Integrated Phosphorus and Extracellular Polymeric Substances Recovery from Aerobic Granular Sludge

Bahgat, T.M.S.M.

DOI
10.4233/uuid:ebb4bdfd-42ea-4313-8f9e-0805a8e830d6

Publication date
2025

Document Version
Final published version

Citation (APA)
Bahgat, T. M. S. M. (2025). *Integrated Phosphorus and Extracellular Polymeric Substances Recovery from Aerobic Granular Sludge*. [Dissertation (TU Delft), Delft University of Technology]. https://doi.org/10.4233/uuid:ebb4bdfd-42ea-4313-8f9e-0805a8e830d6

Important note
To cite this publication, please use the final published version (if applicable).
Please check the document version above.

Integrated Phosphorus and Extracellular Polymeric Substances Recovery from Aerobic Granular Sludge

Nouran Bahgat

Integrated Phosphorus and Extracellular Polymeric Substances Recovery from Aerobic Granular Sludge

Dissertation

for the purpose of obtaining the degree of doctor

at Delft University of Technology

by the authority of the Rector Magnificus,

Prof. dr. ir. T.H.J.J. van der Hagen,

chair of the Board for Doctorates

to be defended publicly on

Friday 14th of February at 12:30

by

Nouran BAHGAT

Master of Science in Water Technology

Wageningen University & Research, University Twente, and University of Groningen (Joint Degree)

born in Cairo, Egypt

This dissertation has been approved by the promotors.

Composition of the doctoral committee:

Rector Magnificus	chairperson
Prof.dr.ir. M.C.M. van Loosdrecht	Delft University of Technology, promotor
Dr. Y. Lin	Delft University of Technology, promotor
Dr. P.K. Wilfert	Delft University of Technology, copromotor

Independent members:

Prof.dr. S.J. Picken	Delft University of Technology
Prof.dr.ir. E.I.P. Volcke	University of Ghent
Prof.dr.ir. H.V.M. Hamelers	Wageningen University & Research
Dr. S.M. Scherrenberg	Royal HaskoningDHV, NL
Prof.dr. P. Osseweijer	Delft University of Technology

Ir. L. Korving of Wetsus has contributed greatly to this dissertation

M.S.c. Nouran Bahgat,

Integrated Phosphorus and Extracellular Polymeric Substances Recovery from Aerobic Granular Sludge

This work was performed in the cooperation framework of Wetsus and Delft University of Technology. This work was part of the “Phosphate Recovery Theme” at Wetsus. This work has received funding from the European Union's Horizon 2020 research and innovation program under grant agreement No 869474.

Printed by: ProefschriftMaken

Cover concept: Nouran Bahgat

Cover design: **Yuwei Huang**

Welcome to a Cosmic Adventure

In the vast space, the bright planet Venus appears in the cosmic landscape just before sunrise, casting its ethereal glow upon the surrounding darkness. Its Greek ancient name, Phosphorus, meaning "light-bearer," seemed fitting for its radiant glow. Known for its bright glow when exposed to oxygen, Phosphorus is also the heart of this PhD thesis.

On Earth, a girl wrapped in a warm yellow scarf gazed up at Venus, her eyes reflecting the wonder of the celestial display. As she looked closer, she noticed four mysterious, undiscovered bodies gracefully orbiting the planet. Each one symbolized an oxygen atom in the iconic phosphate molecule. In her mind, each of these bodies represented a chapter in her thesis. With every chapter, she uncovered new aspects of this glowing element.

To my family….

Summary:

Our current resource consumption practices are unsustainable due to our linear approach, which rapidly depletes resources as populations grow and demands increase. To address this issue, we are transitioning towards circular practices aimed at prolonging the use of products, materials, and resources, thereby minimizing waste. This shift is critical for ensuring a sustainable and secure future for the next generations. Consider wastewater as an example: it's not merely dirty water that needs disposal; rather, it represents a concentrated source of valuable resources such as energy, reusable water, and essential nutrients like nitrogen and phosphorus. By embracing these concentrated streams, we have the opportunity to transform wastewater treatment plants into resource recovery facilities. Here, we can efficiently extract and reuse these precious materials, thus maximizing their value and minimizing environmental impact.

The activated sludge system, which utilizes microbial flocs, remains the predominant wastewater treatment method globally but suffers from inefficiencies in settling, necessitating large land areas. However, in response to the needs of expanding urban areas and the imperative to conserve land, compact and efficient systems like aerobic granular sludge (AGS) technology have been developed. AGS, commercially known as "Nereda®" technology, employs small, rapidly settling microbial granules to treat wastewater more economically and with reduced energy consumption. Beyond its primary function of wastewater treatment,

AGS technology holds promise as a means to recover valuable products such as extracellular polymeric substances (EPS), a bio-based polymer. This highlights the potential of AGS-based wastewater treatment plants to evolve into resource recovery facilities, enhancing sustainability by extracting valuable materials from wastewater streams.

EPS, or extracellular polymeric substances, are polymeric gels produced by bacteria during their metabolic processes, creating a matrix that immobilizes cells into granular particles. EPS have versatile applications, including the production of composite materials, bio-stimulants, and flame retardants, offering sustainable alternatives to petroleum-based polymers.In the Netherlands, there are two demonstration-scale installations dedicated to extracting EPS from Nereda® granules, commercially branded as "Kaumera". This extraction process involves two primary steps: 1) Matrix dissolution: The first step involves elevating the temperature and pH to dissolve the biofilm matrix of aerobic granular sludge. This results in two distinct streams: an alkaline supernatant containing solubilized EPS and an alkaline by-product pellet. 2) EPS precipitation: The solubilized EPS stream is then subjected to a pH adjustment to lower the pH, causing the EPS to precipitate out. This step yields two streams as well: the EPS product and an acidic by-product liquid stream.

Bacteria in aerobic granular sludge wastewater treatment plants efficiently remove phosphorus by storing it as polyphosphate. On the other hand, the EPS extraction method utilizes high temperatures and pH to break down sludge and extract EPS, which can also mobilize

phosphorus present in sludge into a recoverable form. Given that phosphorus is both finite and non-renewable, adopting a dual approach to recover EPS and phosphorus is highly significant. This dual resource recovery approach is particularly innovative because it integrates two distinct resource recovery technologies. Many current methods in literature tend to focus on singular technological solutions for resource recovery, often missing out on the synergistic potential of integrating different recovery processes. By integrating EPS extraction with phosphorus recovery from sludge, there is substantial potential to enhance the efficient use and value of resources present in wastewater. This integrated approach aligns closely with the main motivation of this PhD thesis.

In our research journey, we embarked on meticulously tracking the flow of carbon, phosphorus, and nitrogen through aerobic granular sludge wastewater treatment plants and the EPS extraction process. Our goal was to establish a robust foundation for the next generation of AGS WWTPs equipped with integrated resource recovery capabilities, achieving this by conducting comprehensive mass balances and feasibility evaluations. Focusing on phosphorus, the key element in our study, our research revealed promising results: we identified that up to 60% of the total phosphorus in sludge could potentially be reclaimed. Digestionlly, approximately 20% naturally resides within EPS, about 30% can be recovered from the acidic by-product stream through chemical precipitation, and roughly 10% can be extracted from the digestate if the alkaline by-product undergoes anaerobic digestion (Anaerobic

digestion is a process where microorganisms break down organic matter in the absence of oxygen, producing methane and nutrient-rich digestate). This study was the foundation for subsequent research steps in this PhD thesis.

In our second research phase, our focus shifted to recovering the 30% of phosphorus present in the acidic by-product stream generated during the EPS extraction process. This stream is particularly rich in orthophosphate (PO_4^{3-}), constituting 95% of its phosphorus content, making it the largest and most significant source of phosphorus among the various streams studied. Common minerals like calcium phosphates (CaP), struvite ($MgNH_4PO_4.6H_2O$), and vivianite ($Fe_3(PO_4)_2 \cdot 8H_2O$) are typically recovered through precipitation with the addition of metal ions. However, their precipitation generally requires neutral or alkaline pH levels due to solubility limitations under acidic conditions. Adjusting the pH of acidic streams for mineral recovery poses challenges both environmentally and economically due to chemical dosage requirements and the potential coprecipitation of heavy metals, resulting in lower product purity. In this thesis, we introduced an innovative patented technology for recovering strengite ($FePO_4.2H_2O$) from acidic streams. Unlike traditional methods, our approach eliminates the need for pH adjustment, making it a simpler and more cost-effective process that yields a purer product. Additionally, we developed a novel method to enhance the settleability of strengite by controlling the oxidation of Fe (II) to Fe (III), facilitating easier separation from the liquid phase in WWTPs. This method achieves over 95% phosphorus recovery

efficiency, producing a high-purity product. Research into recovering phosphorus as strengite-type compounds from acidic waste liquid streams represents a growing field with substantial potential for further exploration and development.

In the third phase of our research, our focus centered on recovering the 20% of phosphorus contained within the EPS product, which stands as the second largest source of phosphorus among the streams studied and a key target for recovery in our study. To achieve this, we developed a standardized laboratory protocol and employed ^{31}P NMR spectroscopy as a complementary technique. These methods allowed us to identify various phosphorus species present in EPS, including organic phosphorus (mono and diesters), free orthophosphates, non-apatite inorganic phosphorus (bound to metals such as Fe, Al, Mn), as well as smaller fractions of pyrophosphates and polyphosphates. ^{31}P NMR spectroscopy is an analytical chemistry technique that utilizes nuclear magnetic resonance to analyze compounds containing phosphorus. Our analysis revealed that organic phosphorus species constituted the dominant fraction, accounting for at least 50% of phosphorus within EPS. These organic phosphorus species are highly valuable in industries such as flame retardant manufacturing, typically requiring thermal processing of phosphate rock—a costly and energy-intensive process. Recovering these organic phosphorus species from wastewater presents a novel approach for high-value phosphorus recovery from WWTPs, diverging from conventional methods that predominantly yield mineral-based phosphorus products.

In our final research phase, we explore how to engineer EPS with the manifold of P chemistry, creating a novel recovery route for both phosphorus and EPS. Phosphorus has the potential to enhance EPS properties in ways analogous to its role in improving natural and synthetic polymers in various industries, enhancing characteristics such as flame resistance, viscoelasticity, and water retention. However, there remains a significant gap in understanding how phosphorus specifically influences EPS properties.To address this knowledge gap, we have drawn upon insights from other fields and industries, adapting and applying this knowledge to enhance our understanding and manipulation of EPS. Our research involved a comprehensive review of the various types of phosphorus likely present in EPS, an examination of how phosphorus impacts polymer properties, and developing patented methods to engineer EPS by modifying its phosphorus chemistry either during extraction processes or upstream within wastewater treatment plant operations. This exploration has not only provided valuable insights but has also identified exciting new avenues for future research. Our future investigations aim to engineer EPS to potentially replace or enhance commercial products such as flame retardants, fertilizers, and coatings. Indeed, research is an evolving journey where each answer prompts new questions and opens doors to innovative applications and sustainable solutions.

Samenvatting:

Ons huidige gebruik van grondstoffen is niet duurzaam vanwege onze lineaire aanpak, waarbij grondstoffen snel uitgeput raken naarmate de bevolking groeit en de vraag toeneemt. Om dit probleem aan te pakken, stappen we over op circulaire systemen die gericht zijn op het verlengen van het gebruik van producten, materialen en grondstoffen, waardoor afval wordt geminimaliseerd. Deze verschuiving is cruciaal om een duurzame en veilige toekomst voor de volgende generaties te garanderen. Neem afvalwater als voorbeeld: het is niet alleen vuil water dat moet worden afgevoerd, maar het is een geconcentreerde bron van waardevolle hulpbronnen zoals energie, water en essentiële voedingsstoffen zoals stikstof en fosfor. Door deze geconcentreerde stromen te omarmen, hebben we de mogelijkheid om afvalwaterzuiveringsinstallaties om te vormen tot fabrieken die grondstoffen terugwinnen. Hier kunnen we deze kostbare materialen efficiënt extraheren en hergebruiken, waardoor hun waarde wordt gemaximaliseerd en de impact op het milieu wordt geminimaliseerd.

Het actief slibsysteem, dat gebruik maakt van microbiële vlokken, blijft wereldwijd de belangrijkste afvalwaterbehandelingsmethode, maar heeft te lijden onder inefficiënte bezinking, waardoor grote landoppervlakten nodig zijn. In antwoord op de behoeften van groeiende stedelijke gebieden en de noodzaak om land te sparen, zijn er echter compacte en efficiënte systemen ontwikkeld, zoals de aëroob korrelslib (aerobic granular sludge, AGS) technologie. AGS,

commercieel bekend als de "Nereda®" technologie, maakt gebruik van kleine, snel bezinkende microbiële korrels om afvalwater economisch en met minder energieverbruik te behandelen. Naast de primaire functie van afvalwaterzuivering is de AGS-technologie veelbelovend als middel om waardevolle producten terug te winnen, zoals extracellulaire polymere stoffen (EPS), een polymeer op biologische basis. Dit onderstreept het potentieel van AGS-gebaseerde afvalwaterzuiveringsinstallaties om zich te ontwikkelen tot grondstof fabrieken

EPS, of extracellulaire polymere stoffen, zijn polymere gels die door bacteriën worden geproduceerd tijdens hun metabolische processen, waarbij een matrix wordt gecreëerd die cellen immobiliseert tot korrelvormige deeltjes. EPS heeft veelzijdige toepassingen, waaronder de productie van composietmaterialen, biostimulanten, vlamvertragers, en biedt duurzame alternatieven voor polymeren op basis van aardolie. In Nederland zijn er twee installaties op demonstratieschaal voor het extraheren van EPS uit Nereda®-korrels, commercieel bekend onder de merknaam "Kaumera". Dit extractieproces omvat twee primaire stappen: 1) oplossen van de matrix: het verhogen van de temperatuur en pH om de biofilmmatrix van aëroob korrelslib (AGS) op te lossen. Dit resulteert in twee verschillende stromen: een alkalisch supernatant met opgelost EPS en een alkalische pellet alsbijproduct. 2) EPS-neerslag: De opgeloste EPS-stroom wordt vervolgens onderworpen aan een pH-aanpassing door de pH te verlagen, waardoor het EPS neerslaat.

Ook deze stap levert twee stromen op: het EPS-product en een vloeibaar zuur bijproduct.

Bacteriën in aerobe afvalwaterzuiveringsinstallaties met korrelslib, verwijderen fosfor efficiënt door het op te slaan als polyfosfaat. Aan de andere kant gebruikt de EPS-extractiemethode hoge temperaturen en een hoge pH-waarde om slib af te breken en EPS te extraheren, waardoor ook fosfor in slib kan worden gemobiliseerd in een terugwinbare vorm. Aangezien fosfor zowel eindig als niet-hernieuwbaar is, is een tweeledige aanpak om EPS en fosfor terug te winnen van groot belang. Deze tweeledige aanpak voor het terugwinnen van hulpbronnen is vooral innovatief omdat het twee verschillende technologieën voor het terugwinnen van grondstoffen integreert. Veel van de huidige methoden in de literatuur richten zich op enkelvoudige technologische oplossingen voor het terugwinnen van grondstoffen, waarbij het synergetische potentieel van de integratie van verschillende terugwinningsprocessen vaak over het hoofd wordt gezien. Door EPS-extractie te integreren met fosforterugwinning uit slib, is er een aanzienlijk potentieel om het efficiënte gebruik en de waarde-extractie van hulpbronnen in afvalwater te verbeteren. Deze geïntegreerde aanpak sluit nauw aan bij de belangrijkste motivatie van dit proefschrift.

Tijdens ons onderzoek zijn we begonnen met het nauwgezet volgen van koolstof, fosfor en stikstof bij aërobe afvalwaterzuiveringsinstallaties met korrelslib en bij het EPS-extractieproces. Ons doel was om een robuuste basis te leggen voor de volgende generatie AGS RWZI's met

geïntegreerde terugwinningsmogelijkheden, door uitgebreide massabalansen en haalbaarheidsevaluaties uit te voeren. De focus op fosfor, het belangrijkste element in onze studie, leverde veelbelovende resultaten op: we stelden vast dat tot 60% van de totale hoeveelheid fosfor in slib mogelijk kan worden teruggewonnen. Ongeveer 20% bevindt zich van nature in EPS, ongeveer 30% kan worden teruggewonnen uit de zure bijproductstroom door middel van chemische neerslag en ongeveer 10% kan worden gewonnen uit het digestaat als het alkalische bijproduct anaerobe gisting ondergaat. (Anaerobe vergisting is een proces waarbij micro-organismen organisch materiaal afbreken in afwezigheid van zuurstof, waarbij methaan en voedselrijk digestaat wordt geproduceerd).

In onze tweede onderzoeksfase richtten we ons op het terugwinnen van de 30% fosfor die aanwezig is in de zure nevenstroom die ontstaat tijdens het EPS extractieproces. Deze stroom is bijzonder rijk aan ortho-fosfaat ($PO4^{3-}$) en vormt 95% van het fosforgehalte, waardoor het de grootste en belangrijkste bron van fosfor is onder de verschillende onderzochte stromen. Veel voorkomende mineralen zoals calciumfosfaten (CaP), struviet ($MgNH_4PO_4.6H_2O$) en vivianiet ($Fe_3(PO_4)_2.8H_2O$) worden meestal teruggewonnen door precipitatie met toevoeging van metaalionen. Voor hun precipitatie is echter over het algemeen een neutrale of alkalische pH nodig vanwege de beperkte oplosbaarheid onder zure omstandigheden. Het aanpassen van de pH van zure stromen voor het terugwinnen van mineralen vormt een uitdaging voor zowel het milieu als de economie vanwege de vereiste

chemische dosering en de mogelijke co-precipitatie van zware metalen, wat resulteert in een lagere productzuiverheid. In dit proefschrift introduceren we een innovatieve gepatenteerde technologie voor het terugwinnen van strengiet ($FePO_4.2H_2O$) uit zure stromen. In tegenstelling tot traditionele methoden maakt onze benadering pH-aanpassing overbodig, waardoor het een eenvoudiger en kosteneffectiever proces is dat een zuiverder product oplevert. Daarnaast hebben we een nieuwe methode ontwikkeld om de bezinkbaarheid van strengiet te verbeteren door de oxidatie van Fe(II) tot Fe(III) te controleren, waardoor de scheiding van de vloeibare fase in AWZI's eenvoudiger wordt. Dit proces bereikt een fosforterugwinningsefficiëntie van meer dan 95% en produceert een zeer zuiver product. Onderzoek naar het terugwinnen van fosfor als strengietachtige verbindingen uit zure afvalwaterstromen is een groeiend gebied met een aanzienlijk potentieel voor verdere exploratie en ontwikkeling.

In de derde fase van ons onderzoek richtten we ons op het terugwinnen van de 20% fosfor in het EPS-product, de op één na grootste bron van fosfor in de onderzochte stromen en een belangrijk doel voor terugwinning in ons onderzoek. Om dit te bereiken ontwikkelden we een gestandaardiseerd laboratoriumprotocol en gebruikten we 31P NMR spectroscopie als aanvullende techniek. Met deze spectroscopische methode konden we verschillende fosforsoorten identificeren die aanwezig waren in EPS, waaronder organische fosfor (mono- en diësters), vrije orthofosfaten, niet-apatiet anorganische

fosfor (gebonden aan metalen zoals Fe, Al, Mn), evenals kleinere fracties van pyrofosfaten en polyfosfaten. 31P NMR spectroscopie is een analytisch-chemische techniek die gebruik maakt van kernspinresonantie om fosforhoudende verbindingen te analyseren. Uit onze analyse bleek dat organische fosforsoorten de dominante fractie vormden, goed voor 50% van het fosfor in EPS. Deze organische fosforverbindingen zijn zeer waardevol in industrieën zoals de productie van vlamvertragers, waarvoor meestal thermische verwerking van fosfaatgesteente nodig is - een duur en energie-intensief proces. Het terugwinnen van deze organische fosforsoorten uit afvalwater is een nieuwe benadering voor het terugwinnen van hoogwaardige fosfor uit afvalwaterzuiveringsinstallaties, die afwijkt van conventionele methoden die voornamelijk minerale fosforproducten opleveren.

In onze laatste onderzoeksfase onderzoeken we hoe we EPS kunnen combineren met het veelvoud aan P-chemie, waardoor een nieuwe route ontstaat voor het terugwinnen van zowel fosfor als EPS. Fosfor heeft het potentieel om de eigenschappen van EPS te verbeteren op een manier die vergelijkbaar is met de rol die het speelt bij het verbeteren van natuurlijke en synthetische polymeren in verschillende industrieën, door eigenschappen als vlambestendigheid, visco-elasticiteit en waterretentie te verbeteren. Echter, er blijft een significante kennisklоof over hoe fosfor de specifieke kenmerken van EPS beïnvloedt. Daarom hebben we gebruik gemaakt van inzichten uit andere vakgebieden en industrieën en hebben we deze kennis aangepast en toegepast om ons

begrip en de manipulatie van EPS te verbeteren. Ons onderzoek omvatte een uitgebreid overzicht van de verschillende soorten fosfor die waarschijnlijk aanwezig zijn in EPS, een onderzoek naar de manier waarop fosfor de eigenschappen van polymeren beïnvloedt en een verkenning van methoden om EPS te manipuleren door de chemie van fosfor te wijzigen tijdens extractieprocessen of stroomopwaarts in afvalwaterzuiveringsinstallaties. Dit onderzoek heeft niet alleen waardevolle inzichten opgeleverd, maar ook spannende nieuwe mogelijkheden voor toekomstig onderzoek aan het licht gebracht. Ons toekomstig onderzoek is erop gericht om EPS te ontwikkelen om mogelijk commerciële producten zoals vlamvertragers, meststoffen en coatings te vervangen of te verbeteren. Onderzoek is inderdaad een evoluerende reis waarbij elk antwoord nieuwe vragen oproept en deuren opent naar innovatieve toepassingen en duurzame oplossingen.

ملخص علمي مبسط:

استخدامُنا للمواردِ غيرُ مستدامٍ لأننا نستهلكُ الموارِدَ بطريقةٍ خطِّيَّةٍ، مما يؤدي إلى نضوبِها بسرعةٍ مع نموّ السكانِ وزيادةِ متطلباتِنا. لمكافحةِ هذا النمطِ الاستهلاكيّ للمواردِ، نتجه نحو ممارساتٍ دائريةٍ حيث يتمُّ استخدامُ المنتجاتِ والموادِّ والمواردِ لأطولِ فترةٍ ممكنةٍ، مما يقللُ أيضاً من إنتاجِ النفاياتِ. هذا التحوُّل ضروريٌّ لمستقبلٍ مستدامٍ وآمنٍ للأجيالِ القادمةِ. خذْ مياهَ الصرفِ الصحيّ على سبيلِ المثالِ. إنها ليست مجردَ مياهٍ ملوثةٍ نحتاجُ إلى التخلصِ منها؛ بل هي مصدرٌ مركَّزٌ للمواردِ القيمةِ مثلِ الطاقةِ والمياهِ القابلةِ لإعادةِ الاستخدامِ والموادِّ الغذائيةِ الأساسيةِ مثل النيتروجين والفوسفور. من خلالِ تبنِّي مياهِ الصرفِ كمصدرٍ مركَّزٍ للمواردِ، يمكنُنا تحويلُ محطاتِ معالجةِ مياهِ الصرفِ الصحيّ إلى مصانعَ لاستخراجِ المواردِ، حيث نقومُ باستخراجِ وإعادةِ استخدامِ هذه الموادِّ الثمينةِ كموادٍّ خامٍّ أوليةٍ.

نظامُ الحمأةِ النشطةِ، الذي يستخدمُ التكتلاتِ الميكروبيةِ الصغيرةِ، يمثلُ عمليةَ معالجةِ مياهِ الصرفِ الصحيّ التقليديةِ في جميعِ أنحاءِ العالمِ. وعلى الرغمِ من كفاءتِهِ في المعالجةِ، إلا أنه يتطلبُ مساحاتٍ كبيرةً بسببِ صعوبةِ وبطءِ عمليةِ ترسيبِ التكتلاتِ الميكروبيةِ الصغيرةِ إلى قاعِ الخزانِ مما يصعّبُ إزالةَ المخلفاتِ الصلبةِ عن المياهِ المعالجةِ. ومع ذلك، لتلبيةِ احتياجاتِ المدنِ المتناميةِ والحفاظِ على الأراضي، تمَّ تطويرُ أنظمةٍ مدمجةٍ وفعالةٍ مثل تقنيةِ الحمأةِ الحبيبيةِ الهوائيةِ التي تعتمدُ على حبيباتٍ ميكروبيةٍ كبيرةٍ سريعةِ الترسيبِ لمعالجةِ مياهِ الصرفِ الصحيّ بتكاليفَ أقلَّ واستهلاكٍ أقلَّ للطاقةِ ومساحاتٍ أقلَّ. إلى جانبِ دورِ هذه التكنولوجيا الأساسيّ في معالجةِ مياهِ الصرفِ فهي تظهَرُ كوسيلةٍ واعدةٍ لاستخراجِ منتجاتٍ قيمةٍ مثلَ الموادِّ البوليمريةِ البيولوجيةِ الموجودةِ خارجَ الخلايا البكتيريةِ، مما يبرزُ إمكاناتِ محطاتِ معالجةِ مياهِ الصرفِ الصحيّ القائمةِ على تقنيةِ الحمأةِ الحبيبيةِ للتحوُّل إلى مصانعَ لاستخراجِ المواردِ في المستقبلِ.

يتمُّ إنتاجُ الموادِّ البوليمريةِ كهلامٍ من قِبلِ البكتيريا أثناءَ أيضِ الخلايا، حيث تشكلُ مصفوفةً تُسمى الغشاءَ الحيويَّ تثبتُ فيها الخلايا كجسيماتٍ حبيبيةٍ كبيرةٍ. يمكنُ استخدامُ هذه الموادِّ البوليمريةِ كبديلٍ للبوليمراتِ القائمةِ على البترولِ في تطبيقاتٍ صناعيةٍ متعددةٍ، مثل صناعةِ

الموادِّ المركبةِ ومحفزاتِ النموِّ النباتيةِ والموادِّ المانعةِ للاشتعالِ. أسَّست هولندا محطتين تجريبيتين لاستخراجِ هذه الموادِّ البوليمريةِ من الحمأةِ الحبيبيةِ من خلال عمليةٍ تتكونُ من مرحلتين: المرحلةُ الأولى هي رفعُ درجةِ الحرارةِ والرقمِ الهيدروجينيِّ لذوبانِ مصفوفةِ الغشاءِ الحيويِّ مما يؤدي إلى تكوينِ ناتجٍ أساسيٍّ وهو سائلٌ قلويٌّ يحتوي على الموادِّ البوليمريةِ المذابةِ وناتجٍ فرعيٍّ يحتوي على مخلفاتٍ صلبةٍ قلويةٍ. يتمُّ فصلهما ثم يدخلُ الناتجُ الأساسيُّ إلى المرحلةِ الثانيةِ وهي خفضُ الرقمِ الهيدروجينيِّ لترسيبِ الموادِّ البوليمريةِ المذابةِ مما يؤدي إلى تكوينِ المنتجِ النهائيِّ وهو الموادُّ البوليمريةُ المترسبةُ وناتجٌ فرعيٌّ سائلٌ حامضيٌّ. يتمُّ فصلهما وتخزينُ المنتجِ النهائيِّ.

تزيلُ البكتيريا الفوسفورَ من مياهِ الصرفِ الصحيِّ في محطاتِ المعالجةِ بالحمأةِ الحبيبيةِ الهوائيةِ بكفاءةٍ عاليةٍ عن طريقِ تخزينِهِ كبوليفوسفات. عمليةُ استخراجِ الموادِّ البوليمريةِ التي تعتمدُ على استخدامِ درجاتِ حرارةٍ عاليةٍ ورقمٍ هيدروجينيٍّ عالٍ لتحلُّلِ الحمأةِ السابقِ ذكرُها يمكنُ أن تعززَ أيضاً استخراجَ الفوسفورِ من الحمأةِ إلى شكلٍ قابلٍ لإعادةِ الاستخدامِ. نظرًا لأن الفوسفورَ عنصرٌ محدودٌ وغيرُ قابلٍ للتجديدِ، فإنَّ النهجَ المزدوجَ لاستعادةِ واستخراجِ الموادِّ البوليمراتِ والفوسفورِ من مياهِ الصرفِ الصحيِّ يستحقُّ الدراسةَ والتقييمَ. هذا النهجُ جديدٌ لأنَّ العديدَ من الطرقِ الحاليةِ لاستردادِ الموارِدِ تميلُ إلى التركيزِ على حلولٍ تكنولوجيةٍ فرديةٍ، متجاهلةً في كثيرٍ من الأحيانِ إمكانياتِ التكاملِ. تكاملُ هذه التقنياتِ لديه القدرةُ على تحقيقِ أقصى استخدامٍ كفءٍ وأعلى قيمةٍ للموارِدِ المتوفرةِ في مياهِ الصرفِ الصحيِّ (الحافزُ الرئيسيُّ لأطروحةِ الدكتوراه).

في رحلتِنا البحثيةِ، بدأنا بتتبعِ تدفقِ الكربونِ والفوسفورِ والنيتروجينِ في محطاتِ معالجةِ مياهِ الصرفِ الصحيِّ باستخدامِ الحمأةِ الحبيبيةِ الهوائيةِ وما يليها من عمليةِ استخراجِ الموادِّ البوليمريةِ. هدفُنا كان وضعَ أساسٍ قويٍّ لجيلِ المحطاتِ القادمةِ من الحمأةِ الحبيبيةِ الهوائيةِ المجهزةِ بقدراتِ استعادةِ الموارِدِ المتكاملةِ من خلال إنشاءِ أوزانٍ كتليةٍ لهذه الموارِدِ وتقييمِ جدوى استخراجِها من مياهِ الصرفِ. نظرًا لأن عمليةَ استخراجِ الموادِّ البوليمريةِ هي العمليةُ الرئيسيةُ، وضعنا بشكلٍ استراتيجيٍّ تقنياتِ استخراجِ موادٍّ أخرى داخلَ هذه العمليةِ الرئيسيةِ لتعظيمِ استردادِ الكربونِ والفوسفورِ والنيتروجين. تركيزًا على الفوسفورِ، العنصرِ الرئيسيِّ

في دراستِنا، وجدنا أن ما يصلُ إلى ٦٠٪ من إجماليّ الفوسفورِ في الحمأةِ يمكنُ استرداده حيث: حوالي ٢٠٪ يوجدُ بشكلٍ طبيعيٍّ داخلَ المنتجِ النهائيّ للعمليةِ (الموادُّ البوليمريةُ)، وحوالي ٣٠٪ يمكنُ استردادُه من الناتجِ الفرعيّ الحامضيّ الناتجِ بعدَ الترسيبِ الكيميائيّ للموادّ البوليمريةِ، وحوالي ١٠٪ يمكنُ استردادُه من الناتجِ الفرعيّ الذي يحتوي على مخلفاتٍ صلبةٍ قلويةٍ إذا مرَّ الناتجُ الفرعيُّ بعمليةِ الهضمِ اللاهوائيّ (وهي عمليةٌ حيث تقومُ الكائناتُ الدقيقةُ بتحليلِ الموادّ العضويةِ في غيابِ الأكسجينِ لإنتاجِ الميثانِ وسائلٍ غنيٍّ بالفوسفورِ والنيتروجينِ). هذه الدراسةُ شكلتْ أساسَ الدراساتِ اللاحقةِ في الأطروحةِ.

في المرحلةِ البحثيةِ الثانية، ركَّزْنا على استردادِ الـ ٣٠٪ من الفوسفورِ الذي ينتهي في الناتجِ الفرعيّ السائلِ الحامضيّ أثناءَ استخراجِ الموادّ البوليمريةِ، حيث يحتوي هذا التيارُ على ٩٥٪ من محتواه من الفوسفورِ كأيوناتِ فوسفاتِ الأورثو الحرة، مما يجعله أكبرَ مصدرٍ للفوسفورِ وهدفاً أساسياً للاستخراجِ في دراستِنا. المعادنُ مثل فوسفاتِ الكالسيوم، فوسفاتِ المغنيسيوم (ستروفيت)، وفوسفاتِ الحديدِ ذو رقمِ الأكسدةِ +٢ (فيفيانايت) هي المنتجاتُ الأكثرُ شيوعاً لاستخراجِ فوسفاتِ الأورثو عن طريقِ الترسيبِ الكيميائيّ عند إضافةِ أيوناتِ المعادن. عادةً ما تتطلب هذه المعادنُ رقماً هيدروجينياً معتدلاً أو قاعدياً بسبب ذوبانِها وعدمِ إمكانيةِ تكوينِها تحتَ الظروفِ الحامضية. يواجه تعديلُ الرقمِ الهيدروجينيّ للسوائلِ الحامضيةِ لترسيبِ هذه المعادنِ تحدياتٍ بيئيةٍ واقتصاديةٍ بسبب الجرعاتِ الكيميائيةِ الكبيرةِ اللازمِ إضافتُها وانخفاضِ نقاءِ المنتجِ بسببِ الترسيبِ المشتركِ للمعادنِ الثقيلة. في هذه الأطروحةِ، قدمنا تقنيةً مبتكرةً محميةً ببراءةِ اختراعٍ لترسيبِ واستخراجِ فوسفاتِ الأورثو كفوسفاتِ الحديدِ ذو رقمِ الأكسدةِ +٣ (سترينجايت). على عكسِ الطرقِ التقليدية، هذه التقنيةُ لا تتطلب ضبطَ الرقمِ الهيدروجينيّ أو إضافةَ جرعاتٍ كيميائيةٍ، لذا فهي عمليةٌ بسيطةٌ وفعالةٌ من حيث التكلفةِ مع منتجٍ أكثرَ نقاءً. كما قدمنا طريقةً جديدةً لعملِ تكتلاتٍ كبيرةٍ من السترينجايتِ التي يمكنُ ترسيبُها بوزنِ الجاذبيةِ عن طريق التأكسدِ المنظمِ للحديدِ ذو رقمِ الأكسدةِ +٢ إلى الحديدِ ذو رقمِ الأكسدةِ +٣ لتعزيزِ سرعةِ ترسيبِ المنتجِ وسهولةِ فصلِه عن الطورِ السائلِ في محطاتِ معالجةِ مياهِ الصرفِ الصحيّ. تنتجُ هذه العمليةُ منتجاً نقياً بكفاءةِ استردادٍ للفوسفورِ تزيدُ عن ٩٥٪. البحثُ في

استردادِ الفوسفورِ كمركباتٍ من نوعِ سترينجايتِ من المياهِ الحامضيةِ هو مجالٌ متنامٍ يحملُ المزيدَ من الأبحاثِ لاستكشافِ إمكانياتٍ كبيرة.

في المرحلةِ البحثيةِ الثالثة، ركزنا على الـ ٢٠٪ من الفوسفورِ الذي ينتهي في الموادِّ البوليمريةِ، نظراً لكونهِ ثاني أكبرِ مصدرٍ للفوسفورِ. من خلال تطويرِ بروتوكولٍ معمليٍّ قياسيٍّ واستخدامِ الطيفِ النوويِّ المغناطيسيِّ كتقنيةٍ مكملةٍ، كشفنا أنَّ الموادَّ البوليمريةَ تحتوي على أشكالٍ مختلفةٍ من أنواعِ الفوسفور، بما في ذلك الفوسفورُ العضويُّ، وأيوناتُ فوسفاتِ الأورثو الحرة، والفوسفورُ غيرُ الأباتيتيِّ اللاعضويُّ (المرتبطُ بالفلزاتِ مثل الحديدِ، الألمنيومِ، المنغنيز)، بالإضافة إلى نسبٍ أقلَّ من فوسفاتِ البيرفوسفاتِ والبوليفوسفاتِ. الجزءُ السائدُ من الفوسفورِ في الموادِّ البوليمريةِ هو الفوسفورُ العضويُّ والذي يمثلُ ٥٠٪ من مجموعِ الفوسفورِ. هذه الأنواعُ العضويةُ من الفوسفورِ مطلوبةٌ بشدةٍ في الصناعةِ، على سبيلِ المثال لإنتاجِ موادٍّ مانعةٍ للاحتراقِ، ويتعينُ إنتاجُها من خلالِ عمليةِ التحليلِ الحراريِّ لصخورِ الفوسفاتِ المستخرجةِ من باطنِ الأرضِ، والتي تتطلبُ تكاليفَ عاليةً واستهلاكاً للطاقةِ. استردادُ هذه الأنواعِ العضويةِ من الفوسفورِ من مياهِ الصرفِ الصحيِّ يقدمُ نهجاً جديداً لم يتمَّ طرحُهُ من قبلُ لاستردادِ فوسفورٍ ذي قيمةٍ عاليةٍ من محطاتِ معالجةِ مياهِ الصرفِ الصحيِّ، مختلفاً عن الطرقِ التقليديةِ التي تنتجُ عادةً منتجاتِ فوسفاتٍ معدنيةٍ.

في المرحلةِ النهائيةِ من بحثِنا، نستكشفُ كيفيةَ تصميمِ وهندسةِ هذه الموادِّ البوليمريةِ لتسدَّ احتياجاتِ الصناعةِ باستخدامِ كيمياءِ الفوسفورِ. يمكنُ للفوسفورِ تحسينُ خصائصِ الموادِّ البوليمريةِ المستخرجةِ من الغشاءِ الحيويِّ للبكتيريا تماماً كما يُحسنُ الفوسفورُ خصائصَ البوليمراتِ الصناعيةِ في مختلفِ الصناعاتِ الكيميائيةِ والغذائيةِ وأخرى مثل تحسينِ مقاومةِ اللهبِ، والمرونةِ، واحتباسِ الماءِ وخصائصَ أخرى، مما يخلقُ مسارَ استخراجٍ جديدٍ متكاملٍ لكلا من الفوسفورِ والموادِّ البوليمريةِ من مياهِ الصرفِ. مع ذلك، هناك معلوماتٌ محدودةٌ حول كيفيةِ تأثيرِ الفوسفورِ على خصائصِ هذه الموادِّ البوليمريةِ المستخرجةِ من الغشاءِ الحيويِّ للبكتيريا، فهو مجالٌ لم يتمَّ بحثُهُ سابقاً. لسدِّ هذه الفجوةِ المعرفيةِ، قمنا بمراجعةِ الأنواعِ المختلفةِ من الفوسفورِ التي من المحتملِ أن تكونَ موجودةً في الموادِّ البوليمريةِ المستخرجةِ، وفحصْنا آلياتِ تأثيرِ الفوسفورِ على خصائصِ البوليمراتِ، واستكشفْنا طرقاً مبتكرةً محميةً ببراءةِ

اختراعٍ لتصميمِ وهندسةِ الموادِّ البوليمريةِ من خلالِ تعديلِ كيمياءِ الفوسفورِ أثناءَ عمليةِ الاستخراجِ أو في المراحلِ الأوليةِ خلالَ تشغيلِ محطاتِ معالجةِ مياهِ الصرفِ الصحيّ. يسلطُ هذا البحثُ الضوءَ أيضاً على اتجاهاتٍ بحثيةٍ جديدةٍ مثيرةٍ للتحقيقِ في المستقبلِ، بهدفٍ نهائيٍّ هو تصميمُ هذه الموادِّ البوليمريةِ البيولوجيةِ لتحلَّ محلَّ بعضِ المنتجاتِ التجاريةِ المعتمدةِ على البوليمراتِ البتروليةِ مثل الموادِّ المانعةِ للاحتراقِ، والأسمدةِ، والطلاءاتِ. فالبحثُ هو رحلةُ اكتشافٍ حيثُ يقودُ كلُّ جوابٍ إلى أسئلةٍ جديدةٍ.

Table of Contents:

Chapter 1 1

1.1 Aerobic Granular Sludge Wastewater Treatment Plants 30

1.2 Aerobic Granular Sludge Wastewater Resource Recovery Facilities (WRRFs) 32

1.2.1 EPS Recovery 34

1.2.2 Integrative EPS and Phosphorus Recovery 35

1.3 Phosphorus 38

1.3.1 Mined P rock 38

1.3.2 Phosphorus Recovery- Mineral P Precipitates 42

1.3.3 Phosphorus recovery- Higher value P Products 45

1.4 Innovative Integration of Phosphorus and EPS for High-Value Product Development 47

1.5 Thesis Outline 50

References 52

Chapter 2 59

2.1 Introduction 61

2.2 Materials and Methods 66

2.2.1 Laboratory extractions 66

2.2.2 Epe demonstration extractions 66

2.2.3 Mass balance calculations 69

2.2.4 Analysis 70

2.3 Results 73

2.3.1 Concentrations in laboratory and Epe demonstration extractions 73

2.3.2 The appearance of an alkaline gel layer 73

2.3.3 The potential of carbon recovery (laboratory scale extractions) 76

2.3.4 The potential of phosphorus recovery (laboratory scale extractions) 77

2.3.5 The potential of nitrogen recovery (laboratory scale extractions) 78

2.3.6 Recovery potential in perspective to Epe AGS WWTP+ EPS extraction plant 81

2.4 Discussion 82

2.4.1 Alkaline gel layer formation 83

2.4.2 Epe demonstration-scale extractions 85

2.4.3 Carbon Recovery 87

2.4.4 Phosphorus Recovery 88

2.4.5 Nitrogen recovery 93

2.4.6 Practical Implications 94

2.5 Conclusions 95

References 98

Supplementary Materials 104

Chapter 3 53

3.1 Introduction 123

3.2 Methodology 128

3.2.1 Reagents 128

3.2.2 Preparations 128

3.2.3 Analysis 130

3.2.4 Curve fitting 134

3.3 Results 135

3.3.1 Evaluation of chemical equilibria 135

3.3.2 pH effect on P recovery% 135

3.3.3 Temperature effect on P recovery% 136

3.3.4 Fe (II) oxidation effect on P recovery% 137

3.3.5 Fe (III) versus Fe (II) Settling 141

3.3.6 FeP precipitate identification 144

3.3.7 Proof of principle experiments on acidic by-product stream from EPS extraction process 148

3.4 Discussion 151

3.4.1 $FePO_4.2H_2O$ identification 151

3.4.2 Fe (II) oxidation in acidic conditions 152

3.4.3 $FePO_4.2H_2O$ separation methods 155

3.4.4 Proof of principle experiments on acidic by-product stream from EPS extraction process 157

3.5 Outlook 158
3.6 Conclusion 160
References 162
Supplementary Materials 170
Chapter 4 103
4.1 Introduction 185
4.2 Methodology 187
4.2.1 Sludge samples 187
4.2.2 EPS extraction 188
4.2.3 P-fractionation protocol 189
4.2.4 Analysis 195
4.2.5 Liquid ^{31}P NMR 196
4.3 Results and Discussion 201
4.3.1 P-fractionation protocol 201
4.3.2 Liquid ^{31}P NMR 209
4.4 Recommendations and Outlook 217
4.4.1 Regarding the P-fraction protocol 218
4.4.2 Regarding the ultimate goal of EPS engineering 219
4.5 Conclusion 222
References 224
Supplementary Materials 229

Chapter 5 125

5.1 Introduction 243

5.2 P species in EPS 245

5.2.1 Organic P 246

5.2.2 Polyphosphates, pyrophosphates and orthophosphates 252

5.3 P and functional properties 253

5.3.1 Thermal properties 253

5.3.2 Physiochemical properties 264

5.4 Outlook: EPS engineering via P 273

5.4.1 Translating Literature Knowledge to EPS 273

5.4.2 Engineering P species in EPS 275

5.5 Conclusions 277

References 278

Chapter 6 123

6.1 Integrated P and EPS Recovery Route from Aerobic Granular Sludge – Critical View of This Thesis 294

6.2 Non-Integrated P Recovery Routes from Aerobic Granular Sludge – Alternatives to this Thesis 300

6.2.1 From the surplus AGS before EPS extraction 300

6.2.2 At the end of the anaerobic phase of the SBR cycle 302

6.3 Outlook 304

6.3.1 Expanding the Scope of Phosphorus Recovery Beyond Mineral Precipitation 304

6.3.2 Expanding the Scope of the Innovative Integration of Phosphorus and EPS to Engineer EPS 306

6.3.3 Towards the Future Vision of Aerobic Granular Sludge water-resource Facilties and Circularity 308

References 310

About the Author 312

List of Publications/Patents 314

Acknowledgments 316

Chapter 1

General Introduction

1.1 Aerobic Granular Sludge Wastewater Treatment Plants

1

A hundred years ago, the activated sludge process, which utilizes flocculating bacteria, was introduced and became the conventional treatment process worldwide. However, this technology requires a large surface area due to the poor settling characteristics of microbial flocculent aggregates, low concentrations of solids in aeration tanks, and a restricted maximum sludge loading (kg TSS/m^2.day) on secondary sedimentation tanks. Compact treatment systems were introduced due to population expansion, new human activities, and limited availability of land. During the last decades, different compact treatment systems have developed, such as biofilm systems, membrane bioreactors (MBR), and aerobic granular sludge technology (AGS). A collaboration between the Dutch public and private sectors resulted in the creation of the full-scale aerobic granular sludge technology, commonly referred to as 'Nereda technology.' AGS technology presents several benefits over traditional activated sludge technology, including reduced investment costs and energy consumption. Additionally, it requires a smaller overall footprint due to the rapid settling of granular microbial aggregates, in contrast to the floccular ones found in conventional activated sludge systems (de Bruin et al., 2004). This efficiency is achieved through a feast-famine feeding regime, which favors the growth of slow-growing microorganisms that form granules (Beun et al., 2002; de Kreuk & van Loosdrecht, 2004). The AGS process operates as a sequencing batch reactor (SBR) system. The reactor goes through three consecutive steps, as shown in **Figure 1-1** (Pronk et al., 2020):

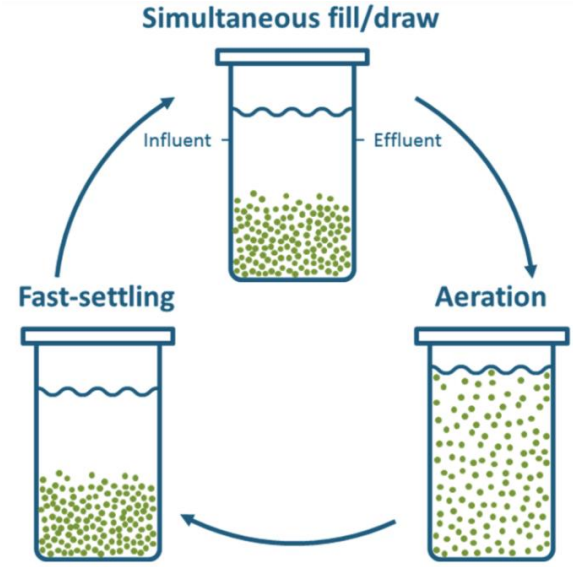

Figure 1-1:The Nereda® cycle (Pronk et al., 2020)

1) simultaneous feeding from the bottom and effluent overflow from the top. Due to the good settling properties of aerobic granular sludge, this can be done at relatively high up-flow velocities without the risk of sludge washout.

2) aeration phase, in which COD and nutrients are simultaneously removed. In practice, aeration is controlled based on a series of different strategies, such as oxygen concentration, redox, pH, ammonium, and phosphate concentrations.

and 3) a short settling period in which the sludge bed settles to prevent the washout of sludge when the simultaneous feeding and decanting start. Granules will settle faster than flocs, and these flocs form a layer

on top of the granular bed. The waste sludge is taken from the top of the sludge blanket and is called “spill sludge.”

1.2 Aerobic Granular Sludge Wastewater Resource Recovery Facilities (WRRFs)

Initially, the primary objective of WWTPs was to protect against health risks and widespread diseases. However, nowadays, wastewater is recognized as a resource rather than just a waste stream. The transition to a circular economy drives a paradigm shift in wastewater treatment from a focus on pollutant removal to an emphasis on resource recovery. This transition will preserve the value of products, materials, and resources within the economic system for an extended duration and will minimize waste generation. Much research has been done within the field of wastewater resource recovery as seen in recovering bio-based products e.g., polyhydroxyalkanoates (PHA) (Werker et al., 2018), extracellular polymeric substances (EPS) (Felz et al., 2016), phosphorus from sludge and liquid streams (Egle et al., 2015), biogas (Bachmann, 2015), water reclamation processes and reuse (Nancarrow et al., 2008) and nitrogen (Rodríguez Arredondo et al., 2015). It is argued that enough innovation has already been developed to implement resource recovery; however, implementation is lagging due to social, economic, and legal obstacles (Velenturf & Jopson, 2019). Additionally, most recovery routes in the literature focus solely on a single technological resource recovery solution and rarely consider integration possibilities (Kehrein et al., 2020), such as integrating the recovery of phosphorus,

carbon, methane, nitrogen, and other valuable resources. Integrating recovery technologies can maximize the utilization of resources in wastewater more economically by reducing the need for chemicals and energy associated with separate technologies. This integration can produce higher value products that address societal demands due to the unique combination of elements. By incorporating these integrations in the early design phases of WWTPs, we can determine the optimal approach to combine these technologies based on the specific wastewater treatment technology used, the quantitative potential for resource recovery, local market demands, and other relevant factors.

Aerobic granular sludge technology is a promising wastewater treatment method with significant potential to operate as a water resource recovery facility. Currently, in practice, aerobic granular surplus sludge is not treated separately but combined with surplus sludge from activated sludge systems and processed through anaerobic digestion or incineration. However, aerobic granular sludge offers an innovative possibility for product recovery from COD, the recovery of EPS. Successful recovery of EPS has been demonstrated at both lab and pilot scales (E. van der Knaap et al., 2019; Felz et al., 2019).

The future scheme of aerobic granular sludge WRRFs can be envisioned as a wastewater treatment process followed by EPS recovery technology to produce biopolymers as a primary recovery process. Additionally, other recovery technologies could be integrated into its by product streams. **In this thesis, the potential for integrating phosphorus with EPS recovery was explored for the first time.**

1.2.1 EPS Recovery

Extracellular polymeric substances are polymeric gel materials generated by bacteria during cell metabolism. These substances comprise proteins, polysaccharides, DNA, lipids, glycoproteins, and humic substances, forming a matrix that immobilizes the cells as granular particles (Seviour et al., 2009). Various extraction methods to solubilize and precipitate EPS from biofilms are reported in the literature based on chemical, physical, or combined approaches (Sheng et al., 2010). These different extraction methods result in different EPS fractions with different compositions, so extraction conditions are considered one of the first differentiation criteria between different EPS (Y. Lin et al., 2010; Pronk et al., 2017). Felz et al., 2016 reported EPS extraction conditions that involve raised temperature and pH conditions to dissolve the biofilm matrix of aerobic granular sludge, then low pH conditions to collect the dissolved EPS, target structural EPS, and have the highest yield compared to other extraction conditions. Using these extraction conditions, the Netherlands developed the world's first two demonstration-scale facilities to extract EPS from Nereda® granules, marketed under the name "Kaumera."

As shown in **Figure 1-2**, the EPS demonstration-scale installations in Epe and Zutphen have a buffer tank where there is a constant flow of Nereda® surplus sludge (granules and flocs) to the extraction installation, followed by a gravity thickener. Steam injections (as in Epe) or heat exchangers (as in Zutphen) are used to introduce heat into the thickened sludge that ends up in the alkaline reactor. The sludge in the

reactor is continuously mixed while heating. Once the sludge in the reactor has reached a temperature of about 80 - 90 °C, potassium hydroxide (KOH) is dosed into the reactor until a pre-set pH is reached (9-11). Hereafter the content of the reactor will continue to be mixed for around 2 hours. From the reactor, the sludge is pumped to a decanter centrifuge separation unit where the alkaline sludge pellet is separated from the alkaline centrate containing solubilized EPS. After the alkaline centrate is cooled down to a temperature of 15-30°C, hydrochloric acid (HCl) is dosed until a pH (2-3) is reached. The acidified alkaline centrate is pumped into a disc centrifuge where the precipitated EPS is separated. The produced EPS is stored in IBCs and can be picked up for processing and application. The acidic centrate is collected and returned to the WWTP to be combined with the wastewater influent. EPS extracted from aerobic granular sludge has diverse applications across agriculture, construction, textiles, and the paper industry (E. van der Knaap et al., 2019; Henze et al., 2020). Additionally, it exhibits distinctive properties as a composite material, bio-stimulant, and flame retardant (Kim et al., 2020; Y. M. Lin et al., 2015).

1.2.2 Integrative EPS and Phosphorus Recovery

In aerobic granular sludge systems, the phosphorus present in the wastewater influent is removed by storage of polyphosphate in the PAOs. Under anaerobic conditions, the PAOs take up VFAs forming intercellular PHA while hydrolyzing polyphosphate for energy production. This leads to phosphate being released into the bulk liquid. In the aerobic phase following the anaerobic feeding phase, the reactor is

aerated to allow microorganism growth. Oxygen allows the PAOs and GAOs to start consuming the anaerobically stored PHA for growth and PAOs to replenish the polyphosphate pool removing the phosphate from the bulk liquid that is eventually removed from the reactor in the spill sludge (Pronk et al., 2020). The EPS extraction conditions explained in section 1.2.1 include extreme pH and temperature that could change the speciation or the mineralogy of phosphorus present in sludge providing opportunities for a multidisciplinary resource recovery process.

Let's first get an overview of why phosphorus recovery is important, how can we recover phosphorus (mineral precipitates versus higher-value products), and later, how the integration of EPS and phosphorus has led to innovative research directions that could potentially maximize the value of both EPS and phosphorus recovered from WWTPs as shown in **this thesis.**

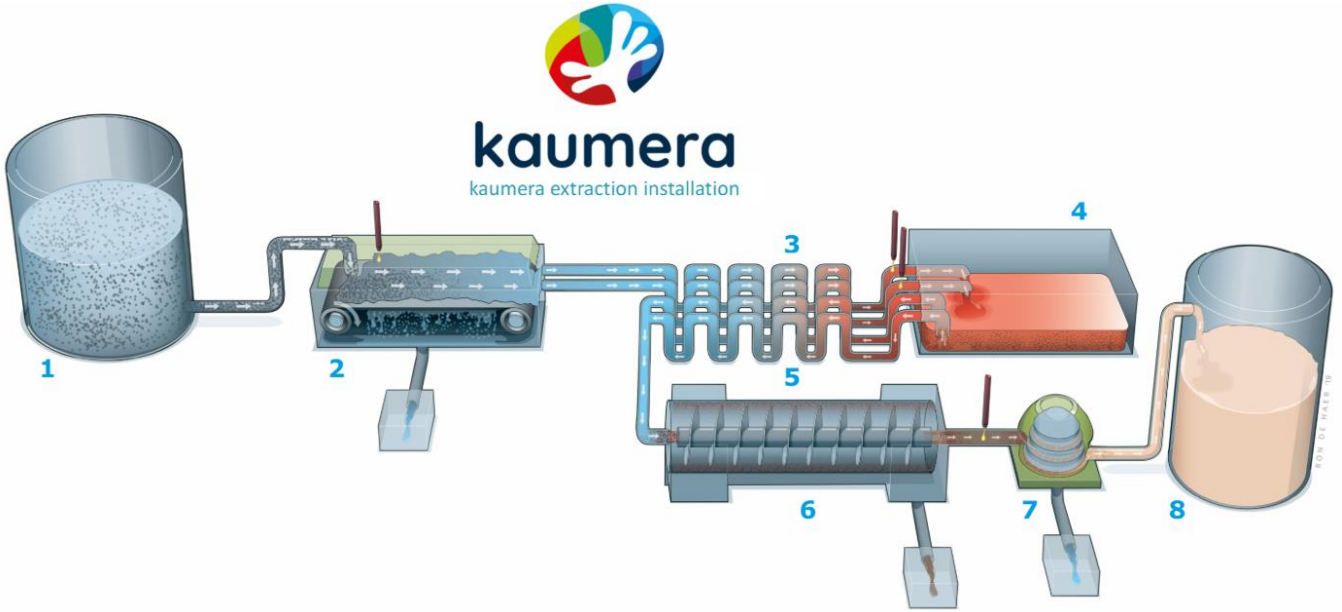

Figure 1-2: **:** EPS extraction process in demonstration-scale installations (Kaumera.com, 2024) : 1) Buffer tank, 2) sludge thickener, 3)& 5) heat exchangers, 4) alkaline reactor, 6) decant centrifuge, 7) disc centrifuge and 8) EPS storage silo

1.3 Phosphorus

1.3.1 Mined P rock

Around 95% of the mined phosphate rock is used as fertilizers (Jupp et al., 2021; Van Vuuren et al., 2010). Fertilization is an essential part of modern agriculture to increase the food needed to match the growing population, and phosphorus is an essential element in those fertilizers. The rest of the mined phosphorus is used in the industrial sector. There are two routes to process phosphate rock to meet our demands both in the fertilization and industrial sectors (de Boer et al., 2018) as shown in **Figure 1-3**:

1) "Wet acid route": phosphate rock is reacted with strong acids (usually sulfuric acid) to produce phosphoric acid (called Merchant Grade Acid (MGA)) that contains various impurities depending on the origin of the phosphate rock, e.g., iron, aluminum, potassium, fluorides, cadmium. Approximately 98% of phosphate rock is processed through this wet acid route, with around 95% being used in the fertilization industry and as animal feed. The remaining 3% is utilized in various other industries, such as for detergents, industrial-grade phosphoric acid for metal treatment, and the production of industrial inorganic phosphates, which often require additional purification of the phosphoric acid (ESPP webinar, 2020; Jupp et al., 2021).
2) "Thermal route": It involves producing elemental phosphorus (P_4, or white phosphorus) from phosphate rock in furnaces at temperatures ranging from 1500 to 1700 °C, with coke serving

as a reducing agent. This process accounts for approximately 2% of global phosphate rock usage (Scholz et al., 2014) . Currently, P_4 production is concentrated in just four countries: the USA, China, Kazakhstan, and Vietnam (de Boer et al., 2018; ESPP webinar, 2020). There is no P_4 production in Europe anymore, and Europe is dependent on these four countries for both P_4 and P_4 derivatives. This process is energy and cost-intensive but necessary to make flame retardants, lubricants, lithium-ion batteries, food additives, catalyst materials, herbicides, and to produce specific grades of polyphosphoric acid. These industries' demand must (and can only) be produced via the thermal route and requires P_4 production for these reasons: 1) to produce extremely pure P_4 product, with almost no impurities that reacts with oxygen and water to produce extremely pure phosphoric acid (called thermal acid) which is not possible to be produced by purifying wet-acid MGA, 2) to make compounds in which the P atom oxidation state is not (+5), e.g., most organophosphorus chemicals, phosphonates (+3), phosphites (+3), hypophosphites (+1), phosphine (-3), phosphine oxides (-1) phosphides (-3), 4) to make compounds in which the P atom is not surrounded by four oxygens e.g., $LiPF_6$, (used in batteries), 5) for some applications of phosphorus chemicals which require very low water content. For example, ammonium polyphosphate (APP), is a common flame retardant, can be manufactured from phosphoric acid using the wet acid route (MGA). However, achieving the extremely low water content required for

many flame-retardant applications, particularly in plastics and electrical components, is not industrially feasible through this route (Bulk inside.com, 2024; ESPP webinar, 2020). Therefore, plastics-grade APP is produced using derivatives of P_4, while APP for other uses, such as in wood products, is made from phosphoric acid (ESPP webinar, 2020). Organophosphorus compounds, which include molecules with P-C and P-O-C bonds, are utilized in flame retardants, metal extractants, pesticides, and various other applications. Most of these compounds are produced using phosphorus trichloride (PCl_3) with P oxidation state (+3), which is obtained from the direct chlorination of white phosphorus.

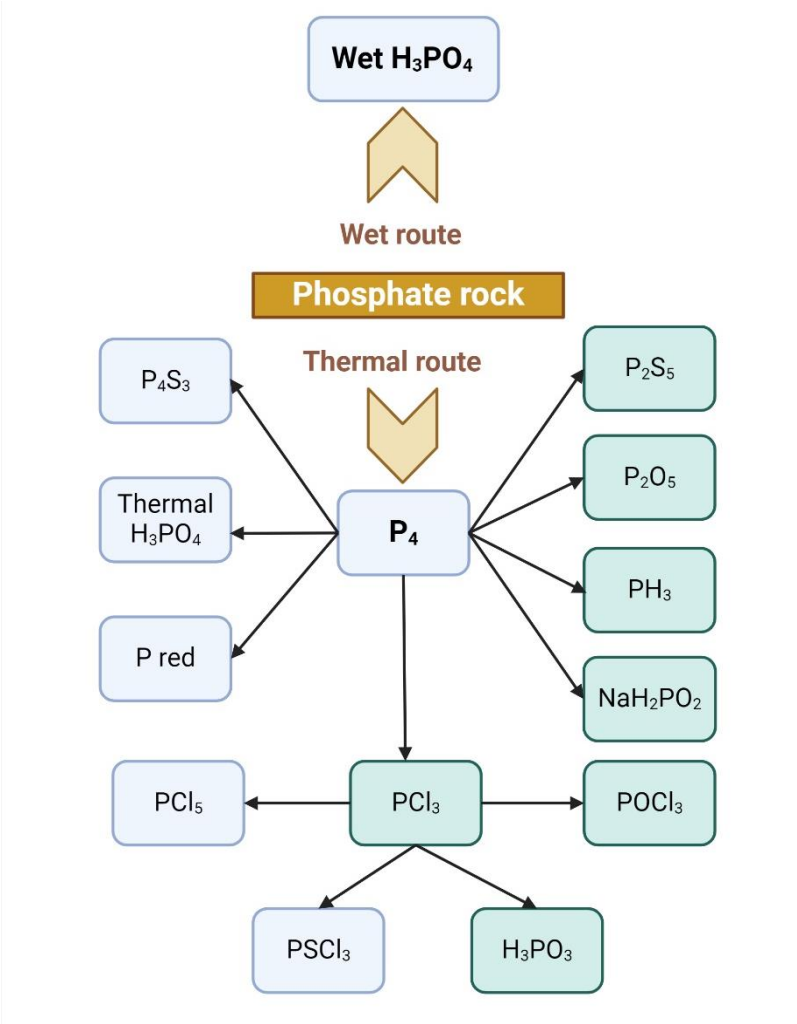

Figure 1-3: P rock processing via wet and thermal routes with precursors to organophosphorus compounds highlighted (adapted from ((Jupp et al., 2021))

1.3.2 Phosphorus Recovery- Mineral P Precipitates

There are different arguments when it comes to the topic of phosphorus recovery. P rock mining is environmentally unfriendly as it releases heavy metals that pollute soil, air, and water (Cordell & White, 2015; El Zrelli et al., 2018). Phosphorus release to the environment is harmful due to eutrophication issues and ecosystem loss. Another argument is that phosphorus is a non-renewable resource that is concentrated in specific locations in the world so alternatives to the P rock need to be found (European Commission, 2014). Concentrated streams are a pivotal factor in advancing phosphorus recovery, facilitating both efficient and economic recovery. For example, the phosphorus content in wastewater, constituting 15% of the total imported phosphorus in Europe, highlights the significance of urban wastewater as a phosphorus hotspot (Cordell et al., 2009; van Dijk et al., 2016). Precipitation is the most common way to recover phosphorus from wastewater by the addition of metal salts. There are opportunities to recover phosphorus from WWTPs from three main phases and e.g.,

1) From aqueous phase:

The concentrated side streams of enhanced biological phosphorus removal (EBPR) sludge anaerobic digesters are ideal for phosphorus recovery by precipitation as struvite or calcium phosphate e.g., Ostara, Nuresys, Phospaq, Struvia, Phosphogreen processes. Struvite is the most common recovery product from the aqueous phase (Kabbe Christian, 2019). However, it has low efficiency as recovery is typically only 10–30%

of the total influent phosphorus load (Cornel & Schaum, 2009; Hermann, 2009) due to the presence of phosphorus fractions that are not extracted during anaerobic digestion (phosphorus fixed in biomass or bound to metals like iron) (Wilfert et al., 2015). That is why the recovery from chemical phosphorus removal systems (CPR) is very limited. Recovering phosphorus as vivianite precipitation from the aqueous phase is another promising technology, though it is still at the pilot scale (Priambodo et al., 2017).

2) From sludge:

Crystallization in a sludge environment heightens the likelihood of contaminants incorporation into the final product but vivianite was found to be a major iron phosphate species in the sludge from CPR systems. It could be separated and recovered from digested sludge thanks to its paramagnetic properties (Wilfert et al., 2016). 60% of the phosphorus present in the influent wastewater could be recovered as vivianite (Prot, 2021). Other recovery methods involve wet-chemical treatments with mineral acids followed by precipitation or thermochemical processes as hydrothermal treatment, pyrolysis or gasification, however, these processes have not seen widespread yet as precipitation technologies.

3) From incinerated sludge ash:

Phosphorus recovery from ash has several advantages as nearly all phosphorus removed can be recovered, unwanted pathogens

and pollutants are destroyed, and the phosphorus remains in a concentrated form. Incineration increases the phosphorus concentration to approximately 10% of the solids, compared to 2-3% in dewatered sludge solids (Kabbe. C, 2019). Then, phosphorus is leached from the ashes by acidic treatment, and phosphorus is recovered as phosphoric acid e.g., Tetraphos and Susphos (Egle et al., 2016; ESPP, 2023), or precipitated as mono/di-ammonium phosphates or mono/di-calcium phosphates e.g., Easymining process. There are also some thermochemical developments e.g., AshDec process that involves magnesium or potassium salts addition to ash at elevated temperatures producing $CaKPO_4$ and $CaNaPO_4$ (Adam et al., 2009; Desmidt et al., 2015; Jupp et al., 2021).

To integrate phosphorus recovery technologies into the EPS extraction process, we need to determine which phase contains the highest P concentrations to select the appropriate recovery technology. Since the distribution of phosphorus in terms of loads and concentrations along the EPS extraction process was previously unknown, **this thesis chapter (2)** investigates it for the first time. The study found that the acidic waste stream had the highest P load, primarily in the form of orthophosphates. Orthophosphate precipitates in the aqueous phase, typically with magnesium, calcium, and iron, forming struvite, calcium phosphates, and vivianite, as explained earlier in this section. This process requires neutral to alkaline pH conditions due to the high solubility of these precipitates under low pH conditions (Cichy et al., 2019; Thant Zin & Kim, 2019). This makes phosphorus recovery from acidic

phosphorus-rich streams challenging due to the need for intensive chemical dosing to adjust the pH. In **this thesis chapter (3)**, we developed and patented a new technology to precipitate phosphorus in acidic waste streams as strengite ($FePO_4.2H_2O$), inspired by natural acidic soils. This technology can potentially be integrated into the acidic by-product stream from the EPS extraction process, integrating EPS and phosphorus recovery. And it could also be used for other streams such as acid leaching of sludge ash and industrial wastewater from cheese production, semiconductors and LCD manufacturing and others (Martin et al., 2020; Priambodo et al., 2017; Lei et al., 2022).

1.3.3 Phosphorus recovery- Higher value P Products

Traditional commercial fertilizer costs are 1.6 €/kg P, whereas the cost of recovering phosphorus from wastewater is estimated at 2 €/kg P, potentially rising to 8 €/kg P under certain conditions (Witek-Krowiak et al., 2022; Xu et al., 2023; Egle et al., 2015). Thus, recovering P products typically used as fertilizers, such as struvite and calcium phosphates, is not particularly encouraging from an economic standpoint. Horstink et al., 2021 estimated the price of P_4 to be roughly €2.9/kg P. The cost of P_4-derived chemicals will be higher since they need to be made from P_4 or PCl_3 as explained in section 1.3.1. This suggests that recovering P from WWTPs as products with functions similar to P_4-derived products would have a higher value compared to recovering P as fertilizers. Recovering these products from sludge could upcycle and produce high-value P products, reducing Europe's dependency on importing P_4 and synthesizing its derivatives. However, even with the higher value of

these P recovery products functioning as P_4 derivatives, recovery costs might still not be fully covered, emphasizing the need to target higher-value products while also reducing costs.

Several companies have investigated the process of producing P_4 from waste products. For example, Thermphos developed a method to produce P_4 from sewage sludge ashes and, together with Slibverwerking Noord-Brabant (SNB), used iron-poor sewage sludge ash as a feedstock for the P_4 process. They performed several tests over several years until Thermphos ended their operations (Schipper & Korving, 2008). The RecoPhos technology, developed in 2014 to produce P_4 from sewage sludge ashes, has remained in the piloting phase since then (ESPP webinar, 2020; de Boer et al., 2018). Spodofos is another new process, developed in 2021 to produce P_4 from ashes, and further scaling up through lab and pilot research is currently being explored (Horstink et al., 2021).

Towards the goal of recovering high-value phosphorus products, in this thesis, we investigate innovative phosphorus recovery pathways and the potential to produce high-value recovery products through the unique integration of phosphorus and EPS. By leveraging phosphorus chemistry, EPS can substitute for some P_4 derivatives.

1.4 Innovative Integration of Phosphorus and EPS for High-Value Product Development

The manifold of P chemistry in extracted EPS lays the foundation for leveraging the incorporated P to manipulate EPS properties and enhance its industrial applications. It could also potentially substitute some derivatives of P_4 required for industries e.g., organophosphorus compounds production from P rock to make flame retardants.

Earlier studies have shown that a significant amount of phosphorus is recovered within extracted EPS (Zhang et al., 2013; Zeng et al., 2019). Since P is an intrinsic part of EPS and could potentially influence its properties and industrial applications, understanding the speciation of P in EPS and how P species change during the EPS extraction process is revealed for the first time in **this thesis chapter (4)**. This knowledge is crucial for comprehending the relevance of P species to EPS properties and for exploring the possibility of manipulating P chemistry during the extraction process to enrich specific P species.

In this thesis, we will show that the class of P species (such as phosphate esters) detected in EPS are also widely used in the chemical industry to enhance properties such as thermal stability, viscoelasticity, emulsification, and water-holding capacity in natural and petroleum-derived polymers. For instance, chemical phosphorylation of polyesters and cotton in textiles to form P-O-C bonds is employed to impart flame resistance (Liang et al., 2013; Salmeia et al., 2016). Despite these potential applications, the knowledge of how P chemistry could influence

EPS properties is currently lacking in the EPS domain, hindering the full utilization of P in EPS. Therefore, in **this thesis chapter (5)**, we discussed how P could impact EPS properties based on an extensive review of experiences from other industries and patented a process design concept on how these P species could be influenced during the EPS extraction process or in WWTPs to engineer EPS properties. Based on this knowledge, we also give recommendations for a new research direction that could shape the future of P and EPS recovery from WWTPs.

1.5 Thesis Outline

Chapter 2: **"Integrated Resource Recovery from Aerobic Granular Sludge"** evaluated the potential of combined phosphorus, EPS, bio-methane, and nitrogen recovery from AGS WWTPs. The foundation of the interesting phosphorus-containing streams was set to be tackled in the rest of the thesis chapters. Results showed that around 60% of the total phosphorus load to AGS WWTP can be recovered:

1) 30% from the acidic liquid by-product stream (tackled in **this thesis chapter 3)**

2) 20% ends in the EPS final product (tackled in **this thesis chapters 4 and 5**)

3) 10% in the liquid fraction of the digested pellet byproduct from the extraction process (future research on alkaline pellet digestion to produce biomethane).

Chapter 3: **"$FePO_4.2H_2O$ Recovery from Acidic Waste Streams"** focuses on recovering the phosphorus that ends in the acidic liquid by-product stream of the EPS extraction process. The acidic by-product stream contains 30% of the TP load of WWTPs and around 95% of this TP is present as free orthophosphates. Inspired by acidic soils literature, strengite ($FePO_4.2H_2O$) chemical precipitation was evaluated on synthetic and real wastewater from EPS extraction, and a method to make quick settleable structures was developed without using crystallizers.

Chapter 4: "Phosphorus Speciation in Extracellular Polymeric Substances extracted from Aerobic Granular Sludge" aimed to reveal the different phosphorus species present in EPS. No research has been reported on P speciation in EPS extracted using the extraction conditions used for extracting EPS from AGS in the two demonstration-scale extraction installations in Zutphen and Epe in the Netherlands. No information was known about how P species change along the EPS extraction process and if this process selects for any specific P species. Creating knowledge was a necessary step toward the goal of EPS engineering. Additionally, a standard protocol to measure P species consistently in EPS samples was developed.

Chapter 5: "Impact of Phosphorus on the Functional Properties of Extracellular Polymeric Substances Recovered from Sludge" aimed to review different industrial polymeric contexts in which P chemistry is used to influence polymers properties and translate the P knowledge from these different fields to EPS. This knowledge helps predict the properties of EPS based on quantifying and characterizing its different phosphorus species. This review also sheds light on the potential of EPS engineering by enriching certain phosphorus species to substitute some P_4 derivatives. It also highlights the research gaps that need to be addressed in future work towards the goal of EPS engineering via P interplay.

Chapter 6: General Discussions and Outlook

References

Adam, C., Peplinski, B., Michaelis, M., Kley, G., & Simon, F. G. (2009). Thermochemical treatment of sewage sludge ashes for phosphorus recovery. Waste Management, 29(3). https://doi.org/10.1016/j.wasman.2008.09.011

Bachmann, N. (2015). Sustainable biogas production in municipal wastewater treatment plants. IEA Bioenergy.

Beun, J. J., Van Loosdrecht, M. C. M., & Heijnen, J. J. (2002). Aerobic granulation in a sequencing batch airlift reactor. Water Research, 36(3). https://doi.org/10.1016/S0043-1354(01)00250-0

Bulk inside.com. (2024). High-Temperature Drying of Flame Retardants in Industrial Scale. https://bulkinside.com/high-temperature-drying-of-flame-retardants-in-industrial-scale/

Cichy, B., Kużdżał, E., & Krztoń, H. (2019). Phosphorus recovery from acidic wastewater by hydroxyapatite precipitation. Journal of Environmental Management, 232. https://doi.org/10.1016/j.jenvman.2018.11.072

Cordell, D., Drangert, J. O., & White, S. (2009). The story of phosphorus: Global food security and food for thought. Global Environmental Change, 19(2). https://doi.org/10.1016/j.gloenvcha.2008.10.009

Cordell, D., & White, S. (2015). Tracking phosphorus security: indicators of phosphorus vulnerability in the global food system. Food Security, 7(2). https://doi.org/10.1007/s12571-015-0442-0

Cornel, P., & Schaum, C. (2009). Phosphorus recovery from wastewater: Needs, technologies and costs. Water Science and Technology, 59(6). https://doi.org/10.2166/wst.2009.045

de Boer, M. A., Wolzak, L., & Slootweg, J. C. (2018). Phosphorus: Reserves, production, and applications. In Phosphorus Recovery and Recycling. https://doi.org/10.1007/978-981-10-8031-9_5

de Bruin, L. M. M., de Kreuk, M. K., van der Roest, H. F. R., Uijterlinde, C., & van Loosdrecht, M. C. M. (2004). Aerobic granular sludge technology: An alternative to activated sludge? Water Science and Technology, 49(11–12). https://doi.org/10.2166/wst.2004.0790

de Kreuk, M. K., & van Loosdrecht, M. C. M. (2004). Selection of slow growing organisms as a means for improving aerobic granular sludge stability. Water Science and Technology, 49(11–12). https://doi.org/10.2166/wst.2004.0792

Desmidt, E., Ghyselbrecht, K., Zhang, Y., Pinoy, L., Van Der Bruggen, B., Verstraete, W., Rabaey, K., & Meesschaert, B. (2015). Global phosphorus scarcity and full-scale P-recovery techniques: A review. Critical Reviews in Environmental Science and Technology, 45(4). https://doi.org/10.1080/10643389.2013.866531

E. van der Knaap, E. Koornneef, K. L., M. Oosterhuis, P. Roeleveld, & M. Schaafsma. (2019). Kaumera Nereda gum: samenvatting NAOP onderzoeken 2013-2018,2019. Retrieved February 18, 2020, from http://edepot.wur.nl/501893

Egle, L., Rechberger, H., Krampe, J., & Zessner, M. (2016). Phosphorus recovery from municipal wastewater: An integrated comparative technological, environmental and economic assessment of P recovery technologies. Science of the Total Environment, 571. https://doi.org/10.1016/j.scitotenv.2016.07.019

Egle, L., Rechberger, H., & Zessner, M. (2015). Overview and description of technologies for recovering phosphorus from municipal wastewater. Resources, Conservation and Recycling, 105. https://doi.org/10.1016/j.resconrec.2015.09.016

El Zrelli, R., Rabaoui, L., Daghbouj, N., Abda, H., Castet, S., Josse, C., van Beek, P., Souhaut, M., Michel, S., Bejaoui, N., & Courjault-Radé, P. (2018). Characterization of phosphate rock and phosphogypsum from Gabes phosphate fertilizer factories (SE Tunisia): high mining potential and implications for environmental protection. Environmental Science and Pollution Research, 25(15). https://doi.org/10.1007/s11356-018-1648-4

ESPP. (2023). ESPP – DPP – NNP phosphorus recovery technology catalogue. https://phosphorusplatform.eu/images/download/ESPP-NNP-DPP_nutrient-recovery_tech_catalogue_v9_6_22.pdf

ESPP webinar. (2020). Summary of joint European Commission-ESPP webinar on P4 (phosphorus) Critical Raw Material. www.phosphorusplatform.eu

European Commission. (2014). Report on Critical Raw Materials for the Eu Critical Raw Materials Profiles. Report of the Ad Hoc Working Group on Defining Critical Raw Materials, May 2014.

Felz, S., Al-Zuhairy, S., Aarstad, O. A., van Loosdrecht, M. C. M., & Lin, Y. M. (2016). Extraction of structural extracellular polymeric substances from aerobic granular sludge. Journal of Visualized Experiments, 2016(115). https://doi.org/10.3791/54534

Felz, S., Vermeulen, P., van Loosdrecht, M. C. M., & Lin, Y. M. (2019). Chemical characterization methods for the analysis of structural extracellular

polymeric substances (EPS). Water Research, 157. https://doi.org/10.1016/j.watres.2019.03.068

Hermann, L. (2009). Rückgewinnung von Phosphor aus der Abwasserreinigung- Eine Bestandsaufnahme. Um.

Horstink, F., Keursten, R., Adamczyk Doradztwo, S., Odegard, I., Uijttewaal, M., de Koning, J., & Korving, L. (2021). SPODOFOS: WITTE FOSFOR PRODUCTIE UIT SLIBVERBRANDINGSASSEN. https://www.stowa.nl/publicaties/spodofos-witte-fosforproductie-uit-slibverbrandingsassen-eerste-evaluatie-van-de

Jupp, A. R., Beijer, S., Narain, G. C., Schipper, W., & Slootweg, J. C. (2021). Phosphorus recovery and recycling-closing the loop. In Chemical Society Reviews (Vol. 50, Issue 1). https://doi.org/10.1039/d0cs01150a

Kabbe Christian. (2019). Global Compendium on Phosphorus Recovery from Sewage/Sludge/Ash Lead Agent: Kompetenzzentrum Wasser Berlin (Germany) and P-REX® Environment (Germany). https://www.vesiyhdistys.fi/wp-content/uploads/2019/12/GWRCPhosphorusCompendiumFinalReport2019-March-20.pdf

Kaumera.com. (2024). Kaumera Extraction Installation. https://kaumera.com/publish/pages/7655/kaumera_extraction_installation_a3_en.pdf

Kehrein, P., Van Loosdrecht, M., Osseweijer, P., & Posada, J. (2020). Exploring resource recovery potentials for the aerobic granular sludge process by mass and energy balances-energy, biopolymer and phosphorous recovery from municipal wastewater. Environmental Science: Water Research and Technology, 6(8). https://doi.org/10.1039/d0ew00310g

Kim, N. K., Mao, N., Lin, R., Bhattacharyya, D., van Loosdrecht, M. C. M., & Lin, Y. (2020). Flame retardant property of flax fabrics coated by extracellular polymeric substances recovered from both activated sludge and aerobic granular sludge. Water Research, 170. https://doi.org/10.1016/j.watres.2019.115344

Lei, Y., Zhan, Z., Saakes, M., van der Weijden, R. D., & Buisman, C. J. N. (2022). Electrochemical Recovery of Phosphorus from Acidic Cheese Wastewater: Feasibility, Quality of Products, and Comparison with Chemical Precipitation. ACS ES and T Water, 1(4). https://doi.org/10.1021/acsestwater.0c00263

Liang, S., Neisius, N. M., & Gaan, S. (2013). Recent developments in flame retardant polymeric coatings. In Progress in Organic Coatings (Vol. 76, Issue 11). https://doi.org/10.1016/j.porgcoat.2013.07.014

Lin, Y., de Kreuk, M., van Loosdrecht, M. C. M., & Adin, A. (2010). Characterization of alginate-like exopolysaccharides isolated from aerobic granular sludge in pilot-plant. Water Research, 44(11). https://doi.org/10.1016/j.watres.2010.03.019

Lin, Y. M., Nierop, K. G. J., Girbal-Neuhauser, E., Adriaanse, M., & van Loosdrecht, M. C. M. (2015). Sustainable polysaccharide-based biomaterial recovered from waste aerobic granular sludge as a surface coating material. Sustainable Materials and Technologies, 4. https://doi.org/10.1016/j.susmat.2015.06.002

Martin, N., Ya, V., Leewiboonsilp, N., Choo, K. H., Noophan, P. (Lek), & Li, C. W. (2020). Electrochemical crystallization for phosphate recovery from an electronic industry wastewater effluent using sacrificial iron anodes. Journal of Cleaner Production, 276. https://doi.org/10.1016/j.jclepro.2020.124234

Morgan-Sagastume, F., Valentino, F., Hjort, M., Cirne, D., Karabegovic, L., Gerardin, F., Johansson, P., Karlsson, A., Magnusson, P., Alexandersson, T., Bengtsson, S., Majone, M., & Werker, A. (2014). Polyhydroxyalkanoate (PHA) production from sludge and municipal wastewater treatment. Water Science and Technology, 69(1). https://doi.org/10.2166/wst.2013.643

Nancarrow, B. E., Leviston, Z., Po, M., Porter, N. B., & Tucker, D. I. (2008). What drives communities' decisions and behaviours in the reuse of wastewater. Water Science and Technology, 57(4). https://doi.org/10.2166/wst.2008.160

Priambodo, R., Shih, Y. J., & Huang, Y. H. (2017). Phosphorus recovery as ferrous phosphate (vivianite) from wastewater produced in manufacture of thin film transistor-liquid crystal displays (TFT-LCD) by a fluidized bed crystallizer (FBC). RSC Advances, 7(65). https://doi.org/10.1039/c7ra06308c

Pronk, M., Neu, T. R., van Loosdrecht, M. C. M., & Lin, Y. M. (2017). The acid soluble extracellular polymeric substance of aerobic granular sludge dominated by Defluviicoccus sp. Water Research, 122. https://doi.org/10.1016/j.watres.2017.05.068

Pronk, M., van Dijk, E. J. H., & van Loosdrecht, M. C. M. (2020). Aerobic granular sludge. In Biological Wastewater Treatment: Principles, Modeling and Design (2nd ed.). https://doi.org/10.2166/9781789060362

Prot, T. (2021). Phosphorus recovery from iron-coagulated sewage sludge. In TU Delft University.

Rodríguez Arredondo, M., Kuntke, P., Jeremiasse, A. W., Sleutels, T. H. J. A., Buisman, C. J. N., & Ter Heijne, A. (2015). Bioelectrochemical systems for nitrogen removal and recovery from wastewater. In Environmental

Science: Water Research and Technology (Vol. 1, Issue 1). https://doi.org/10.1039/c4ew00066h

Salmeia, K. A., Gaan, S., & Malucelli, G. (2016). Recent advances for flame retardancy of textiles based on phosphorus chemistry. Polymers, 8(9). https://doi.org/10.3390/polym8090319

Schipper, W., & Korving, L. (2008). Full-scale plant test using sewage sludge ash as raw material for phosphorus production.

International Conference on Nutrient Recovery from Wastewater Streams. https://www.researchgate.net/publication/270510294_Full-scale_plant_test_using_sewage_sludge_ash_as_raw_material_for_phosphorus_production

Scholz, R. W., Roy, A. H., Hellums, D. T., Ulrich, A. E., & Brand, F. S. (2014). Sustainable phosphorus management: A global transdisciplinary roadmap. In Sustainable Phosphorus Management: A Global Transdisciplinary Roadmap. https://doi.org/10.1007/978-94-007-7250-2

Seviour, T., Pijuan, M., Nicholson, T., Keller, J., & Yuan, Z. (2009). Understanding the properties of aerobic sludge granules as hydrogels. Biotechnology and Bioengineering, 102(5). https://doi.org/10.1002/bit.22164

Sheng, G. P., Yu, H. Q., & Li, X. Y. (2010). Extracellular polymeric substances (EPS) of microbial aggregates in biological wastewater treatment systems: A review. In Biotechnology Advances (Vol. 28, Issue 6). https://doi.org/10.1016/j.biotechadv.2010.08.001

Thant Zin, M. M., & Kim, D. J. (2019). Struvite production from food processing wastewater and incinerated sewage sludge ash as an alternative N and P source: Optimization of multiple resources recovery by response surface methodology. Process Safety and Environmental Protection, 126. https://doi.org/10.1016/j.psep.2019.04.018

van Dijk, K. C., Lesschen, J. P., & Oenema, O. (2016). Phosphorus flows and balances of the European Union Member States. Science of the Total Environment, 542. https://doi.org/10.1016/j.scitotenv.2015.08.048

Van Vuuren, D. P., Bouwman, A. F., & Beusen, A. H. W. (2010). Phosphorus demand for the 1970-2100 period: A scenario analysis of resource depletion. Global Environmental Change, 20(3). https://doi.org/10.1016/j.gloenvcha.2010.04.004

Velenturf, A. P. M., & Jopson, J. S. (2019). Making the business case for resource recovery. Science of the Total Environment, 648. https://doi.org/10.1016/j.scitotenv.2018.08.224

Werker, A., Bengtsson, S., Korving, L., Hjort, M., Anterrieu, S., Alexandersson, T., Johansson, P., Karlsson, A., Karabegovic, L., Magnusson, P., Morgan-Sagastume, F., Sijstermans, L., Tietema, M., Visser, C., Wypkema, E., Van Der Kooij, Y., Deeke, A., & Uijterlinde, C. (2018). Consistent production of high quality PHA using activated sludge harvested from full scale municipal wastewater treatment - PHARIO. Water Science and Technology, 78(11). https://doi.org/10.2166/wst.2018.502

Wilfert, P., Kumar, P. S., Korving, L., Witkamp, G. J., & Van Loosdrecht, M. C. M. (2015). The Relevance of Phosphorus and Iron Chemistry to the Recovery of Phosphorus from Wastewater: A Review. Environmental Science and Technology, 49(16). https://doi.org/10.1021/acs.est.5b00150

Wilfert, P., Mandalidis, A., Dugulan, A. I., Goubitz, K., Korving, L., Temmink, H., Witkamp, G. J., & Van Loosdrecht, M. C. M. (2016). Vivianite as an important iron phosphate precipitate in sewage treatment plants. Water Research, 104. https://doi.org/10.1016/j.watres.2016.08.032

Witek-Krowiak, A., Gorazda, K., Szopa, D., Trzaska, K., Moustakas, K., & Chojnacka, K. (2022). Phosphorus recovery from wastewater and bio-based waste: an overview. In Bioengineered (Vol. 13, Issue 5). https://doi.org/10.1080/21655979.2022.2077894

Xu, Y., Zhang, L., Chen, J., Liu, T., Li, N., Xu, J., Yin, W., Li, D., Zhang, Y., & Zhou, X. (2023). Phosphorus recovery from sewage sludge ash (SSA): An integrated technical, environmental and economic assessment of wet-chemical and thermochemical methods. In Journal of Environmental Management (Vol. 344). https://doi.org/10.1016/j.jenvman.2023.118691

Zhang, H. L., Fang, W., Wang, Y. P., Sheng, G. P., Zeng, R. J., Li, W. W., & Yu, H. Q. (2013). Phosphorus removal in an enhanced biological phosphorus removal process: Roles of extracellular polymeric substances. Environmental Science and Technology, 47(20). https://doi.org/10.1021/es403227p


15

Chapter 2

Integrated Resource Recovery from Aerobic Granular Sludge

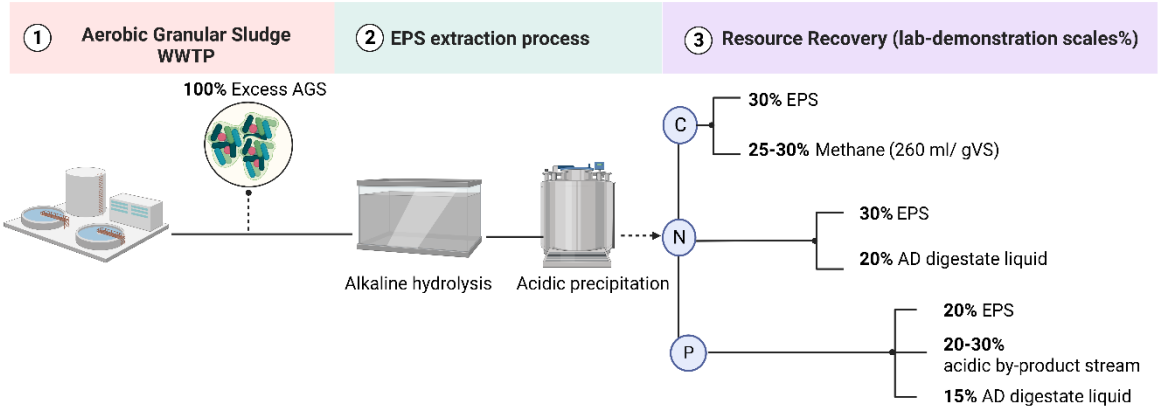

This chapter has been published as:

Bahgat, N. T., Wilfert, P., Korving, L., & van Loosdrecht, M. (2023). Integrated resource recovery from aerobic granular sludge plants. Water Research. https://doi.org/10.1016/j.watres.2023.119819

Abstract

The study evaluated the combined phosphorus, nitrogen, methane, and extracellular polymeric substances (EPS) recovery from aerobic granular sludge (AGS) wastewater treatment plants. About 30% of sludge organics are recovered as EPS and 25-30% as methane (≈260 ml methane/g VS) by integrating alkaline anaerobic digestion (AD). It was shown that 20% of excess sludge total phosphorus (TP) ends in the EPS. Further, 20-30% ends in an acidic liquid waste stream (≈600 mg PO_4-P/L), and 15% in the AD centrate (≈800 mg PO_4-P/L) as ortho-phosphates in both streams and is recoverable via chemical precipitation. 30% of sludge total nitrogen (TN) is recovered as organic nitrogen in the EPS. Ammonium recovery from the alkaline high-temperature liquid stream is attractive, but it is not feasible for existing large-scale technologies because of low ammonium concentration. However, ammonium concentration in the AD centrate was calculated to be 2600 mg NH_4-N/L and ≈20% of TN, making it feasible for recovery. The methodology used in this study consisted of three main steps. The first step was to develop a standard laboratory protocol mimicking demonstration-scale EPS extraction conditions. The second step was to establish mass balances over the EPS extraction process on laboratory and demonstration scales within a full-scale AGS WWTP. Finally, the feasibility of resource recovery was evaluated based on concentrations, loads, and integration of existing technologies for resource recovery.

2.1 Introduction

Wastewater is considered a valuable resource rather than a waste due to resource scarcity, market demand, and economic interests. Therefore, the transition of conventional wastewater plants into resource recovery plants has become of interest recently (van Loosdrecht & Brdjanovic, 2014). Wastewater provides opportunities to recover energy, biosolids, reusable water, and other valuable nutrients such as nitrogen, phosphorus, and other elements (Kehrein, van Loosdrecht, Osseweijer, Garfí et al., 2020; Hao et al., 2019).

A Dutch public-private partnership led to the development of the full-scale aerobic granular sludge technology, also known as "Nereda technology" for wastewater treatment. Aerobic granular sludge (AGS) is a promising technology as it offers key advantages compared to conventional activated sludge technologies (Pronk et al., 2015; de Kreuk et al., 2005). These advantages include a 75% reduction in footprint, a 30% reduction in energy, and less operating costs associated with phosphorus removal. The study of AGS not only opened a door for a more resource-efficient wastewater treatment technology but also created new opportunities for resource recovery, with the recovery of extracellular polymeric substances (EPS) as a successful example (Y. Lin et al., 2018; Sam & Dulekgurgen, 2016; Seviour et al., 2009).

EPS is a polymeric gel material produced by bacteria during cell metabolism that consists of proteins, polysaccharides, DNA, lipids, glycoproteins, and humic substances that form the matrix in which the cells are immobilized as granular particles (Seviour et al., 2019). EPS from

aerobic granular sludge offers various applications in agriculture, building, textile, and paper industries (E. van der Knaap, 2019; Henze et al., 2020). It also showed unique properties as a composite material, biostimulant, and flame retardant (Kim et al., 2020a; Feng et al., 2019; Y. M. Lin et al., 2015). The Netherlands has the world's first two demonstration-scale installations to extract EPS from Nereda® granules under the product name Kaumera. The EPS extraction process involves elevated temperature and pH conditions to dissolve the biofilm matrix in granules and target structural EPS, as reported by Felz, 2019. EPS recovery introduces an innovative concept to valorize the COD instead of converting COD into energy. According to the bio-based recovery value pyramid, biomass should ideally be first delegated as a material (higher value) before it is delegated to final energetic use (lower value) (Stegmann et al., 2020). COD has a relatively large exergy content that should be preserved and converted into carbonaceous materials. Moreover, there has always been a perception that chemical energy is the only source of recoverable energy in wastewater; however, studies showed that the potential of thermal energy recovery is around ten times larger than chemical energy recovery as biogas (Hao, Li et al., 2019). For these reasons, it is argued that COD recovery should be in the form of materials (i.e., EPS) rather than energy. The EPS extraction process under elevated pH and temperature conditions might also offer recovery opportunities for other elements, such as phosphorus, nitrogen, or methane, which could create a new generation of AGS WWTPs with integrated resource recovery. However, EPS yield should not be affected

by resource recovery since it is likely the main driver for a recovery facility.

Phosphorus is on the list of critical raw materials issued by the EU because its supply security is at risk and its economic importance is high. Phosphorus is considered a bottleneck due to its life-essential nature and low abundance. Phosphorus recovery from wastewater is experiencing increased interest as sewage is one of the richest streams of phosphorus (Childers et al., 2011; ESPP webinar, 2020; Eynard et al., 2020). According to van Dijk et al., 2016, phosphorus in wastewater accounts for 15% of total imported phosphorus in Europe. In AGS WWTPs, phosphorus removal relies on phosphorus-accumulating organisms (PAOs) taking phosphate in wastewater as intracellular phosphorus during the alternation of anaerobic and aerobic phases in the Nereda tank (de Kreuk et al., 2005). High pH and temperature extraction conditions could potentially change phosphorus speciation or mineralogy in sludge, enabling or exacerbating recovery. Nitrogen is another essential nutrient found in wastewater. In AGS WWTP, ammonium-nitrogen is removed in the form of nitrogen gas through simultaneous nitrification and denitrification, and a small part of it ends in the sludge (de Kreuk et al., 2005; Henze et al., 2020). During the EPS extraction process, the AGS undergoes thermo-alkaline conditions, potentially releasing organic and inorganic nitrogen into the liquid streams (Siami et al., 2020; Toutian et al., 2020). Evaluating the nitrogen fate over the process is to be considered to assess its recovery potential. Anaerobic digestion could also be integrated into the EPS extraction process as a secondary technology to recover further COD as methane from the alkaline sludge

residuals by-product stream from the EPS extraction process. This integration is interesting as alkaline pre-treatment of sludge increases the anaerobic degradability of organics and biogas yields (Fang et al., 2014; Li et al., 2012). Evaluating the potential of phosphate and ammonium recovery from digestate liquid fraction is also to be considered as they are released during organics digestion (Uysal et al., 2010). Nitrogen and phosphorus recovery from the EPS extraction process by-product streams is also crucial to prevent operational issues due to their recirculation to the WWTP influent. Due to all these reasons, investigating the status of organics, phosphorus, and nitrogen over the EPS extraction process is of interest.

The fate of nutrients through the EPS extraction process is unknown. A careful analysis of the EPS production process is vital to identify the best synergies to combine these elements' recovery within the EPS extraction process. Mass balances can provide insight into how and what to expect from integrated recovery technologies to evaluate these synergies. They are a robust decision tool to estimate quantities of elements of interest in all relevant streams, recovery potential, make value chains, and evaluate market potential (Kehrein, van Loosdrecht, Osseweijer, & Posada, 2020; Solon et al., 2019). However, the existing laboratory-scale EPS extraction protocol by Felz et al., 2016 shows differences compared to large/demonstration-scale extractions which are relevant for resource recovery as summarized in **Table 2-1**. The most significant difference is the dilution factor during the extraction, as dilution affects concentrations and saturation conditions, so it does not allow for accurate judging of the potential of combined nutrient recovery. A

representative translation of large-scale conditions to laboratory scale is essential for a realistic evaluation of concentrations and quantities.

Therefore, this study involved the development of a modified standard laboratory protocol to simulate large/demonstration-scale conditions. This was crucial for conducting future experiments to test resource recovery technologies on sludge from various sources and seasons, and to make predictions about large-scale impacts in later stages. This study aims to set the foundation for a new generation of AGS WWTPs with integrated resource recovery by answering two main research questions. The first question relates to the recovery potential of combined phosphorus, nitrogen, EPS, and methane from AGS WWTP. So, mass balances were established on laboratory and demonstration scales EPS extractions and extrapolated to a full-scale Nereda AGS WWTP to address this question. The second question is about the possible existing technologies that can be applied to recover these elements to reach a fully integrated AGS WWTP. To address this, concentrations, stream composition, speciation of nutrients, and loads were used to qualitatively evaluate the feasibility of existing technologies.

2.2 Materials and Methods

2.2.1 Laboratory extractions

Laboratory extractions were performed using AGS surplus sludge samples collected after belt thickening from Epe AGS WWTP. The sludge samples are a mix of flocs and small granules, so-called "selection spill" which is the sludge removed after every cycle. Sludge samples had the following average composition: 5 %TS, 4.3 %VS, 30 g P/Kg TS, and 60 g N/Kg TS. Extractions were performed based on a newly developed modified protocol adapted from demonstration-scale practices in Epe and Zutphen. **Table 2-1** summarizes how the modified laboratory protocol mimics Zutphen/Epe demonstration-scale EPS extractions. The detailed laboratory protocol steps are listed in section (3) of the supplementary material.

2.2.2 Epe demonstration extractions

The resemblances and differences between the modified laboratory and Epe demonstration extractions were assessed in this study. Epe AGS WWTP is the first full-scale domestic wastewater treatment plant in the Netherlands to install the innovative Nereda sewage treatment technology, operated by the water authority Waterschap Vallei en Veluwe. The WWTP treats wastewater produced by the town of Epe with an average daily influent equal to 6200 m^3, and 37.167 p.e. At the time of this sampling campaign, the Nereda® reactors had a sludge concentration of 8 g MLSS/L and were operated with process cycles of approximately

Table 2-1: Differences between Felz et al., 2016 laboratory extraction, Epe&Zutphen demonstration extractions (other steps not mentioned in the table were similar), and the established new modified protocol

Parameters	**Original (diluted) laboratory protocol (Felz et al., 2016)**	**Epe/Zutphen demonstration scale practice**	**New modified (undiluted) laboratory protocol in this study**
Sludge used	Granules ≥2mm	Excess granular sludge (small granules +flocs)	Excess granular sludge (small granules +flocs)
Sludge concentration	<0.8 w/v%	5 w/v%	5 w/v%
Base used	0.5% (w/v) Sodium carbonate	25% (w/v) Potassium hydroxide	25% (w/v) Potassium hydroxide
Base addition	No pH control	pH-controlled 9-11	pH-controlled 9-11
Alkaline extraction	80°C, 30 minutes	80°C,2 hours	80°C, 2 hours
Acid used	1 M Hydrochloric acid-pH 2-4	9.5 M hydrochloric acid- pH 2-4	9.5 M hydrochloric acid- pH 2-4
Centrifugation	4 Celsius (4000xg, 20 mins)	30 Celsius -Decanter (3300xg, HRT= 5mins) -Disc (9000xg, HRT=1min)	30 Celsius (4000xg, 20 mins)
Mixing	- 400 rpm during alkaline extraction -100 rpm during acidification	-3 kW in the first two compartments of the alkaline reactor -0,55 kW in the acidification tank	-400 rpm during alkaline extraction -100 rpm during acidification

6 h: 3 h of aeration, 1 h of settling, and 2 h of anaerobic feeding/simultaneous effluent withdrawal (these data are site-specific and vary between different WWTPs). The excess sludge was stored in an aerated sludge buffer tank before being transported to the belt thickener in the EPS extraction installation. The EPS extraction installation in Epe is the second installation in the Netherlands. Before our investigation, many extraction runs had been performed at the site, and in general, extraction runs in the demonstration plant are for a few days only. Sampling for this study was performed on a continuous EPS extraction process treating 0.5 m^3 spill sludge/hour. KOH and HCl dosing rates were 11 and 7 L/ hour, respectively. 20th June 2021 was the starting day of the campaign to run the system and ensure steady-state conditions. Then, samples were collected two days after the start of the operational run. So, two-time samples were collected on the 22nd and 23rd of June 2021.

Figure 2-1 shows the process flow in Epe demonstration with sampling points:

- Stream B is the initial thickened sludge stream,
- D is the alkaline liquid stream containing the hydrolyzed EPS,
- G is the alkaline sludge residue stream that remains after EPS hydrolysis and separation,
- F is the EPS production stream,
- and H is the acidic liquid stream after EPS production and separation.

To confirm that our sampling days are representative, we compared results from our study with earlier results from Epe (E. van der Knaap, 2019) and other unpublished measurements performed by RHDHV as described in section (2) in the supplementary material in detail. This comparison showed that the measurements of 23rd June 2021 were more typical for the normal operation of the plant than the results of 22nd. On this first day, the operation of the alkaline centrifuge was different than normal. Therefore, we focus in the result section on the results of June 23rd. The results of the 22nd can be found in the supplemental information. The differences between the 22nd and 23rd are interesting and discussed in section 2.4.2..22.4.2.

Correspondingly, sludge samples from the 22nd and 23rd were collected to perform laboratory extractions as described in **Table 2-1** at a similar pH as Epe. For all laboratory and Epe demonstration-scale samples, measurements were done in triplets, and average values and their standard deviation were calculated.

2.2.3 Mass balance calculations

Regarding laboratory-scale mass balances, concentrations, masses, and volumes of different fractions were measured experimentally. Regarding demonstration-scale mass balances, concentrations were measured experimentally for collected samples. D, G, F, and H flow rates were calculated using measured concentrations instead of using flow meters data logger to ensure the accuracy of these flows using B (sludge feed) as the initial condition, as shown in section (1) of the supplementary material. Epe demonstration installation does not treat the full sludge

flow from Epe Nereda WWTP, but the results were extrapolated to give the effect if it would be full scale. The mass balances over Nereda WWTP were evaluated based on the 2021 one-year average flows and the composition of influent, effluent, and sludge data were collected from the plant database. The plant has the following average wastewater influent composition: 835 mg COD/L, 81 mg N/L, and 7.2 mg P/L, and a daily load of 4174 Kg COD/day, 497 kg N/day and 44 kg P/day. Sankey diagrams depicted mass flows, where flow sizes are proportional to the influent mass flow expressed in %.

2.2.4 Analysis

2.2.4..1 Total Solids (TS) and Volatile Solids (VS)

TS and VS were analyzed according to the Standard Methods for the Examination of Water and Wastewater (APHA, 1999).

2.2.4..2 Total Chemical Oxygen Demand and Total Nitrogen

Both TCOD and TN were measured using Hach Lange test kits, Hach Lange) to 170 Celsius, and then analyzed using a spectrophotometer (DR 3900 VIS spectral photometer, wavelength range 320-750 nm). Carbon and nitrogen fate through the EPS extraction process was further confirmed by analyzing total carbon and total nitrogen using an Elemental analyzer (Mettler Toledo, America).

2.2.4..3 Microwave digestion

All solid samples were destructed by microwave digestion to convert them to liquid analyses. Samples were digested in an Ethos Easy from Milestone with an SK-15 High-Pressure Rotor. Around 50 mg of solids

were put in a Teflon vessel in which 10 mL of ultrapure HNO_3 (64.5-70.5% from VWR Chemicals) was poured. The digester is set to reach 200 Celsius in 15 minutes, run at this temperature for 15 minutes, and cool down for 1 hour.

2.2.4..4 ICP-OES

The inorganic elemental composition was measured via Inductively Coupled Plasma (Perkin Elmer, type Optima 5300 DV) with an Optical Emission Spectroscopy as a detector. The device was equipped with an Autosampler, Perkin Elmer, type ESI-SC-4 DX fast, and the data were processed with the software Perkin Elmer WinLab32. The rinse and internal standard solutions were 2%HNO_3 and 10 mg/L of Yttrium.

2.2.4..5 IC

Liquid samples were pre-treated first by filtering the samples through 0.45 µm followed by 0.22 µm membrane filters before analysis. Anions and cations (free dissolved ions) were measured by Metrohm Compact ion chromatograph Flex 930. To confirm these measurements and to avoid small colloidal particles squeezed through the filters, ultrafiltration was used. Liquid samples were filtered using ultrafiltration centrifugal tubes with polyethersulfone (PES) members with a molecular weight cutoff (MWCO) of 3K (ThermoFisher, UK).

2.2.4..6 X-Ray diffraction (XRD)

Room-temperature dried samples were used for XRD analysis. The sample was filled in a 0.7 mm glass capillary and tamped so the solid settled. The capillaries were sealed with a burner and mounted in a

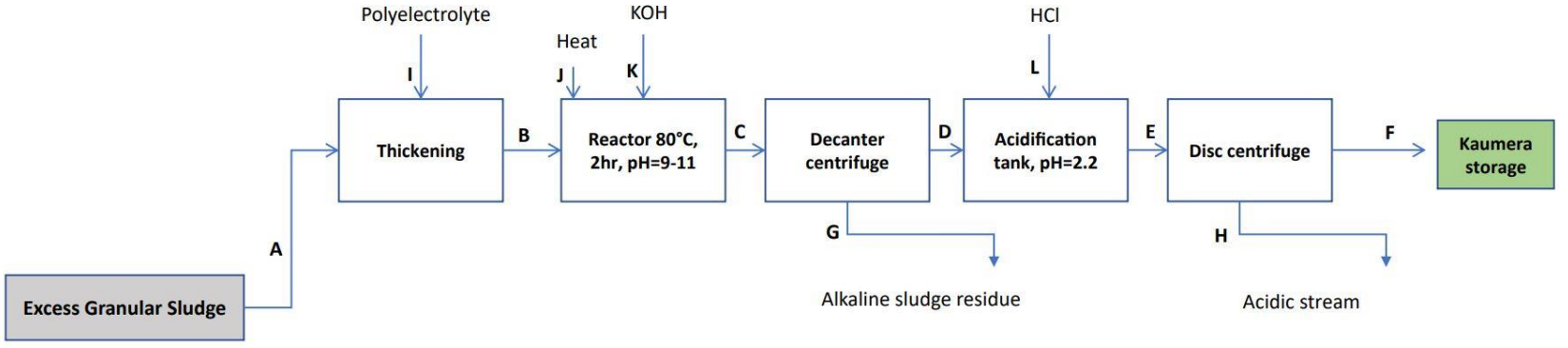

Figure 2-1: EPS extraction process from excess aerobic granular sludge in Epe installation

sample holder. The device used was a Bruker D8 Advance diffractometer with Cu Ka radiation (Coupled θ -2θ scan 10° - 110°, step size 0.030 ° 2θ, counting time per step 2 s). The data evaluation was performed using Burker software DiffracSuite.EVA vs. 6

2.3 Results

2.3.1 Concentrations in laboratory and Epe demonstration extractions

Table 2-2 shows the total solids, TCOD, total nitrogen, total phosphorus, and dissolved species relevant for nutrient recovery as phosphate, ammonium, calcium, and magnesium ions in the alkaline and acidic liquid streams.

Table *2-3* shows the EPS-Kaumera and alkaline sludge residue composition in laboratory and Epe extractions. Unlike the original laboratory protocol, the new modified laboratory protocol concentrations are comparable and have the same order of magnitude as the demonstration-scale concentrations. It was also observed that the concentrations of Ca^{2+} and Mg^{2+} in the alkaline stream are (6-10) times lower than in the acidic liquid stream both in the modified laboratory protocol and Epe demonstration scale, which could be due to the EPS nature as discussed, in section 2.4.4..2.

2.3.2 The appearance of an alkaline gel layer

After the thermal-alkaline hydrolysis step and centrifugation, there was a stratification of the granular matrix into a residue part (lower layer), a gel layer (middle layer), and a soluble layer (upper layer) shown in **Figure 2-2**. Despite the appearance of the alkaline gel layer, it was

observed that the Kaumera yield is ≈30% of TCOD (or volatile solids) of sludge both in the original (diluted) and modified (undiluted) laboratory extraction protocol when this alkaline gel layer is not included in the EPS soluble fraction. Understanding the fate of this alkaline gel layer in both laboratory and Epe demonstration scales is discussed in section 2.4.2. **Table 2-4** shows the average composition of this alkaline gel layer compared to the Kaumera-EPS on the laboratory scale. The gel layer has higher inorganic content than Kaumera as it has a higher P, Ca, and Fe content. XRD analysis also showed that the alkaline gel layer contains vivianite; however, no crystalline P-mineral was detected in Kaumera, which shows that P speciation in both fractions is different. The presence of vivianite can be explained by the fact that Fe precipitates in neutral to alkaline conditions, and there is always Fe in the raw sewage (Wilfert et al., 2015). There is also a slaughterhouse discharge to Epe WWTP, which contains most likely high levels of Fe. Spectra are shown in section (5) of the supplementary material.

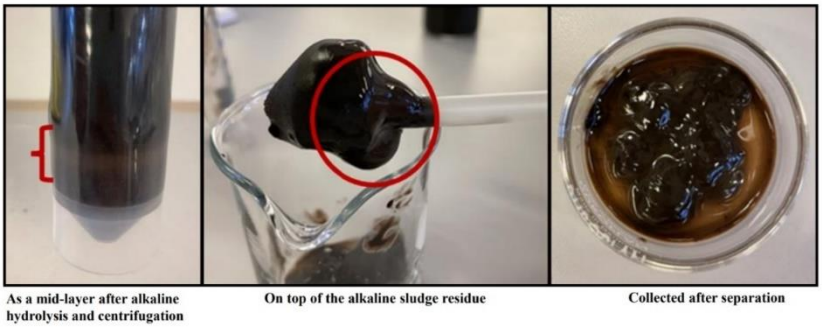

Figure 2-2: The alkaline gel appearance with the modified laboratory protocol

Table 2-2: Alkaline and acidic liquid streams concentrations comparison between laboratory protocols and Epe demonstration

	Original laboratory protocol		**Modified laboratory protocol**		**Epe demonstration-scale**	
	Alkaline stream	**Acidic stream**	**Alkaline stream**	**Acidic stream**	**Alkaline stream (D)**	**Acidic stream (H)**
TS%	0.7± 0.01	0.8 ± 0.10	3.4±0.03	1.9±0.05	3.5±0.04	1.9±0.05
			mg/L			
TP	94 ±0.5	71 ±0.4	879±6.0	680±7.0	960± 15	702 ±7.0
TN	339± 2.0	229 ±8.0	2230±160	1000± 3.0	2475 ±15	1248 ±5.0
TCOD	4600± 10	2400± 30	38000 ±500	11400 ±240	33000±1500	12400±30
PO_4^{3-}-P	40±0.6	48 ±0.3	615 ±3.0	630 ±2.6	572±8.0	604 ±10
NH_4^+-N	18 ±0.4	22 ±0.1	105 ±0.2	110 ±1.0	85 ±0.5	82 ±1.2
Ca^{2+}	13 ±0.3	6 ±0.1	35 ±0.8	204 ±8.0	30 ±0.5	267 ±1.9
Mg^{2+}	<5.00	6 ±0.1	10 ±1.0	105 ±0.8	11 ±0.2	110 ±0.8

Table 2-3: Alkaline sludge residue and Kaumera-EPS concentrations comparison between laboratory protocol and Epe demonstration

	Modified laboratory protocol		**Epe demonstration-scale**	
	Alkaline sludge residue	**Kaumera-EPS**	**Alkaline sludge residue (G)**	**Kaumera-EPS (F)**
TS%	9.7±0.1	8.3 ±0.7	8 ±0.1	8.6 ±0.1
		g/Kg TS		
TCOD	1170 ±70	1260 ±90	1210 ±20	1260± 20
TN	50± 1.0	65 ± 1.0	56± 2.0	70±4.0
TP	25 ±0.1	20± 0.2	23 ±0.1	23±0.2

Table 2-4: Average composition of Kaumera-EPS and alkaline gel layer in the laboratory extraction

	Alkaline Gel layer	Kaumera-EPS
g TCOD/ Kg TS	1260 ±25	1260±90
g TP/ Kg TS	30± 0.3	20±0.15
g TN/ Kg TS	65 ±2	65±0.6
g Ca/ Kg TS	12 ± 0.1	2.5±0.1
g Fe/ Kg TS	16± 0.2	5.6± 0.1

2.3.3 The potential of carbon recovery (laboratory scale extractions)

The TCOD mass balance over the EPS extraction using the modified laboratory protocol (undiluted) was established, as shown in **Figure 2-3a**. TCOD balances were confirmed by the fate of volatile solids along the process, data shown in Table S2-4 of the supplementary material. During the alkaline step, the high pH enriches the negative charges of the EPS, causing its repulsion and solubilization (Lotti et al., 2019), and around 40% of sludge TCOD ended in the alkaline liquid stream. Then, during the acidification step, the low pH reduces the negative charge of the EPS, causing its precipitation as a hydrogel with a yield of 30% of excess granular sludge TCOD. It was estimated that 35% of the initial COD was present in the alkaline gel layer, 25% in the alkaline sludge residue, and only 10% ended in the acidic liquid stream, possibly a fraction of organics that cannot precipitate at low pH conditions. By comparing the TCOD (volatile solids) fate in original (diluted) and modified (undiluted) laboratory protocols, it was observed that the gel layer ended in the acidic liquid stream in diluted conditions, increasing the TCOD percentage to 45% instead of 10%, as indicated by the shaded grey arrow in **Figure 2-3a**. Instead, the modified laboratory

protocol shows this layer as an independent fraction on top of alkaline sludge residue.

The alkaline sludge residue by-product stream could function as an input for an alkaline mesophilic anaerobic digester (AD). The alkaline sludge residue theoretical composition was calculated as described in Kleerebezem, 2014 based on its dry organic matter, TCOD, and TN content. From these measurements, the elemental substrate composition $C_cH_hO_oN_n$ and the stoichiometry of the anaerobic digestion are estimated as shown in **Table 2-5**. The model predicts the maximum methane production to be 516 ml/ g VS, assuming 100% degradation. However, in practice, around 50% degradation of organics occurs at maximum, as discussed in section 2.4.3, which makes the potential of methane production ≈260ml/g VS, recovering 30% of sludge TCOD as methane.

Table 2-5: Theoretical substrate composition and degradation equation of alkaline sludge residue (lab), calculated as described in (Kleerebezem, 2014)

Substrate composition	Degradation Equation
$C\ H_{2.8}O_{0.66}\ N_{0.13}$	$-1\ CH_{2.8}\ O_{0.66}\ N_{0.13} - 0.25\ H_2O$ $+ 0.66\ CH_4 + 0.26\ CO_2 + 0.13\ NH_4HCO_3$

2.3.4 The potential of phosphorus recovery (laboratory scale extractions)

A phosphorus mass balance over laboratory scale using the modified protocol (undiluted) was established, as shown in **Figure 2-3b**, including the bound and free dissolved ortho-phosphate species. 20% of excess sludge total phosphorus ends in the EPS fraction. Bound

phosphorus in liquid streams was calculated as the difference between the measured values of total phosphorus and free ortho-phosphates.

Total phosphorus in EPS was estimated to be divided into a 3:1 ratio of bound phosphorus to free dissolved phosphorus, assuming that the subtraction of P species in the alkaline and acidic liquid streams calculates the P fraction in EPS. However, this should be measured directly to be confirmed in future research.

Since most of the current phosphorus recovery systems recover ortho-phosphates from liquid streams, ortho-phosphate fractions in alkaline and acidic liquid streams were measured. The ortho-phosphate% in the spill sludge was initially measured as 10% of sludge TP. 25% of sludge TP was released to the alkaline stream during the alkaline hydrolysis step as ortho-phosphate and 20% in the acidic liquid stream. The concentrations of ortho-phosphates in alkaline and acidic liquid streams were 615 and 630 mg PO_4-P/L, respectively.

Orthophosphate in the anaerobic digestion centrate was also assessed. It was calculated using the laboratory measurements of alkaline sludge residue as the influent and some basic assumptions from literature research, as described in section (7) in the supplementary material. 15% of sludge TP would end in the liquid digestate with a concentration of 900 mg PO_4-P/L.

2.3.5 The potential of nitrogen recovery (laboratory scale extractions)

The nitrogen mass balance for modified laboratory scale extractions of Epe sludge was established, as shown in **Figure 2-3c**, including the

organic and inorganic dissolved species. In spill sludge, nitrate and nitrite concentrations were negligible, ammonium was less than 2% of sludge TN, and the rest was organic nitrogen. So, the nitrogen mass balance was dominated by organic nitrogen. 30% of excess sludge TN ends in the EPS fraction, primarily as organic nitrogen. The nitrate and nitrite species concentrations were negligible in the liquid streams, and ammonium concentrations in the alkaline and acidic liquid streams were low. The fraction of ammonium-nitrogen was around 2% of sludge TN, with 105 and 110 mg NH_4-N/L for alkaline and acidic streams, respectively. The ammonium fraction possibly ending in the liquid digestate was also calculated using the laboratory measurements of the alkaline sludge residue and some basic assumptions from literature research, as described in section (6) of the supplementary material. It was estimated that around 25% of TN in sludge would end in the effluent with a concentration equal to 2600 mg NH_4-N/L.

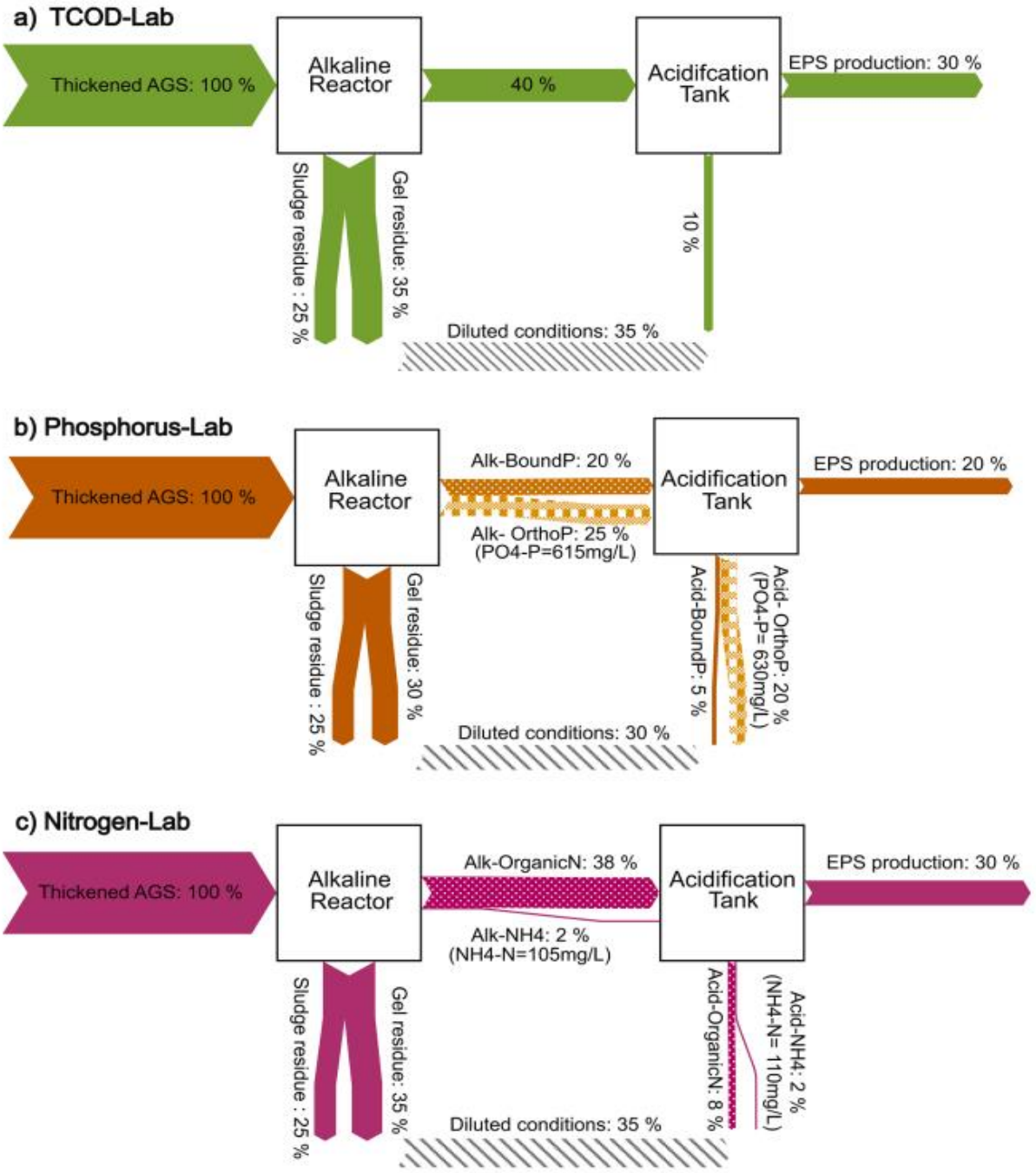

Figure 2-3: Mass balanced for laboratory scale undiluted extractions performed on AGS samples from Epe WWTP. Results are average from triplicates measurements. All percentages express % of the original sludge sample. The shaded grey arrow shows the amount of C, P, or N going to the acidic stream in the case of the diluted protocol. a) TCOD (organic solids), b) The dotted orange arrow shows the amount of bound phosphorus, and the shaded orange arrow shows the amount of free ortho-phosphate, c) The dotted arrow shows the amount of organic nitrogen

2.3.6 Recovery potential in perspective to Epe AGS WWTP+ EPS extraction plant

Figure 2-4 shows TCOD, total phosphorus, and total nitrogen over Epe Nereda WWTP and its large-scale EPS extraction installation. TCOD balance showed that 40% of the plant TCOD daily load ends in excess aerobic granular sludge. The excess sludge goes into the EPS extraction process, in which the final EPS yield is 30% of excess sludge TCOD. With the potential integration of biogas production into the process, 25% of sludge TCOD is calculated to be recovered by AD technology. Methane production was estimated, as explained earlier (Kleerebezem, 2014), as shown in **Table 2-6**, assuming 50% organic degradation occurs at max at practice. Potential methane production from Epe is around 260 ml/g VS and 64 m^3/day.

Table 2-6: Theoretical substrate composition and degradation equation of alkaline sludge residue (Epe), calculated as described in (Kleerebezem, 2014)

Substrate composition	Degradation Equation
$C\ H_{2.8}O_{0.65}\ N_{0.11}$	$-1\ CH_{2.8}\ O_{0.65}\ N_{0.11}\ -0.16\ H_2O$ $+\ 0.65\ CH_4 + 0.25\ CO_2 + 0.11\ NH_4HCO_3$

Total phosphorus balance revealed that 90% of the daily phosphorus load of Epe Nereda WWTP ends in the excess sludge and is removed from the system. The phosphorus ends in the EPS fraction represent 20% of the excess sludge TP. Ortho-phosphate fractions in the alkaline and acidic liquid streams are 35% and 30% of excess sludge TP, respectively, with ≈ 600 mg PO_4-P/L. The ortho-phosphate fraction potentially

present in the AD centrate was calculated as ≈15% of sludge TP with ≈800 mg PO_4-P/L.

Total nitrogen balance showed that 67% of the WWTP daily nitrogen load is removed from the system as nitrogen gas through the simultaneous nitrification-denitrification process, and around 24% enters the EPS extraction process. 30% of excess sludge TN is recovered in the EPS fraction as organic nitrogen. The ammonium concentration in alkaline and acidic streams is ≈ 80-100 mg NH_4-N/L. Ammonium concentration in the AD centrate was also calculated to be ≈ 2600 mgNH_4-N/L and represents 17% of sludge TN. Sections (8) and (9) in the supplementary material provide detailed calculations over the AD.

2.4 Discussion

The fate of the alkaline gel layer is first discussed to provide a basic understanding required for the following discussions on the observed differences between the mass balances in Epe demonstration plant on the 22nd and 23rd of June and laboratory extractions in section 2.4.2. This gel layer has implications on the recovery% reported and later sections discuss how the layer distributes over either the liquid or the solid phase depending on the decanter operation and design. The focus of this study is to evaluate the potential of carbon, phosphorus, and nitrogen recovery from the EPS extraction process as discussed in sections 2.4.3, 2.4.4, and 2.4.5.

2.4.1 Alkaline gel layer formation

The modified laboratory protocol revealed a new alkaline gel layer as a middle layer between the sludge residue and the hydrolyzed EPS supernatant. This layer was not observed with the earlier laboratory protocol as the gel layer probably ended in the acidic liquid stream after separation, as indicated by grey arrows in **Figure 2-3**. On the demonstration scale, due to inefficient solid-liquid separation, it was only easy to observe it once the current work pointed it out. There are several possible explanations for the appearance of this layer: 1) dilution affects the supersaturation and solubility of organics and polymers, similar to inorganic systems, so EPS might precipitate due to higher concentration in the new laboratory protocol/on demo scale; 2) polymers differentiate into different polymer fractions based on molecular weight, higher molecular weight precipitates, and lower molecular weight dissolves, or 3) this fraction has less negative charge density compared to the rest of the dissolved EPS, so it is not readily soluble (Lotti et al., 2019). The exact reason for this layer's appearance has yet to be explored, and further characterization is needed. Fractionation of EPS samples and using advanced analytical methods can help with more accurate EPS characterization. Pre-treatments can achieve this by enriching targeted compounds, followed by purification steps. The purification can be based on solubility using different solvents, charge using chromatography, or size exclusion chromatography (Felz, 2019; Seviour et al., 2019). Such advanced analytical methods can be applied to reveal the differences between Kaumera and the alkaline gel layer in terms of quality and the reason for its appearance. Understanding the mechanism of this layer

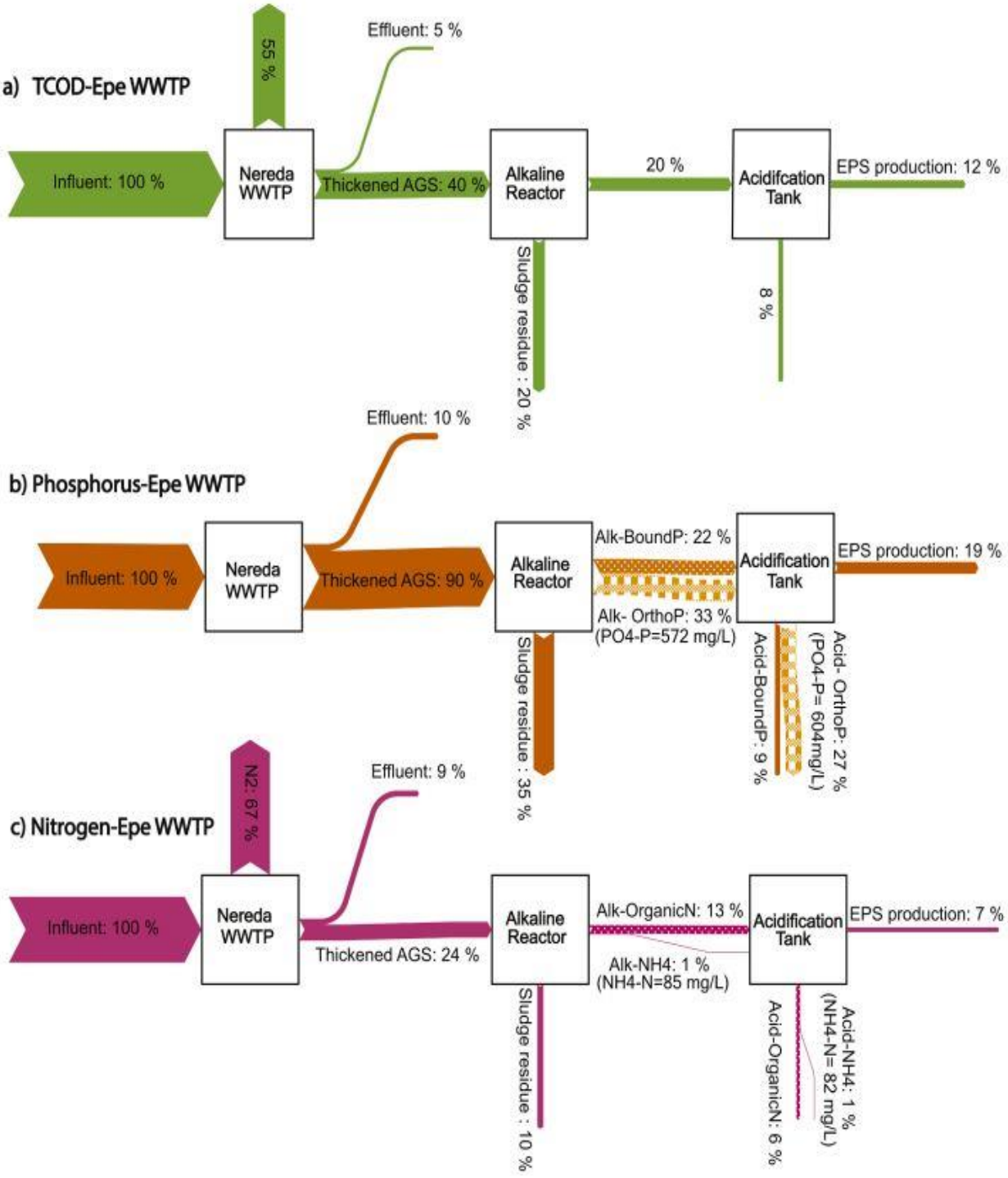

Figure 2-4: a) TCOD, b) phosphorus, c) nitrogen balances for Epe Nereda WWTP+ EPS extraction process. Results are average from triplicate measurements. All mass flows are expressed in % of WWTP daily load.

formation could also open a new direction to separate EPS into different polymer fractions, and each fraction is oriented to specific applications.

2.4.2 Epe demonstration-scale extractions

2.4.2..1 Fate of the alkaline gel layer in Epe

Comparing the 22nd results to the 23rd showed that the 22nd had a much larger Kaumera VS% yield, reaching around 50%. That revealed two implications: 1) that there is a potential to increase the yield of Kaumera by recovering this alkaline gel layer as well, or 2) insufficient solid/liquid separation leads to higher yield but quality deterioration of Kaumera (i.e., a lower fraction of gel-forming polymer). This observation shows that optimizing the decanter separation is crucial in the EPS extraction process and needs further attention. Further research is required to identify the quality difference between the 30%VS Kaumera yield (no alkaline gel layer) and the 50% VS Kaumera yield (including alkaline gel layer + undiluted conditions) to assess if this gel layer can be combined with Kaumera for higher recovery without deteriorating the quality. The fate of this gel layer affects the elemental mass distribution over the process.

2.4.2..2 Epe demonstration versus laboratory extractions

Epe mass balances showed that the potential of TCOD, TP, and TN recovery% by the EPS fraction is similar to the laboratory scale. The concentrations have the same order of magnitude on both scales, as shown in **Table 2-2**. However, there is a difference in the mass% distribution of nutrients at the decanter separation step following the alkaline

hydrolysis, causing a larger fraction of elements to end in the alkaline liquid stream in Epe demonstration and eventually the acidic liquid stream. The TCOD, TP, ortho-phosphate, and TN in the alkaline liquid stream in Epe are 10%, 15%, 10%, and 20%, respectively, higher than the laboratory scale. These observations are explained by two main differences: the decanter solid/liquid separation efficiency and steam injection for heating up sludge to 80 Celsius. The solid/liquid separation efficiency of the decanter would affect the fate of the alkaline gel layer and consequently make a difference in the mass distribution. Steam injection is used in Epe to increase the temperature of the excess sludge before alkaline hydrolysis, and it accounts for 20% of the inlet flow to the alkaline reactor (dilution factor =1.2). Since the concentrations of Epe demonstration and laboratory extractions are in the same order of magnitude, and the dilution effect of steam injection is not significant enough to change that magnitude, it is concluded that a small fraction of the alkaline gel layer ends in the alkaline liquid stream. On the other hand, the solid/liquid separation at the laboratory scale is fully controlled and efficient, so the alkaline gel layer ends on top of the alkaline sludge residue fraction.

The steam injection is an Epe-specific case. For instance, in Zutphen, the first EPS-Kaumera extraction demonstration-scale installation, heating is done through a heat exchanger. Also, decanter centrifuge settings could differ from one extraction plant to another. The comparison showed that the modified laboratory protocol gives results comparable to the demonstration scale installation in Epe. The laboratory protocol can be tailored to specific conditions to predict full-scale mass balances

reasonably well in later stages, i.e., for other sludges from different installations or seasons without the need to realize a pilot installation. It also showed that the operators should be aware that the gel layer fate at full scale will depend on the alkaline solid-liquid separation efficiency.

2.4.3 Carbon Recovery

COD balances showed a 30% EPS yield in the laboratory and Epe demonstration scales. It was reported that the amount of Kaumera extracted is approx. 25-35% of the organic matter in the waste sludge in e in an earlier study (E. van der Knaap et al., 2019). Calculations also showed that 25-30% of sludge TCOD can be recovered as methane by anaerobically digesting the alkaline sludge residue. The AD is proposed to be mesophilic (35°C) and alkaline (pH=9-11), similar to the characteristics of the alkaline sludge residue after solid-liquid separation. Alkaline conditions are commonly used as an effective sludge pre-treatment step for better degradability, higher biogas production, and methane content. In neutral pH digestion systems, 25-60% CO_2 and 40-75% CH_4 ratios are usually obtained (Ryckebosch et al., 2011). According to CO_2/HCO_3 speciation against pH, the vapor pressure of CO_2 is minimal at pH 9-11, as most CO_2 stays in solution as (bi)carbonate. In high pH digestion systems, CO_2 remains in solution, yielding biogas predominantly composed of methane (>95%) (Nolla-Ardevol et al., 2015). The potential of methane production using the alkaline sludge residue is calculated to be ≈260 ml/g VS, according to (Kleerebezem, 2014), and the degradation of around 50% of organics based on Literature and industrial practice (A.F. van Nieuwenhuijzen et al., 2011; Roš

& Zupančič, 2002). The first proof of principle batch experiments on digestion of this residue under mesophilic alkaline conditions (pH=9.5) showed that the methane content was around 98%, with 2% CO_2 as expected. The same experiments also showed methane yield equal to 200-240 ml/g VS; the substrate recovered as methane was about 40-50% (V.Sels, MSc, TU Delft,2019)(unpublished results), which is in line with the calculations in this study. However, some crucial points still need to be investigated in future anaerobic digestion research of this residue, such as the need for pH adjustment during digestion because of CO_2 solubility and VFA production, the evaluation of ammonia toxicity, microbial community, and media composition.

2.4.4 Phosphorus Recovery

According to the established mass balances, phosphorus recovery is realized in two ways during the EPS chemical extraction process. The first one is phosphorus present in the EPS fraction, which is potentially considered recovered phosphorus after understanding the role of phosphorus in polymer properties and its industrial applications. The second way is ortho-phosphate recovery from alkaline or acidic and digestate liquid streams.

2.4.4..1 Phosphorus recovery in the EPS fraction

Market competition is one of the problems facing phosphorus recovery implementation because phosphate rock is cheap. Phosphorus recovery costs from wastewater on a large scale are estimated at €2 per kg P as a bare minimum and could be more than €10 per kg P (Egle et al., 2016; Molinos-Senante et al., 2011). However, the value of phosphorus in

phosphate rock is less than €1 per Kg P. It is argued that upcycling P-recovery products with higher value and quality than fertilizer phosphates is a way to accelerate the P- recovery market. The production of P_4 derivatives from waste streams has gained interest recently (ESPP webinar, 2020; Jupp et al., 2021). P_4 derivatives are P compounds that are cost-intensive as they must be produced via the thermal route of phosphate rock and used in specific industrial applications. EPS-Kaumera from AGS is a potential example of upcycling P-recovery products as it can substitute some P_4 derivatives, i.e., as a flame retardant. Kim et al., 2020 reported that EPS-Kaumera acts as a high-performance bio-based flame retardant as it shows self-extinguishing properties. It also meets the flame retardancy requirements in US Federal Aviation Regulation standards. In addition, EPS from granules has the advantage that it can be produced at a large scale as flame retardants, unlike other biomacromolecules such as DNA, whey proteins, or caseins (Alongi et al., 2014), as sufficient waste granular streams can be provided from Nereda® WWTPs.

Future research focused on understanding the phosphorus speciation in EPS is needed to establish the role of phosphorus for Kaumera properties, which can be manipulated to enhance and change its properties to maximize the usage of recovered phosphorus in EPS in more comprehensive industrial applications. Mass balances showed some assumptions about P-speciation in Kaumera, which will be measured directly in future research for a properly confirmed speciation. According to these assumptions, around 70-75% of phosphorus in EPS is bound phosphorus, and 30-25% is free ortho-phosphates. Free ortho-phosphate is

not an integral part of the polymer, and it is present since EPS is precipitated in the acidic stream, which contains high amounts of free ortho-phosphates. Bound phosphorus in EPS could be organic, inorganic, or ortho-phosphate loosely bound by electrostatic interactions. Organically bound phosphorus and loosely bounded ortho-phosphate are expected to be the most dominant fractions. EPS is expected to have phosphorylated proteins, phospholipids, and phosphosugars due to the extracellular and intracellular components released during alkaline hydrolysis (García Becerra et al., 2010). Also, EPS hydrogel is precipitated at around pH=2-4, which is very low to expect any mineral inorganic phosphorus present, as they would dissolve.

2.4.4..2 Ortho-phosphates recovery from alkaline, acidic, and AD centrate

The potential of ortho-phosphate recovery from alkaline or acidic liquid streams is attractive. According to laboratory extractions, 25%-20% of sludge TP, and 35%-30%, according to Epe demonstration, end in these two fractions as ortho-phosphates. The ortho-phosphate% increase from 10% of sludge TP initially in spill sludge to 25-35% of sludge TP in the alkaline liquid stream could be attributed to polyphosphate hydrolysis. The phosphate concentration is 600 mg PO4-P/L, comparable to concentrations reported for mature full-scale phosphate recovery processes for municipal and industrial wastewater (Desmidt et al., 2015). There are possible technologies to consider for phosphorus recovery from these two streams. For example:

1- nanofiltration on the alkaline stream can bleed off the phosphate (and other salts) to the permeate and keep the EPS in the retentate. That would concentrate the EPS and might reduce acid consumption in the later step. However, organic fouling of the membrane could be challenging (Wang et al., 2009).

2- the acidic stream has a low pH, meaning that most phosphate is present as $H_3PO_4/H_2PO_4^-$. Further lowering the pH to <1 would get all the phosphate to the unionized form as H_3PO_4, and this could create a way to separate phosphoric acid from other salts via ion-selective membranes. However, this would require an extra acid dosage and is cost intensive.

3- chemical precipitation by metal addition as magnesium and calcium is the most common straightforward technology for ortho-phosphate recovery from liquid streams. Alkaline and acidic liquid streams are expected to have pros and cons for chemical phosphorus precipitation. For instance, the alkaline liquid stream has an advantage as it has a high pH value, making it suitable for calcium phosphate and struvite recovery. Struvite consists of equimolar amounts of magnesium, ammonium, and phosphate and forms at pH=8-9 (Desmidt et al., 2015; Doyle & Parsons, 2002), calcium phosphate forms at pH ≥ 9 when the concentrations of phosphorus and calcium are high (Jupp et al., 2021). So, there will be no need to adjust the pH of the alkaline stream to form these minerals. However, this stream also contains solubilized EPS. Metal addition could interfere with its solubilization as it might get complexed or trapped by the polymer, causing the soluble polymers to co-precipitate,

affecting the final EPS yield. **Table 2-2** shows that soluble Ca^{2+} and Mg^{2+} in the alkaline stream are significantly lower than in the acidic stream. This suggests that the highly negatively charged polymers trapped these ions at high pH conditions. Similar observations were reported in soil literature that EPS contains metal binders, such as phosphate, amine, carboxyl, and hydroxyl groups, that trap divalent cations such as Ca^{2+} and Mg^{2+} and inhibit the precipitation of calcium carbonate as it reduces the saturation of calcium (Dittrich & Sibler, 2010; Kremer et al., 2008). The second reason is that visual Minteq modeling showed that the calcium phosphates and struvite are to be formed in the alkaline supernatant; saturation indexes are shown in section (4) of the supplementary material. So, the alkaline liquid stream is already supersaturated; however, no precipitation is seen. That reflects the possible complexity of phosphorus recovery from this stream. On the other hand, the acidic stream has a low pH=2-4, requiring intensive chemical addition for pH adjustment and extra costs to precipitate struvite or calcium phosphate (Cichy et al., 2019). The acidic by-product stream would not interfere with the EPS production as it is already precipitated and removed, and the organics interference would be minimal. It seems that the acidic stream is more promising, so current research is ongoing to validate the possibility of phosphorus recovery in the acidic stream through chemical precipitation.

Ortho-phosphate fraction in the AD centrate was calculated based on our measurements and assumptions from Literature. Phosphorus remains in solution after digesting EBPR excess sludge, as reported by Jardin & Popel, 1994, is 38% of the total phosphorus brought to the

digester. No data is available for granular sludge. The calculations showed that this centrate would contain 12% (Epe)-15% (laboratory) of sludge TP with concentrations ≈700-900 mg PO_4-P/L, showing promising feasible recovery.

2.4.5 Nitrogen recovery

Figure 2-3 and **Figure 2-4** show the fate of nitrogen through the EPS extraction process. 30% of sludge TN is recovered in the EPS mainly as organic nitrogen, which fits with its composition of proteins, and complex glycoconjugates as glycoprotein (Felz, 2019). The concept of recovering ammonium from the alkaline liquid stream is attractive since it has high pH and high temperature, which are required for commercial ammonium recovery technologies. Air stripping and membrane stripping are the most advanced applied technologies on a large scale for ammonium recovery. Both technologies require high pH of about 9-10 and high temperatures of 70-80°C (van der Hoek et al., 2018). The energy efficiency of the recovery depends highly on the ammonium concentration. Ammonium recovery should not require more energy than ammonium production by the Haber-Bosch process. Ammonium concentration in the alkaline supernatant is 105 mg NH_4-N mg/L which is too low to be efficiently recovered (Maurer et al., 2006; Ye et al., 2020) as reported in the recent STOWA report on mature ammonium recovery technologies (R. Elbersen et al., 2021). So, ammonium recovery from the alkaline liquid stream would be a no-go. However, the ammonium fraction in the anaerobic digestion centrate was calculated to be 17% (Epe) and 25%(laboratory) of sludge TN with a concentration of around

2600 mg NH_4-N/L, which would make it feasible for ammonium recovery. These numbers were calculated assuming digestion releases 55% of the sludge nitrogen content (J Soerensen et al., 1999; Suschka & Grübel, 2014).

2.4.6 Practical Implications

Resource recovery from wastewater is still in its infancy but the consensus is that it should be developed in the context of a more sustainable society (Kehrein, van Loosdrecht, Osseweijer, & Posada, 2020; Kehrein, van Loosdrecht, Osseweijer, Garfí, et al., 2020). This paper is taking the first steps towards this and setting a base for decision-makers. Several aspects are relevant to consider for a smooth implementation in the future. Firstly, the technologies used are quite different from operating a standard WWTP, and the goals are different. Utilities will have to consider how they can manage resource recovery at the WWTP, either by adaptation or by partly outsourcing the resource recovery operations. Secondly, the EPS extraction process is the primary process, and other integrated recovery technologies are associated with its by-product streams, so there should be a substantial market demand for Kaumera for such a treatment scheme to make sense. The EPS from AGS forms an interesting new resource for gel-forming biopolymers with much higher market potential and new applications than i.e. alginate or carrageenan. Kaumera could comprise 50% of the turnover Energy & Raw Materials Factory (ERMF) of the Dutch Water Authorities (van Leeuwen et al., 2018). It can be used in agricultural, horticulture, paper, coatings, and construction industries and can be applied as a gel,

foam, or fiber. In 2022, Koppert Biological Systems, Chaincraft, and RHDHV signed a long-term contract for collaboration in applying Kaumera as a bio-stimulant. Another promising application is flame retardancy, as described in section 2.4.42.4.4..1, so it can be used to produce materials and coatings (Kim et al., 2020). EPS can also be used in composite material production as it can hold up to 80% of inorganic filler material. Using Kaumera in composite materials makes it an excellent option to replace many of the current applications of oil-based plastics (Henze et al., 2020).

2.5 Conclusions

Mass balances allowed the quantification of loads and concentrations of carbon, phosphorus, and nitrogen species relevant for recovery to set the foundation for a new generation of AGS WWTP with integrated resource recovery. It was shown that combined EPS, methane, phosphorus, and nitrogen recovery is promising. 30% of sludge TCOD is recovered as EPS, which has wide possible applications, and 25-30% of sludge TCOD could be recovered as biomethane by integrating alkaline anaerobic digestion (AD). 20% of sludge TP is recovered in the EPS. About 20-30% of TP ends in the acidic liquid waste stream and, 15% in the AD centrate as ortho-phosphates. These ortho-phosphate fractions are recoverable by integrating chemical precipitation. 30% of sludge TN ends in the EPS mainly as organic nitrogen and 20% in the AD centrate as ammonium which membrane or air stripping technologies can feasibly recover. This study showed that the developed modified laboratory protocol is an excellent tool for predicting large-scale EPS

extractions. It can be used for futural experimental work focused on nutrient recovery or to test the effect of sludge from different installations or seasons and predict the consequences on a large scale. With the new laboratory protocol, a gel layer was discovered. Comparing the demonstration and laboratory extractions revealed that the fate of the alkaline gel layer depends on the solid/liquid separation efficiency of the decanter centrifuge. This layer could offer additional EPS recovery however its formation, character, and effect on the quality of the recovered EPS needs further research.

References

A.F. van Nieuwenhuijzen, E. Koornneef, P.J. Roeleveld, A. Visser, D. Berkhout, F. van den Berg van Saparoea, v. Miska, E. van Voorthuizen, & C. van Erp Taalman Kip. (2011). STOWA 2011-16. https://www.stowa.nl/publicaties/handboek-slibgisting

Alongi, J., Bosco, F., Carosio, F., di Blasio, A., & Malucelli, G. (2014). A new era for flame retardant materials? In Materials Today (Vol. 17, Issue 4). https://doi.org/10.1016/j.mattod.2014.04.005

APHA [American Public Health Association]. (1999). Standard Methods for the Examination of Water and Wastewater (Twentieth Edition). In American Public Health Association.

Childers, D. L., Corman, J., Edwards, M., & Elser, J. J. (2011). Sustainability challenges of phosphorus and food: Solutions from closing the human phosphorus cycle. BioScience, 61(2). https://doi.org/10.1525/bio.2011.61.2

Cichy, B., Kużdżał, E., & Krztoń, H. (2019). Phosphorus recovery from acidic wastewater by hydroxyapatite precipitation. Journal of Environmental Management, 232. https://doi.org/10.1016/j.jenvman.2018.11.072

De Kreuk, M. K., Heijnen, J. J., & van Loosdrecht, M. C. M. (2005). Simultaneous COD, nitrogen, and phosphate removal by aerobic granular sludge. Biotechnology and Bioengineering, 90(6). https://doi.org/10.1002/bit.20470

Desmidt, E., Ghyselbrecht, K., Zhang, Y., Pinoy, L., van der Bruggen, B., Verstraete, W., Rabaey, K., & Meesschaert, B. (2015). Global phosphorus scarcity and full-scale P-recovery techniques: A review. Critical Reviews in Environmental Science and Technology, 45(4). https://doi.org/10.1080/10643389.2013.866531

Dittrich, M., & Sibler, S. (2010). Calcium carbonate precipitation by cyanobacterial polysaccharides. Geological Society Special Publication, 336.

https://doi.org/10.1144/SP336.4

Doyle, J. D., & Parsons, S. A. (2002). Struvite formation, control, and recovery. In Water Research (Vol. 36, Issue 16).

https://doi.org/10.1016/S0043-1354(02)00126-4

E. van der Knaap, E. Koornneef, K. L., M. Oosterhuis, P. Roeleveld, & M. Schaafsma. (2019). Kaumera Nereda gum: samenvatting NAOP onderzoeken 2013-2018,2019. Retrieved February 18, 2020, from http://edepot.wur.nl/501893

Egle, L., Rechberger, H., Krampe, J., & Zessner, M. (2016). Phosphorus recovery from municipal wastewater: An integrated comparative technological, environmental and economic assessment of P recovery technologies. Science of the Total Environment, 571. https://doi.org/10.1016/j.scitotenv.2016.07.019

ESPP webinar. (2020). Summary of joint European Commission-ESPP webinar on P4 (phosphorus) Critical Raw Material. www.phosphorusplatform.EU

Eynard, U., Wittmer, D., Latunussa, C., & di Milano, P. (2020). Study on the EU's list of Critical Raw Materials (2020) Non-Critical Raw Materials Factsheets SAFEWATER View project Design for Sustainability Fiji View project. https://doi.org/10.2873/587825

Fang, W., Zhang, P., Zhang, G., Jin, S., Li, D., Zhang, M., & Xu, X. (2014). Effect of alkaline addition on anaerobic sludge digestion with combined pretreatment of alkaline and high-pressure homogenization. Bioresource Technology, 168. https://doi.org/10.1016/j.biortech.2014.03.050

Felz, S. (2019). Structural Extracellular Polymeric Substances from Aerobic Granular Sludge. Ph.D. Thesis, TU Delft. https://doi.org/10.4233/uuid:93e702d1-92b2-4025-ab57-6d2c141ed14d

Felz, S., Al-Zuhairy, S., Aarstad, O. A., van Loosdrecht, M. C. M., & Lin, Y. M. (2016). Extraction of structural extracellular polymeric substances from aerobic granular sludge. Journal of Visualized Experiments, 2016(115). https://doi.org/10.3791/54534

Feng, C., Lotti, T., Lin, Y., & Malpei, F. (2019). Extracellular polymeric substances extraction and recovery from anammox granules: Evaluation of methods and protocol development. Chemical Engineering Journal, 374. https://doi.org/10.1016/j.cej.2019.05.127

García Becerra, F. Y., Acosta, E. J., & Grant Allen, D. (2010). Alkaline extraction of wastewater activated sludge biosolids. Bioresource Technology, 101(18). https://doi.org/10.1016/j.biortech.2010.04.021

Hao, X., Li, J., van Loosdrecht, M. C. M., Jiang, H., & Liu, R. (2019). Energy recovery from wastewater: Heat over organics. In Water Research (Vol. 161). https://doi.org/10.1016/j.watres.2019.05.106

Hao, X., Wang, X., Liu, R., Li, S., van Loosdrecht, M. C. M., & Jiang, H. (2019). Environmental impacts of resource recovery from wastewater treatment plants. Water Research, 160. https://doi.org/10.1016/j.watres.2019.05.068

Henze, M., van Loosdrecht, M. C. M., Ekama, G. A., Brdjanovic, D., Pronk, M., & van Dijk, E. J. H. (2020). Biological Wastewater Treatment: Principles, Modeling and Design. In Biological Wastewater Treatment: Principles, Modeling and Design. https://doi.org/10.2166/9781789060362

J Soerensen, G Tholstrup, & K Andreasen. (1999). Anaerobic digestion and thermal hydrolysis to reduce production of sludge in WWTPs. Vatten, 55(1), 45–51.

Jardin, N., & Popel, H. J. (1994). Phosphate release of sludges from enhanced biological P-removal during digestion. Water Science and Technology, 30(6 pt 6). https://doi.org/10.2166/wst.1994.0279

Jupp, A. R., Beijer, S., Narain, G. C., Schipper, W., & Slootweg, J. C. (2021). Phosphorus recovery and recycling-closing the loop. In Chemical Society Reviews (Vol. 50, Issue 1). https://doi.org/10.1039/d0cs01150a

Kehrein, P., van Loosdrecht, M., Osseweijer, P., Garfí, M., Dewulf, J., & Posada, J. (2020). A critical review of resource recovery from municipal wastewater treatment plants-market supply potentials, technologies, and bottlenecks. In Environmental Science: Water Research and Technology (Vol. 6, Issue 4).https://doi.org/10.1039/c9ew00905a

Kehrein, P., van Loosdrecht, M., Osseweijer, P., & Posada, J. (2020). Exploring resource recovery potentials for the aerobic granular sludge process by mass and energy balances-energy, biopolymer, and phosphorous recovery from municipal wastewater. Environmental Science: Water Research and Technology, 6(8). https://doi.org/10.1039/d0ew00310g

Kim, N. K., Mao, N., Lin, R., Bhattacharyya, D., van Loosdrecht, M. C. M., & Lin, Y. (2020). Flame retardant property of flax fabrics coated by extracellular polymeric substances recovered from both activated sludge and aerobic granular sludge. Water Research, 170. https://doi.org/10.1016/j.watres.2019.115344

Kleerebezem, R. (2014). Biochemical Conversion: Anaerobic Digestion. In Biomass as a Sustainable Energy Source for the Future: Fundamentals of Conversion Processes (Vol. 9781118304914). https://doi.org/10.1002/9781118916643.ch14

Kremer, B., Kazmierczak, J., & Stal, L. J. (2008). Calcium carbonate precipitation in cyanobacterial mats from sandy tidal flats of the North Sea. Geobiology, 6(1). https://doi.org/10.1111/j.1472-4669.2007.00128.x

Lee, K. Y., & Mooney, D. J. (2012). Alginate: Properties and biomedical applications. In Progress in Polymer Science (Oxford) (Vol. 37, Issue 1). https://doi.org/10.1016/j.progpolymsci.2011.06.003

Li, H., Li, C., Liu, W., & Zou, S. (2012). Optimized alkaline pre-treatment of sludge before anaerobic digestion. Bioresource Technology, 123.

https://doi.org/10.1016/j.biortech.2012.08.017

Lin, Y., Reino, C., Carrera, J., Pérez, J., & van Loosdrecht, M. C. M. (2018). Glycosylated amyloid-like proteins in the structural extracellular polymers of aerobic granular sludge enriched with ammonium-oxidizing bacteria. MicrobiologyOpen, 7(6). https://doi.org/10.1002/mbo3.616

Lin, Y. M., Nierop, K. G. J., Girbal-Neuhauser, E., Adriaanse, M., & van Loosdrecht, M. C. M. (2015). Sustainable polysaccharide-based biomaterial recovered from waste aerobic granular sludge as a surface coating material. Sustainable Materials and Technologies, 4. https://doi.org/10.1016/j.susmat.2015.06.002

Lotti, T., Carretti, E., Berti, D., Martina, M. R., Lubello, C., & Malpei, F. (2019). Extraction, recovery, and characterization of structural extracellular polymeric substances from anammox granular sludge. Journal of Environmental Management, 236. https://doi.org/10.1016/j.jenvman.2019.01.054

Maurer, M., Pronk, W., & Larsen, T. A. (2006). Treatment processes for source-separated urine. In Water Research (Vol. 40, Issue 17). https://doi.org/10.1016/j.watres.2006.07.012

Molinos-Senante, M., Hernández-Sancho, F., Sala-Garrido, R., & Garrido-Baserba, M. (2011). Economic feasibility study for phosphorus recovery processes. Ambio, 40(4). https://doi.org/10.1007/s13280-010-0101-9

Nolla-Ardevol, V., Strous, M., & Tegetmeyer, H. E. (2015). Anaerobic digestion of the microalga Spirulina at extreme alkaline conditions: Biogas production, metagenome and metatranscriptome. Frontiers in Microbiology, 6(MAY). https://doi.org/10.3389/fmicb.2015.00597

Pronk, M., de Kreuk, M. K., de Bruin, B., Kamminga, P., Kleerebezem, R., & van Loosdrecht, M. C. M. (2015). Full-scale performance of the aerobic granular sludge process for sewage treatment. Water Research, 84. https://doi.org/10.1016/j.watres.2015.07.011

R. Elbersen, D. Roelofsen, J. Dan, A.L. de Jong, J. Boorsma & M.Bovee (2021). stikstofterugwinning uit rioolwater; van marktambitie naar praktijk. https://edepot.wur.nl/555277

Roš, M., & Zupančič, G. D. (2002). Thermophilic aerobic digestion of waste activated sludge. Acta Chimica Slovenica, 49(4). http://acta-arhiv.chem-soc.si/49/49-4-931.pdf

Ryckebosch, E., M. Drouillon, and H. Vervaeren. 2011. “Techniques for Transformation of Biogas to Biomethane.” Biomass and Bioenergy 35(5): 1633–45.

Sam, S. B., & Dulekgurgen, E. (2016). Characterization of exopolysaccharides from floccular and aerobic granular activated sludge as alginatelike-exoPS. Desalination Water Treat, 57(6), 2534–2545. https://doi.org/10.1080/19443994.2015.1052567

Seviour, T., Derlon, N., Dueholm, M. S., Flemming, H. C., Girbal-Neuhauser, E., Horn, H., Kjelleberg, S., van Loosdrecht, M. C. M., Lotti, T., Malpei, M. F., Nerenberg, R., Neu, T. R., Paul, E., Yu, H., & Lin, Y. (2019). Extracellular polymeric substances of biofilms: Suffering from an identity crisis. In Water Research (Vol. 151). https://doi.org/10.1016/j.watres.2018.11.020

Seviour, T., Pijuan, M., Nicholson, T., Keller, J., & Yuan, Z. (2009). Understanding the properties of aerobic sludge granules as hydrogels. Biotechnology and Bioengineering, 102(5), 1483–1493. https://doi.org/10.1002/bit.22164

Siami, S., Aminzadeh, B., Karimi, R., & Hallaji, S. M. (2020). Process optimization and effect of thermal, alkaline, H2O2 oxidation and combination pretreatment of sewage sludge on solubilization and anaerobic digestion. BMC Biotechnology, 20(1). https://doi.org/10.1186/s12896-020-00614-1

Solon, K., Volcke, E. I. P., Spérandio, M., & van Loosdrecht, M. C. M. (2019). Resource recovery and wastewater treatment modeling. In Environmental Science: Water Research and Technology (Vol. 5, Issue 4). https://doi.org/10.1039/c8ew00765a

Stegmann, P., Londo, M., & Junginger, M. (2020). The circular bioeconomy: Its elements and role in European bioeconomy clusters. In Resources, Conservation and Recycling: X (Vol. 6). https://doi.org/10.1016/j.rcrx.2019.100029

Suschka, J., & Grübel, K. (2014). Nitrogen in the process of waste activated sludge anaerobic digestion. Archives of Environmental Protection, 40(2). https://doi.org/10.2478/aep-2014-0021

Toutian, V., Barjenbruch, M., Loderer, C., & Remy, C. (2020). A pilot study of thermal alkaline pre-treatment of waste activated sludge: Seasonal effects on anaerobic digestion and impact on dewaterability and refractory COD. Water Research, 182. https://doi.org/10.1016/j.watres.2020.115910

Uysal, A., Yilmazel, Y. D., & Demirer, G. N. (2010). The determination of fertilizer quality of the formed struvite from the effluent of a sewage sludge anaerobic digester. Journal of Hazardous Materials, 181(1–3). https://doi.org/10.1016/j.jhazmat.2010.05.004

van Leeuwen, K., de Vries, E., Koop, S., & Roest, K. (2018). The Energy & Raw Materials Factory: Role and Potential Contribution to the Circular Economy of the Netherlands. Environmental Management, 61(5). https://doi.org/10.1007/s00267-018-0995-8

Van der Hoek, J. P., Duijff, R., & Reinstra, O. (2018). Nitrogen recovery from wastewater: Possibilities, competition with other resources, and adaptation pathways. Sustainability (Switzerland), 10(12). https://doi.org/10.3390/su10124605

Van Dijk, K. C., Lesschen, J. P., & Oenema, O. (2016). Phosphorus flows and balances of the European Union Member States. Science of the Total Environment, 542. https://doi.org/10.1016/j.scitotenv.2015.08.048

Van Loosdrecht, M. C. M., & Brdjanovic, D. (2014). Anticipating the next century of wastewater treatment. In Science (Vol. 344, Issue 6191). https://doi.org/10.1126/science.1255183

V.Sels. (2019). 190802 MSc Thesis Sels, Valerie_b0daa2cf-1eeb-4118-ac5b-b9b9c5ecbe7a. Master Thesis, TU Delft.

Wang, Z., Wu, Z., & Tang, S. (2009). Extracellular polymeric substances (EPS) properties and their effects on membrane fouling in a submerged membrane bioreactor. Water Research, 43(9). https://doi.org/10.1016/j.watres.2009.02.026

Ye, Y., Ngo, H. H., Guo, W., Chang, S. W., Nguyen, D. D., Zhang, X., Zhang, J., & Liang, S. (2020). Nutrient recovery from wastewater: From technology to economy. In Bioresource Technology Reports (Vol. 11). https://doi.org/10.1016/j.biteb.2020.10042

Supplementary Materials

1. The mass balance equation set used to determine the unknown flows in the EPS extraction process:

P, Fe, Mg, Ca, Al, and volatile solids concentrations were used to calculate the unknown flows of D, G, F, and H using B (the thickened excess sludge) flow as an initial condition, shown in **Figure 2-1**. Although only two mass balance equations (known concentrations) are needed to calculate two unknown flows, the mass balance equations were extended to multiple elements to confirm that flow values converge to the same value.

For the alkaline hydrolysis reactor + decanter part of the system, the following equations were used:

$$G\ P_G + D\ P_D - B\ P_B = zero$$

$$G\ Fe_G + D\ Fe_D - B\ Fe_B = zero$$

$$G\ Mg_G + D\ Mg_D - B\ Mg_B = zero$$

$$G\ Ca_G + D\ Ca_D - B\ Ca_B = zero$$

$$G\ Al_G + D\ Al_D - B\ Al_B = zero$$

$$G\ VS_G + D\ VS_D - B\ VS_B = zero$$

Where B is the initial thickened sludge stream, G is the alkaline sludge residue byproduct stream, and D is the alkaline liquid stream all in (Kg/day). For the acidification tank+ Disc centrifuge part of the system, the following equations were used:

$$F\ P_F + H\ P_H - D\ P_D = zero$$

$$F\ Fe_F + H\ Fe_H - D\ Fe_D = zero$$

$$F\ Mg_F + H\ Mg_H - D\ Mg_D = zero$$

$$F\ Ca_F + H\ Ca_H - D\ Ca_D = zero$$

$$F\ Al_F + H\ Al_H - D\ Al_D = zero$$

$$F\ VS_F + H\ VS_H - D\ VS_D = zero$$

Where F is the EPS production stream, H is the acidic liquid byproduct stream after EPS production and separation, and D is the alkaline liquid stream containing the hydrolyzed EPS all in (Kg/day).

Table S2-1: Average estimated flows in (Kg/h) based on concentrations measured in g/Kg

Flow	**Alkaline liquid stream**	**Alka-line residue pellet**	**Acidic liquid stream**	**Kaumera-EPS**	**Kaumera-EPS VS yield%**
22nd - Kg/h	514	90	380	112	47
23rd- Kg/h	497	172	390	90	30

2. 22nd and 23rd sampling days in Epe

As described in the methods section, samples for this study were collected from Epe on the 22nd and 23rd, one day after the system startup (20th). It was observed that the mass balances on the 22nd are different from the 23rd showing a much larger Kaumera Gum VS% (COD%) yield than expected reaching around 50% compared to 30% VS yield on the second day. This value is much higher than observed in earlier lab extractions and reported by demonstration plants in Epe or Zutphen.

To carefully validate the data, the following steps were taken:

- The concentrations of TS%, VS%, TP, TN, Fe, COD, Ca, Al, and Mg were compared between the 22nd and 23rd of June. Higher concentrations and higher mass end in the alkaline liquid stream on the 22nd compared to the 23rd as shown in Table S2-2. Together with the onsite observation that the 22nd alkaline dissolved EPS liquid samples were much more turbid than on the 23rd, it was concluded that the decanter centrifuge was not working optimally during the 22nd. This caused higher mass fractions (alkaline gel layer) to end in the alkaline liquid stream, and eventually in the EPS fraction and acid stream.

- However, the differences between the 22nd and 23rd samples showed two possibilities:

1) that there is a potential to increase the yield of Kaumera due to this alkaline gel layer's presence if it is derived to end in the alkaline supernatant under undiluted conditions or

2) Insufficient solid/liquid separation led to higher Kaumera yield but quality deterioration of yielded Kaumera (i.e., a lower fraction of gel-forming polymer).

- To confirm if our data represents the general operation of the plant, they were validated by other data for confirmation:

1) The data reported by STOWA report on Kaumera E. van der Knaap et al., 2019 was compared to ours:

EPS with 25-35% yield, 5-12% TS (in the range of our results)

Eps with 2-3% TP and 6-9%TN (in the range of our results)

Acidic centrate with 200-400 mgP/L, 500-1000 mgN/L and < 100 mgNH4-N/L (in the range of our results)

2) To further confirm, our measurements were compared to other data collected by RHDHV from Epe in November 2021 (unpublished):

+/- 2% VS of Kaumera yield, +/- 4% VS in alkaline sludge residue, +/- 5% VS in acidic centrate

+/-2% P in Kaumera, +/-5% P in alkaline sludge residue, +/- 8% P in acidic centrate

+/- 2% N in Kaumera, +/-6% N in alkaline sludge residue+/-4% N in acidic stream

Table S2-2: Mass balances of Fe, Ca, Mg, Al, and composition in Epe (22nd and 23rd June 2021)

	Alkaline stream	**Alkaline residue pellet**	**Acidic stream**	**Kaumera-EPS**
%Mass balances and composition	**mg/L**	**g/ Kg TS**	**mg/L**	**g/Kg TS**
Fe				
22nd June, 2021	52% (340)	48% (20)	22% (210)	30% (9.0)
23rd June, 2021	30% (247)	70% (21)	15% (142)	15% (7.1)
Ca				
22nd June, 2021	63% (307)	37% (12)	50% (343)	13% (3.2)
23rd June, 2021	43% (233)	57% (12)	35% (250)	8% (2.5)
Mg				
22nd June, 2021	60% (136)	40% (5.7)	50% (149)	10% (1.4)
23rd June, 2021	36% (92)	64% (6)	30% (97)	6% (0.9)
Al				
22nd June 2021	65% (342)	35% (12)	37% (282)	28% (7.1)
23rd June 2021	46% (284)	54% (12)	30% (241)	16% (5.8)

Table S2-3: Mass balances of TCOD, TN, TP, and composition on 22nd June in Epe (for comparison with 23rd Epe or lab data in the manuscript)

22nd June, 2021	**Alkaline stream**	**Alkaline residue pellet**	**Acidic stream**	**Kaumera-EPS**
TS%	4.1	9.5	2.9	10.5
	mg/L	**g/Kg TS**	**mg/L**	**g/Kg TS**
TCOD	70% (44900)	30% (1090)	22% (21200)	48% (1346)
TN	80% (2750)	20% (41)	35% (1651)	45% (65)
TP	80% (1247)	20% (23)	47% (981)	33% (22)

Table S2-4: Mass balances% of other elements over the extraction process

VS%	Alkaline Liquid stream	Alkaline residue pellet	Acidic liquid stream	Kaumera-EPS
22nd June, 2021	3	6.2	1.7	9.2
23rd June, 2021	2.5	6.6	0.96	7.4
Lab	2.8	6.6	0.98	7.4

3. Detailed modified lab protocol (EPS extraction)

1- Excess thickened aerobic granular sludge samples were collected (5%TS)

2- Heating 90 grams of fresh excess thickened sludge in a water bath to 80 Celsius.

3- Add 25%(w/v) KOH to the heated sludge (pH-controlled process)(9-11)

Note: Selection of the probe is critical, as the pH is measured at 80 Celsius. The calibration is either: 1) a probe with ATC and you can calibrate the probe using buffers at room temperature, 2) a probe with no ATC and you calibrate the probe using buffers at 80 celsius. In this case, the Endress+Hauser pH ATC probe with a pH range: of 0 to 14, and a process temperature: of 0 to 135 °C was used. So, during calibration, ATC reads the true temperature of the buffer and assigns the exact correct value and during testing, ATC reads the true temperature of the sample and adjusts the slope to remain in collaboration. So, the accuracy of the probe is maintained regardless of the temperature.

4- Cover the flask and the beaker separately with aluminum foil to prevent evaporation

5- Stir the mixture for two hours at 400 rpm and 80 °C

6- let it cool down to room temperature.

7- Transfer the mixture into 50 ml centrifugation tubes, and centrifuge at 4,000 × g and 30 °C for 20 min.

8- Collect the alkaline sludge residue for analysis

9- Transfer the alkaline supernatant extract to a 250 ml glass beaker and stir it slowly at 100 rpm and room temperature while adding 30 wt% HCl until it reaches a final pH 2-4

10- Transfer the acidified extract into 50 ml centrifugation tubes, and centrifuge at 4,000 x g and 30°C for 20 min.

11- Collect the acidic supernatant for analysis and collect the gel-like EPS pellet.

4. Visual Minteq modelling of the alkaline liquid stream from EPS extraction process

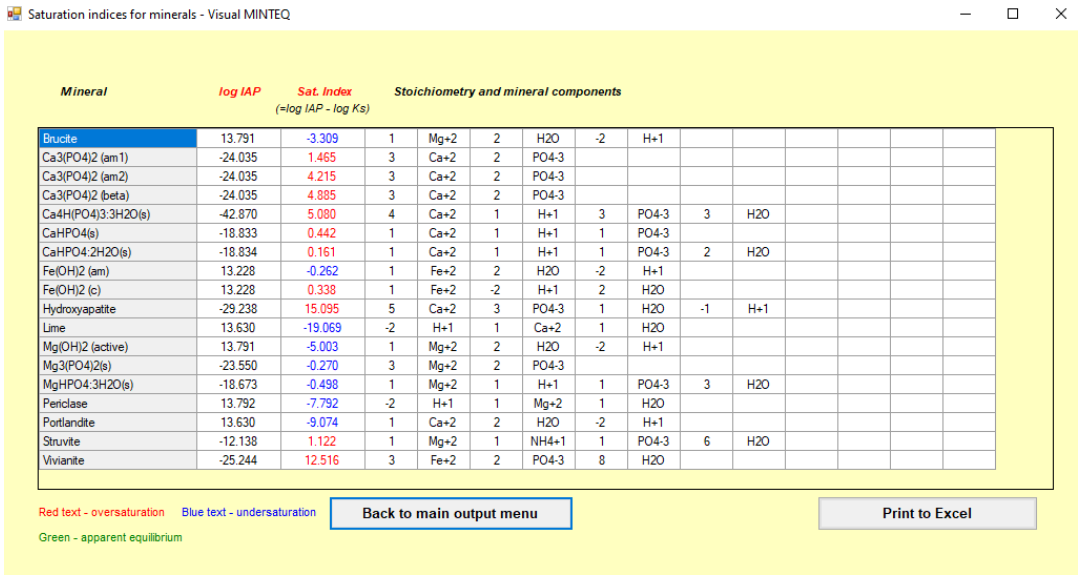

Mineral	log IAP	Sat. Index (=log IAP - log Ks)	Stoichiometry and mineral components												
Brucite	13.791	-3.309	1	Mg+2	2	H2O	-2	H+1							
Ca3(PO4)2 (am1)	-24.035	1.465	3	Ca+2	2	PO4-3									
Ca3(PO4)2 (am2)	-24.035	4.215	3	Ca+2	2	PO4-3									
Ca3(PO4)2 (beta)	-24.035	4.885	3	Ca+2	2	PO4-3									
Ca4H(PO4)3:3H2O(s)	-42.870	5.080	4	Ca+2	1	H+1	3	PO4-3	3	H2O					
CaHPO4(s)	-18.833	0.442	1	Ca+2	1	H+1	1	PO4-3							
CaHPO4:2H2O(s)	-18.834	0.161	1	Ca+2	1	H+1	1	PO4-3	2	H2O					
Fe(OH)2 (am)	13.228	-0.262	1	Fe+2	2	H2O	-2	H+1							
Fe(OH)2 (c)	13.228	0.338	1	Fe+2	-2	H+1	2	H2O							
Hydroxyapatite	-29.238	15.095	5	Ca+2	3	PO4-3	1	H2O	-1	H+1					
Lime	13.630	-19.069	-2	H+1	1	Ca+2	1	H2O							
Mg(OH)2 (active)	13.791	-5.003	1	Mg+2	2	H2O	-2	H+1							
Mg3(PO4)2(s)	-23.550	-0.270	3	Mg+2	2	PO4-3									
MgHPO4:3H2O(s)	-18.673	-0.498	1	Mg+2	1	H+1	1	PO4-3	3	H2O					
Periclase	13.792	-7.792	-2	H+1	1	Mg+2	1	H2O							
Portlandite	13.630	-9.074	1	Ca+2	2	H2O	-2	H+1							
Struvite	-12.138	1.122	1	Mg+2	1	NH4+1	1	PO4-3	6	H2O					
Vivianite	-25.244	12.516	3	Fe+2	2	PO4-3	8	H2O							

Figure S2-1: Saturation indices for minerals in the alkaline liquid stream calculate by Visual Minteq

5. XRD

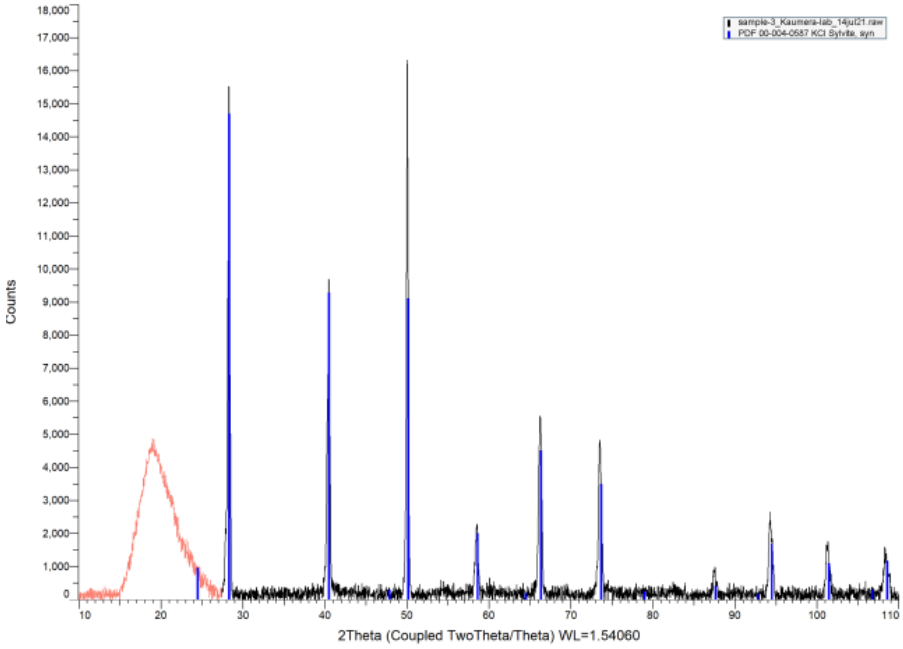

Figure S2-2: XRD pattern sample (Kaumera-Lab)

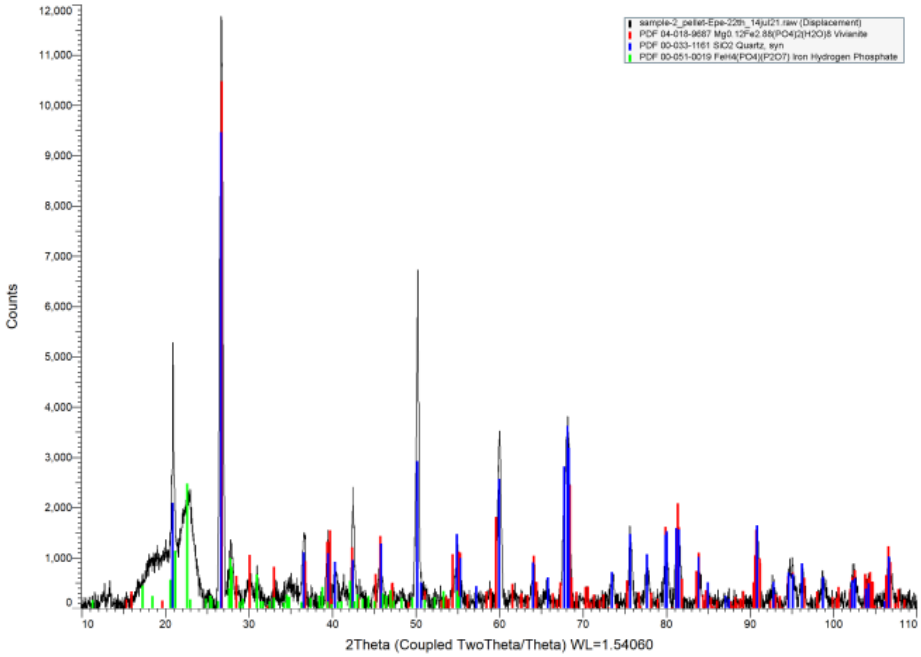

Figure S2-3: XRD pattern (Alkaline sludge pellet-lab)

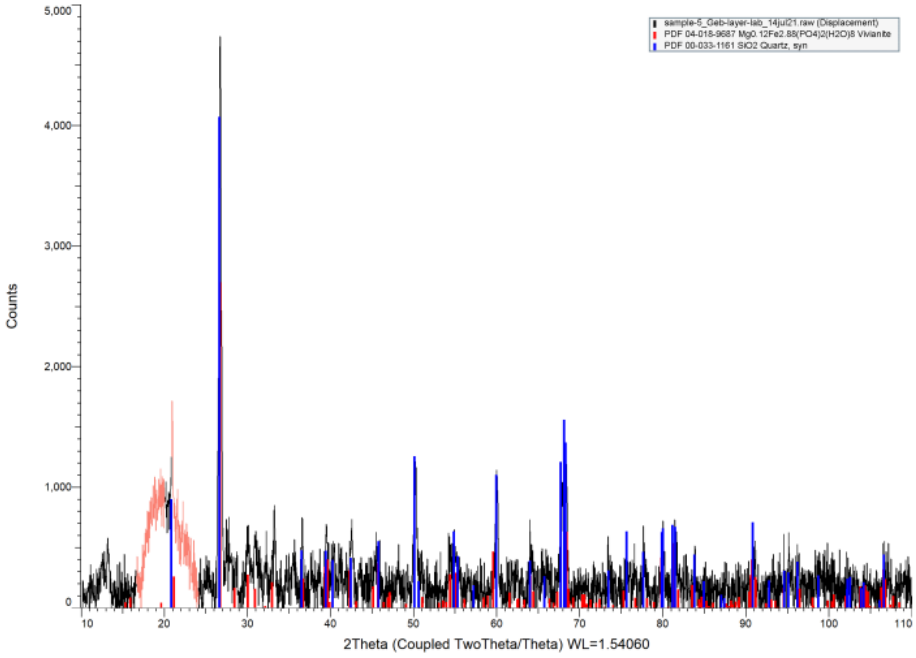

Figure S2-4:XRD pattern (Alkaline gel layer-lab)

6. Nitrogen balance over anaerobic digester (Lab scale)

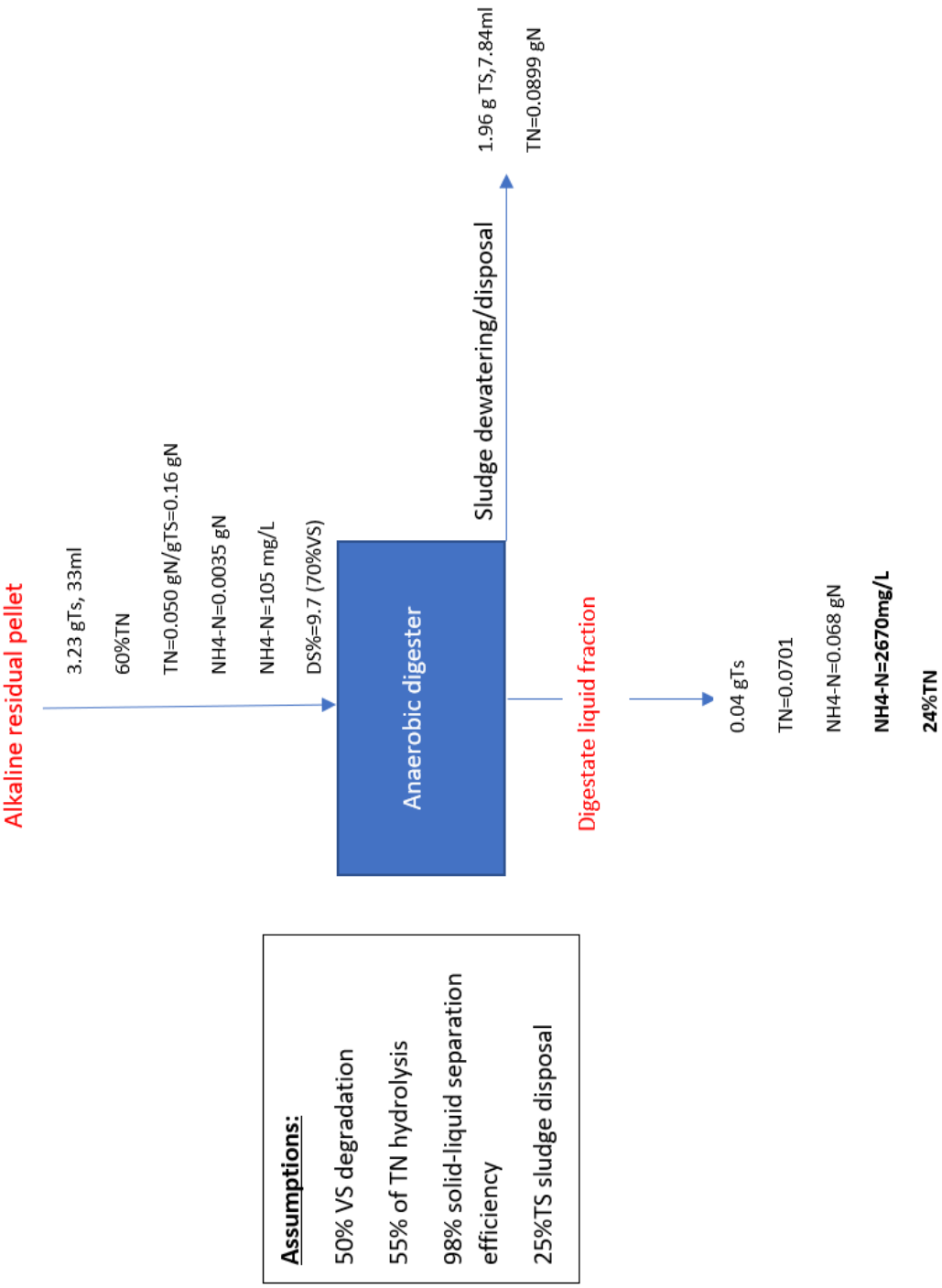

7. Phosphorus balance over anaerobic digester (Lab scale)

8. Nitrogen balance over anaerobic digester (Epe)

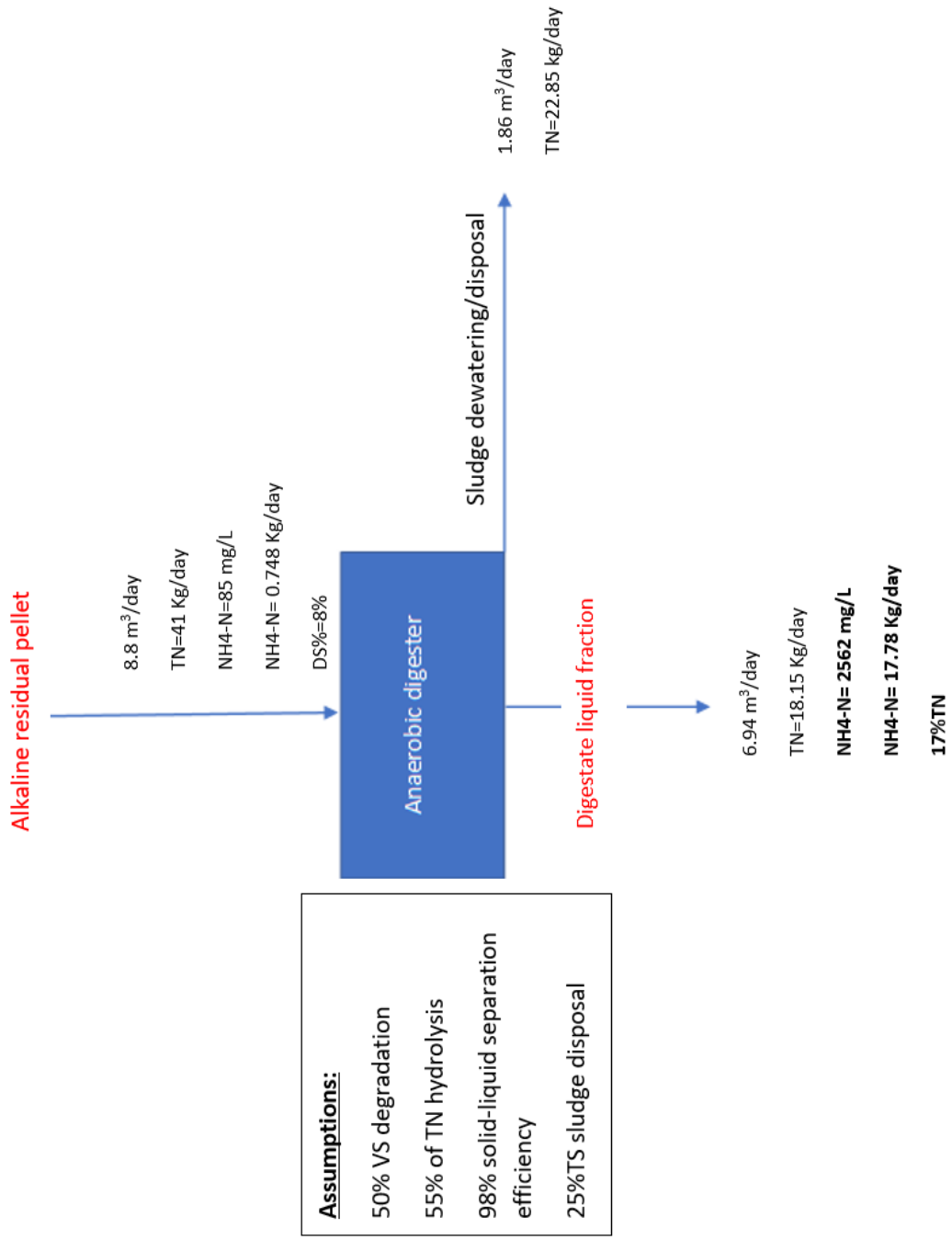

9. Phosphorus balance over anaerobic digester (Epe)


15

Chapter 3

$FePO_4.2H_2O$ Recovery from Acidic Waste Streams

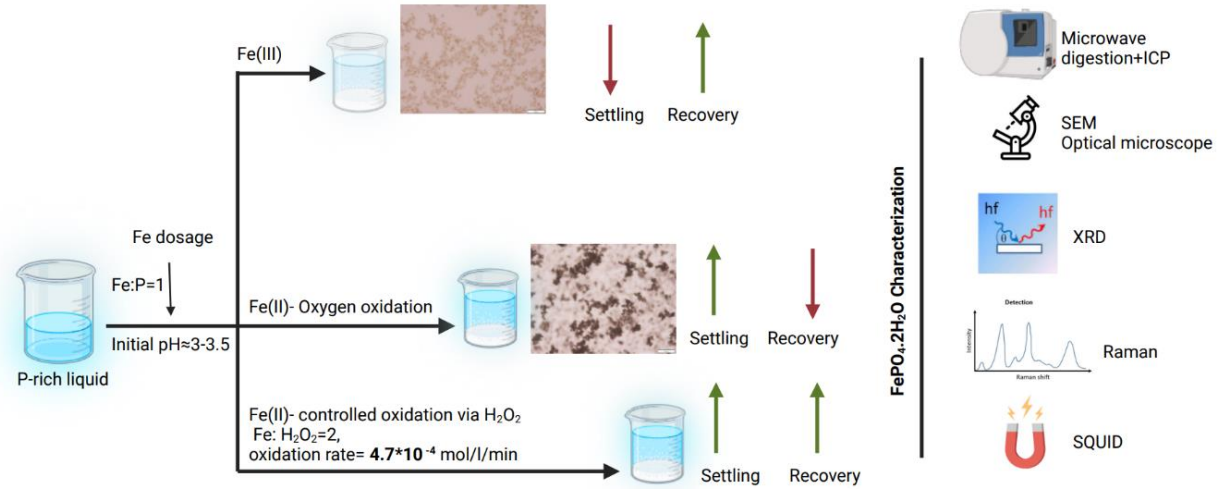

This chapter has been published as:

Bahgat, N. T., Siddiqui, A., Wilfert, P., Korving, L., & van Loosdrecht, M. C. M. (2024). $FePO_4.2H_2O$ recovery from acidic phosphate-rich waste streams. Water Research. https://doi.org/10.1016/j.watres.2024.121905

This chapter was patented as: METHOD FOR PHOSPHATE AND/OR ARSENATE RECOVERY FROM AN ACIDIC STREAM, SYSTEM THEREFORE, AND USE OF A PRECIPITATE OBTAINABLE BY SAID METHOD.

Abstract

Phosphorus not only needs to be removed to prevent eutrophication of wastewater effluent receiving surface water bodies, but it also has to be recovered as a scarce finite reserve. Phosphorus chemical precipitation as $NH_4MgPO_4 \cdot 6H_2O$, $Ca_3(PO_4)_2$, or $Fe_3(PO_4)_2 \cdot 8H_2O$ is the most common method of phosphorus recovery from phosphorus-rich streams. These minerals ideally form under neutral to alkaline pH conditions, making acidic streams problematic for their formation due to the need for pH adjustments. This study proposes $FePO_4 \cdot 2H_2O$ (strengite-like compounds) recovery from acidic streams due to its simplicity and high efficiency, while also avoiding the need for pH-adjusting chemicals. The effect of initial pH, temperature, Fe (III) dosing rates, and Fe (II) dosage under different oxidation conditions (pO_2=0.2, 1, 1.5 bar, different H_2O_2 dosing rates) on phosphorus recovery percentage and product settleability were evaluated in this study. The precipitates formed were analyzed using optical microscopy, SEM, XRD, SQUID, Raman, and ICP. Experiments showed that Fe (III) dosing achieved phosphorus recovery of over 95% at an initial pH of 3 or higher, and the product exhibited poor settleability in all initial pH (1.5-5), and temperature (20-80 Celsius) tests. On the other hand, Fe (II) dosage instead of Fe (III) resulted in good product settleability but varying phosphorus recovery percentages depending on the oxidation conditions. The novelty of the study lies in revealing that the Fe (II) oxidation rate serves as a crucial process-design parameter, significantly enhancing product settleability without the requirement of carrier materials or crystallizers. The study proposes a novel strategy with controlled Fe^{2+}-H_2O_2 dosing, identifying an Fe (II) oxidation rate of $4.7 * 10^{-4}$ mol/l/min as the optimal rate for achieving over 95% total phosphorus recovery, along with excellent settleability with a volumetric index equal to only 8 ml/gP.

3.1 Introduction

Phosphorus is an essential element for life, responsible for various functions in all forms of life, often serving as a limiting nutrient for crops and a crucial component of fertilizers. The primary source of phosphorus is mining phosphate rock, with mined phosphorus primarily utilized for agricultural fertilizers (80%), along with applications in animal feed additives (5%), detergents (12%), metal treatments, and other industrial processes (3%) (Smit et al., 2009). Despite rising demand, the sustainability of phosphorus use remains uncertain due to diminishing phosphate rock reservoirs and quality concerns arising from cadmium content (Kratz et al., 2016; Ridder, 2012). Moreover, the majority of phosphate reservoirs are concentrated in a few countries, with over 85% located in Morocco, China, the US, Jordan, and South Africa (Ashley et al., 2011). Regional imbalances in phosphorus distribution can lead to phosphate accumulation or excessive phosphorus discharge into ecosystems, contributing to pollution (van Dijk et al., 2016). Recognizing the critical importance of phosphorus, the European Commission listed phosphorus rock as a critical raw material in 2017 due to its significance for economic development and the risks associated with its supply (Eynard et al., 2020). Consequently, the current EU policy emphasizes phosphorus recovery and improved resource management, aiming to increase the utilization of waste streams for reuse while minimizing losses (ESPP webinar, 2020). This underscores the necessity of cyclic use and phosphorus recovery from secondary sources (Childers et al., 2011).

Phosphorus recovery from wastewater can occur from liquid side streams, sludge, or ash, all of which have high phosphate concentrations. Phosphorus chemical precipitation is the most well-established method for phosphorus recovery from phosphorus-rich streams, utilizing metal salts such as magnesium, calcium, or iron. Struvite recovery is the most widely implemented technology among commercialized phosphorus recovery techniques due to its simplicity (Jupp et al., 2021), with struvite crystals forming at pH ≈ 9 (Desmidt et al., 2015; Doyle & Parsons, 2002; Thant Zin & Kim, 2019). Calcium phosphate recovery occurs when calcium is added in the form of $Ca(OH)_2$, and then calcium precipitates with phosphates at pH ≥9 (Cichy et al., 2019). To enhance the settleability of struvite and calcium phosphate crystals, crystallizers such as AirPrex®, NuReSys®, Pearl®, Crystalactor®, and PHOSPAQ™ are used (Metcalf & Eddy, 2014). Vivianite ($Fe_3(PO_4)_2 \cdot 8H_2O$) is also recovered at a pH range of 6-8 when the Fe:P ratio =1.5. Initially observed in surplus anaerobically digested sludge (Frossard et al., 1997; Wilfert et al., 2016), technology has been developed to crystallize and recover vivianite from liquid streams (Priambodo et al., 2017a). All these techniques for phosphorus recovery require neutral or alkaline pH conditions, as these minerals are soluble under low-pH conditions (Luyckx et al., 2021). This makes phosphorus recovery from low-pH phosphorus-rich streams challenging due to the need for intensive chemical dosing to adjust the pH. It's intriguing that low pH recovery technologies aren't more prevalent, given the substantial impact these streams have on overall phosphorus loads and their widespread presence. The niche of these streams can be separated into:

1) Acidic industrial waste streams: an economically interesting niche for removal and recovery, relatively easy to implement, such as wastewater from cheese production (Carvalho et al., 2013; Danalewich et al., 1998; Lei et al., 2022; Slavov, 2017), wastewater from semiconductors or LCD manufacturing (Martin et al., 2020; Priambodo et al., 2017), wastewater from phosphoric acid production (Monat et al., 2022; Nawghare et al., 2001), wastewater from some pulp and paper industries (Leo et al., 2011; J. C. Zhang et al., 2019), and streams from leaching processes of steelmaking slag (Iwama et al., 2020).
2) Acidic waste streams related to municipal WWTPs: these streams have far bigger phosphorus loads compared to loads from industries (Eicher, 2018; Meyer et al., 2018) as leaching/acidification processes for metal/nutrient recovery of sludge or ash from incinerators. A new niche is wastewater from EPS (Kaumera) extraction processes from aerobic granular sludge (Bahgat et al., 2023). Although the EPS extraction process is quite new, this niche might have high recovery potential as more aerobic granular sludge (Nereda) wastewater plants are established worldwide, and EPS is proving successful as a product. Other potential streams could be identified through further engagement with various industries.

The only available technology to recover phosphorus from these streams is raising the pH to neutral or alkaline conditions (Cichy et al., 2019; Monat et al., 2022), followed by precipitation. Membranes have

also been reported as a potential method to concentrate phosphates in wastewater at low pH regions (Koh et al., 2020; Leo et al., 2011). However, this only concentrates these phosphates and does not yet recover them; the concentrated stream can still contain impurities that need to be removed and requires further processing. Additionally, the use of membranes makes the technology capital-intensive. In this study, a new approach to recover phosphate more effectively from acidic liquid streams is presented. The idea was inspired by acidic soils literature (pH= 3- 5.7) where $FePO_4 \cdot 2H_2O$ strengite-like minerals (strengite and metastrengite) are reported to be naturally formed (CHAKRAVARTI & TALIBUDEEN, 1962; Iuliano et al., 2007; Oxmann & Schwendenmann, 2014). Recovering $FePO_4 \cdot 2H_2O$ from acidic waste streams would have advantages over conventional phosphorus recovery products because: 1) no need for chemical dosing to adjust the pH compared to struvite, calcium phosphates, or vivianite; 2) it is insoluble under acidic conditions; 3) it has Fe:P ratio=1 which means less iron dosing compared to vivianite Fe: P=1.5; 4) it does not require reducing conditions to form as vivianite so it can form in the ambient conditions of any WWTP; and 5) the precipitated product will be cleaner and purer, e.g., compared to high pH precipitation products because of high solubility of heavy metals under these low pH conditions (Ain Zainuddin et al., 2019; Marchioretto et al., 2005).

According to $FePO_4 \cdot 2H_2O$ crystallization literature, at room temperature, amorphous Fe (III) phosphates would initially form and then transform into crystalline structures after prolonged aging (Hsu, 1982).

Additionally, $FePO_4 \cdot 2H_2O$ formation at pH 1.6 after 12 hours of reaction at 50 and 100 degrees Celsius was reported to be amorphous and persisted for a substantial time. However, at 200 degrees Celsius, crystalline strengite and metastrengite formed (Roncal-Herrero et al., 2009). Accordingly, It is expected that $FePO_4 \cdot 2H_2O$ forms under WWTPs ambient conditions will be amorphous, not crystalline, and settle poorly. $FePO_4 \cdot 2H_2O$ recovery from synthetic effluents was reported in earlier studies in which a phosphate recovery percentage of 95% was achieved, and product settleability was improved by adding carriers in fluidized bed reactors (Priambodo et al., 2017; Xing et al., 2021).

In this study, our approach was to enhance the settleability of $FePO_4 \cdot 2H_2O$ to the level that gravity-based separation techniques are sufficient, without the need for crystallizers or seed material, while maintaining an acceptable recovery via varying operating conditions. First, the optimum initial pH (1.5-5) for recovery was tested. Then, temperature (25 - 80 degrees Celsius) was tested as a way to induce partial crystallization and better settleability of the precipitate at higher temperatures. Controlled Fe (III) supply was also tested to prevent high supersaturation, where nucleation dominates over crystal growth, and to improve settleability. Different Fe (III) dosing rates, Fe (II), and different oxidation conditions (pO_2 = 0.2 bar, 1 bar, and 1.5 bar, and different H_2O_2 dosing rates) were tested. The novelty of our research lies in presenting a Fe^{2+} controlled oxidation system via H_2O_2 wherein both high recovery and rapid precipitate settleability are achieved by controlling the supply of Fe (III) through controlled Fe (II) oxidation, without the need to add carriers or further crystallizers, as previously reported in

the literature (Priambodo et al., 2017; Xing et al., 2021). The $FePO_4 \cdot 2H_2O$ precipitate was characterized using ICP, SEM, optical microscope, XRD, Raman spectroscopy, and SQUID. Precipitate settleability was also measured using Imhoff sedimentation cones, and volume indexes were calculated in ml/gP.

3.2 Methodology

3.2.1 Reagents

$FeNH_4(SO_4)_2.12H_2O$, $Fe(NH_4)_2(SO_4)_2.6H_2O$, and $NH_4H_2PO_4$ salts (Sigma-Aldrich) were used for precipitation experiments adopted from Lundager Madsen & Koch, 2018 protocol. 1M NaOH was prepared with ≈99% pure NaOH pellets to adjust the initial pH in experiments (VWR chemicals). 0.01 M H_2O_2 was used for Fe (II) oxidation experiments (VWR chemicals). Milli-Q water was used as a solvent to prepare these solutions.

3.2.2 Preparations

3.2.2..1 Fe (III) Synthetic experiments

0.085 M equimolar solution of $FeNH_4(SO_4)_2$ as a source of Fe (III) and $NH_4H_2PO_4$ as a P source was prepared. Fe (III) solutions were initially adjusted by adding 1M NaOH in pH experiments. The temperature was controlled using shaking incubators in different temperature experiments. Fe (III) dosing to the P solution was carried out in two ways: one-time quick addition and drop-wise (for 3 hours) using a glass lab decanter funnel while stirring. The solid precipitation was separated from the liquid fraction by centrifugation at 4000xg for 10 minutes. The

precipitate was then washed three times by adding MilliQ water and separated by centrifugation. Both solid and liquid fractions were analyzed.

3.2.2..2 Fe (II) synthetic experiments

0.085 M equimolar solution of Fe $(NH_4)_2(SO_4)_2.6H_2O$ as a source of Fe (II) and $NH_4H_2PO_4$ as a P source was prepared. Open-air oxidation (pO_2 = 0.2 bar) experiments were left on the lab bench overnight and for 10 days at room temperature. Non-pressurized (pO_2 = 1 bar) and pressurized (pO_2 = 1.5 bar) pure oxygen experiments were performed in serum-stoppered bottles and left overnight. In H_2O_2 oxidation experiments, H_2O_2 was dosed to Fe (II)P equimolar solution: one-time quick and drop-wise (for 4 mins, 10 mins, 3 hours) using a glass lab decanter funnel. The dosage of H_2O_2 was calculated according to Fenton's reaction equation (Truong et al., 2004), with a molar ratio Fe: H_2O_2 = 2:1. Solid and liquid fractions were separated and analyzed.

3.2.2..3 Real acidic waste from EPS extraction installation in Epe WWTP

Acidic liquid samples from the EPS extraction pilot installation in Epe WWTP were collected as an example of complex wastewater, containing organic and inorganic impurities, to confirm the potential of phosphorus recovery from real acidic streams as $FePO_4 \cdot 2H_2O$. Epe WWTP was the first full-scale domestic wastewater treatment plant in the Netherlands to install the innovative aerobic granular sludge (AGS) treatment technology, operated by the water authority Waterschap Vallei en Veluwe. The EPS extraction process is operated as described in detail

by Bahgat et al., 2023. AGS goes through an alkaline reactor in which the pH is within 9-11 and the temperature is 80 degrees Celsius for two hours, followed by an acidification reactor in which the pH is within 2.5-3 and an acidic phosphate-rich liquid stream is produced as a by-product. To perform the experiments, the phosphate concentration of the acidic stream from EPS extraction was measured, and the dosage of Fe (III) or Fe (II) and H_2O_2 was determined according to the theoretical molar ratios of Fe:P = 1 and Fe: H_2O_2= 2.

3.2.2..4 Settling experiments

Precipitate settleability measurements were conducted by pouring 1L samples into Imhoff sedimentation cones and allowing them to settle. The settled solids volume was recorded at 5, 10, and 30 minutes, and results were recorded as ml/L. Volumetric indexes were calculated as ml/gP recovered.

3.2.3 Analysis

3.2.3..1 Elemental and Composition Analyses

a. Microwave digestion

With the help of microwave digestion, solids and organics are completely decomposed and dissolved in a strong inorganic acid. Concentrated nitric acid was used to fully digest the samples after they were subjected to high temperature and pressure inside the microwave. The purpose of microwave digestion is to enable a quantitative elemental analysis of solid samples using ICP-OES and IC which require aqueous inorganic samples. Samples were digested in an Ethos Easy from

Milestone with an SK-15 High-Pressure Rotor. Around 50 mg of solids were put in a Teflon vessel where 10 mL of ultrapure HNO_3 (64.5-70.5% from VWR Chemicals) was poured. The digester is set to reach 200 Celsius in 15 minutes, run at this temperature for 15 minutes, and cool down for 1 hour.

b. ICP-OES

The elemental inorganic composition was measured via Inductively Coupled Plasma (Perkin Elmer, type Optima 5300 DV) with an Optical Emission Spectroscopy as a detector (ICP-OES). The device was equipped with an Autosampler, Perkin Elmer, type ESI-SC-4 DX fast, and the data were processed with the software Perkin Elmer WinLab32. The rinse and standard internal solutions were 2%HNO_3 and 10 mg/L of Yttrium.

c. C/H/N/O elemental analysis

The solid precipitate from the real acidic samples experiments was analyzed using an Elemental analyzer (Mettler Toledo, America) to check the estimate of the organics co-precipitated.

d. IC (Ion chromatography)

Liquid samples were pre-treated first by filtering the samples through 0.45 µm followed by 0.22 µm membrane filters before analysis. Anions and cations (free dissolved ions) were measured by Metrohm Compact ion chromatograph Flex 930.

e. LCK 320 Iron Hach Lange kits

In this study, Fe (II) and Fe (III) were measured using iron Hach Lange kits which depend on the strong Fe (II)-binding ligand phenanthroline. Three molecules of phenanthroline chelate a single Fe (II) molecule to form an orange-red complex. Any Fe (III) ions in the sample are reduced to Fe (II) in a secondary step by ascorbic acid before the complex is formed again. Phenanthroline is better than ferrozine (another standard Fe (II) colorimetric reagent) at low pH samples. Ferrozine can induce reduction and interfere with the reliable measurement of Fe (II) (Anastácio et al., 2008; Jones et al., 2014).

f. Gas Chromatography

The gas composition was analyzed using gas chromatography to ensure that the serum bottles were completely purged by pure oxygen in Fe (II) experiments. A glass syringe (1 mL) was connected to the serum bottles, and a sample was collected and analyzed using Micro GC (CP-4900) using argon as carrier gas. The module was connected to a Thermal Conductivity Detector (TCD) for data acquisition, and the Galaxy Chromatography Data System controls the instrument.

3.2.3..2 Morphology observations

g. SEM (Scanning Electron Microscopy)

The dried precipitate was observed under SEM (Jeol JSM-6480LV) to determine the shape and size of the precipitate. The samples were coated with a 10 nm layer of gold at 15 Pa and 25 mA to make the surface electrically conductive. The following settings were applied:

Accelerating Voltage: 6 kV, Working distance: 10 mm. The software used was JEOL SEM Control User Interface.

h. Optical microscope

Liquid samples were analyzed under a light microscope. The sample was placed on the glass slide, and then a cover slide was placed. The sample was observed under 4x, 10x, 20x, and 100x magnifications bright field using the Leica (DMI 6000B) stereo microscope and Olympus (Model BX43F) light microscope. The pictures were captured using the Leica Application Suite (LAS V4.6) and cellSens Standard.

3.2.3..3 Advanced analytical identification techniques

i. XRD (X-Ray diffraction)

Room-temperature dried samples were used for XRD analysis. The sample was filled in a 0.7 mm glass capillary and tamped so the solid settled. The capillaries were sealed with a burner and mounted in a sample holder. The device used was a Bruker D8 Advance diffractometer with Cu Ka radiation (Coupled $\theta - 2\theta$ scan 10° - 110°, step size 0.030 ° 2θ, counting time per step 2 s). The data evaluation was performed using Burker software DiffracSuite.EVA vs. 6.

j. Raman Spectroscopy

Raman Spectroscopy was used to compare $FePO_4$ $2H_2O$ prepared from synthetic solution experiments with strengite and metastrengite minerals from the literature. The processed data of samples was obtained from Raman (LabRam Olympus MPlan N 100x/0.9 Lens). The following settings for Raman Analysis were used: Exposition: 100 seconds,

Spectro: Auto, Accumulation: 1x8, Binning: 1, Slit: 100 µm, Hole: 100 µm, Laser: 532.13 nm, Grating: 600, Objective: x100, Detector: Synapse CCD, Detector size: 1024. The spectrum was processed using Origin-pro by performing baseline correction and smoothing.

k. SQUID (Superconducting Quantum Interference Device)

Field-dependent magnetization (M-H) curves at a temperature of 300 K were measured in an interference devices (SQUID) MPMS-XL magnetometer equipped with a reciprocating sample option (RSO). The SQUID MPMS provides exceptional sensitivity, as high as 10^5 Am^2. The typical sample mass used in this work is about 2~3 mg. The temperature range is between 1.7 and 400 K, and the applied magnetic field is up to 5 T.

3.2.4 Curve fitting

The nonlinear regression function of Sigma Plot (version 14) was used to fit the phosphorus recovery percentages and volumetric indexes to sigmoidal, 4 parameter function provided in the standard regression library (shown in equation [1]), where a is the maximum asymptote, b is the slope, y_0 is the ground asymptote and x_0 is the point of inflection. This function was chosen because the measurement points seemed to behave like a sigmoid function constrained by a pair of horizontal asymptotes (S-shaped curves). The fitting showed an R-squared value of 1 for the P recovery curve and 0.9982 for the volumetric indexes showing the goodness of fit chosen. Details on the fitting are shown in the supplementary material.

$$f = y_0 + \frac{a}{1+e^{-(\frac{x-x_0}{b})}} \quad [1]$$

3.3 Results

3.3.1 Evaluation of chemical equilibria

Visual Minteq was utilized for simulating the Fe (III) and phosphate solutions to confirm the potential of $FePO_4 \cdot 2H_2O$ formation under acidic conditions. The inputs included the initial Fe (III) and P concentration in the synthetic solutions, pH, and temperature, as referenced in section 3.2.2..1. The calculated saturation indexes indicated $FePO_4 \cdot 2H_2O$ as the only phosphate mineral to form under these conditions. The pKsp used in the calculations is 26.4, as reported by (Nriagu, 1972). As shown in the supplementary material, strengite, goethite, and hematite are supersaturated; however, as discussed later in section 3.4.2, the formation of oxide species is almost negligible under the tested acidic conditions. Therefore, only strengite was added to the list of "Possible Solid Phases." The "Equilibrated Mass Distribution" revealed that the fraction of Fe and P precipitate is 99.9%, indicating that thermodynamically all phosphorus can be recovered as $FePO_4 \cdot 2H_2O$ by the addition of Fe (III).

3.3.2 pH effect on P recovery%

Fe (III) reacted directly with PO_4^{3-} which led to the instantaneous formation of $FePO_4.2H_2O$ white precipitate in these experiments. The initial pH in Fe (III) experiments was 1.5 upon Fe (III) addition and mixing of the solutions. The effect of pH was studied at room

temperature by adjusting the pH from 1.5 to 3, 4, and 5. Total phosphorus (TP) removal from the liquid fraction and TP precipitated are reported in **Table 3-1**. pH 3 was the optimum among the tested pH values, achieving a phosphorus recovery rate of approximately 96%, similar to pH 4 and 5 but with minimal pH adjustment, and surpassing the recovery rate observed at pH 1.5, which stood at 60%. pH 4 and 5 formed a slightly reddish precipitate, unlike pH 1.5 and 3, indicating a greater formation of hydroxide species at higher pH values. The initial pH dropped by the end of the experiments due to the liberation of H^+ during the precipitation process. Previous literature has also identified pH 3 as optimum for $FePO_4 \cdot 2H_2O$ solubility and purity. The optimal solubility level of $FePO_4 \cdot 2H_2O$ under acidic conditions falls within the range of 2-4, with an optimum value of around 3 (Eastman, 2017; T. Zhang et al., 2017). Additionally, pure $FePO_4 \cdot 2H_2O$ precipitates typically form only below pH 3.5. With increasing pH above 3.5, a mixture of ferric phosphate and hydroxide emerges, with ferric hydroxide precipitates becoming more predominant above pH 4.5 (Morgan & Lahav, 2007a; Takács et al., 2006), further discussion on this is in section 3.4.2. Consequently, the initial pH values of our experiments were maintained within the range of 3 and 3.5.

3.3.3 Temperature effect on P recovery%

The effect of temperature was studied at 25, 40, 60, and 80 ℃ at pH 1.5. The experiment aimed to assess the feasibility of improving settling efficiency by partially crystallizing the precipitate at higher temperatures. This approach was inspired by the observation that

crystalline $FePO_4.2H_2O$ formation was reported at elevated temperatures (150-200°C), as discussed in section 3.4.1. In the EPS extraction process, the sludge undergoes heating to 80°C and then cools down to room temperature before the acidification step. Therefore, the temperature range of room temperature to 80 °C was chosen for testing, as it aligns with the existing process and could potentially be integrated into the acidic by-product stream from the EPS extraction process. Results showed that there was no effect on the crystal size or XRD spectra as discussed in section 3.3.6..3. Still, the temperature influenced the phosphorus recovery as shown in **Table 3-1**. Higher temperature induced higher phosphorus recovery, increasing temperature from 25 to 40 increased phosphate recovery by 20%. However, it reached a plateau value as increasing temperature from 60 to 80 ℃ had negligible effect.

3.3.4 Fe (II) oxidation effect on P recovery%

In these experiments, Fe (III) was replaced by Fe (II), and it was allowed to oxidize to Fe (III) by O_2 and H_2O_2 and eventually form $FePO_4.2H_2O$. The initial pH in the Fe (II) experiments was 3.5 after the addition of Fe (II) and mixing the solutions. Since Fe (II)-P solutions already fell within the optimal pH range discussed in section 3.3.2, there was no need for pH adjustments.

3.3.4..1 Oxidation via O_2

Phosphate recovery was very low in open-air oxidation systems (pO_2 = 0.2 bar), with approximately 7% of total phosphorus recovered over-night, as shown in **Table 3-1**. When the experiment was extended to 10 days, the recovery increased to approximately 45%, indicating that

more precipitation formed over time, as shown in **Figure 3-1.** These two experiments demonstrated that Fe (II) oxidation under atmospheric conditions is very slow and is the rate-limiting step. One approach to accelerate Fe (II) oxidation under these conditions is by increasing the dissolved oxygen concentration in the system. As the oxygen partial pressure (pO_2) increases, the dissolved oxygen concentration will also increase, following Henry's law. Increasing pO_2 from 0.2 bar to 1 and 1.5 bar with pure oxygen systems was conducted in serum bottles and tested. The recovery increased from approximately 7% to 34% and 50% of the total phosphorus for 1 and 1.5 bar overnight, respectively, as shown in **Table 3-1**.Although these results demonstrate that Fe (II) oxidation fastened and recovered phosphorus increased compared to open-air experiments, the low recovery percentage and long duration still pose challenges for WWTPs.

3.3.4..2 Oxidation via H_2O_2

H_2O_2 is a stronger oxidant than oxygen that can be used to rapidly oxidize Fe (II) to Fe (III). These experiments aimed to increase the speed of the Fe (II) oxidation process by adding H_2O_2. The phosphate recovery in H_2O_2 experiments was higher, approximately around 99%, close to Fe (III) experiments.

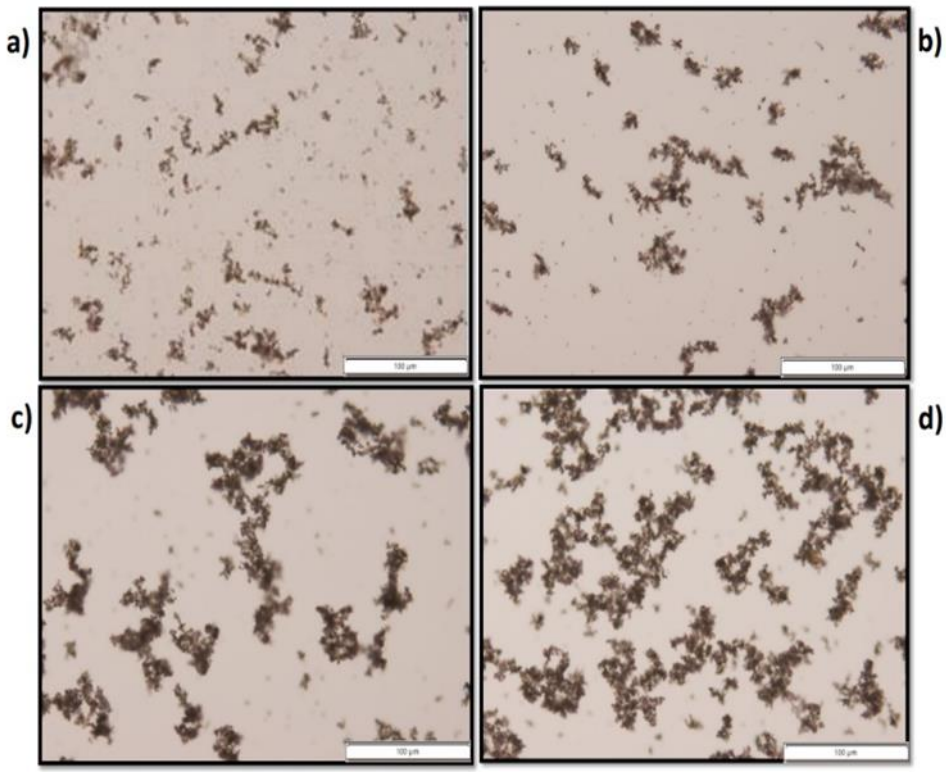

Figure 3-1: Fe (III)-P precipitation growth dosing Fe (II) over time under air oxidation conditions pO2= 0.2 bar a) 2 days, b) 4 days, c) 6 days, d) 10 days under the optical microscope. Scale =100µm

Table 3-1: Phosphate recovery % in Fe (III) tests (different pH and temperature) and Fe (II) tests (different oxidation conditions). TP% (liquid) is phosphate removal from the liquid fraction measured by IC, and TP% (precipitate) is phosphates recovered as a solid fraction measured by microwave digestion+ ICP, and the molar ratio of Fe:P of the precipitate is calculated. All experiments were performed in triplets, and averages and standard deviations were calculated. The discrepancy between TP% (precipitate) and TP% (liquid) is between 1% to 6% and is due to using different instrumental techniques and sample preparation methods to perform the two different measurements.

Synthetic- Fe (III)					
Initial pH	**Initial pH**	**Final pH**	**TP% (liquid)**	**TP% (precipitate)**	**Molar ratio precipitate (Fe:P)**
1.5	-	1.3	62±0.0	60±0.3	1.04±0.03
3	-	2.8	98±0.00	94±0.2	1.08±0.01
4	-	3.9	98±0.1	94±0.1	1.07±0.03
5	-	5	98±0.1	94±0.2	1.06±0.00
Temperature					
25°C	1.5	1.3	61±2.0	60 ±0.3	1.04±0.03
40°C	1.5	1.4	81±0.0	77±0.1	1.03±0.01
60°C	1.5	1.4	87±0.0	84±0.6	1.04±0.00
80°C	1.5	1.3	87±0.00	89±1.0	1.00±0.00
Synthetic- Fe (II) Oxidation to Fe (III)					
Open-air (pO_2 =0.2 bar)			**TP% (liquid)**	**TP% (precipitate)**	**Molar ratio (Fe:P)**
Overnight	3.5	3.1	9 ±0.5	5 ±0.1	0.95±0.01
10 days	3.5	2.7	46±0.3	40 ±0.2	0.89±0.01
Pure oxygen					
pO_2 = 1 bar-overnight	3.5	2.8	32±1.0	36±0.2	0.90±0.00

pO_2 = 1.5 bar-overnight	3.5	2.6	50± 1.0	51 ±0.1	0.89±0.00
Another oxidant					
H_2O_2	3.5	2.2	99±0.2	98±0.2	1.04±0.02
Stream from the EPS extraction process with a pH of 2.5					
Fe (III)-quick	1.6	1.2	75 ±0.4	75±0.2	1.02±0.01
Fe (III) -3 hours	3	2.6	95 ± 0.3	93 ± 0.2	1.07 ±0.02
Fe (II) H_2O_2- 3 hours	3	2.7	99 ± 0.4	96± 0.1	1.04 ± 0.04

3.3.5 Fe (III) versus Fe (II) Settling

The settling behavior of the precipitate was measured and compared between Fe (II) and Fe (III) experiments. The precipitate formed instantly with the quick addition of Fe (III), and its settleability was poor under all pH and temperature conditions tested, with a volumetric index (VI) equal to 263 ml/gP. However, the controlled addition of Fe (III) for 3 hours enhanced the settleability (VI = 40 ml/gP) because of the lower saturation level. Fe (III) formation via Fe (II) oxidation with O_2 and H_2O_2 further enhanced the settleability of the precipitate. Oxygen's slow oxidation resulted in the most settleable precipitate, while H_2O_2 oxidation could influence settling behavior based on how quickly it was added to the Fe (II) system. Comparing H_2O_2 dosage over 3 hours, 10 minutes, 4 minutes, or one-time addition revealed different settling speeds. These varied oxidation conditions indicate that controlling the Fe (II) oxidation rate is a method to manage the settleability of the precipitate without requiring crystallizers or seed

addition. Fe (II) oxidation rates from different experiments were calculated based on Fe (II) consumption over time, as shown in **Table 3-2.** Saturation levels could not be measured directly in these experiments as it was impossible to measure Fe^{3+} concentration with the Hach Lange kits because of the instant formation of $FePO_4.2H_2O$ and the low concentrations of Fe^{3+} left in solutions that could not be detected using these kits. Still, an estimation for Fe(III)-(3 hours) and Fe(II)-H_2O_2 (3 hours) systems could be given based on one droplet volume (0.05 mL) of F^{3+} solution or H_2O_2 introduced to the P solution and its Fe^{3+} equivalence. The two systems had an initial SI of 2.42, indicating that although the saturation levels were the same, there was a difference in the settling behavior, suggesting that another mechanism besides saturation level is influencing the settleability. The effect of oxidation rate on settling and recovery was fitted to a sigmoidal function as shown in **Figure 3-2.** Combining the phosphate recovery curve (time-dependent) with the settling curve shows an ideal system for recovery that combines both a high recovery percentage and low volumetric index (ml/gP) at Fe (II) oxidation rate of 4.7 *10 $^{-4}$ mol/l/min. Further characterization of the precipitate from Fe (II)-H_2O_2 (3 hours) is in section 3.3.6.

Table 3-2: Volumetric index of the precipitate formed in different Fe (II) and Fe (III) experiments, calculated by measuring the volume of settled solids after 30 min as ml/g phosphorus and Fe (II) average oxidation rates in different experiments in mol/l/min

Experimental systems (synthetic)	Volumetric index (ml/gP)	Fe (II) oxidation rate (mol/l/min) *10^{-6}
Fe^{3+}(Quick)	263	-
Fe^{3+}(3 hours)	40	-
Fe^{2+}-O_2 0.2 bar (20 hours)	2.3	5
Fe^{2+}-O_2 1 bar (20 hours)	3	23
Fe^{2+}-O_2 1.5 bar (20 hours)	3	35
Fe^{2+}-H_2O_2 (Quick)	250	425000
Fe^{2+}-H_2O_2 (4 mins)	115	21000
Fe^{2+}-H_2O_2 (10 mins)	88	9400
Fe^{2+}-H_2O_2 (3 hours)	8	470

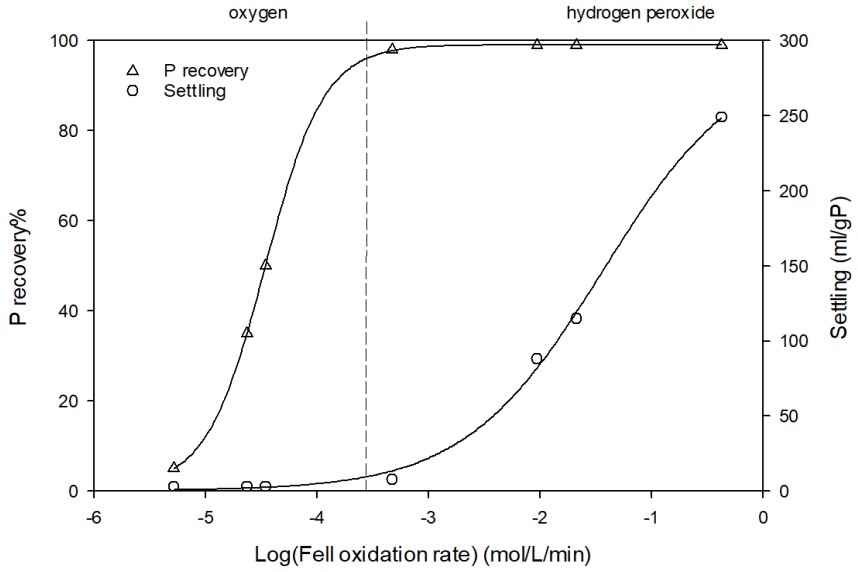

Figure 3-2: Log Fe (II) oxidation rate (mol/L/min) versus settling (ml/gP) and P recovery% in both oxygen experiments (slow oxidation) and H_2O_2 experiments (medium to fast oxidation)

3.3.6 FeP precipitate identification

3.3.6..1 Composition

$FePO_4.2H_2O$ has an equimolar ratio of iron and phosphorus. $FePO_4.2H_2O$ precipitates from all experiments were collected, solubilized, and analyzed by ICP to determine the Fe:P molar ratio as shown in **Table 3-1**. In all experiments, the Fe: P molar ratio in the precipitate was around 1; however, for Fe (II)-O_2 oxidation experiments, the ratio was slightly lower (0.89- 0.95), which could indicate another mechanism to remove phosphates besides $FePO_4$ $2H_2O$ formation is taking place (e.g., adsorption).

3.3.6..2 Morphology

The surface morphology features of the precipitate were demonstrated by SEM in **Figure 3-4**. The precipitate was observed to be agglomerations of small particles in size of 2-3 µm which formed larger clusters in different Fe (III) and Fe (II) experiments. Optical microscope images of the samples showed that the precipitate consists of clusters of small particles (**Figure 3-3)**. There was distinction between the precipitates from Fe (II) and Fe (III). In the case of Fe (II), the agglomerations appeared denser and had a stronger dark hue compared to the precipitate from Fe (III). This observation aligns with the superior settling characteristics observed.

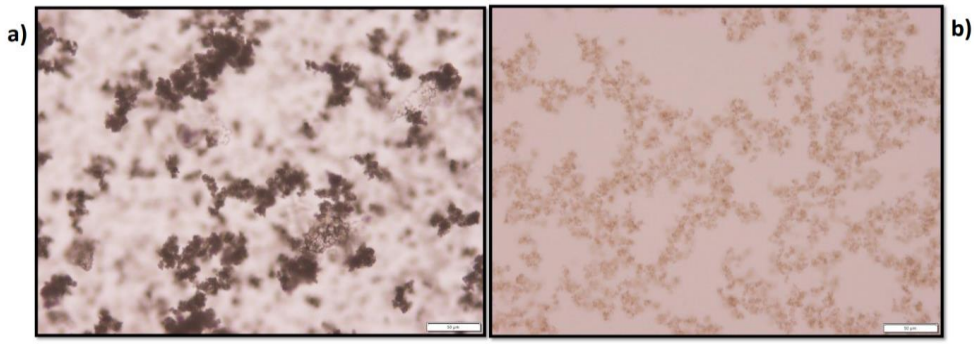

Figure 3-3: Microscopic pictures of the wet precipitate from **a)** Fe (II) pO_2=0.2 bar, and **b)** Fe^{3+}quick (one-time) addition pH 3

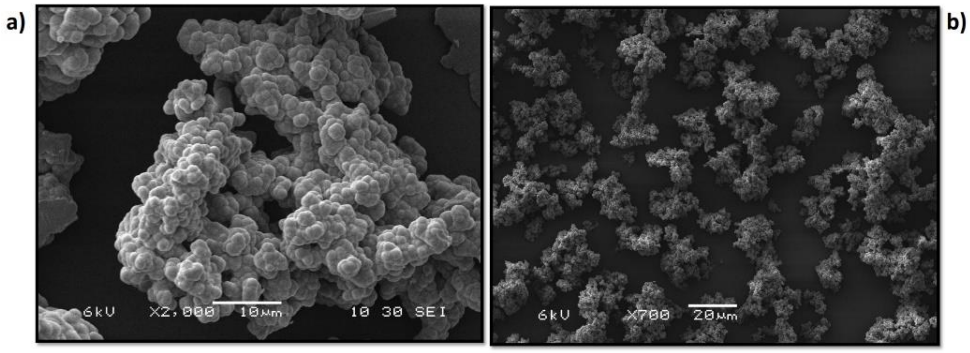

Figure 3-4: SEM pictures of the precipitate from Fe (II)- H_2O_2 (3 hours) at different magnification levels a) 10 µm and b) 20 µm

3.3.6..3 Advanced Analytical Identification

In this section, further characterization of the precipitate from Fe (III) quick addition, Fe (II)-H_2O_2 (3 hours), and Fe (II)-O_2 =0.2 bar (20 hours) is provided, as these three points would govern all different experiments tested: no (or rapid) oxidation, Fe (II) ideal rate of oxidation, and Fe (II) slowest oxidation.

Precipitates from Fe (III) quick addition at pH3, Fe (II)- H_2O_2 (3 hours), and Fe (II)- pO_2=0.2 bar (20 hours) had identical XRD spectra. They were all amorphous as no crystalline peaks of $FePO_4.2H_2O$ were visible. Also, the XRD spectra from different temperature experiments showed amorphous precipitate (as shown in supplementary material). **Figure 3-5** shows the measured XRD pattern for the proposed ideal precipitation system of Fe (II)-H_2O_2 (3 hours).

Samples from Fe (III) quick addition at pH3, Fe (II)- H_2O_2 (3 hours), and Fe (II)- pO_2=0.2 bar (20 hours) were also analyzed by Raman, (all spectra are shown in the supplementary material), the precipitates showed similar peaks. The Raman spectra of the precipitates were obtained in the region 900–2000 cm^{-1} at 298 K. Peaks at ≈1000 cm^{-1} were ascribed to the stretching vibrations of the PO_4^{3-}; peaks at ≈ 1600 cm^{-1} were assigned to HOH bending, and other peaks were observed at ≈606, 467, and 248 cm^{-1} (**Figure 3-5**). Precipitates were also analyzed at 298 K by SQUID. The magnetic moment (emu) was measured against the applied magnetic field (Oe). The magnetic susceptibility (emu Oe^{-1} g^{-1}) was calculated based on the slope shown in equation [2] and **Figure 3-5**, where M is the material's magnetization, and H is the magnetic field strength. The magnetic susceptibility was 6.7 $x10^{-5}$, 5.4$x10^{-5}$, and 5.4 $x10^{-5}$ emu Oe^{-1} g^{-1} for Fe (III) quick addition at pH3, Fe (II)- H_2O_2 (3 hours), and Fe (II)- pO_2=0.2 bar (20 hours) respectively. The detailed calculations are in the supplementary material.

$$M = x_v H \qquad [2]$$

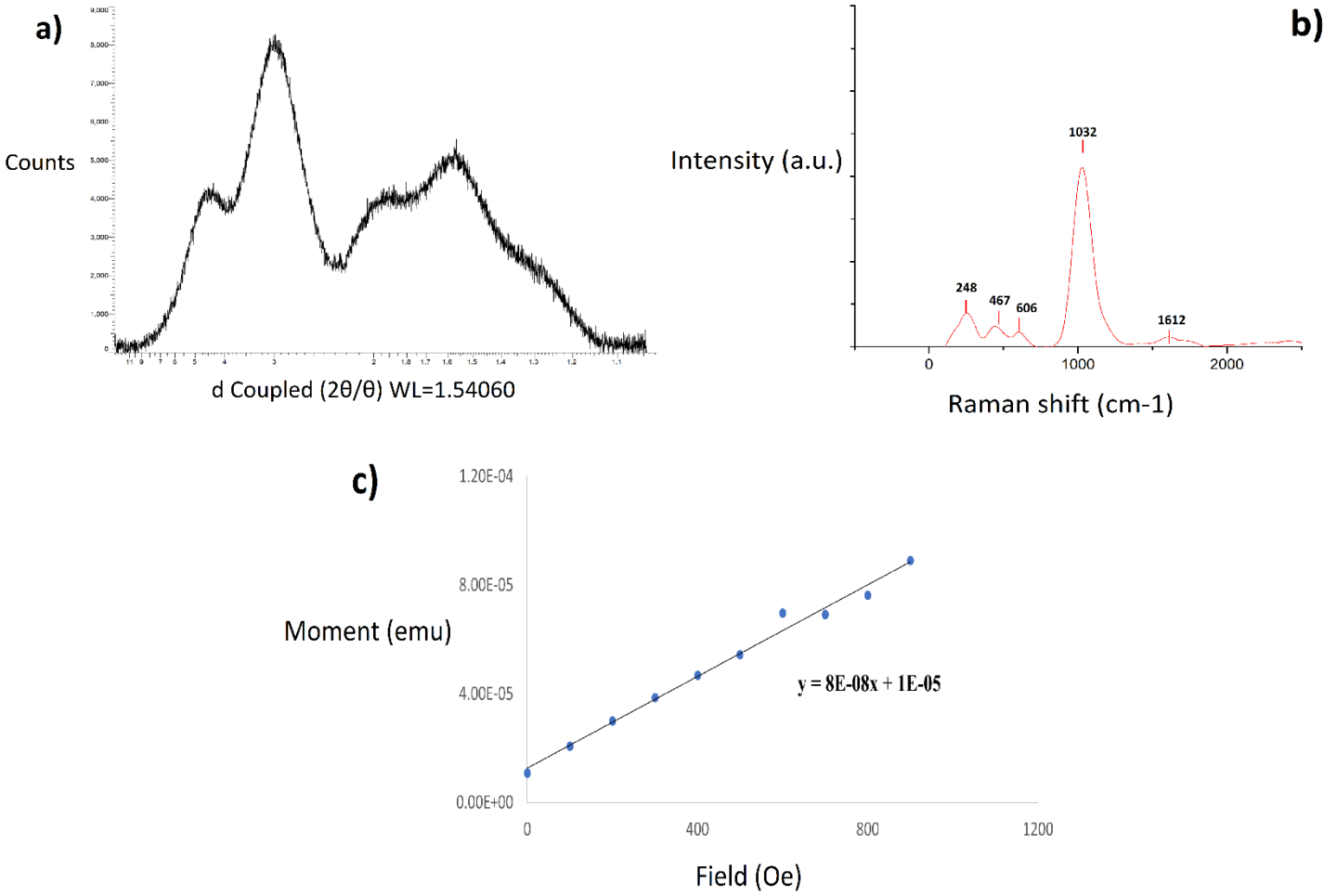

Figure 3-5: a) XRD powder pattern, b) Raman spectra, and c) SQUID measurement of the precipitate from Fe (II)-H_2O_2 (3 hours)

3.3.7 Proof of principle experiments on acidic by-product stream from EPS extraction process

Acidic samples were collected from the by-product stream from the EPS extraction process from aerobic granular sludge Epe WWTP in the Netherlands (Bahgat et al., 2023); the composition is shown in **Table 3-3**. The pH of the waste acidic by-product stream is usually between 2.5-3. The acidic liquid samples collected for these experiments from Epe WWTP had a pH of 2.5. In the first test, the quick addition of Fe (III) to the system without any pH adjustment was tested as it would be the easiest way to recover $FePO_4.2H_2O$ in WWTPs. Similar to the synthetic solution, pH dropped to 1.6 upon salt addition (low solubility range) and the recovery was low (75%). So, to ensure that the initial and final pH is within the optimum range to achieve the highest recovery and purity, it was adjusted to pH 3, and the experiments with a controlled dosage of Fe (III) and Fe (II)-H_2O_2 were performed to evaluate settleability. P recovery values were 95% and 99% for Fe (III)-(3 hours) and Fe (II)- H_2O_2 (3 hours) systems, respectively, with a Fe:P molar ratio of 1 for the dosed Fe. The elemental composition of the precipitates is shown in **Table 3-3** and it shows that organic precipitation also occurred. Additionally, it was observed during the experiments that the precipitate formed was brown, unlike the white precipitate observed in synthetic experiments. Moreover, the acidic liquid after precipitation became much less turbid and less brownish compared to its original state. Based on the percentages of Fe and P in the TS of the precipitate and the theoretical percentage in $FePO_4.2H_2O$, it is estimated that the purity of the product is around 60-65%. The difference in precipitate

settleability in both Fe (III)- (3 hours) and Fe (II)- H_2O_2 (3 hours) was not as significant as in the synthetic experiments, as both systems had a volumetric index of 16 ml/gP. The difference between the microscopic pictures in **Figure 3-6** showed that the precipitate clusters from the EPS extraction acidic waste stream looked bigger and denser than the synthetic precipitates.

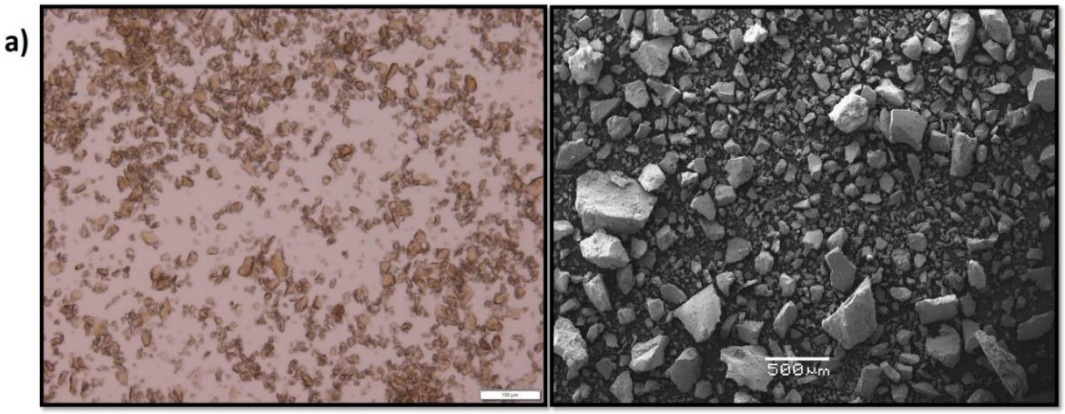

Figure 3-6: Iron phosphates precipitate from the acidic by-product stream of the EPS extraction process after dosing Fe (III) - 3 hours: a) optical microscope (wet sample) with 100 µm scale, b) SEM (dried sample).

Table 3-3: Elemental composition mg/L of the crude acidic by-product stream from EPS extraction and the TS% of the precipitates after the addition of Fe

Elements	EPS-acidic stream (mg/L)	Precipitate (%TS)	
COD	11600	**Fe (III)pH3-3h**	**Fe (II) H_2O_2- 3h**
P	P-$PO4^{3-}$=455 TP= 470	9.9	10.3
Fe	Fe^{2+}= 114, Fe^{3+}= 66 TFe= 185	19.9	20.1
K	4532	0.68	0.9
Al	35	0.07	0.09
Ca	157	0.09	0.13
Mg	78	0.02	0.03
Na	173	0.11	0.12
S	50	1	0.81
C	-	8.5	8.5
H	-	4.0	4.0
N	-	1.3	1.3
O	-	34	37

3.4 Discussion

3.4.1 $FePO_4.2H_2O$ identification

The formation of tiny particles that tend to agglomerate to form larger clusters or blocks was earlier reported by Lundager Madsen, 2014 and Lundager Madsen & Koch, 2018 when Fe (III) was used to form $FePO_4 \cdot 2H_2O$. They also reported that the precipitate formed under similar ambient conditions is nanocrystalline (XRD amorphous) which fits with our results. These observations align with findings by Hsu, 1982; Reale et al., 2003; Roncal-Herrero et al., 2009, who reported that XRD crystalline $FePO_4 \cdot 2H_2O$ forms only at high temperatures (150-200 Celsius) and that at ambient temperature range, amorphous phases of $FePO_4 \cdot 2H_2O$ are favored and can persist for a substantial time. The Raman spectrum peaks observed in this study were also compared to crystalline $FePO_4 \cdot 2H_2O$ compounds from the RRUFF database (shown in the supplementary material) and to Frost et al., 2004. The peaks observed at 1016 and 1629 cm^{-1} were similar to those observed in the spectrum for Strengite and metastrengite at around 1000 and 1600 cm^{-1}. Lundager Madsen & Koch, 2018 reported the formation of big orthorhombic crystals when Fe (II) was air oxidized at 35 Celsius for 15 days. However, this differs from what was observed in this work, as Fe (II) air oxidized at 25 Celsius for 10 days formed big aggregates of small particles observed by microscopy, while still being amorphous by XRD.

3.4.2 Fe (II) oxidation in acidic conditions

Fe (II) oxidation experiments showed that Fe (II) oxidation under open atmospheric conditions (pO_2=0.2 bar) was very limited, and it was accelerated by increasing the oxygen partial pressure (pO_2=1 and 1.5 bar) or by directly adding H_2O_2 as a replacement of oxygen. The Fe (II) oxidation via O_2 under acidic conditions is the rate-limiting step and how this step is skipped by the addition of H_2O_2 can be explained by the equilibrium chemistry of Fe (II) in aqueous solutions and some models reported in literature. Oxidation of Fe (II) in aqueous solutions is widely reported in the literature due to its presence in wide aquatic contexts such as fresh and marine water environments, acid mine drainage, and industrial water treatment processes. Stumm & Morgan, 1996 presented a kinetic equation for the oxidation of Fe(II) to Fe (III) with $O_{2(aq)}$ as the electron acceptor in which the rate of oxygenation of Fe (II) in solutions of pH≥ 5 is first-order with respect to the concentrations of both Fe (II) and O_2 and second order with respect to the ion OH^-, thus the oxidation reaction rate is strongly pH dependent. At pH 4 or below, the oxidation rate becomes very low and is fundamentally independent of pH. The slow oxidation rate at pH 4 or below can be explained by:

1) the equilibrium chemistry of Fe (II) in aqueous solutions, Morgan & Lahav, 2007 explained that at pH 4 or below, Fe^{2+} is the most dominant and ferrous hydroxide $FeOH^+$and $Fe(OH)_2$ species are almost negligible. Ferrous hydroxide species are the most significant for oxidation, as shown by the reaction constants in equation [3].

2) as shown in **Table 3-4**, thermodynamically, all oxidation steps (1), (2), and (3) are endergonic, but ΔG^0 decreases going from Fe^{2+} to $FeOH^+$ and $Fe(OH)_2$ based on the data calculated by Stumm & Morgan, 1996 , which explains the faster reaction at higher pH. Also, by combining equation reaction (0) with A, B, C, and D, we can conclude that reaction A is the slowest step and rate-determining as ΔG^0 for the full reaction is 89.8 kJ/mol, which explains the limited Fe (II) oxidation and P recovery in air oxidation experiments. These ΔG^0 values also show that adding directly H_2O_2 will fasten the Fe (II) oxidation process.

Based on the studies of Lowson, 1982; and Millero (1985), a heuristic model of the oxidation kinetics of Fe (II) to (III) by O_2 was proposed by Morgan & Lahav, 2007 where dFe(II)/dt is the rate of ferrous oxidation in mole per liter per min and rate constants were determined with pO_2=0.2 bar as shown in equation [3]. Since Fe^{2+} dominates at conditions below pH 4, so equation [3] can be further simplified to equation [4]. Based on the calculated Fe^{2+} oxidation rate and initial Fe^{2+} concentration in air oxidation experiments (pO_2=0.2 bar) the oxidation rate constant was calculated to be 6.3 x 10^{-5} min^{-1}, which is similar to the value suggested by the model.

$$-\frac{d[Fe^{2+}]}{dt} = 6 * 10^{-5}[Fe^{2+}] + 1.7\,[Fe(OH)^{+}] + 4.3 * 10^{5}[Fe(OH)_2^0] \quad [3]$$

$$-\frac{d[Fe2+]}{dt} = 6 * 10^{-5}[Fe^{2+}] \quad [4]$$

Table 3-4: ΔG^0 for the oxidation of Fe (II) and the One-Electron Steps in the reduction of O_2

Reaction number	Reaction equation	ΔG^0 (kJ/mol)
0	$Fe^{2+} \rightarrow Fe^{3+} + e^-$	74.2
1	$FeOH^+ \rightarrow FeOH^{2+} + e^-$	48.0
2	$Fe(OH)_2 \rightarrow Fe(OH)_2^+ + e^-$	3
A	$O_{2(aq)} + e^- \rightarrow O_2^{\cdot -}{}_{(aq)}$	15.5
B	$O_2^{\cdot -}{}_{(aq)} + e^- + 2\,H^+ \rightarrow H_2O_{2(aq)}$	-165.9
C	$H_2O_{2(aq)} + e^- + H^+ \rightarrow OH^{\cdot}_{(aq)} + H_2O$	-95.3
D	$OH^{\cdot}_{(aq)} + e^- + H^+ \rightarrow H_2O$	-244.9

3.4.3 $FePO_4.2H_2O$ separation methods

3.4.3..1 Fe (II) systems fast settleability

Improving settleability is an essential parameter in industrial-scale phosphorus precipitation processes. Quick and good settleability will minimize the loss of the precipitate due to washout, enhance phosphorus recovery efficiency, ensure effluent quality, and minimize separation equipment. Different factors can affect settling velocity, such as size, shape, and density of the precipitated particles (Tarragó et al., 2016). As presented in **Table 3-2**, using Fe (II) instead of Fe (III) to precipitate phosphate was better for settleability. The XRD spectra confirm that the precipitates in both Fe (II) and Fe (III) systems are amorphous, so the formation of bigger crystals is not the reason behind the improved settleability. The aggregates formed in both Fe (II)-O_2 or H_2O_2 systems appear bigger and denser, and the color of the particles under the microscope is more pronounced compared to Fe (III), as shown in the microscopic and SEM pictures in **Figure 3-3** and **Figure 3-4.** These denser aggregates in Fe (II) systems can be explained based on differences in surface charge (Kofina & Koutsoukos, 2005; Le Corre et al., 2007) or the effect of low initial supersaturation, which causes the metastable zone to be maintained for a longer time during growth; hence, particle aggregation is improved (Shaddel et al., 2019).

The volumetric index of the $FePO_4.2H_2O$ (strengite-like precipitates) calculated in the results section 3.3.5 was compared to previous indexes reported for magnesium and potassium struvite. Volumetric indexes were reported as 116 ml/gP for the conventional struvite precipitation

approach, and 15 ml/gP for a new approach using microwave-induced decomposition product of struvite pellet to achieve good solid-liquid separation of struvite by Chen et al., 2020. Wilsenach et al., 2007 also reported VI= 44 ml/gP and 310-500 ml/gP for ammonium and K-struvite, respectively. This comparison reflects that the ideal point chosen from our experiments (Fe (II) oxidation rate= 4.7 $x10^{-4}$ mol/l/min) indeed exhibits excellent settleability compared to common precipitation practices, as it had a volumetric index of only 8 ml/gP. Although Fe (II) oxidation by O_2 (slow oxidation) can further lower the VI of the precipitate to 2-3 ml/gP, it requires a long retention time to achieve acceptable recoveries, which is problematic in practice.

3.4.3..2 Magnetic separation

This research showed that excellent settleability of $FePO_4.2H_2O$ can be achieved, and the use of simple settling tanks is possible; however, magnetic separation of the precipitate is also possible. Precipitate characterization showed that $FePO_4$ $2H_2O$ precipitates are magnetic both from Fe (II) and Fe (III) systems. Mass susceptibility measurements were 6.7 $x10^{-5}$, 5.4$x10^{-5}$, and 5.4 $x10^{-5}$ emu Oe^{-1} g^{-1} for Fe (III) quick addition, Fe (II)-H_2O_2 (3 hours), and Fe (II)- pO_2=0.2 bar (20 hours), respectively. These measurements were in the same order of magnitude as the calculated values 6.74 x 10^{-5} emu Oe^{-1} g^{-1} for strengite and 6.37 x 10^{-5} emu Oe^{-1} g^{-1} for meta-strengite from molar susceptibility data reported by (Kim, 2009). However, little to no literature on strengite magnetic susceptibility exists. These measurements are significantly higher (x100) than the values reported for vivianite 8$x10^{-7}$ emu $Oe^{-1}g^{-1}$

(Minyuk et al., 2013). ViviMag is an upscaling project for the magnetic separation of vivianite from digested sewage sludge (Wijdeveld et al., 2022). Since $FePO_4.2H_2O$ precipitates have higher magnetic susceptibility, this could potentially allow for higher recovery/separation compared to vivianite with the same magnetic strength. This advanced separation technique can be useful for toxic or high organic load waste streams where co-settling can be problematic.

3.4.4 Proof of principle experiments on acidic by-product stream from EPS extraction process

Proof-of-principle experiments on the acidic samples from the EPS extraction process from AGS WWTPs were conducted to confirm the potential of integrating this technology to recover phosphorus from EPS installations. Experiments showed that the theoretical iron dosage to maintain the Fe: P molar ratio at 1 and the theoretical H_2O_2 dosage to maintain Fe: H_2O_2 at 2 were sufficient to achieve a phosphate recovery of over 95%. This was surprising, as it was expected that a higher Fe or H_2O_2 dosage would be required due to the presence of organics in these samples (COD=11600 mg/L). Complexation of Fe by organic matter presence was reported in the literature to alter iron speciation, redox reactivity by manipulating the energetics of the Fe (III)/Fe (II) redox couple, and possible electron transfer reactions (Wang et al., 2013). The Fenton reaction is widely reported to oxidize organic micropollutants under acidic conditions (Ijpelaar et al., 2002). Organics precipitated with $FePO_4.2H_2O$ as shown in the precipitate elemental analysis in **Table 3-3** and which was also observed during settling experiments as large

brown filaments were observed to settle in both Fe (III) and Fe (II) systems. Both systems exhibited a good volumetric index for the precipitate equal to 16 ml/gP, as the presence of organics significantly improved the settleability of the Fe (III) system. The exact mechanistic explanation of why organics enhance aggregation and settling is not clear yet in this study, but the presence of a high organic load could have altered the charge of the $FePO_4.2H_2O$ particles, leading to their rapid settleability in Fe (III) systems, making it comparable to the Fe (II)-H_2O_2 system (Angelico et al., 2014; Dalas et al., 1990). It is shown that Fe (III) can be added to the current EPS extraction installations to achieve high phosphate recovery and good settleability instead of the Fe (II)-H_2O_2 system. However, to obtain a pure product, it may be necessary, depending on the intended application, to remove the organics priorly with ultrafiltration to prevent undesired precipitation and utilize the Fe (II)-H_2O_2 system instead.

3.5 Outlook

The recovery of phosphorus as $FePO_4 \cdot 2H_2O$ (strengite-like compounds) from acidic waste liquid streams represents a novel research avenue, yet numerous research gaps remain to be explored. The primary research gap pertains to the fundamental understanding of $FePO_4 \cdot 2H_2O$ formation in the presence of Fe (II)-H_2O_2, aiming to determine whether the regulation of supersaturation, charge, or both accounts for the denser agglomeration and rapid settleability observed in these systems. It is also proposed to perform particle size measurements for the precipitate to confirm that the formation of larger agglomerations in Fe

(II)-H_2O_2 systems contributes to improved settleability. The second research gap involves the process optimization of real waste streams and the potential challenges associated with upscaling. It would be intriguing to evaluate other acidic municipal and industrial streams and to assess the functionality of the Fe (II)-H_2O_2 system. Although our experiments were not conducted at different initial concentrations, the outcomes based on the Fe (II) oxidation rate versus recovery and settleability curve are still anticipated. A higher concentration of phosphorus would necessitate a slower addition of Fe (II) to the system to achieve the optimum Fe (II) oxidation rate. For lower concentrations, Fe (II) addition would be quicker, resulting in a faster process, which is advantageous. However, dedicated experiments to investigate the formation mechanism should be conducted in future research to also evaluate if the surface charge (e.g., measuring zeta potential) plays a role in settleability and if changing the concentrations would influence the surface charge, as it alters the saturation levels.

To facilitate the potential scale-up of the technology, it is also recommended to conduct a detailed economic analysis of the Fe (II)-H_2O_2 method of phosphorus recovery, comparing it with other conventional phosphorus recovery processes such as struvite or vivianite recovery. At this stage, an estimation of economic comparison based on OPEX (operating expenses, e.g., Fe salt usage, addition of chemicals such as NaOH or KOH, and H_2O_2) has been performed. The analysis indicates that the recovery of $FePO_4 \cdot 2H_2O$ via the Fe (II)- H_2O_2 method will be at least 2 times more cost-effective than vivianite recovery from EPS extraction acidic by-product stream. Detailed calculations are provided

in the supplementary material. Although the CAPEX remains unknown at this stage, it is anticipated that it will be lower for $FePO_4 \cdot 2H_2O$ recovery due to the novel method developed in this study, which enables the recovery of gravity-settleable precipitates without the need for engineered crystallizers, as required by vivianite recovery. The third research gap involves evaluating and testing the potential applications of such recovery products in fertilization or the manufacturing process of electrode materials, catalysts, precursors of $LiFePO_4$, or as an adsorbent for lead pollutants (Li et al., 2020; Reale et al., 2003; Y. Wang et al., 2018; Zhou et al., 2017). This would require double-checking the purity of $FePO_4.2H_2O$ recovered from different acidic streams, and how it is comparable to calcium phosphates, struvite, or vivianite.

3.6 Conclusion

Recovery of $FePO_4.2H_2O$ from acidic streams appears promising due to its simplicity and high efficiency, while also reducing the need for pH adjustment and excessive usage of ferric salts. However, an integrated optimization of recovery efficiency and product properties (aggregation and settling) is necessary to achieve feasible recovery from low pH and phosphate-rich streams. This research presents a novel strategy to integrate Fe (II) and H_2O_2 controlled dosing systems as the best approach to achieve high P% recovery (> 95%) and form a quick-settling precipitate with a volumetric index equal to only 8 ml/gP. The Fe (II) oxidation rate is the design parameter to enhance the settling process without adding a carrier material or further crystallizers. Extremely low Fe (II) oxidation rates will result in a quick-settling

precipitate but a low recovery percentage over short durations, while rapid oxidation rates will result in a high recovery percentage over short durations but poor settleability. Accordingly, the oxidation rate value of $4.7x10^{-4}$ mol/l/min was the optimum point for achieving both high recovery and settling. Experiments on the acidic by-product stream from EPS extraction installations confirmed high phosphate recovery (> 95%) while dosing the theoretical amounts of Fe and H_2O_2. Additionally, the organics present in that stream enhanced aggregation and settling. The mechanism is not yet fully understood, requiring further experiments in future research. $FePO_4.2H_2O$ compounds have potential applications in fertilization, lithium batteries, and electrode materials production.

References

Ain Zainuddin, N., Azwan Raja Mamat, T., Imam Maarof, H., Wahidah Puasa, S., & Rohana Mohd Yatim, S. (2019). Removal of Nickel, Zinc and Copper from Plating Process Industrial Raw Effluent Via Hydroxide Precipitation Versus Sulphide Precipitation. IOP Conference Series: Materials Science and Engineering, 551(1). https://doi.org/10.1088/1757-899X/551/1/012122

Anastácio, A. S., Harris, B., Yoo, H. I., Fabris, J. D., & Stucki, J. W. (2008). Limitations of the ferrozine method for quantitative assay of mineral systems for ferrous and total iron. Geochimica et Cosmochimica Acta, 72(20). https://doi.org/10.1016/j.gca.2008.07.009

Angelico, R., Ceglie, A., He, J. Z., Liu, Y. R., Palumbo, G., & Colombo, C. (2014). Particle size, charge and colloidal stability of humic acids coprecipitated with ferrihydrite. Chemosphere, 99. https://doi.org/10.1016/j.chemosphere.2013.10.092

Ashley, K., Cordell, D., & Mavinic, D. (2011). A brief history of phosphorus: From the philosopher's stone to nutrient recovery and reuse. Chemosphere, 84(6). https://doi.org/10.1016/j.chemosphere.2011.03.001

Bahgat, N. T., Wilfert, P., Korving, L., & van Loosdrecht, M. (2023). Integrated resource recovery from aerobic granular sludge plants. Water Research, 234. https://doi.org/10.1016/j.watres.2023.119819

Carvalho, F., Prazeres, A. R., & Rivas, J. (2013). Cheese whey wastewater: Characterization and treatment. In Science of the Total Environment (Vols. 445–446). https://doi.org/10.1016/j.scitotenv.2012.12.038

CHAKRAVARTI, S. N., & TALIBUDEEN, O. (1962). PHOSPHATE EQUILIBRIA IN ACID SOILS. Journal of Soil Science, 13(2). https://doi.org/10.1111/j.1365-2389.1962.tb00701.x

Chen, S., Yang, Y., Zheng, M., Cheng, X., Xu, K., & Dou, X. (2020). Thermal decomposition of struvite pellet by microwave radiation and recycling of its product to remove ammonium and phosphate from urine. Environmental Research, 188. https://doi.org/10.1016/j.envres.2020.109774

Childers, D. L., Corman, J., Edwards, M., & Elser, J. J. (2011). Sustainability challenges of phosphorus and food: Solutions from closing the human phosphorus cycle. BioScience, 61(2). https://doi.org/10.1525/bio.2011.61.2.6

Cichy, B., Kużdżał, E., & Krztoń, H. (2019). Phosphorus recovery from acidic wastewater by hydroxyapatite precipitation. Journal of Environmental Management, 232. https://doi.org/10.1016/j.jenvman.2018.11.072

Dalas, E., Koutsoukos, P., & Karaiskakis, G. (1990). The effect of carrier solution on the particle size distribution of inorganic colloids measured by steric field-flow fractionation. Colloid & Polymer Science, 268(2). https://doi.org/10.1007/BF01513194

Danalewich, J. R., Papagiannis, T. G., Belyea, R. L., Tumbleson, M. E., & Raskin, L. (1998). Characterization of dairy waste streams, current treatment practices, and potential for biological nutrient removal. Water Research, 32(12). https://doi.org/10.1016/S0043-1354(98)00160-2

Desmidt, E., Ghyselbrecht, K., Zhang, Y., Pinoy, L., Van Der Bruggen, B., Verstraete, W., Rabaey, K., & Meesschaert, B. (2015). Global phosphorus scarcity and full-scale P-recovery techniques: A review. Critical Reviews in Environmental Science and Technology, 45(4). https://doi.org/10.1080/10643389.2013.866531

Doyle, J. D., & Parsons, S. A. (2002). Struvite formation, control and recovery. In Water Research (Vol. 36, Issue 16). https://doi.org/10.1016/S0043-1354(02)00126-4

Eastman, K. (2017). Digital Commons @ Montana Tech SUPERGENE MINERALIZATION OF THE CONTINENTAL PIT, BUTTE, SILVER BOW COUNTY, MONTANA. http://digitalcommons.mtech.edu/grad_rschhttp://digitalcommons.mtech.edu/grad_rsch/125

Eicher, N. (2018). The LeachPhos process at the waste-to-energy plant Bern (Switzerland). In Phosphorus: Polluter and Resource of the Future – Removal and Recovery from Wastewater. https://doi.org/10.2166/9781780408361_411

ESPP webinar. (2020). Summary of joint European Commission-ESPP webinar on P4 (phosphorus) Critical Raw Material. www.phosphorusplatform.eu

Eynard, U., Wittmer, D., Latunussa, C., & Di Milano, P. (2020). Study on the EU's list of Critical Raw Materials (2020) Non-Critical Raw Materials Factsheets SAFEWATER View project Design for Sustainability Fiji View project. https://doi.org/10.2873/587825

Frossard, E., Bauer, J. P., & Lothe, F. (1997). Evidence of vivianite in FeSO4 - Flocculated sludges. Water Research, 31(10). https://doi.org/10.1016/S0043-1354(97)00101-2

Frost, R. L., Weier, M. L., Erickson, K. L., Carmody, O., & Mills, S. J. (2004). Raman spectroscopy of phosphates of the variscite mineral group. Journal of Raman Spectroscopy, 35(12), 1047–1055. https://doi.org/10.1002/jrs.1251

Hsu, P. H. (1982). Crystallization of Iron(III) Phosphate at Room Temperature. Soil Science Society of America Journal, 46(5). https://doi.org/10.2136/sssaj1982.03615995004600050009x

Ijpelaar, G. F., Groenendijk, M., Kruithof, J. C., & Schippers, J. C. (2002). Fenton process for the combined removal of iron and organic micropollutants in groundwater treatment. Water Science and Technology: Water Supply, 2(2). https://doi.org/10.2166/ws.2002.0068

Iuliano, M., Ciavatta, L., & De Tommaso, G. (2007). On the Solubility Constant of Strengite. Soil Science Society of America Journal, 71(4). https://doi.org/10.2136/sssaj2006.0109

Iwama, T., Du, C. M., Koizumi, S., Gao, X., Ueda, S., & Kitamura, S. Y. (2020). Extraction of phosphorus and recovery of phosphate from steelmaking slag by selective leaching. ISIJ International, 60(2). https://doi.org/10.2355/isijinternational.ISIJINT-2019-298

Jones, A. M., Griffin, P. J., Collins, R. N., & Waite, T. D. (2014). Ferrous iron oxidation under acidic conditions - The effect of ferric oxide surfaces. Geochimica et Cosmochimica Acta, 145. https://doi.org/10.1016/j.gca.2014.09.020

Kim, J. (2009). Investigation of Surface Adsorption of Li + and Phosphate on Iron Oxyhydroxides via Solid-State NMR Spectroscopy. https://dspace.sunyconnect.suny.edu/bitstream/handle/1951/52354/000000842.sbu.pdf?sequence=1

Kofina, A. N., & Koutsoukos, P. G. (2005). Spontaneous precipitation of struvite from synthetic wastewater solutions. Crystal Growth and Design, 5(2). https://doi.org/10.1021/cg049803e

Koh, K. Y., Zhang, S., & Chen, J. P. (2020). Improvement of Ultrafiltration for Treatment of Phosphorus-Containing Water by a Lanthanum-Modified Aminated Polyacrylonitrile Membrane. ACS Omega, 5(13). https://doi.org/10.1021/acsomega.9b03573

Kratz, S., Schick, J., & Schnug, E. (2016). Trace elements in rock phosphates and P containing mineral and organo-mineral fertilizers sold in Germany. Science of the Total Environment, 542. https://doi.org/10.1016/j.scitotenv.2015.08.046

Le Corre, K. S., Valsami-Jones, E., Hobbs, P., Jefferson, B., & Parsons, S. A. (2007). Struvite crystallisation and recovery using a stainless steel structure as a seed material. Water Research, 41(11). https://doi.org/10.1016/j.watres.2007.03.002

Lei, Y., Zhan, Z., Saakes, M., van der Weijden, R. D., & Buisman, C. J. N. (2022). Electrochemical Recovery of Phosphorus from Acidic Cheese Wastewater: Feasibility, Quality of Products, and Comparison with Chemical Precipitation. ACS ES and T Water, 1(4). https://doi.org/10.1021/acsestwater.0c00263

Leo, C. P., Chai, W. K., Mohammad, A. W., Qi, Y., Hoedley, A. F. A., & Chai, S. P. (2011). Phosphorus removal using nanofiltration membranes. Water Science and Technology, 64(1). https://doi.org/10.2166/wst.2011.598

Li, R., Li, Q., Sun, X., Li, J., Shen, J., Han, W., & Wang, L. (2020). Removal of lead complexes by ferrous phosphate and iron phosphate: Unexpected favorable role of ferrous ions. Journal of Hazardous Materials, 392. https://doi.org/10.1016/j.jhazmat.2020.122509

Lowson, R. T. (1982). Aqueous Oxidation of Pyrite by Molecular Oxygen. Chemical Reviews, 82(5). https://doi.org/10.1021/cr00051a001

Lundager Madsen, H. E. (2014). Redox process catalysed by growing crystal - Strengite, FePO4,2H2O, crystallizing from solution with iron(II) and hydroxylamine. Journal of Crystal Growth, 401. https://doi.org/10.1016/j.jcrysgro.2013.11.025

Lundager Madsen, H. E., & Koch, C. B. (2018). Kinetics of solution crystal growth of strengite, FePO4,2H2O. Journal of Crystal Growth, 482. https://doi.org/10.1016/j.jcrysgro.2017.10.014

Luyckx, L., Sousa Correia, D. S., & Van Caneghem, J. (2021). Linking Phosphorus Extraction from Different Types of Biomass Incineration Ash to Ash Mineralogy, Ash Composition and Chemical Characteristics of Various Types of Extraction Liquids. Waste and Biomass Valorization, 12(9). https://doi.org/10.1007/s12649-021-01368-3

Marchioretto, M. M., Bruning, H., & Rulkens, W. (2005). Heavy metals precipitation in sewage sludge. Separation Science and Technology, 40(16). https://doi.org/10.1080/01496390500423748

Martin, N., Ya, V., Leewiboonsilp, N., Choo, K. H., Noophan, P. (Lek), & Li, C. W. (2020). Electrochemical crystallization for phosphate recovery from an electronic industry wastewater effluent using sacrificial iron anodes. Journal of Cleaner Production, 276. https://doi.org/10.1016/j.jclepro.2020.124234

Metcalf, W., & Eddy, C. (2014). Wastewater Engineering: Treatment and Resource Recovery, Fifth Edition. In Wastewater Engineering: Treatment and Resource Recovery, Fifth Edition.

Meyer, C., Preyl, V., Steinmetz, H., Maier, W., Mohn, R. E., & Schönberger, H. (2018). The stuttgart process (Germany). In Phosphorus Recovery and Recycling. https://doi.org/10.1007/978-981-10-8031-9_19

Millero, F. J. (1985). The effect of ionic interactions on the oxidation of metals in natural waters. Geochimica et Cosmochimica Acta, 49(2). https://doi.org/10.1016/0016-7037(85)90046-8

Minyuk, P. S., Subbotnikova, T. V., Brown, L. L., & Murdock, K. J. (2013). High-temperature thermomagnetic properties of vivianite nodules, Lake El'gygytgyn, Northeast Russia. Climate of the Past, 9(1). https://doi.org/10.5194/cp-9-433-2013

Monat, L., Zhang, W., Jarošíková, A., Haung, H., Bernstein, R., & Nir, O. (2022). Circular Process for Phosphoric Acid Plant Wastewater Facilitated by Selective Electrodialysis. ACS Sustainable Chemistry and Engineering, 10(35). https://doi.org/10.1021/acssuschemeng.2c03132

Morgan, B., & Lahav, O. (2007a). The effect of pH on the kinetics of spontaneous Fe(II) oxidation by O2 in aqueous solution - basic principles and a simple heuristic description. Chemosphere, 68(11). https://doi.org/10.1016/j.chemosphere.2007.02.015

Morgan, B., & Lahav, O. (2007b). The effect of pH on the kinetics of spontaneous Fe(II) oxidation by O2 in aqueous solution - basic principles and a simple heuristic description. Chemosphere, 68(11). https://doi.org/10.1016/j.chemosphere.2007.02.015

Nawghare, P., Rao, N. N., Bejankiwar, R., Szyprkowicz, L., & Kaul, S. N. (2001). Treatment of phosphoric acid plant wastewater using Fenton's reagent and coagulants. Journal of Environmental Science and Health - Part A Toxic/Hazardous Substances and Environmental Engineering, 36(10). https://doi.org/10.1081/ESE-100107444

Nriagu, J. O. (1972). Solubility equilibrium constant of strengite. American Journal of Science, 272(5). https://doi.org/10.2475/ajs.272.5.476

Oxmann, J. F., & Schwendenmann, L. (2014). Quantification of octacalcium phosphate, authigenic apatite and detrital apatite in coastal sediments using differential dissolution and standard addition. Ocean Science, 10(3). https://doi.org/10.5194/os-10-571-2014

Priambodo, R., Shih, Y. J., & Huang, Y. H. (2017a). Phosphorus recovery as ferrous phosphate (vivianite) from wastewater produced in manufacture of thin film transistor-liquid crystal displays (TFT-LCD) by a fluidized bed crystallizer (FBC). RSC Advances, 7(65). https://doi.org/10.1039/c7ra06308c

Priambodo, R., Shih, Y. J., & Huang, Y. H. (2017b). Phosphorus recovery as ferrous phosphate (vivianite) from wastewater produced in manufacture of thin film transistor-liquid crystal displays (TFT-LCD) by a fluidized bed crystallizer (FBC). RSC Advances, 7(65). https://doi.org/10.1039/c7ra06308c

Reale, P., Scrosati, B., Delacourt, C., Wurm, C., Morcrette, M., & Masquelier, C. (2003a). Synthesis and Thermal Behavior of Crystalline Hydrated Iron(III) Phosphates of Interest as Positive Electrodes in Li Batteries. Chemistry of Materials, 15(26). https://doi.org/10.1021/cm031107z

Reale, P., Scrosati, B., Delacourt, C., Wurm, C., Morcrette, M., & Masquelier, C. (2003b). Synthesis and Thermal Behavior of Crystalline Hydrated Iron(III) Phosphates of Interest as Positive Electrodes in Li Batteries. Chemistry of Materials, 15(26). https://doi.org/10.1021/cm031107z

Ridder, M. de. (2012). Risks and opportunities in the global phosphate rock market : robust strategies in times of uncertainty. The Hague Centre for Strategic Studies.

Roncal-Herrero, T., Rodríguez-Blanco, J. D., Benning, L. G., & Oelkers, E. H. (2009). Precipitation of iron and aluminum phosphates directly from aqueous solution as a function of temperature from 50 to 200 °C. Crystal Growth and Design, 9(12), 5197–5205. https://doi.org/10.1021/cg900654m

Shaddel, S., Ucar, S., Andreassen, J. P., & Sterhus, S. W. (2019). Engineering of struvite crystals by regulating supersaturation - Correlation with phosphorus recovery, crystal morphology and process efficiency. Journal of Environmental Chemical Engineering, 7(1). https://doi.org/10.1016/j.jece.2019.102918

Slavov, A. K. (2017). General characteristics and treatment possibilities of dairy wastewater -a review. In Food Technology and Biotechnology (Vol. 55, Issue 1). https://doi.org/10.17113/ft b.55.01.17.4520

Smit, A. L., Bindraban, P. S., Shroeder, J. J., Conijin, J. G., & G, V. D. M. H. (2009). Phosphorus in agriculture: global resources, trends and developments [C]. Wageningen, Plant Research International BV, 282(January 2009).

Stumm, & Morgan. (1996). Aquatic chemistry: chemical equilibria and rates in natural waters. Choice Reviews Online, 33(11). https://doi.org/10.5860/choice.33-6312

Takács, I., Murthy, S., Smith, S., & McGrath, M. (2006). Chemical phosphorus removal to extremely low levels: Experience of two plants in the Washington, DC area. Water Science and Technology, 53(12). https://doi.org/10.2166/wst.2006.402

Tarragó, E., Puig, S., Ruscalleda, M., Balaguer, M. D., & Colprim, J. (2016). Controlling struvite particles' size using the up-flow velocity. Chemical Engineering Journal, 302. https://doi.org/10.1016/j.cej.2016.06.036

Thant Zin, M. M., & Kim, D. J. (2019). Struvite production from food processing wastewater and incinerated sewage sludge ash as an alternative N and P source: Optimization of multiple resources recovery by response surface methodology. Process Safety and Environmental Protection, 126. https://doi.org/10.1016/j.psep.2019.04.018

Truong, G. Le, De Laat, J., & Legube, B. (2004). Effects of chloride and sulfate on the rate of oxidation of ferrous ion by H2O2. Water Research, 38(9). https://doi.org/10.1016/j.watres.2004.01.033

van Dijk, K. C., Lesschen, J. P., & Oenema, O. (2016). Phosphorus flows and balances of the European Union Member States. Science of the Total Environment, 542. https://doi.org/10.1016/j.scitotenv.2015.08.048

Wang, Y., Feng, Z., Laul, D., Zhu, W., Provencher, M., Trudeau, M. L., Guerfi, A., & Zaghib, K. (2018). Ultra-low cost and highly stable hydrated FePO4 anodes for aqueous sodium-ion battery. Journal of Power Sources, 374, 211–216. https://doi.org/10.1016/j.jpowsour.2017.10.088

Wang, Z., Bush, R. T., & Liu, J. (2013). Arsenic(III) and iron(II) co-oxidation by oxygen and hydrogen peroxide: Divergent reactions in the presence of organic ligands. Chemosphere, 93(9). https://doi.org/10.1016/j.chemosphere.2013.06.076

Wijdeveld, W. K., Prot, T., Sudintas, G., Kuntke, P., Korving, L., & van Loosdrecht, M. C. M. (2022). Pilot-scale magnetic recovery of vivianite from digested sewage sludge. Water Research, 212. https://doi.org/10.1016/j.watres.2022.118131

Wilfert, P., Mandalidis, A., Dugulan, A. I., Goubitz, K., Korving, L., Temmink, H., Witkamp, G. J., & Van Loosdrecht, M. C. M. (2016). Vivianite as an important iron phosphate precipitate in sewage treatment plants. Water Research, 104. https://doi.org/10.1016/j.watres.2016.08.032

Wilsenach, J. A., Schuurbiers, C. A. H., & van Loosdrecht, M. C. M. (2007). Phosphate and potassium recovery from source separated urine through struvite precipitation. Water Research, 41(2). https://doi.org/10.1016/j.watres.2006.10.014

Xing, C., Shi, J., Cui, F., Shen, J., & Li, H. (2021). Fe2+/H2O2-Strengite method with the enhanced settlement for phosphorus removal and recovery from pharmaceutical effluents. Chemosphere, 277. https://doi.org/10.1016/j.chemosphere.2021.130343

Zhang, J. C., Wu, C. J., & Yu, D. M. (2019). Effect of phosphoric acid in the pre-hydrolysis process of dissolving pulp production from Bamboo-willow. BioResources, 14(2). https://doi.org/10.15376/biores.14.2.3117-3131

Zhang, T., Lu, Y., & Luo, G. (2017). Effects of temperature and phosphoric acid addition on the solubility of iron phosphate dihydrate in aqueous solutions. Chinese Journal of Chemical Engineering, 25(2). https://doi.org/10.1016/j.cjche.2016.06.009

Zhou, D., Qiu, X., Liang, F., Cao, S., Yao, Y., Huang, X., Ma, W., Yang, B., & Dai, Y. (2017). Comparison of the effects of FePO4 and FePO4·2H2O as precursors on the electrochemical performances of LiFePO4/C. Ceramics International, 43(16), 13254–13263. https://doi.org/10.1016/j.ceramint.2017.07.023

1. Visual Minteq:

Mineral	log IAP	Sat. Index (=log IAP - log Ks)	Stoichiometry and mineral components							
Femihydrite	1.273	-1.927	1	Fe+3	3	H2O	-3	H+1		
Femihydrite (aged)	1.273	-1.417	1	Fe+3	-3	H+1	3	H2O		
Goethite	1.275	0.784	1	Fe+3	2	H2O	-3	H+1		
Hematite	2.553	3.971	2	Fe+3	3	H2O	-6	H+1		
Lepidocrocite	1.275	-0.096	-3	H+1	1	Fe+3	2	H2O		
Maghemite	2.553	-3.833	-6	H+1	2	Fe+3	3	H2O		
Strengite	-22.607	3.793	1	Fe+3	1	PO4-3	2	H2O		

Distribution of components between dissolved, sorbed and precipitated phases

(Concentrations in molal)

Component	Total dissolved	% dissolved	Total sorbed	% sorbed	Total precipitated	% precipitated
Fe+3	6.4543E-05	0.076	0	0.000	8.4935E-02	99.924
H+1	3.6313E-02	100.000	0	0.000	0	0.000
PO4-3	6.4539E-05	0.076	0	0.000	8.4935E-02	99.924

Figure S3-1: Visual Minteq Modelling, 0.085M Fe^{3+} and P solutions, pH=1.5, temperature 25C

2- XRD spectra

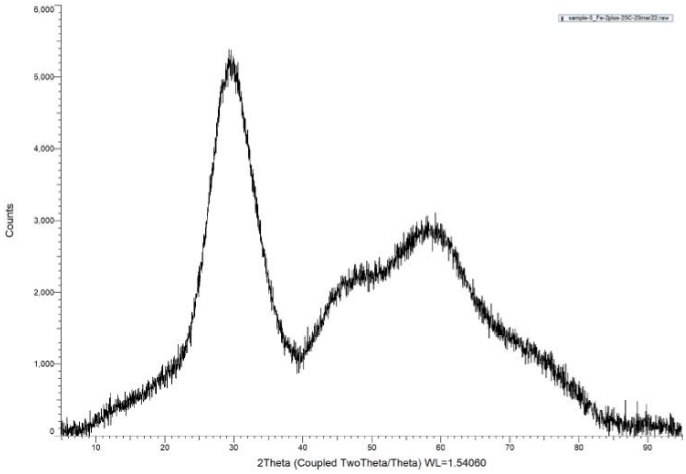

Figure S3-2: XRD of Fe^{3+} quick addition pH3 precipitate

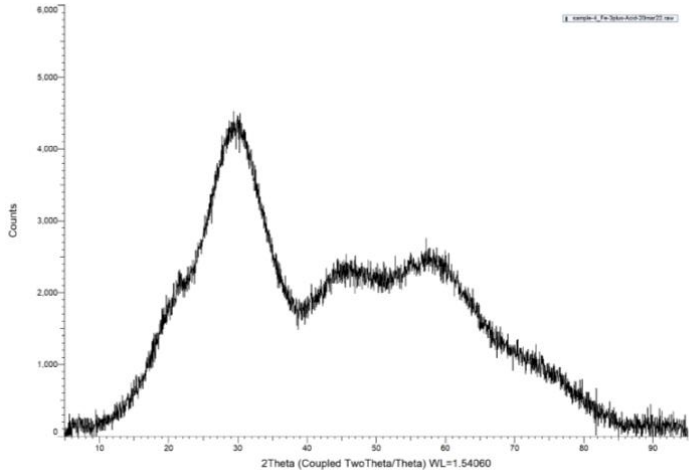

Figure S3-3: XRD of the precipitate from the real acidic stream from EPS extraction process

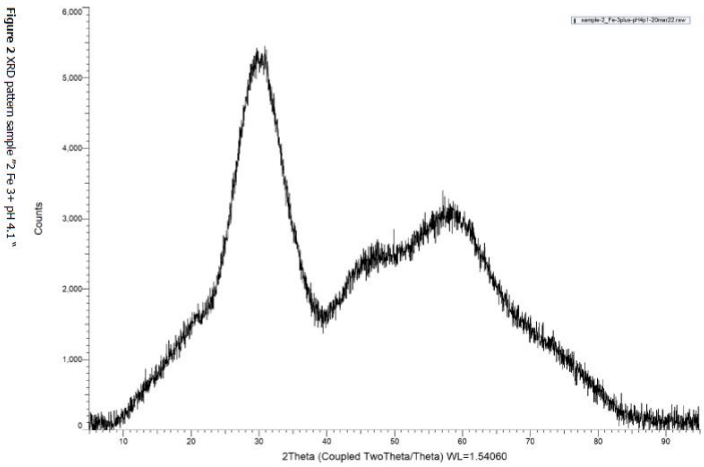

Figure S3-4: XRD of pO2=0.2 bar-Fe (II)-20 hours precipitate

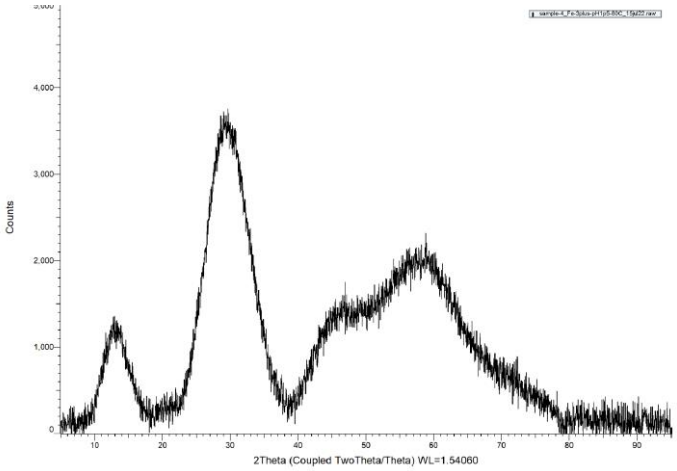

Figure S3-5: XRD of Fe^{3+} quick addition pH1.5 at 80 Celsius

3- Raman spectra

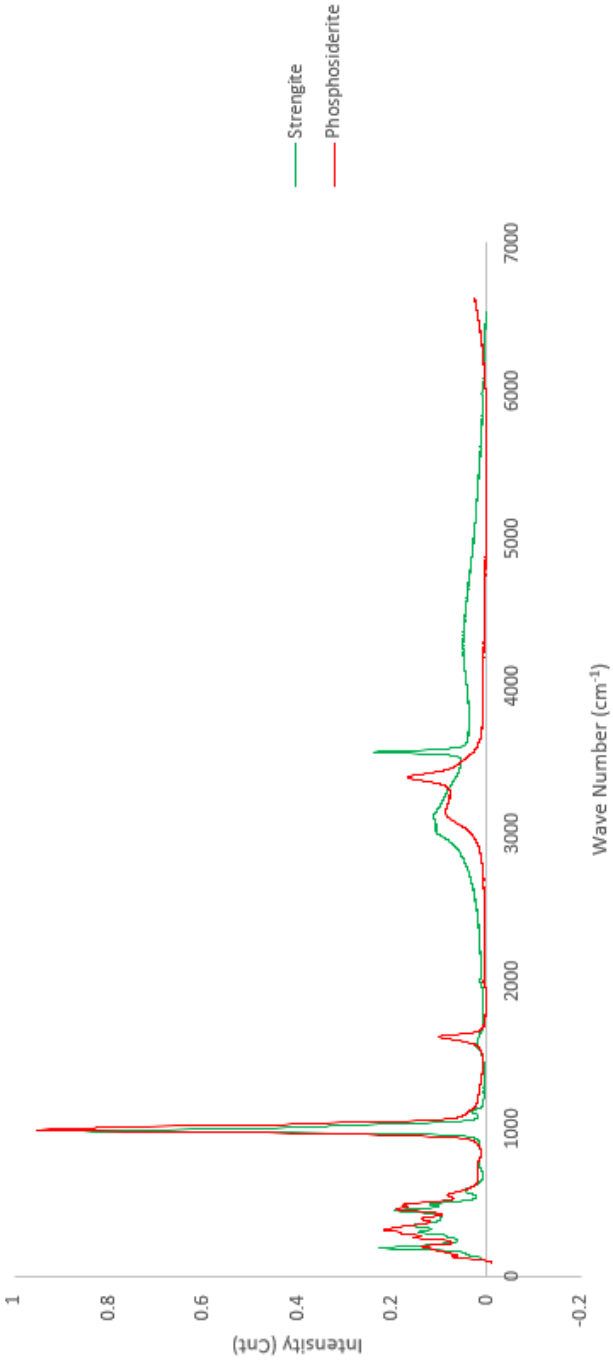

Figure S3-6: RRUFF database- Raman spectra of $FePO_4.2H_2O$

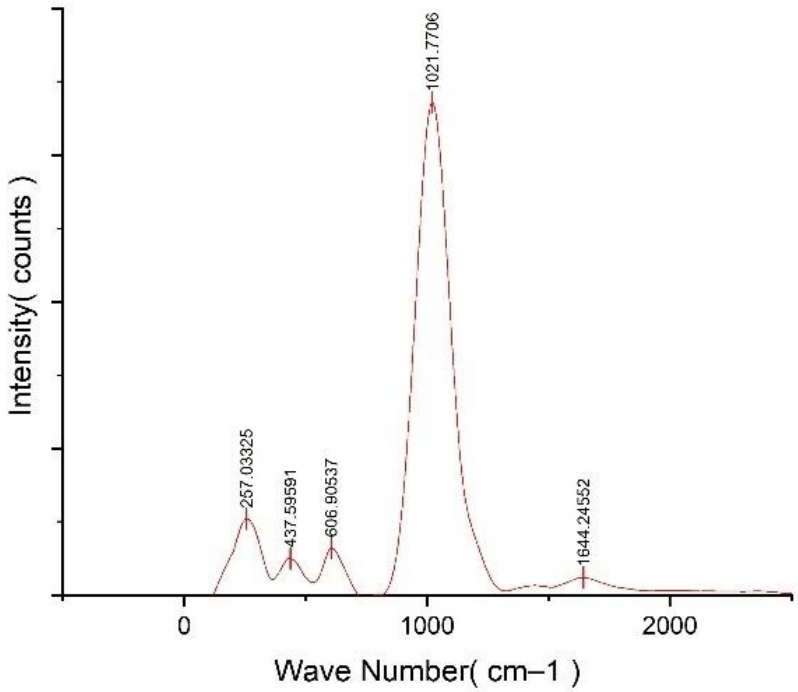

Figure S3-7: Raman spectrum of Fe3+ quick addition pH3 precipitate

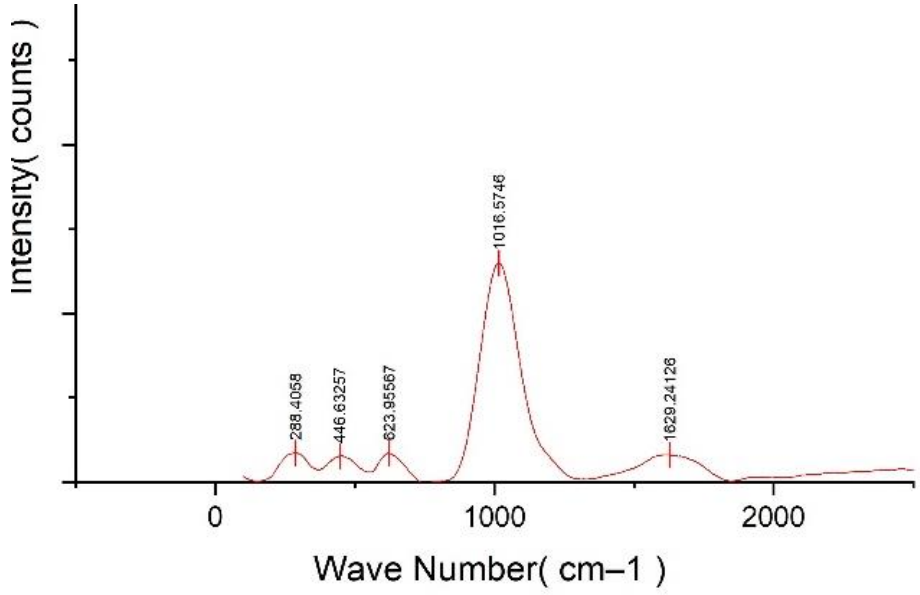

Figure S3-8: Raman spectrum of pO2=0.2 bar-Fe (II)-20 hours precipitate

4. SQUID measurements

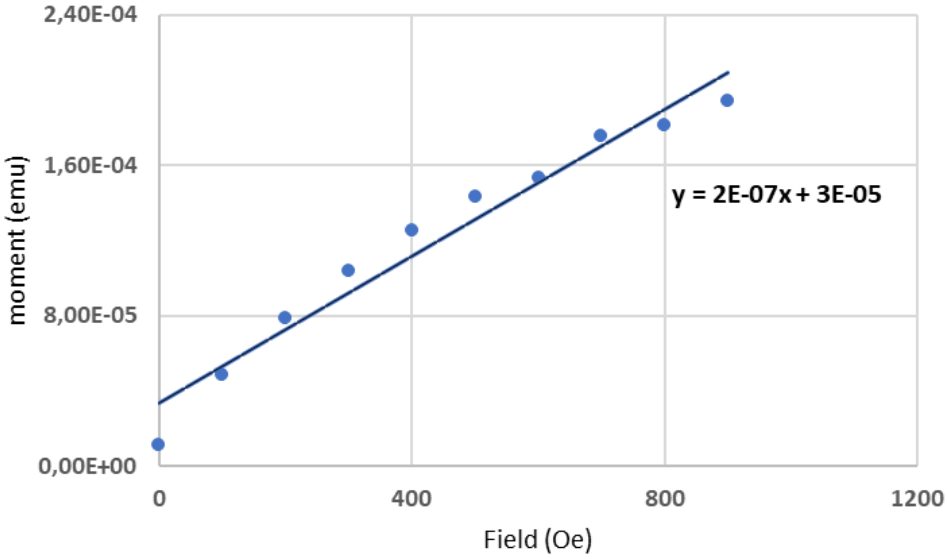

Figure S3-9: SQUID measurement of pO2=0.2 bar-Fe (II)-20 hours precipitate

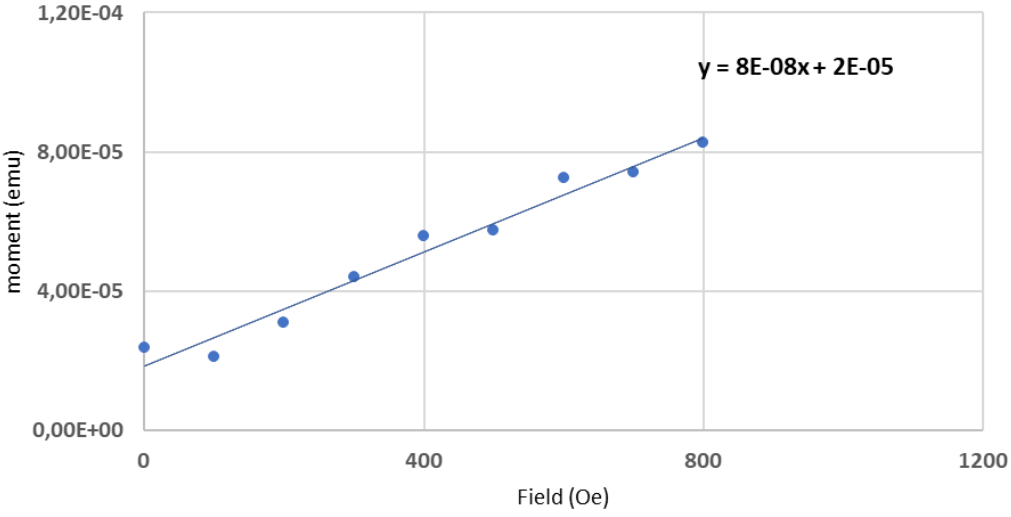

Figure S3-10: SQUID measurement of Fe3+ quick addition pH3 precipitate

5- Sigma Plot curve fitting

Nonlinear Regression **donderdag 16 maart 2023 16:10:46**

Data Source: Data 1 in IronOxidation_Settling_Recovery
Equation: Sigmoidal; Sigmoid, 4 Parameter
f = y0+a/(1+exp(-(x-x0)/b))

R	Rsqr	Adj Rsqr	Standard Error of Estimate
1,0000	1,0000	1,0000	0,1420

	Coefficient	Std. Error	t	P
a	98,1186	0,2970	330,3534	<0,0001
b	0,2615	0,0039	67,6151	<0,0001
x0	-4,4654	0,0017	-2659,3552	<0,0001
y0	0,9428	0,2713	3,4749	0,0402

Analysis of Variance:

	DF	SS	MS
Regression	4	42756,9395	10689,2349
Residual	3	0,0605	0,0202
Total	7	42757,0000	6108,1429

Corrected for the mean of the observations:

	DF	SS	MS
Regression	3	9153,3680	3051,1227
Residual	3	0,0605	0,0202
Total	6	9153,4286	1525,5714

95% Confidence:

Row	Predicted	95% Conf-L	95% Conf-U	95% Pred-L	95% Pred-U
1	5,0170	4,5661	5,4680	4,3785	5,6556
2	34,9142	34,4905	35,3379	34,2947	35,5338
3	50,0844	49,6598	50,5090	49,4642	50,7046
4	97,8110	97,5217	98,1003	97,2743	98,3477
5	99,0527	98,8149	99,2904	98,5419	99,5635
6	99,0592	98,8206	99,2977	98,5480	99,5703
7	99,0614	98,8225	99,3004	98,5501	99,5727

Fit Equation Description:
[Variables]
x = col(1)
y = col(2)
reciprocal_y = 1/abs(y)
reciprocal_ysquare = 1/y^2
reciprocal_x = 1/abs(x)
reciprocal_xsquare = 1/x^2
reciprocal_pred = 1/abs(f)

Figure S3-11: Curve fitting of the experimental phosphate recovery percentages

Nonlinear Regression **donderdag 16 maart 2023 16:10:58**

Data Source: Data 1 in IronOxidation_Settling_Recovery
Equation: Sigmoidal; Sigmoid, 4 Parameter
f = y0+a/(1+exp(-(x-x0)/b))

R	Rsqr	Adj Rsqr	Standard Error of Estimate
0,9991	0,9982	0,9963	5,6325

	Coefficient	Std. Error	t	P
a	292,9954	32,4655	9,0248	0,0029
b	0,6200	0,1296	4,7850	0,0174
x0	-1,4388	0,1737	-8,2847	0,0037
y0	0,3085	3,9448	0,0782	0,9426

Analysis of Variance:

	DF	SS	MS
Regression	4	83077,7587	20769,4397
Residual	3	95,1766	31,7255
Total	7	83172,9353	11881,8479

Corrected for the mean of the observations:

	DF	SS	MS
Regression	3	51628,6980	17209,5660
Residual	3	95,1766	31,7255
Total	6	51723,8746	8620,6458

95% Confidence:

Row	Predicted	95% Conf-L	95% Conf-U	95% Pred-L	95% Pred-U
1	0,8985	-10,3031	12,1001	-20,2389	22,0359
2	1,9980	-7,8277	11,8237	-18,4436	22,4396
3	2,5166	-6,9276	11,9609	-17,7443	22,7776
4	13,5917	-0,4124	27,5959	-9,1553	36,3388
5	82,0961	68,0663	96,1260	59,3333	104,8590
6	119,2558	103,1267	135,3849	95,1423	143,3693
7	248,8376	230,9230	266,7523	223,4950	274,1802

Fit Equation Description:
[Variables]
x = col(1)
y = col(3)
reciprocal_y = 1/abs(y)
reciprocal_ysquare = 1/y^2
reciprocal_x = 1/abs(x)
reciprocal_xsquare = 1/x^2
reciprocal_pred = 1/abs(f)

Figure S3-12: Curve fitting of the experimental volumetric indexes

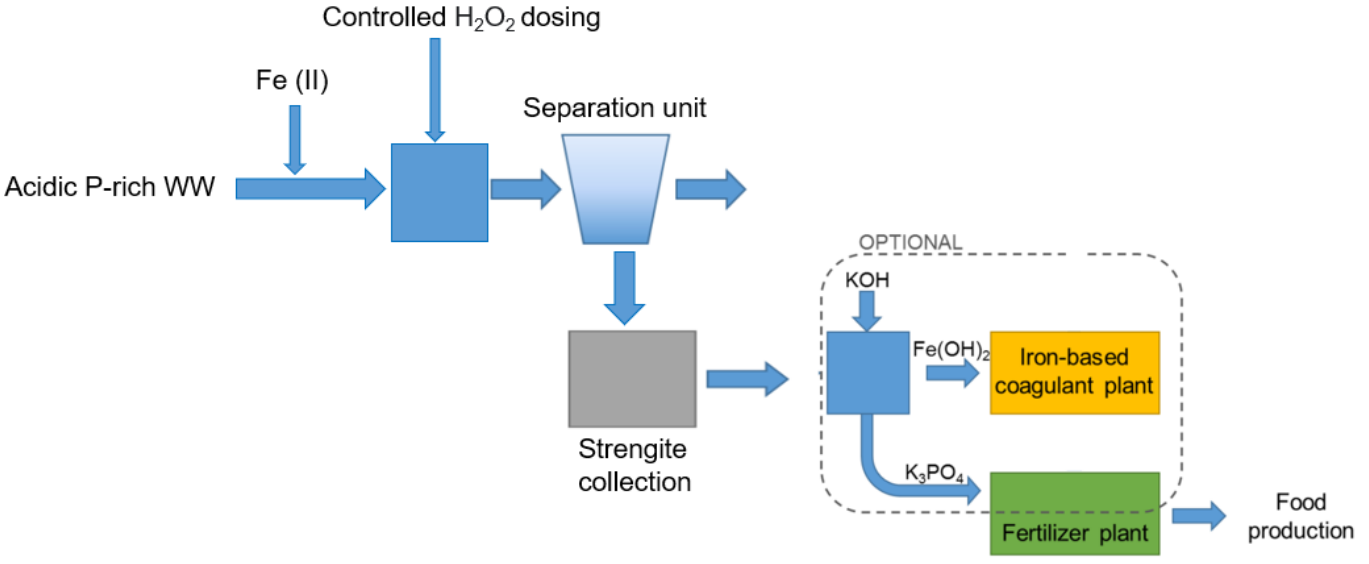

Figure S3-13: Process scheme of quick settleable strengite recovery from acidic WW

Concentration of P in the acidic stream from EPS extraction process (0.02 M)					
Strengite			**Vivianite**		
pH	3		PH	7	
H+	0.001	mol/l	H+	0.0000001	mol/l
			pH adjustment of the sample from 3 to 7 (Experimental including the buffer capacity of the stream)		
			OH added	0.210	mol/l
		OH- needed	0.210		
		Fe(II)Cl2	1.24	euro/kg	
			198.84	g/mol	
			0.20	kg/mol	
			0.25	euro/mol	
H2O2	0.55	euro/kg	**NaOH**	0.25	euro/kg
	34.01	g/mol		40.00	g/mol
	0.03	kg/mol		0.04	Kg/mol
	0.02	euro/mol		**0.01**	euro/mol
			KOH	0.56	euro/kg
				56.11	g/mol
				0.06	Kg/mol
				0.03	euro/mol
(NaOH is cheaper than KOH, however, KOH is sometimes prefered if the final product intended to be introduced to the soil as fertilizer)					
so calculations for both chemicals are done					
FePO4.2H20	1L		Fe3(PO4)2.8H20	1L	
1mole Fe2+	0.0049	euro	1.5 mol Fe2+	0.0074	euro
0.5 mole H2O2	0.0002	euro	OH moles NaOH	0.0021	euro
			OH moles KOH	0.0066	euro
Total	0.005	euro	Total using NaOH	0.009	euro
			Total using KOH	0.014	euro

Figure S3-14: OPEX estimation of strengite versus vivianite recovery from the acidic by-product stream from the EPS extraction process

6. References (for the cost of the chemicals):

https://www.indiamart.com/proddetail/ferrous-chloride-lr-8022045330.html

https://businessanalytiq.com/procurementanalytics/index/sodium-hydroxide-price-index/

https://businessanalytiq.com/procurementanalytics/index/potassium-hydroxide-price-index/

https://businessanalytiq.com/procurementanalytics/index/hydrogen-peroxide-price-index/


15

Chapter 4

Phosphorus Speciation in Extracellular Polymeric Substances extracted from Aerobic Granular Sludge

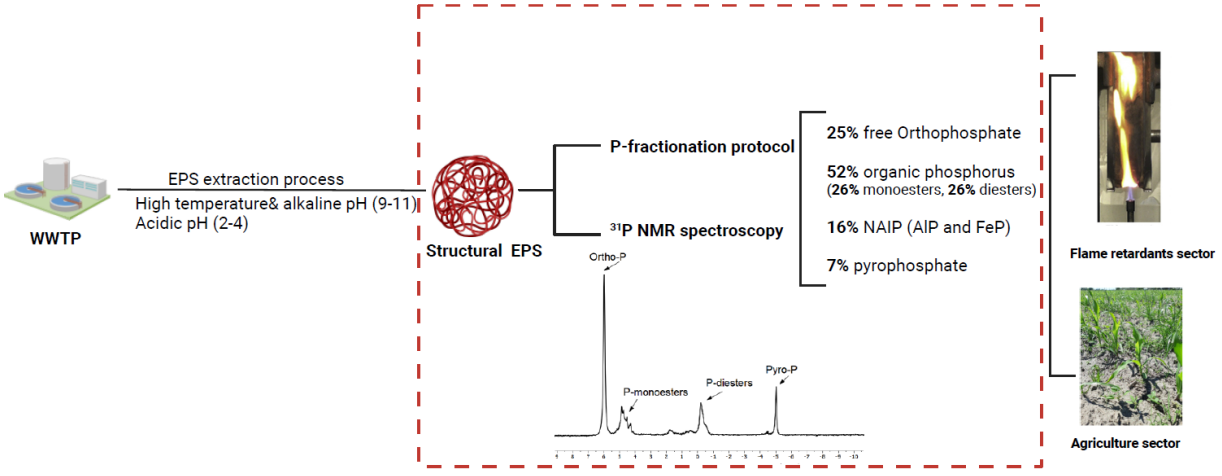

This chapter was published as:

Bahgat, N. T., Wilfert, P., Eustace, S. J., Korving, L., & van Loosdrecht, M. C. M. (2024). Phosphorus speciation in EPS extracted from Aerobic Granular Sludge. Water Research. https://doi.org/10.1016/j.watres.2024.122077

Abstract

Wastewater treatment technologies opened the door for recovery of extracellular polymeric substances (EPS), presenting novel opportunities for use across diverse industrial sectors. Earlier studies showed that a significant amount of phosphorus (P) is recovered within extracted EPS. P recovered within the extracted EPS is an intrinsic part of the recovered material that potentially influences its properties. Understanding the P speciation in extracted EPS lays the foundation for leveraging the incorporated P in EPS to manipulate its properties and industrial applications. This study evaluated P speciation in EPS extracted from aerobic granular sludge (AGS). A fractionation lab protocol was established to consistently distinguish P species in extracted EPS liquid phase and polymer chains. ^{31}P nuclear magnetic resonance (NMR) spectroscopy was used as a complementary technique to provide additional information on P speciation and track changes in P species during the EPS extraction process. Findings showed the dominance of organic phosphorus and orthophosphates within EPS, besides other minor fractions. On average, 25% orthophosphates in the polymer liquid phase, 52% organic phosphorus (equal ratio of mono and diesters) covalently bound to the polymer chains, 16% non-apatite inorganic phosphorus (NAIP) precipitates mainly FeP and AlP, and 7% pyrophosphates (6% in the liquid phase and 1% attached to the polymer chains) were identified. Polyphosphates were detected in initial AGS but hydrolyzed to orthophosphates, pyrophosphates, and possibly organic P (forming new esters) during the EPS extraction process. The knowledge created in this study is a step towards the goal of EPS engineering, manipulating P chemistry along the extraction process and enriching certain P species in EPS based on target properties and industrial applications.

4.1 Introduction

Utilization of microbial-produced phosphorus compounds could lead to more circular and economic phosphorus usage (Blank, 2023). Microorganisms can make very defined products, such as poly-P or organic P esters, out of a complex matrix, such as wastewater. Besides many other P_4 "so-called elemental phosphorus or white phosphorus," derivatives, poly-P, and organic P compounds are often synthesized from P_4, through a cost and energy-intensive thermal route from phosphate rock. These compounds are used to produce flame retardants, lubricants, or organophosphorus chemicals (ESPP webinar, 2020; Horstink et al., 2021; Jupp et al., 2021). The use of P products made by microorganisms has the potential to create a higher value of P recovered from wastewater via its use in high-value industrial niches and, in this way, reduce dependence on cost and energy-intensive processes to produce similar products from P_4 and boost the P recovery market.

Extracellular Polymeric Substances (EPS) extracted from waste sludge contain significant amounts of P, as reported by Huang et al., 2015, Zhang et al., 2013, Zeng et al., 2019, and Bahgat et al., 2023. These polymeric substances have potential applications across sectors such as agriculture, construction, textiles, and paper industry since it has demonstrated distinctive properties, serving as composite materials, bio-stimulants, or flame retardants (E. van der Knaap et al.,2019; Pronk et al., 2020; Feng et al., 2019; Kim et al., 2020). P is already intensively used in various contexts to modify polymers to improve or endow many properties. For instance, chemical phosphorylation of polyesters and

cotton in textiles and polyvinyl chloride in construction materials make these materials flame-resistant (Liang et al., 2013; Salmeia et al., 2016; ESPP webinar, 2020). Similarly, protein phosphorylation is used in food industries to change the properties of substances such as egg white, potatoes, and rice to enhance wettability, dispersibility, and water absorption capacity (Y. Hu et al., 2023; Z. Hu et al., 2019; Li et al., 2020; Miedzianka & Pęksa, 2013). Understanding the role of P in EPS will assist in making high-value P products from WWTPs and potentially replace some of the P_4 derivatives. Still, it will also assist in modifying the recovered EPS with certain processing characteristics or even engineering EPS to target specific industrial applications.

The Netherlands has established the world's first two large-scale demonstration facilities for extracting EPS from sludge. These two facilities are in Epe municipal and Zutphen industrial WWTPs, where EPS is extracted from aerobic granular sludge (AGS) (Bahgat et al., 2023; E. van der Knaap et al., 2019). The EPS extraction process consists of two main steps. The first step is to combine high pH (9-11) and temperature (80 °C) to solubilize EPS, and the second step is acidification, pH (2-4), to precipitate the EPS (Bahgat et al., 2023; E. van der Knaap et al., 2019; Felz et al., 2019). Bahgat et al., 2023 reported that approximately 20% of the total P within AGS ultimately becomes incorporated into the recovered EPS. No research has been reported on P speciation in EPS extracted using the extraction conditions used for extracting EPS from sewage sludge on a large scale (i.e., for application). Furthermore, no information is available on how P speciation in AGS changes under these conditions and whether they select for a certain P

species compared to other EPS extraction conditions. Addressing these knowledge gaps leads to the opportunity to make high-value use of P in WWTPs to promote EPS properties and industrial applications.

In this study, the phosphorus speciation was determined by 1) establishing a P-fractionation protocol that can distinguish between different P species in the liquid phase and polymer chains in the EPS gel-forming polymer and 2) using ^{31}P nuclear magnetic resonance (NMR) spectroscopy as a complementary method to reveal additional information about different organic and inorganic bound P species. ^{31}P NMR was also used to show how P-speciation changes along the EPS extraction process by analyzing P in all different stages of the extraction process.

The knowledge of P chemistry during the extraction process and how much and in what manner P ends up incorporated in EPS serves as a basis to produce EPS with desired or optimized properties (analogue to phosphorylation of synthetic polymers). Based on the results obtained in this study, P distribution in EPS was better elucidated, which opens more opportunities for combined P and EPS recovery from WWTPs and sets the foundation for future research into leveraging the incorporated P in EPS to manipulate its properties and industrial applications.

4.2 Methodology

4.2.1 Sludge samples

Laboratory extractions were performed using AGS surplus sludge samples collected after belt thickening from Epe AGS WWTP. Epe WWTP was selected as it is a municipal WWTP, and the majority of AGS

WWTPs worldwide are municipal, so it is a good representative of the majority of AGS plants. When sampling, the Nereda® reactors had an 8 g MLSS/L sludge concentration. They were operated with process cycles of approximately 6 h: 3 h of aeration, 1 h of settling, and 2 h of anaerobic feeding/simultaneous effluent withdrawal. The so-called "selection spill" is the sludge removed after every cycle and stored in a buffer tank for 4 hours before it partially goes to the EPS extraction installation. The sludge was collected after the belt thickener and had the following average composition: 5.1 %TS, 4.4 %VS, 33 g P/kg TS, and pH 5.9-6.2. The sludge samples were stored in the fridge for 2-3 days at 4 °C until all EPS extractions were performed. AGS sample from Zutphen WWTP, dairy industrial wastewater from FrieslandCampina, was also collected in this study, as shown in detail in the supplementary material. ^{31}P NMR was performed on Zutphen EPS as a quick method to confirm P speciation in EPS from another different source.

4.2.2 EPS extraction

Lab extractions were performed based on the lab protocol adapted from demonstration-scale practice (Bahgat et al., 2023). The sludge samples were first heated to 80 Celsius in a water bath; 25% (w/v) KOH was then added to the heated sludge until it reached pH 10± 0.05; the mixture was stirred for two hours at 400 rpm and 80 °C and then cooled down for centrifugation at 4,000 × g and 30 °C for 20 min. 9.5 M HCl acidified the alkaline supernatant until it reached a final pH of 2.2 ± 0.05, centrifuged at 4,000 × g and 30 °C for 20 min, then the acidified

gel-like EPS pellet precipitates. Samples along the extraction process were collected for analysis.

4.2.3 P-fractionation protocol

The acidic EPS (obtained by the end of the extraction process) was used for P fractionation and analysis. EPS consists of a polymer chain in a liquid phase, and each of these two fractions has P species, as shown in **Figure 4-1**. Total phosphorus in EPS (TP) can be either part of the polymer chain via covalent bonds (organic P), it can also be slightly bound/ adsorbed to the polymer chain via charge (exchangeable O-P) or just floating around in the liquid phase as free orthophosphate ions (O-P) or as bound inorganic and/or organic P in the liquid phase. P could also be present as a precipitate mineral as a non-apatite mineral (NAIP) (iron phosphate, aluminum phosphate, or magnesium phosphate) or an apatite mineral (AIP) (calcium phosphate). Since the EPS analyzed is acidic EPS at a pH of 2.2, it is not expected to find AIP because of its solubility at this pH, and therefore, only NAIP is expected to be found (predicted by visual Minteq as shown in supplementary material Table S4-1 and Figure S4-1).

The P fractions determined with the protocol are summarized as follows:

- TP (liquid+ chain): Total phosphorus in the liquid phase and polymer chains in the EPS.
- Bound inorganic and/or organic P (liquid): The bound phosphorus is either organic or inorganic in the liquid phase of EPS.

- O-P (Liquid): The free orthophosphates in the liquid fraction of EPS
- NAIP: The non-apatite inorganic fractions of phosphorus present in the EPS matrix as a precipitate. FeP, AlP, and MnP were presumed to be possibly present due to the supersaturation conditions of these ions as predicted by Visual Minteq (shown in supplementary material Table S4-1 and Figure S4-1).
- Exchangeable O-P (chain): The exchangeable orthophosphates are adsorbed to the EPS chains by electrostatic interactions and can be displaced by changes in pH or ionic strength.
- Organic-P (chain): The organic phosphorus fraction is covalently bound to the EPS chain and not present in the liquid fraction.

Based on these expected P groups, the P-fractionation protocol was developed to measure and validate the measurements of these fractions in four steps, as described in sections 4.2.3..1,4.2.3..2, 4.2.3..3, and 4.2.3..4, summarized in **Table 4-1** and **Figure 4-2**. Each step in the protocol was performed in triplets, and average values and standard deviations were obtained.

4.2.3..1 Characterization (crude samples)

This step was included in the protocol to measure TP (chain+ liquid) in the acidic EPS and O-P (liquid) and bound inorganic and/or organic P (liquid) in the acidic supernatant. So, the precipitated EPS and the acidic supernatant at the end of the EPS extraction process were collected and

analyzed: TS/VS, pH, conductivity, elemental analysis by IC, ICP, and liquid state ^{31} P NMR.

4.2.3..2 Highly- spun EPS

This step was undertaken to obtain the full liquid phase from the interior of the EPS matrix to evaluate its similarity in composition, O-P (liquid) and bound inorganic and/or organic P (liquid) fractions, with the acidic supernatant and assess if any pocket effects are present in the polymer or not. The pocket effect phenomenon occurs when some regions within the polymer can have different compositions/concentrations than the bulk matrix, as reported in polymer systems containing different monomers or blocks (Henderson & Clarke, 2004). EPS was encapsulated in 5 mL Eppendorf tubes and subjected to high-speed centrifugation at 21,000 xg for 20 minutes at 20°C. After centrifugation, the liquid was collected and analyzed using ICP, IC, and COD kits. The gel compression was validated visually and by TS% change from ≈ 7% to ≈12%.

4.2.3..3 EPS washing

EPS washing was done to remove the P fractions present in the liquid phase, O-P (liquid), bound inorganic and/or organic P (liquid), and keep organic-P (chain), exchangeable O-P (chain), and NAIP precipitates in the pellet. The concept was to wash EPS with a solution that has similar pH, ionic strength, and temperature as polymers are most prone to changes in solubility, swelling, dissolution, hydrophobicity, or others by those conditions due to changes in intermolecular forces which we wanted to avoid in our P-fractionation protocol (Lv et al., 2022; Hong et al., 2017). An HCl/KCl solution used for EPS washing (purification)

with a pH of 2.2, and a conductivity level of 19 mS/cm was made by adding 12 g of KCl (chem-lab 99%) and 12. 5 ml of 0.1 M HCl in a 500 ml volumetric flask. Washings are carried out by adding 25 mL of solvent to 25 g EPS tubes with a 1:1 ratio. The tubes are then shaken vigorously until homogeneous. Subsequently, the tubes were placed in a centrifuge and subjected to centrifugation at 4000 xg for 20 minutes at a temperature of 20°C. After each wash cycle, the supernatant was collected from the tubes for analysis, and the pellet went through the next washing step. The supernatants were analyzed by IC and ICP, and the pellet was analyzed by ICP and liquid state ^{31}P NMR.

4.2.3..4 EPS at pH=0

This step aimed to estimate non-apatite phosphorus (NAIP) fraction in EPS due to its dissolution at extremely low pH conditions. This step was adopted from the SMT (Standards in Measurements and Testing) protocol to determine non-apatite inorganic phosphorus as FeP, AlP, and MnP (Pardo et al., 2004; Zeng et al., 2019b). Additionally, according to the pKa values of phosphate species, at that pH, phosphates are non-ionized, and H_3PO_4 species dominate, so if there are exchangeable orthophosphates adsorbed to the polymer chains, they were also expected to be released into the solution. 3.5 M HCl was added to EPS samples to lower the pH to close to zero, while the pH meter was immersed inside the EPS samples. The EPS samples were shaken vigorously until homogeneous and centrifuged at 21,000 xg for 20 minutes to obtain the supernatant and the pellet separately for analysis. Two confirmation steps were performed at this step. The first is to confirm

with calculations that the added amount of acid was enough to lower pH to zero as pH meters are sensitive at this pH range (calculations are shown in the supplementary material Table S4-2). The second step is to confirm that lowering the pH did not cause polymer disintegration. For this purpose, the COD of the liquid phase of EPS at pH=0 was measured and compared to the original COD value of the liquid phase of EPS at pH=2.2 and the COD of the total EPS (chain and liquid fractions) as explained in the results section 4.3.1..4. Liquid samples were analyzed by IC and ICP.

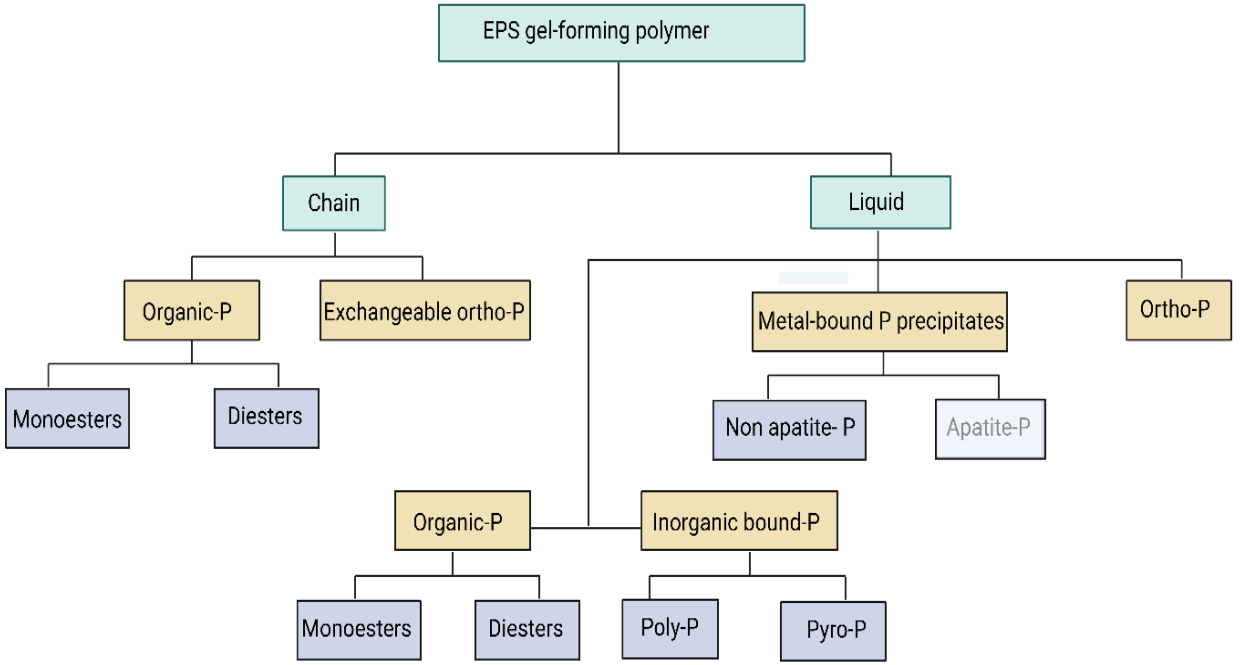

Figure 4-1: Summary of possible P-species present in both chain and liquid phases of the EPS gel-forming polymer. In this study, P fractions in yellow are measured with the P-fractionation protocol, and P fractions in grey are measured with ^{31}P NMR. Apatite-P is shaded as it is thermodynamically not expected in the EPS analyzed in this study.

4.2.4 Analysis

4.2.4..1 Microwave digestion

All solid samples were destructed by microwave digestion to convert them to liquid analyses. Samples were digested in an Ethos Easy from Milestone with an SK-15 High-Pressure Rotor. Around 50 mg of solids were put in a Teflon vessel in which 10 mL of ultrapure HNO_3 (64.5-70.5% from VWR Chemicals) was poured. The digester is set to reach 200 Celsius in 15 minutes, run at this temperature for 15 minutes, and cool down for 1 hour.

4.2.4..2 ICP-OES (Inductively Coupled Plasma with optical emission spectrometer)

The elemental inorganic composition was measured via Inductively Coupled Plasma (Perkin Elmer, type Optima 5300 DV) with an Optical Emission Spectroscopy as a detector (ICP-OES). The device was equipped with an Autosampler, Perkin Elmer, type ESI-SC-4 DX fast, and the data were processed with the software Perkin Elmer WinLab32. The rinse and standard internal solutions were 2%HNO_3 and 10 mg/L of Yttrium.

4.2.4..3 IC (Ion chromatography)

Liquid samples were pre-treated first by filtering the samples through 0.45 µm followed by 0.22 µm membrane filters before analysis. Anions and cations (free dissolved ions) were measured by Metrohm Compact ion chromatograph Flex 930.

4.2.4..4 Chemical oxygen demand (COD)

Total COD was measured using a Hach Lange test kit (LCK514 Hach Lange, UK), heated in a thermostat (HT200S, Hach Lange) to 170 Celsius, and then analyzed using a spectrophotometer (DR. 3900 VIS spectral photometer, wavelength range 320–750 nm).

4.2.4..5 TS/VS

TS and VS were analyzed according to the Standard Methods for the Examination of Water and Wastewater.

4.2.5 Liquid ^{31}P NMR

The presence of phosphor-containing compounds in the sludge, alkaline supernatant, alkaline pellet, acidic supernatant, crude EPS, and washed EPS pellet (described in section 4.2.3..3) was evaluated using ^{31}P NMR as a complementary method to the P-fractionation protocol. Samples preparation included EDTA and NaOH extractions. The dose of EDTA and NaOH solutions was to avoid the interference of divalent cations and to adjust the pH above 12 to ensure consistent chemical shifts and optimal spectral resolution during the NMR measurement (Turner et al., 2003). After adjusting the pH, alkaline, acidic supernatants, crude EPS, and washed EPS samples were completely dissolved. The sludge and alkaline pellet samples had insoluble residual material, which was removed by centrifuging the sample (3900 rpm, 22 Celsius, 20 min); the P extraction efficiency was ≈ 97% and 92% for sludge and alkaline pellet, respectively (calculations are shown in figure S4-5 in the supplementary material). The samples were prepared as follows:

- Alkaline supernatant, alkaline pellet (including the alkaline gel layer described by Bahgat et al., 2023), acidic supernatant, crude EPS, and washed EPS samples: phosphorus was extracted using one-step extraction with 0.1M EDTA and 1M NaOH solution. This method represents the most commonly used extraction protocol for environmental samples (Cade-Menun & Liu, 2014; Turner et al., 2003) and EPS samples (Zeng et al., 2019; Zhang et al., 2013). The samples were prepared one hour before acquiring data.
- Sludge sample: the phosphorus was extracted with a two-step extraction with EDTA pre-extraction followed by NaOH extraction. Staal et al., 2019 reported that a two-step EDTA and NaOH extraction protocol achieved complete poly-P from activated sludge extraction compared to a single-step EDTA-NaOH extraction protocol. So, freeze-dried AGS was pre-extracted with 0.1M EDTA solution for one hour, followed by centrifugation at 3900 rpm for 10 mins and decanting the EDTA extract. The resulting pellet was extracted with 1M NaOH for 16 hours. The sample was being prepared for almost 18 hours before acquiring data.

All liquid samples were placed in a 10 mm NMR tube (Norel). The spectra were obtained using a Bruker Ascend- 600 MHz spectrometer operating at 162.00 MHz for ^{31}P. The acquisition parameters were as follows: acquisition time, 0.8 s; relaxation delay, 50 s (to ensure full relaxation); 90°pulse width, number of scans 1500, and the total

measurement period per sample was 23 hours. The spectrum was acquired twice for the sludge sample, one after four hours (Staal et al., 2019) and another after 23 hours, to confirm that the measurement length did not affect polyphosphate content. The ratio between orthophosphate and polyphosphate peaks was the same in the two spectra (shown in the supplementary material Figure S4-2). The NMR data processing software determined individual signals' chemical shift and area (MestReNova, version 12.0.4-22023, Mestrelab Research S.L., Spain).

Table 4-1: Summary of the measurements and calculations of P-fractions measured with the P-fractionation protocol. The numbers in blue are related to the numbers shown in Figure 4-2 on the top left of measured P fractions

Numbers in Figure 4-2	**Measurements**
(1)	TP (chain+ liquid)
(2)	O-P (liquid)
(3)	Exchangeable O-P (chain)
(4)	O-P (liquid) + bound inorganic and/or organic P (liquid)
(5)	Organic (chain)+ Exchangeable O-P (chain)+ NAIP precipitates
(6)	O-P (liquid) + Exchangeable O-P (chain) + NAIP precipitates
P fractions	**Measured or calculated**
TP (liquid +chain)	(1) measured
O-P (liquid)	(2) measured
bound inorganic and/or organic P (liquid)	**(7)** calculated= (4) measured – (2) measured
NAIP precipitates	**(8)** calculated= (6) measured – (2) measured – (3) estimated
Exchangeable O-P (chain)	(3) estimated from the EPS washing curve
Organic (chain)	**(9)** calculated= (5) measured- (3) estimated - (8) calculated

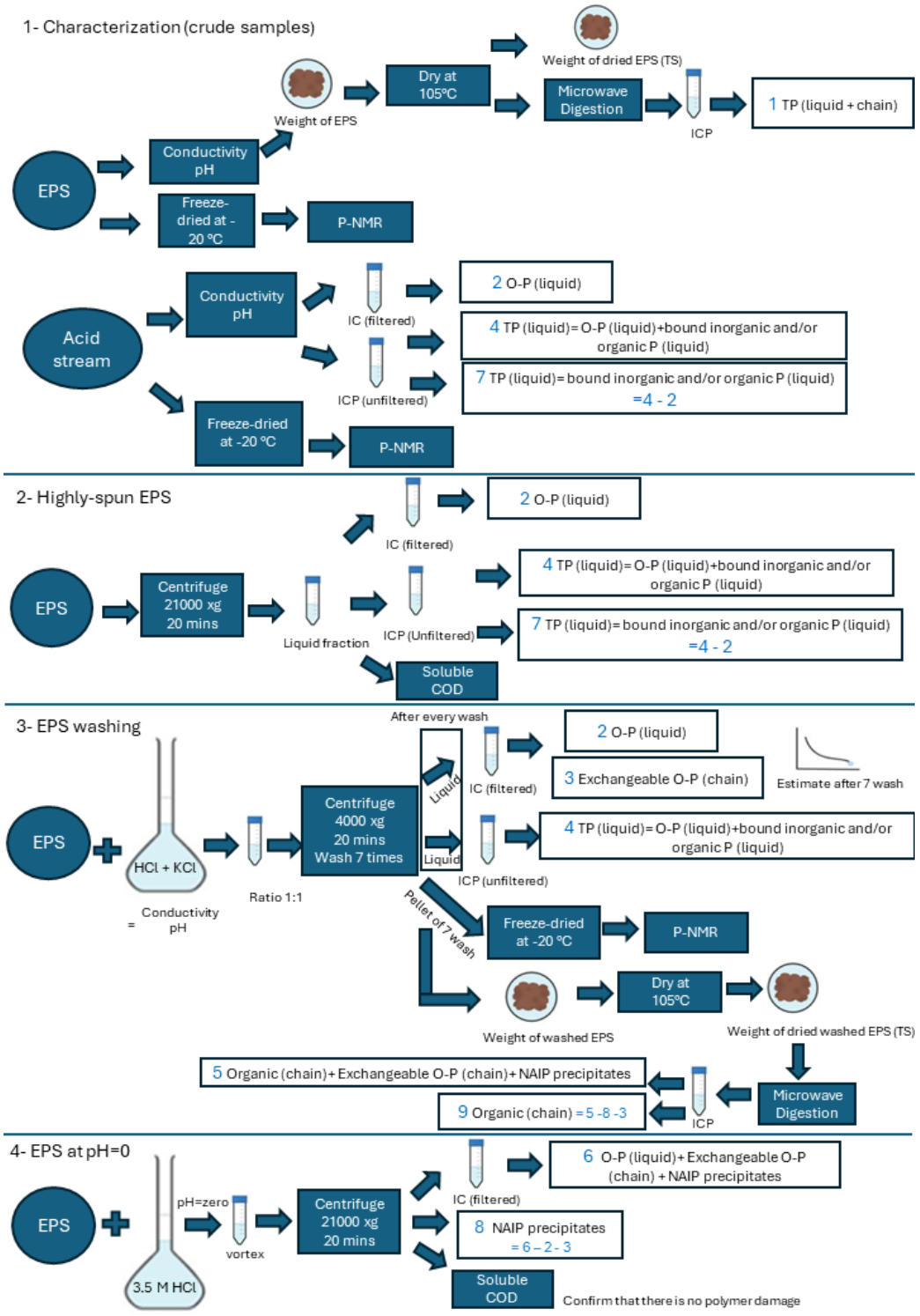

Figure 4-2: Schematic diagrams of the four steps in the P- fractionation lab protocol- analysis performed.

4.3 Results and Discussion

4.3.1 P-fractionation protocol

The results of the phosphorus species measured with the P-fractionation protocol are summarized in **Figure 4-3**. It shows that EPS consists of, on average, 24% of O-P (liquid), 18% of NAIP precipitates with iron and aluminum, < 1% of exchangeable O-P (chain), 6% of bound inorganic and/or organic P (liquid), and 51% of organic (chain) phosphorus integrated into the polymer chains. Detailed calculations and validation steps for each step of the fractionation protocol are described in the below sections.

4.3.1..1 Characterization (crude samples)

The EPS acidic gel samples were characterized as summarized in **Table 4-2** and **Table 4-3**. **Table 4-2** summarizes the EPS samples TS, VS, water content, pH, conductivity, and COD. **Table 4-3** shows the TP in EPS polymer (liquid+ chain) as ≈ 1.4 gP/kg EPS, the O-P (liquid), and the bound inorganic and/or organic P (liquid) in the acidic supernatant as ≈ 350 and 97 mgP/L, respectively. The measurements are in line with measurements reported in Bahgat et al., 2023 for the general characterization of EPS and acidic by-product stream from EPS extraction installation in Epe WWTP.

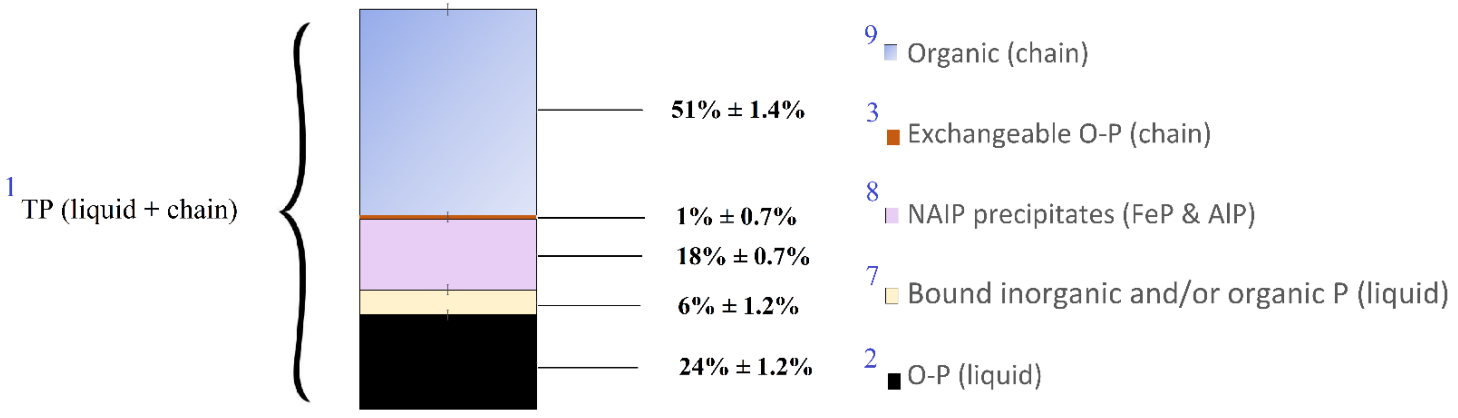

Figure 4-3: % of phosphorus fractions in crude EPS extracted from AGS-Epe WWTP measured by established P-fractionation protocol. Extractions were performed in triplets, average values are shown, standard deviation of all fractions was approximately1%. Blue numbers on the top left are related to numbers in figure 4-2 and Table 4-1 in the methodology section

4.3.1..2 Highly- spun EPS

The EPS was centrifuged at high g force to observe if there was a different O-P (liquid) concentration in the acidic supernatant and the liquid trapped by the EPS gel-forming polymer (pocket effect). The liquid fraction of EPS squeezed via high centrifugal spinning had O-P (liquid) and the bound inorganic and/or organic P (liquid) concentrations ≈ of 340 and 110 mgP/L, respectively, as shown in **Table 4-3**. These concentrations are similar to the concentrations of the acidic supernatant obtained after EPS precipitation at pH 2.2 measured in step 4.3.1..1, indicating phosphate in the liquid phase was distributed equally between the acid supernatant and EPS and it was not influenced by any pocket effects. The liquid phase retrieval from the EPS matrix interior was confirmed as the TS% increased from ≈7% to ≈12%, as shown in **Table 4-2**. This step is unnecessary in future EPS P speciation measurements since no pocket effect on phosphate concentration was observed, and the results are similar to those of the previous step.

4.3.1..3 EPS Washing

EPS washing was performed with a synthetic solution to evaluate the O-P (liquid) and the exchangeable O-P (chain) fractions. The free orthophosphates and the total phosphorus concentrations in the washing solution after each washing step are shown in Figure S4-4 in the supplementary material. Free orthophosphates were observed to be approximately halving each time, indicating no "binding" interactions till the 6^{th} washing step. If there had been a binding interaction, the phosphate concentration of the washing solution would not have

followed the halving trend, as the polymer would have interfered with the washing process. Total phosphorus measurements followed a similar trend but did not decrease linearly, which can be explained by the bound phosphorus in the liquid fraction of EPS washed out. The O-P (liquid) washed from EPS was calculated as ≈ 350 mgP/L and bound inorganic and/or organic P (liquid) as the subtraction of washed total phosphorus and O-P (liquid) ≈ 90 mgP/L. Starting from the 6th washing step, the concentration of O-P was stable, then slightly increased in the 8th washing step, and decreased again, not following the earlier halving trend anymore, indicating binding interactions taking place starting from the 6th washing step. The concentration of exchangeable O-P (chain) was estimated to leave the polymer at the point of these binding interactions taking place after the 6th washing step as ≈ 16 mg P/L. The exchangeable O-P (chain) is negligible as it is less than 1% of the total phosphorus in EPS, so measuring this fraction is not needed in future measurements of EPS. The O-P (liquid), bound inorganic and/or organic P (liquid) fractions are in line with measurements in the previous two steps, as shown in **Table 4-3**.

4.3.1..4 EPS at pH=0

The pH of EPS was adjusted to zero to evaluate the metal-bound (NAIP) fraction of phosphorus. This step resulted in an increase in the free orthophosphate concentrations O-P (liquid) up to 640 mgP/L (20720 µmole P/L) due to the dissolution of P metal-bound precipitates (NAIP, e.g., FeP, AlP, and MnP), and the release of exchangeable O-P (chain) to the liquid. Although $CaPO_4$ and $MgNH_4PO_4$ are commonly

present in sludge, they are not expected to be found in acidic EPS as they will be dissolved during the acid precipitation step of EPS extraction. Two validation steps were performed in this experiment:

1) The first one was to confirm our assumption that the release of NAIP (Fe, Al, Mn) to the liquid is equivalent to P release, considering the small fraction of exchangeable O-P estimated in section 4.3.1..3. Fe release from FeOOH was also assumed not to occur or occur to a minimum extent as it would have already been dissolved at pH 2.2 during the acid precipitation step of EPS. The P-precipitates, as predicted by visual Minteq, are Strengite ($FePO_4.2H_2O$), Variscite ($ALPO_4.2H_2O$), and $MnHPO_4$ (figure S4-1 in supplementary material), all have a ratio of 1:1 to phosphate. Table S4-3 in the supplementary material shows the measurements of the P, Fe, Al, and Mn moles released upon decreasing the pH from 2.2 to zero. Fe and Al are the main fractions of the NAIP present in the EPS sample, as the contribution of Mn is almost negligible. Subtracting the initial O-P (liquid) measured in 4.3.1..1 and 4.3.1..2 as 10970 µmole P/L, exchangeable O-P fraction which was estimated as 16 mgP/L (520 µmole P/L) from the total P released, the moles of P released upon NAIP dissolution are calculated as 9230 µmole P/L. The total Fe and Al moles released are measured to be 9460 µmoles/L, with a 1.02 ratio to P released moles. This ratio agrees with our assumptions and VisualMinteq predictions.
2) The second validation step was to confirm that lowering the pH to zero did not cause polymer damage and that no P attached to

polymer chains dissolved to the liquid fractions, causing an overestimation of the phosphorus measured in the liquid. At pH= zero, the COD of EPS (chain) decreased by ≈ 7 g COD/L as calculated by subtracting the initial COD of EPS (chain) at pH=2.2 ≈ 85 g/L and the COD of EPS (chain) at pH=0 ≈ 78 g/L. The COD decrease of EPS (chain) is probably due to some minor hydrolysis of organics. Since the ratio between TCOD and TP in EPS at pH 2.2 is calculated as ≈ 0.00015 g P/ g COD, we could correlate the COD of EPS (chain) change with the change of P concentrations to assess its influence on the measured phosphorus species. The change in P concentrations due to the minor hydrolysis organics was estimated to be 0.007%, which is negligible. Calculations are shown in detail in Table S4-4 in the supplementary material.

Table 4-2: Measurements of pH, conductivity, COD, and TS% performed in each step of the P-fractionation protocol- EPS extracted from Epe WWTP

(1)-characterization (crude samples)	EPS (liquid+chain)	TS%	7.0±0.4
		VS%	5.9± 0.3
		pH	2
		Conductivity (mS/cm)	19
		COD^{1} (mg/L)	99,000 ± 7,000
(2)-highly spun EPS	EPS (liquid+chain)	TS% of the centrifuged pellet	12.3 ± 0.1
	EPS (liquid)	COD^{2} (mg/L)	14,000± 300
	EPS (chain)	COD^{3} (mg/L) = COD^{1}- COD^{2}	85,000±6,000
(3)-EPS washing	EPS pellet after washing	TS% of the washed pellet	17.4 ±0.4
		TS% of EPS (corrected)	6.0±0.6
(4)-pH=zero EPS	EPS (liquid)	COD^{4} (mg/L)	21,000 ±700
	EPS (chain)	COD^{5}= COD^{1}-COD^{4}	78,000±6,000

Table 4-3: Concentration of different phosphorus fractions (gP/kg EPS) measured by the P-fractionation protocol in EPS extracted from Epe WWTP

Phosphorus fractions	**Concentrations**	
	mg/L	**g P/kg EPS**
(1)- Characterization		
TP (liquid+ chain)	-	1.41±0.01
O-P (liquid)	353± 6	0.33 ± 0.01
bound inorganic and/or organic P (liquid)	97±12	0.09±0.01
(2)-Highly Spun EPS		
O-P (liquid)	340±10	0.32± 0.01
bound inorganic and/or organic P (liquid)	110± 10	0.10± 0.01
(3)-EPS washing		
O-P (liquid)	360± 10	0.35± 0.01
bound inorganic and/or organic P (liquid)	95± 10	0.07 ± 0.01

Exchangeable O-P (chain)	15±5	0.01 ± 0.00
Organic (chain)+ Exchangeable O-P (chain)+ NAIP precipitates	-	0.99± 0.02
Organic (chain)		0.73± 0.02
(4)- EPS at pH=0		
O-P (liquid) + Exchangeable O-P (chain) + NAIP precipitates	640 ±10	0.60 ± 0.01
NAIP precipitates	-	0.25± 0.01

4.3.2 Liquid ^{31}P NMR

4.3.2..1 ^{31} P NMR peaks assignment

^{31}P NMR measurements were performed on initial sludge, alkaline supernatant, alkaline pellet, acidic supernatant, acidic EPS, and washed EPS. The primary goal of these measurements was to confirm the EPS phosphorus speciation obtained by the fractionation protocol and to provide additional information about the organic phosphorus fraction.

The secondary goal was to gain more insights regarding the changes in phosphorus species along the extraction process. The results are shown in **Figure 4-4** and **Figure 4-5**. The peaks in the ^{31}P NMR spectrum were assigned as previously reported (Cade-Menun & Liu, 2014; McDowell et al., 2006; Turner et al., 2003). The pH of the extracts (12.6) was close enough to the pH in those studies that the chemical shifts can be compared (Grouse et al., 2000). Detected inorganic P compounds included orthophosphate (fixed at 6.00 ppm to compare between different spectra easily), pyrophosphate at -5 ppm, polyphosphate middle groups between -19 and -24 ppm, and terminal groups between -4 and -4.5 ppm, organic P included orthophosphate monoesters between 5.9 and 3.7 ppm, and orthophosphate diesters between 2 and -1 ppm. Peaks in the monoester region could possibly be derived from monoribonucleotides due to RNA hydrolysis under alkaline conditions (Lemire et al., 2016), inositol phosphates, metabolic phosphate compounds such as nicotinamide adenine dinucleotide (NAD), sugar phosphates (e.g., glucose 6-P), phosphoproteins (e.g., 3-phosphoserine), or other compounds present due to the degradation of orthophosphate diesters as reported in the literature (Cade-Menun, 2015). Additionally, the peaks in the diester region could possibly be derived from DNA, but also from phospholipids (e.g., phosphatidylcholine, phosphatidylglycerol). Spiking was recommended as the only way to specifically identify phosphorus forms in complex matrices (Koopmans et al., 2007). Therefore, future spiking experiments could be performed on EPS with standard purchased phosphorus compounds and their degradation products if the intention is to identify a specific phosphorus compound in EPS.

4.3.2..2 P species in EPS- complementary to the P-fractionation protocol

From spectrum E) in **Figure 4-5**, of total phosphorus present in crude EPS, total orthophosphate (includes free O-P(liquid), and dissolved NAIP) was calculated as 40%, organic phosphorus as 50% (25% as monoesters, and 25% as diesters), and pyrophosphates as 10% (includes pyrophosphate in liquid or attached to the polymer chains). From spectrum F) in **Figure 4-5**, the washed EPS had a less intense peak of orthophosphate compared to graph E) as expected, showing that O-P (liquid) was removed upon washing, and the remaining phosphates represented the NAIP, which will remain with the washed EPS pellet after washing and centrifugation. The orthophosphates (representing dissolved NAIP due to the high pH <12 of ^{31}P NMR sample) in washed EPS were calculated as 15% of the total phosphorus in crude EPS. Comparing the orthophosphate peaks in spectrum F) and spectrum E), the removed orthophosphates (O-P (liquid)) were calculated as 25% of the total phosphorus present in crude EPS. The organic phosphorus in spectrum F) was estimated as 53 % (27% as monoesters,27% as diesters) of total phosphorus present in crude EPS, confirming the organic P fraction calculated in spectrum E). Comparing the pyrophosphate peaks in spectrum F) and E), the removed pyrophosphate (free in the liquid) was calculated as 9%, and the remaining attached to the organics in washed EPS was 1%. The ^{31}P NMR results were in line with the P-fractionation protocol developed. In comparison to the protocol, ^{31}P NMR showed a 1% difference in O-P (liquid), a 3% difference in NAIP, < 1% difference in organic P (chain), and a 4% difference in the bound inorganic

and/or organic P (liquid) which was revealed to be only pyrophosphates and no organics.

To understand how variant the P speciation could be in EPS samples from different sources, EPS was extracted from Zutphen (dairy industrial AGS) WWTP, and its ^{31}PNMR was compared to Epe (municipal AGS) as described in Figure S4-3 in the supplementary material. Of total phosphorus present in crude Zutphen EPS, 47% orthophosphates (O-P(liquid) and NAIP), 46% organic phosphorus (28% diesters, and 18% monoesters), 1% pyrophosphates, and 6% polyphosphates were present. Compared to Epe, P speciation of Zutphen EPS showed a similar trend despite the sludge being from municipal or industrial sources. Orthophosphates and organic phosphorus are still the dominant species, with 7% and 6% differences from Epe, respectively. The diesters and monoesters do not have an equal ratio as Epe; Zutphen had a higher content of diesters compared to monoesters. A minor fraction of polyphosphate was also detected, unlike Epe. Still, these differences are minor, not affecting the major trend of the dominant P-species and the expected % range of these species.

4.3.2..3 Change of P species along the extraction process

Figure 4-4 shows the ^{31}P NMR spectra of the initial AGS, alkaline supernatant, and alkaline pellet streams produced along the first step (EPS alkaline solubilization) of the extraction process, and all % are related to total P in the initial sludge. **Figure 4-5** shows the ^{31}P NMR spectra of the acidic supernatant, crude EPS, and washed EPS produced along the second step of the extraction process, and all % are related to total

P in the initial sludge. Spectrum A) shows the excess AGS used for EPS extraction contained ≈ 24% polyphosphates, 60% orthophosphates, and 16% organic phosphorus (8% monoesters and 8% diesters). It was anticipated that polyphosphate would be the dominant fraction, as reported by Huang et al. (2015). However, our findings showed that orthophosphate was the predominant form. This discrepancy can be attributed to poly-P hydrolysis to orthophosphate during storage in the buffer tank (with an average SRT of approximately 4 hours, slightly anaerobic conditions, and a pH of around 6) in the WWTP. Storage sludge samples in the fridge for 2-3 days before laboratory extractions could have further contributed to this transformation. Furthermore, most of the phosphorus could have been initially present as inorganic phosphorus precipitates, such as apatite (AIP) and non-apatite (NAIP) in the core of granules not as poly-P. There is a slaughterhouse discharge to Epe WWTP, which contains most likely high levels of Fe. Mañas et al., 2011 reported that biologically induced precipitation of hydroxyapatite was responsible for 45% of the overall P removal in AGS, and Cai et al., 2018 also reported vivianite and siderite precipitation in the core of the granules with iron dosing to the reactor.

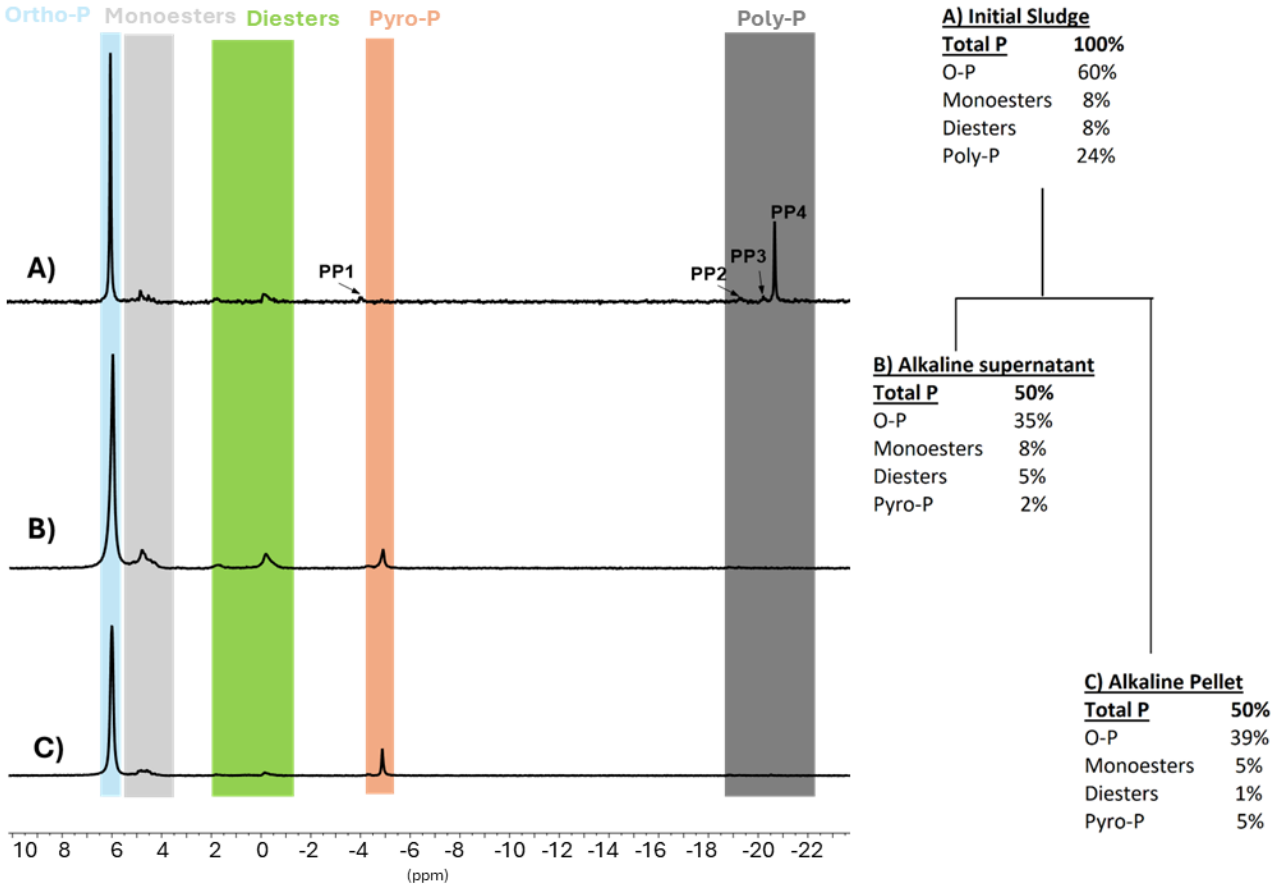

Figure 4-4: ^{31}P NMR spectra of the first step of EPS extraction step: A) initial AGS, B) alkaline supernatant, C) alkaline pellet, -Epe municipal WWTP- All % are related to the initial total P in initial sludge approximated to the first whole numbers or first decimal point

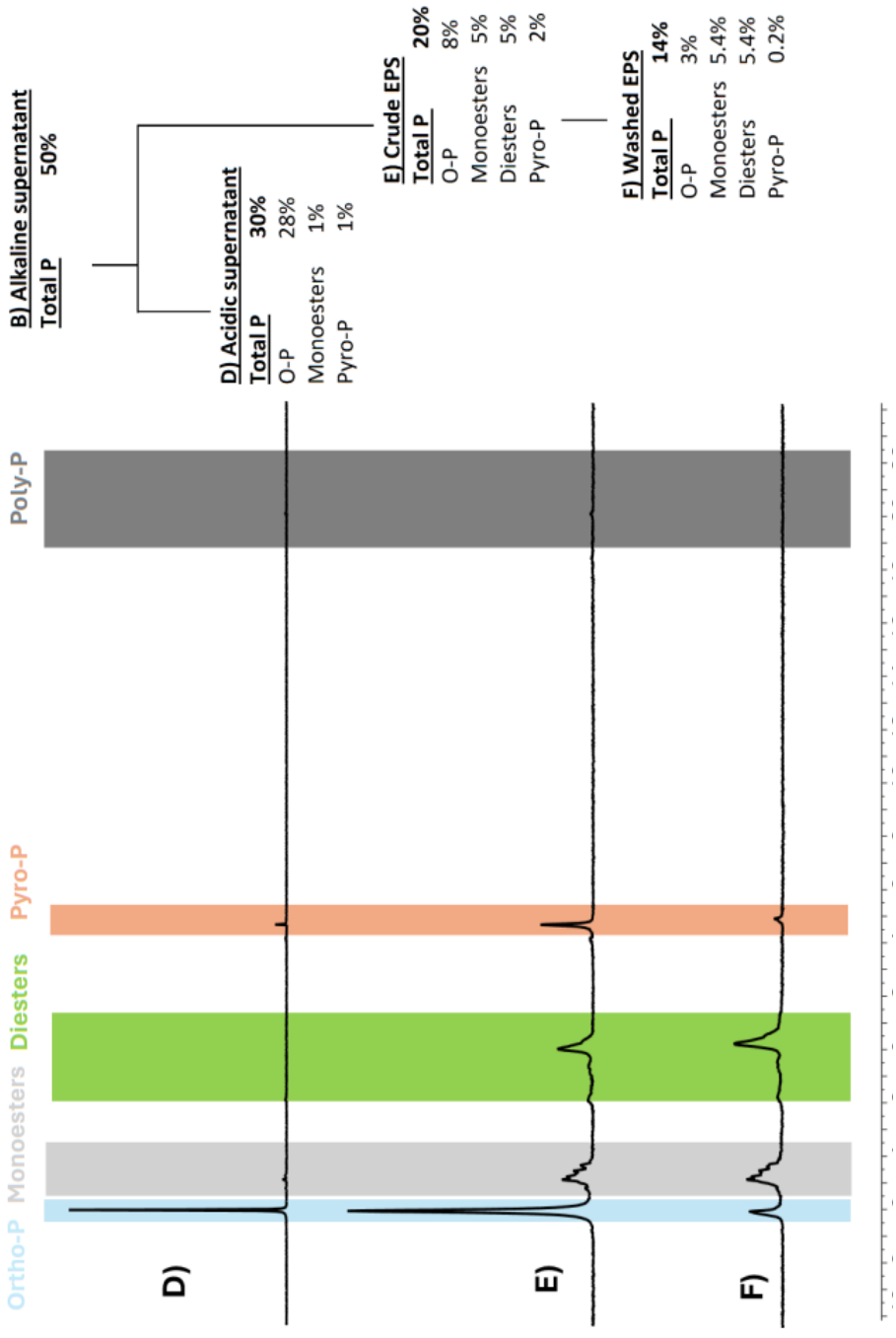

Figure 4-5: ^{31}P NMR spectra of the second step of the EPS extraction process: D) acidic supernatant, E) crude EPS, F) washed EPS- Epe municipal WWTP- All % are related to the initial total P in initial sludge approximated to the first whole numbers or first decimal point

Comparing spectrum A (initial AGS) to B (alkaline supernatant) and C (alkaline pellet) in **Figure 4-4** and the mass balances of P species over the alkaline extraction step, it is observed that polyphosphate was completely hydrolyzed as it only appeared in the initial sludge. Pyro-P peaks appeared in the alkaline supernatant (spectrum B) and pellet (spectrum C). Polyphosphates (≈24% in initial sludge) hydrolyzed into pyrophosphates and orthophosphates. Orthophosphates increased by ≈14% and pyrophosphate by ≈7%, but ≈ 3% of polyphosphates remained. Similarly, the total organic-P content increased compared to the initial sludge by ≈ 3 %. We hypothesize that this could indicate that phosphorylation is taking place, and that part of the polyphosphates was used to form ester bonds. Compared to chemical phosphorylation conditions reported in literature (Cen et al., 2022; Kaewruang et al., 2014 ; Xiong & Ma, 2017; Miedzianka & Pęksa, 2013), the EPS extraction conditions are promising to induce phosphorylation because of the presence of high energy P bonds (P-O-P) in polyphosphates, high temperature, alkaline conditions, and long residence times in the alkaline reactor. However, confirming the hypothesis from a 3% increase of peak integration in the NMR spectra is challenging because it is a very small percentage to be trusted. Consequently, we recommend performing experiments that specifically target phosphorylation effects to substantiate or refute our hypothesis. In these experiments, different parameters that could influence phosphorylation have to be assessed e.g., the type of P salt used, P concentration, pH, temperature, residence time, molecular configuration, and available phosphorylation sites.

Comparing the P speciation in our study with other EPS extracted under different conditions, reported in the literature, showed that extraction conditions used in our study are selecting for organic phosphorus. For example, Huang et al., 2015 reported no organic phosphorus in EPS extracted by EDTA–ultrasound from AGS, Zhang et al., 2013 also reported no organic phosphorus in EPS extracted by cation exchange resin (CER) from WAS, and Zeng et al., 2019 reported poly-P and ortho-P were the dominant forms with negligible organic P in EPS extracted by formaldehyde-NaOH from WAS. Then, the extraction conditions we use in our study are hypothesized to produce EPS with high organic-P content, as around 51%-54% of total phosphorus in EPS is organic phosphorus as measured by the P-fractionation protocol and ^{31}P NMR. This hypothesis was further confirmed since EPS extracted from Zutphen under the same conditions also had organic-P as a dominant species in EPS, similar to Epe, despite the difference in the type of wastewater and sludge in the two WWTPs.

Spectrum D) in **Figure 4-5**, confirmed Bahgat et al., 2024 findings that around 30% of TP as ortho-P in sludge ends in the acidic by-product stream, and it is a relatively pure stream as O-P represents 95% of its total phosphorus composition, so it is suitable for phosphate recovery by precipitation.

4.4 Recommendations and Outlook

This section provides recommendations for future studies on P species in EPS using the P-fractionation protocol established in this study. Also, it offers insights into the ultimate objective of EPS engineering and the

goal to leverage the incorporated P in EPS to manipulate its properties and enhance its industrial applications.

4.4.1 Regarding the P-fraction protocol

1) The P-fractionation protocol to measure EPS samples extracted under similar conditions: The protocol involved four steps, but future studies could be more concise. For example, the "highly spun EPS" step may be omitted in future speciation evaluations as it showed no pocket effects or concentration difference compared to the acidic by-product. Similarly, the "EPS washing" step can be skipped since the exchangeable O-P (chain) is negligible (<1%). The steps "Characterization of crude samples" and "EPS at pH=0" are essential for assessing the main P fractions. "Characterization of crude samples" identifies O-P (liquid) (25% of TP in EPS) and bound inorganic and/or organic P (liquid) (7% of TP in EPS). "EPS at pH=0" identifies organic P covalently bound to the polymer chains (52% of TP in EPS) and non-apatite inorganic phosphorus NAIP (15% of TP in EPS).
2) The P-fractionation protocol to measure EPS samples extracted under different conditions: It's crucial to note that the EPS analyzed in this study was acidic, with a pH of 2.2, so no apatite inorganic phosphorus (AIP) was anticipated. However, caution is needed for EPS at higher pH values, as when EPS is brought to pH=0, combined NAIP and AIP will be released, and a method to differentiate them must be incorporated into the protocol. One approach could involve adjusting the pH to high alkaline conditions to dissolve NAIP and

precipitate AIP and then bringing the EPS to zero to dissolve AIP. Additionally, the exchangeable O-P fraction may not be negligible for higher pH EPS, as P is more ionized (with a higher charge of -2 or -3), potentially having a greater affinity for polymer chains.

4.4.2 Regarding the ultimate goal of EPS engineering

The results reveal the P species incorporated in EPS and how P changes throughout the extraction process. These results highlight opportunities to tailor the P species in EPS according to industrial needs. Comparing EPS extraction conditions to the chemical phosphorylation work done on biopolymers in the literature and considering the resultant phosphorus content (wt%) and its influence on properties as shown in **Table 4-4**, the potential for follow-up research focused on EPS engineering and tailoring its properties to meet industry needs is evident. For example, since P esters are commonly added to macromolecules to make them flame retardants, and approximately 50% of the P in EPS was found to be organic phosphorus, EPS could create an effective flame retardant (Kim et al., 2020, 2022). Further increasing the organic P content in EPS could be a way to make an EPS super flame retardant that competes with commercial flame retardants. Also, further research into phosphorylation under extraction conditions, as pinpointed in this study, could be a way to influence the P chemistry to form higher organic P content to maximize EPS thermal stability property and its application as a flame retardant. Another way to change the speciation could be introducing excess Fe or Al cations in the wastewater treatment reactors or during the EPS extraction process to increase non-

apatite inorganic phosphorus (NAIP) in EPS and reduce O-P (liquid), potentially useful for creating slow-release fertilizers from EPS to prevent rapid O-P (liquid) leaching from the soil. Other possibilities will appear with further research on how different P species/content influence different EPS properties.

Table 4-4: Phosphorylation conditions, %wt P content and the effect on the properties of some biopolymers from literature in comparison to EPS extraction conditions from AGS and EPS %P content. TSPP stands for tetrasodium pyrophosphate salt, STPP stands for sodium tripolyphosphate, and STMP stands for sodium trimetaphosphate

Polymer	P-salt added	Temp	Time	P wt%	pH	Ref	Effect
Gelatin	TSPP	50 °C	0.5 h	3.2%	Aqueous solution pH7	Cen et al., 2022	Enhanced rheological behavior, emulsifying properties, and hydrophobicity
Gelatin	STPP	65°C	1-3 h	0.25%-1%	Aqueous solution pH5-11	Kaewruang et al., 2014	Enhanced rheological behavior
Chitin or chitosan	TSPP	60 °C	3 h	6-7%	-	Yalpani, 1992	Creating metal-chelating agents and enhanced thermal stability
Cellulose paper	STMP	25°C	4 weeks	0.17%	Aqueous solution pH12	Inoue et al., 1995	Creating metal-chelating agents
		50 °C	2 weeks	0.15%			
***EPS from AGS**	NA	80 °C	2 h	2-2.5%	Aqueous solution pH 9-11	Bahgat et al., 2023	*Follow-up studies

4.5 Conclusion

The P-fractionation protocol established in this study and ^{31}P NMR showed that P species in acidic EPS extracted from aerobic granular sludge are free orthophosphate in the liquid phase as 25%, organic P (covalently bound to polymer chains) as 52%, NAIP metal bound-precipitates as 15%, free pyrophosphates in the liquid phase as7%, and <1% of exchangeable orthophosphate adsorbed to the polymer chains. ^{31}P NMR also showed that polyphosphates detected in the initial AGS completely/partially transformed along the extraction process to pyrophosphates, orthophosphates, and possibly to new P-esters (phosphorylation) as hypothesized in this study, which is to be further confirmed in future studies. The knowledge about P-speciation in EPS will set the foundation for future work on utilizing P to engineer EPS properties for industrial applications.

References

Bahgat, N. T., Siddiqui, A., Wilfert, P., Korving, L., & van Loosdrecht, M. C. M. (2024). FePO4.2H2O recovery from acidic phosphate-rich waste streams. Water Research, 121905. https://doi.org/10.1016/j.watres.2024.121905

Bahgat, N. T., Wilfert, P., Korving, L., & van Loosdrecht, M. (2023). Integrated resource recovery from aerobic granular sludge plants. Water Research, 234. https://doi.org/10.1016/j.watres.2023.119819

Blank, L. M. (2023). (Poly)phosphate biotechnology: Envisaged contributions to a sustainable P future. In Microbial Biotechnology (Vol. 16, Issue 8). https://doi.org/10.1111/1751-7915.14250

Cade-Menun, B. J. (2015). Improved peak identification in 31P-NMR spectra of environmental samples with a standardized method and peak library. Geoderma, 257–258. https://doi.org/10.1016/j.geoderma.2014.12.016

Cade-Menun, B., & Liu, C. W. (2014). Solution Phosphorus-31 Nuclear Magnetic Resonance Spectroscopy of Soils from 2005 to 2013: A Review of Sample Preparation and Experimental Parameters. Soil Science Society of America Journal, 78(1). https://doi.org/10.2136/sssaj2013.05.0187dgs

Cai, W., Jin, M., Zhao, Z., Lei, Z., Zhang, Z., Adachi, Y., & Lee, D. J. (2018). Influence of ferrous iron dosing strategy on aerobic granulation of activated sludge and bioavailability of phosphorus accumulated in granules. Bioresource Technology Reports, 2. https://doi.org/10.1016/j.biteb.2018.03.004

Cen, S., Zhang, L., Liu, L., Lou, Q., Wang, C., & Huang, T. (2022). Phosphorylation modification on functional and structural properties of fish gelatin: The effects of phosphate contents. Food Chemistry, 380. https://doi.org/10.1016/j.foodchem.2022.132209

E. van der Knaap, E. Koornneef, K. L., M. Oosterhuis, P. Roeleveld, & M. Schaafsma. (2019). Kaumera Nereda gum: samenvatting NAOP onderzoeken 2013-2018,2019. http://edepot.wur.nl/501893

ESPP webinar. (2020). Summary of joint European Commission-ESPP webinar on P4 (phosphorus) Critical Raw Material. https://phosphorusplatform.eu/images/scope/ScopeNewsletter136.pdf

Felz, S., Vermeulen, P., van Loosdrecht, M. C. M., & Lin, Y. M. (2019). Chemical characterization methods for the analysis of structural extracellular polymeric substances (EPS). Water Research, 157. https://doi.org/10.1016/j.watres.2019.03.068

Feng, C., Lotti, T., Lin, Y., & Malpei, F. (2019). Extracellular polymeric substances extraction and recovery from anammox granules: Evaluation of methods and protocol development. Chemical Engineering Journal, 374. https://doi.org/10.1016/j.cej.2019.05.127

Grouse, D. A., Sierzputowska-Gracz, H., & Mikkelsen, R. L. (2000). Optimization of sample pH and temperature for phosphorus-31 nuclear magnetic resonance spectroscopy of poultry manure extracts. Communications in Soil Science and Plant Analysis, 31(1–2). https://doi.org/10.1080/00103620009370432

Henderson, I. C., & Clarke, N. (2004). Two-Step Phase Separation in Polymer Blends. Macromolecules, 37(5). https://doi.org/10.1021/ma034718l

Horstink, F., Keursten, R., Doradztwo, S., Odegard, I., Uijttewaal, M., de Koning, J., & Korving, L. (2021). SPODOFOS: WITTE FOSFOR PRODUCTIE UIT SLIBVERBRANDINGSASSEN. https://www.stowa.nl/sites/default/files/assets/PUBLICATIES/Publicaties%202021/STOWA%202021-57%20%20Spodofos.pdf

Hong, T., Iwashita, K., & Shiraki, K. (2017). Viscosity Control of Protein Solution by Small Solutes: A Review. Current Protein & Peptide Science, 19(8). https://doi.org/10.2174/1389203719666171213114919

Hu, Y., Du, L., Sun, Y., Zhou, C., & Pan, D. (2023). Recent developments in phosphorylation modification on food proteins: Structure characterization, site identification and function. In Food Hydrocolloids (Vol. 137). https://doi.org/10.1016/j.foodhyd.2022.108390

Hu, Z., Qiu, L., Sun, Y., Xiong, H., & Ogra, Y. (2019). Improvement of the solubility and emulsifying properties of rice bran protein by phosphorylation with sodium trimetaphosphate. Food Hydrocolloids, 96. https://doi.org/10.1016/j.foodhyd.2019.05.037

Huang, W., Huang, W., Li, H., Lei, Z., Zhang, Z., Tay, J. H., & Lee, D. J. (2015). Species and distribution of inorganic and organic phosphorus in

enhanced phosphorus removal aerobic granular sludge. Bioresource Technology, 193. https://doi.org/10.1016/j.biortech.2015.06.120

Inoue, H., Baba, Y., & Tsuhako, M. (1995). Phosphorylation of Cellulose with cyclo-Triphosphate. Chemical and Pharmaceutical Bulletin, 43(4). https://doi.org/10.1248/cpb.43.677

Jupp, A. R., Beijer, S., Narain, G. C., Schipper, W., & Slootweg, J. C. (2021). Phosphorus recovery and recycling-closing the loop. In Chemical Society Reviews (Vol. 50, Issue 1). https://doi.org/10.1039/d0cs01150a

Kaewruang, P., Benjakul, S., & Prodpran, T. (2014). Characteristics and gelling property of phosphorylated gelatin from the skin of unicorn leatherjacket. Food Chemistry, 146. https://doi.org/10.1016/j.foodchem.2013.09.111

Kim, N. K., Lin, R., Bhattacharyya, D., van Loosdrecht, M. C. M., & Lin, Y. (2022). Insight on how biopolymers recovered from aerobic granular wastewater sludge can reduce the flammability of synthetic polymers. Science of the Total Environment, 805. https://doi.org/10.1016/j.scitotenv.2021.150434

Kim, N. K., Mao, N., Lin, R., Bhattacharyya, D., van Loosdrecht, M. C. M., & Lin, Y. (2020). Flame retardant property of flax fabrics coated by extracellular polymeric substances recovered from both activated sludge and aerobic granular sludge. Water Research, 170. https://doi.org/10.1016/j.watres.2019.115344

Koopmans, G. F., Chardon, W. J., & McDowell, R. W. (2007). Phosphorus Movement and Speciation in a Sandy Soil Profile after Long-Term Animal Manure Applications. Journal of Environmental Quality, 36(1). https://doi.org/10.2134/jeq2006.0131

Lemire, K. A., Rodriguez, Y. Y., & McIntosh, M. T. (2016). Alkaline hydrolysis to remove potentially infectious viral RNA contaminants from DNA. Virology Journal, 13(1). https://doi.org/10.1186/s12985-016-0552-0

Li, P., Jin, Y., & Sheng, L. (2020). Impact of microwave assisted phosphorylation on the physicochemistry and rehydration behaviour of egg white powder. Food Hydrocolloids, 100. https://doi.org/10.1016/j.foodhyd.2019.105380

Liang, S., Neisius, N. M., & Gaan, S. (2013). Recent developments in flame retardant polymeric coatings. In Progress in Organic Coatings (Vol. 76, Issue 11). https://doi.org/10.1016/j.porgcoat.2013.07.014

Lv, X., Huang, X., Ma, B., Chen, Y., Batool, Z., Fu, X., & Jin, Y. (2022). Modification methods and applications of egg protein gel properties: A review. Comprehensive Reviews in Food Science and Food Safety, 21(3). https://doi.org/10.1111/1541-4337.12907

Mañas, A., Biscans, B., & Spérandio, M. (2011). Biologically induced phosphorus precipitation in aerobic granular sludge process. Water Research, 45(12). https://doi.org/10.1016/j.watres.2011.04.031

Miedzianka, J., & Pęksa, A. (2013). Effect of pH on phosphorylation of potato protein isolate. Food Chemistry, 138(4). https://doi.org/10.1016/j.foodchem.2012.12.028

Pardo, P., Rauret, G., & López-Sánchez, J. F. (2004). Shortened screening method for phosphorus fractionation in sediments: A complementary approach to the standards, measurements and testing harmonised protocol. Analytica Chimica Acta, 508(2). https://doi.org/10.1016/j.aca.2003.11.005

Pronk, M., van Dijk, E. J. H., & van Loosdrecht, M. C. M. (2020). Aerobic granular sludge. In Biological Wastewater Treatment: Principles, Modeling and Design (2nd ed.), Chapter 11. https://doi.org/10.2166/9781789060362_0497

Salmeia, K. A., Gaan, S., & Malucelli, G. (2016). Recent advances for flame retardancy of textiles based on phosphorus chemistry. Polymers, 8(9). https://doi.org/10.3390/polym8090319

Staal, L. B., Petersen, A. B., Jørgensen, C. A., Nielsen, U. G., Nielsen, P. H., & Reitzel, K. (2019). Extraction and quantification of polyphosphates in activated sludge from waste water treatment plants by 31P NMR spectroscopy. Water Research, 157. https://doi.org/10.1016/j.watres.2019.03.065

Turner, B. L., Mahieu, N., & Condron, L. M. (2003). Phosphorus-31 Nuclear Magnetic Resonance Spectral Assignments of Phosphorus Compounds in Soil NaOH–EDTA Extracts. Soil Science Society of America Journal, 67(2). https://doi.org/10.2136/sssaj2003.4970

Xiong, Z., & Ma, M. (2017). Enhanced ovalbumin stability at oil-water interface by phosphorylation and identification of phosphorylation site using MALDI-TOF mass spectrometry. Colloids and Surfaces B: Biointerfaces, 153. https://doi.org/10.1016/j.colsurfb.2017.02.027

Yalpani, M. (1992). Syntheses of some sulfur- and phosphorus-containing carbohydrate polymer derivatives. Carbohydrate Polymers, 19(1). https://doi.org/10.1016/0144-8617(92)90052-R

Yang, M., Zhang, J., Guo, X., Deng, X., Kang, S., Zhu, X., & Guo, X. (2022). Effect of Phosphorylation on the Structure and Emulsification Properties of Different Fish Scale Gelatins. Foods, 11(6). https://doi.org/10.3390/foods11060804

Zayas, J. F. (1997). Functionality of Proteins in Food. In Functionality of Proteins in Food. https://doi.org/10.1007/978-3-642-59116-7

Zeng, F., Jin, W., & Zhao, Q. (2019). Temperature effect on extracellular polymeric substances (EPS) and phosphorus accumulating organisms (PAOs) for phosphorus release of anaerobic sludge. RSC Advances, 9(4). https://doi.org/10.1039/C8RA10048A

Zhang, H. L., Fang, W., Wang, Y. P., Sheng, G. P., Zeng, R. J., Li, W. W., & Yu, H. Q. (2013). Phosphorus removal in an enhanced biological phosphorus removal process: Roles of extracellular polymeric substances. Environmental Science and Technology, 47(20). https://doi.org/10.1021/es403227p

Supplementary Materials

Table S4-1: Average elemental composition of different cations and phosphorus in the alkaline and acidic supernatants

Element	Unfiltered alkaline supernatant (mg/L)	Filtered alkaline supernatant (mg/L)	Filtered acidic supernatant (mg/L)
P	1301	218	340
Ca	712	2	298
Fe	344	1	30
K	3653	-	2740
Mg	197	3	119
Al	283	2	70
Na	242	107	84
Mn	2	-	1.3

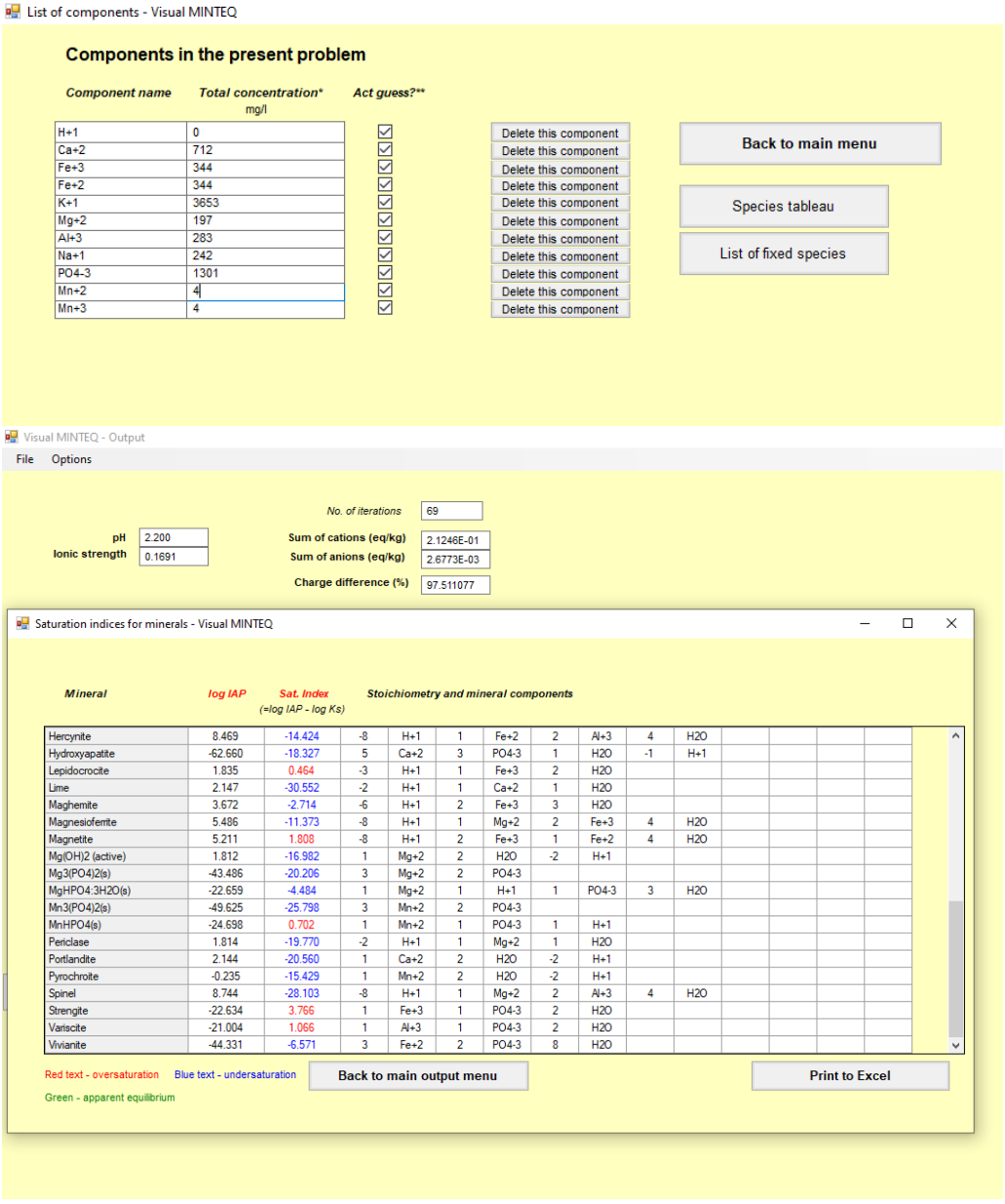

Figure S4-1: Visual MINTEQ showing the possible P-precipitates present in the acidic EPS gel

Table S4-2: Calculations to confirm that HCl addition was enough to drop the EPS from pH 2.2 to zero

pH	2.2	
H+	0.006	mol/L
pH	0	
H+	1	mol/L
H+ to be added to drop pH from 2.2 to zero	0.994	mol/L
Added HCl	7	ml
Concentration	3.5	mol/L
Total sample	21.71	mL
	0.0245	mol H+
	0.0011	mol/ml
	1.13	mol/L

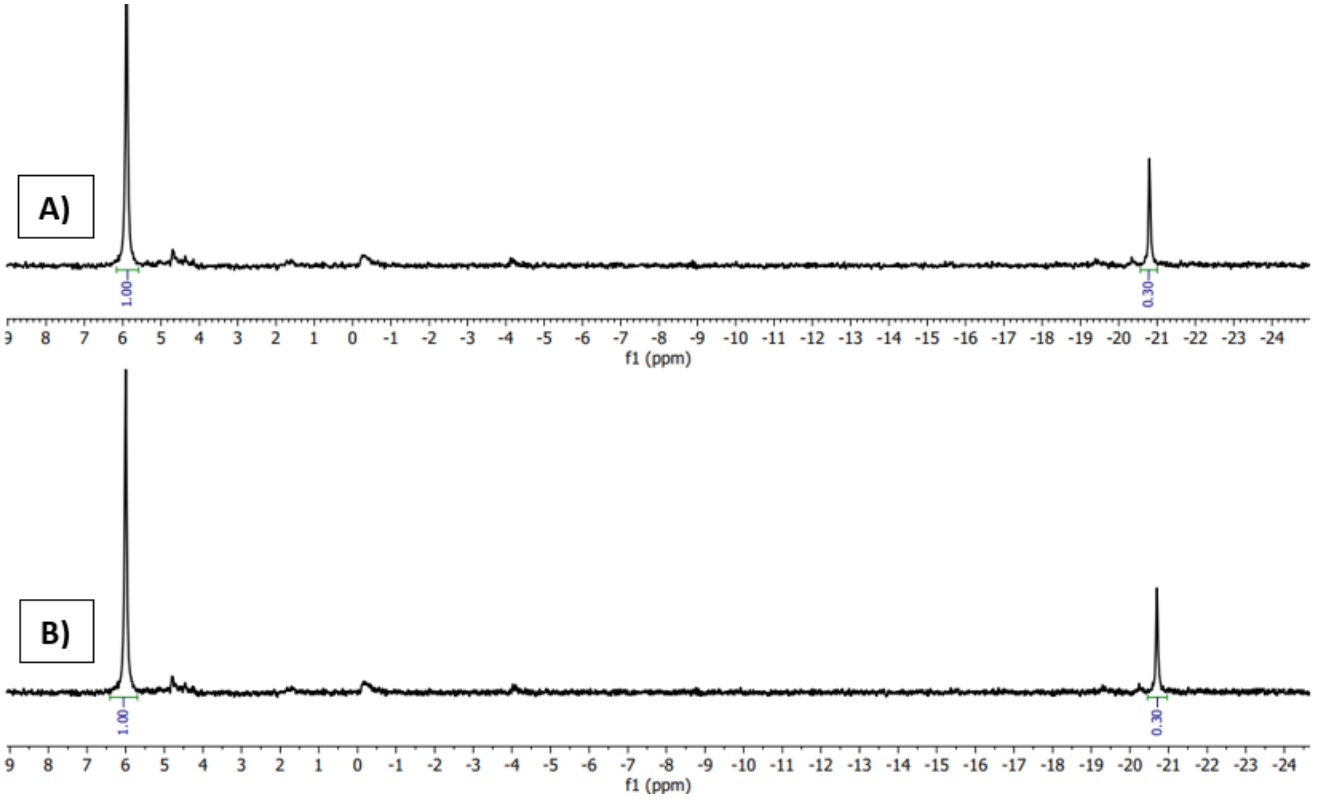

Figure S4-2: ^{31}PNMR spectra for AGS sample after B) 4 hours (300 scan) and A) 23 hours (1500 scan) measurement time

Table S4-3: EPS at pH= zero- validation step-non-apatite inorganic phosphorus dissolution (comparing moles released of P, Fe, Al and Mn) from EPS extracted from Epe WWTP

Elements	Concentration at pH 2.2 (mol/L)	Concentration at pH zero (mol/L)	Released (mol/L)
P	0.01097 ±0.00021	0.02072 ±0.00020	0.00975 ±0.00021
Fe	0.00089 ± 0.00000	0.00332 ± 0.00007	0.00243 ± 0.00007
Al	0.00261 ± 0.00006	0.00964 ±0.00023	0.00703 ±0.00020
Mn	0.00002 ±0.00000	0.00003 ± 0.00000	0.00000 ± 0.00000

Table S4-4: EPS at pH=zero -validation step-correlating COD changes to P changes

	Concentrations	
EPS (liquid+chain)	1.411	g P/kg Kaumera
	92745	g COD/kg Kaumera
	6587	g COD/ g P
Change in EPS (chain) by lowering pH to zero	6.974	g COD/L (COD^5- COD^3) from **Table *4-1***
	0.00106	gP/L
	9.9E-05	gP/kg Kaumera
	0.007%	Change of P concentration

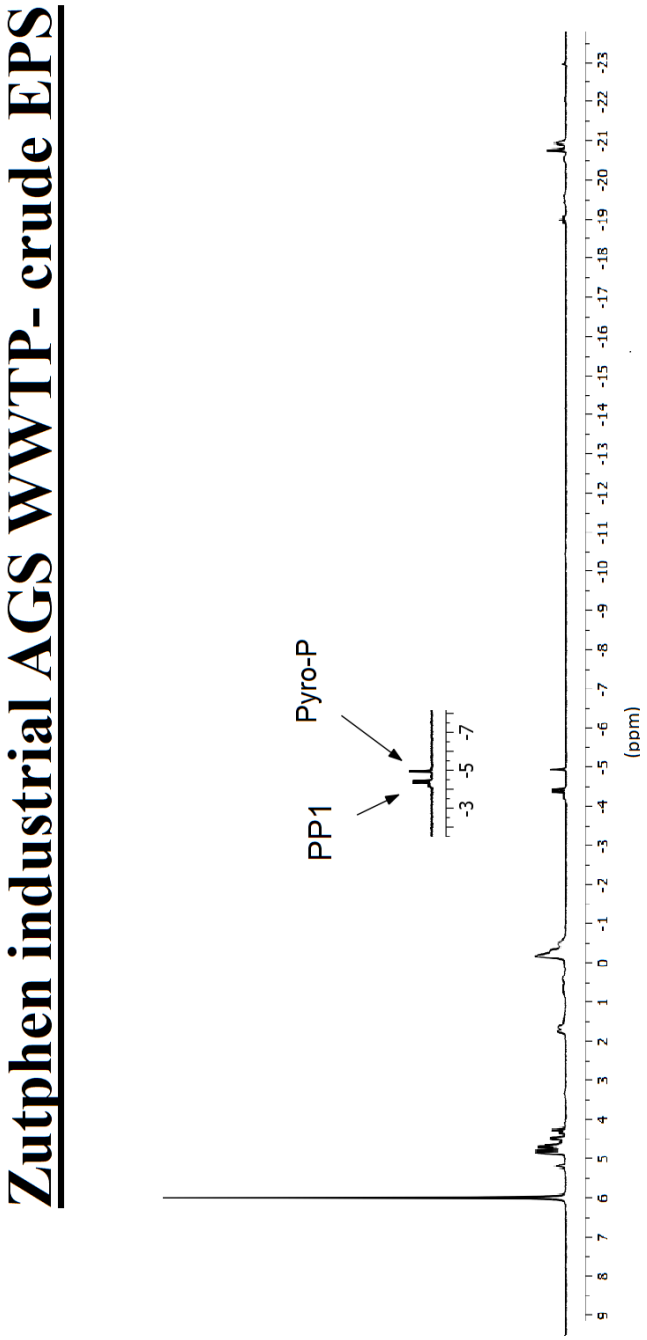

Figure S4-3: ^{31}P NMR spectrum of EPS extracted from Zutphen AGS WWTP

Zutphen Industrial AGS WWTP-crude EPS

This study aimed to establish the P-fractionation protocol so it can be used as a consistent method to look at P-speciation in EPS, not to assess the similarity/ differences of P-speciation in different EPS samples from different sources/ wastewater composition/ or extraction conditions. However, to get an idea of how variant the P speciation could be in EPS samples from different sources, an excess AGS sample from Zutphen WWTP was collected and EPS was extracted as described in section 4.2.2 similarly to Epe. The crude EPS sample from Zutphen was analyzed by ^{31}P NMR as a quick scanning method to observe the general trend of the speciation and compare it to Epe. Zutphen WWTP is operated by the water authority Rhine en Ijssel. It was chosen as it treats dairy industrial wastewater from FrieslandCampina, not municipal WWTP as Epe, so it was a logical choice to get an indication of how different the P speciation could be by choosing a very different type of wastewater.

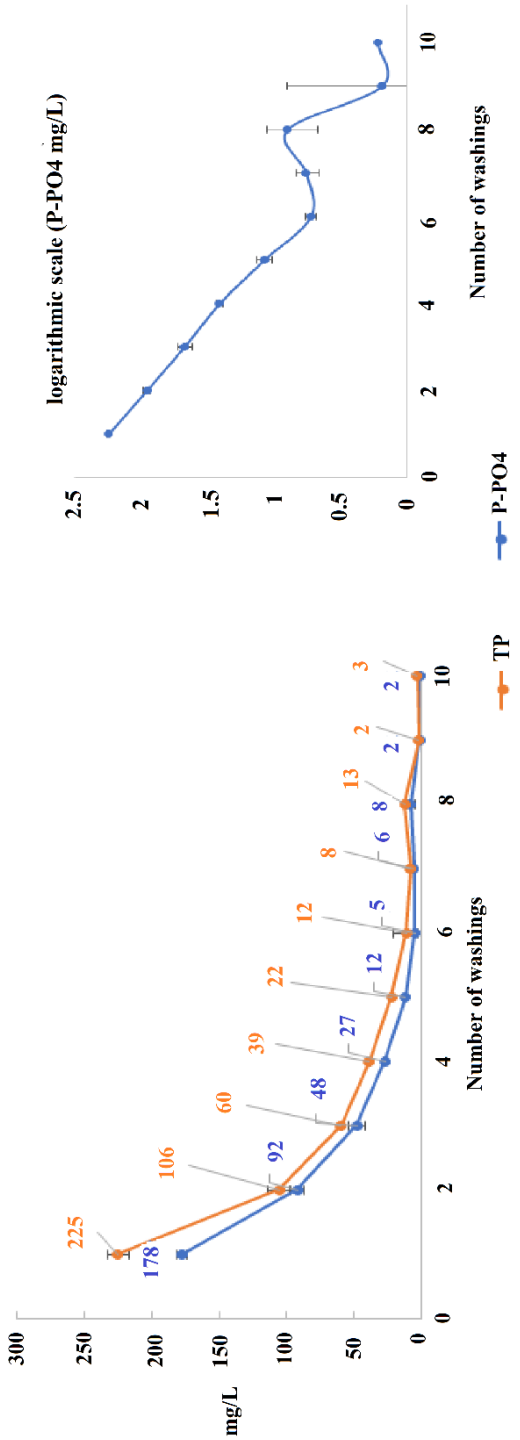

Figure S4-4: EPS washing with synthetic HCl/KCl solution- Total phosphorus (ICP-OES) and free ortho-phosphates (IC) in the washing solutions upon washing steps- All performed in triplets, average values in mg/L and standard deviation.

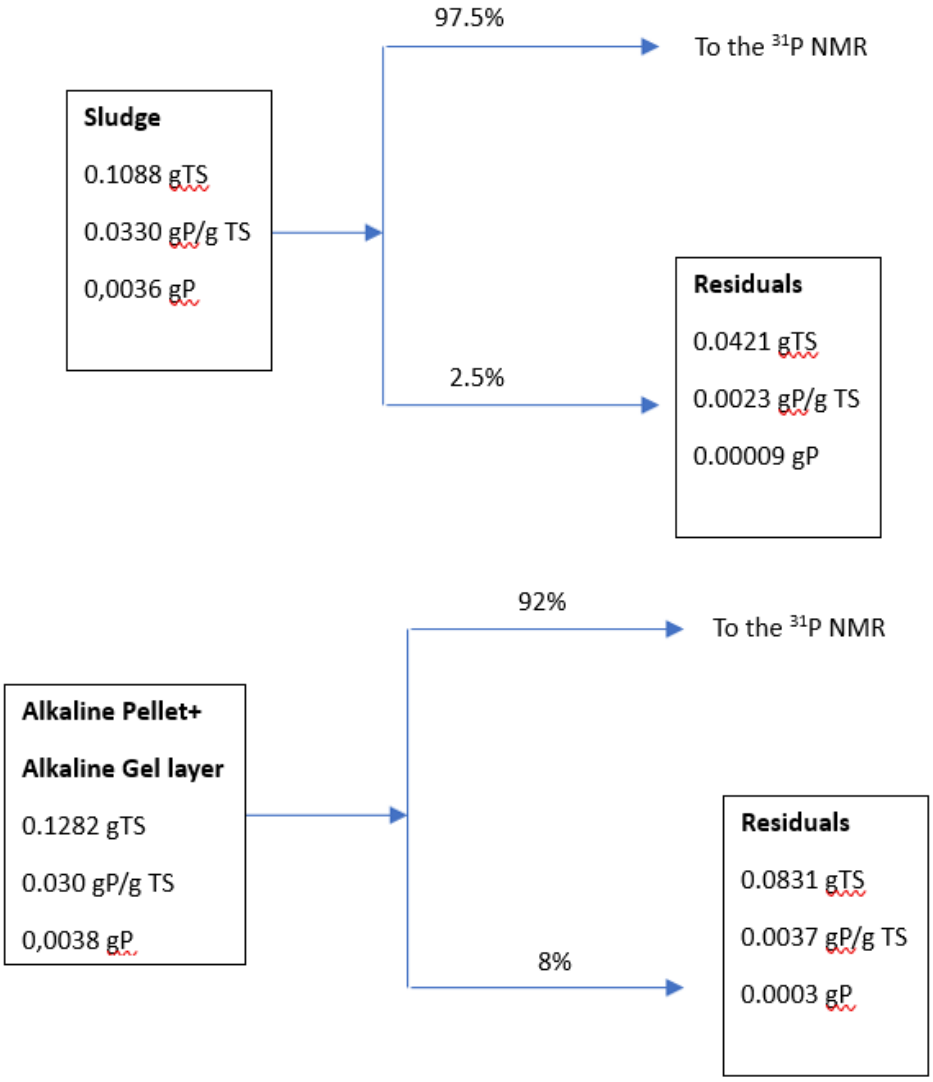

Figure S4-5: EDTA-NaOH extraction efficiency of phosphorus in sludge and alkaline pellet after removing the residuals.


15

Chapter 5

Impact of Phosphorus on the Functional Properties of Extracellular Polymeric Substances Recovered from Sludge

This chapter has been published as:

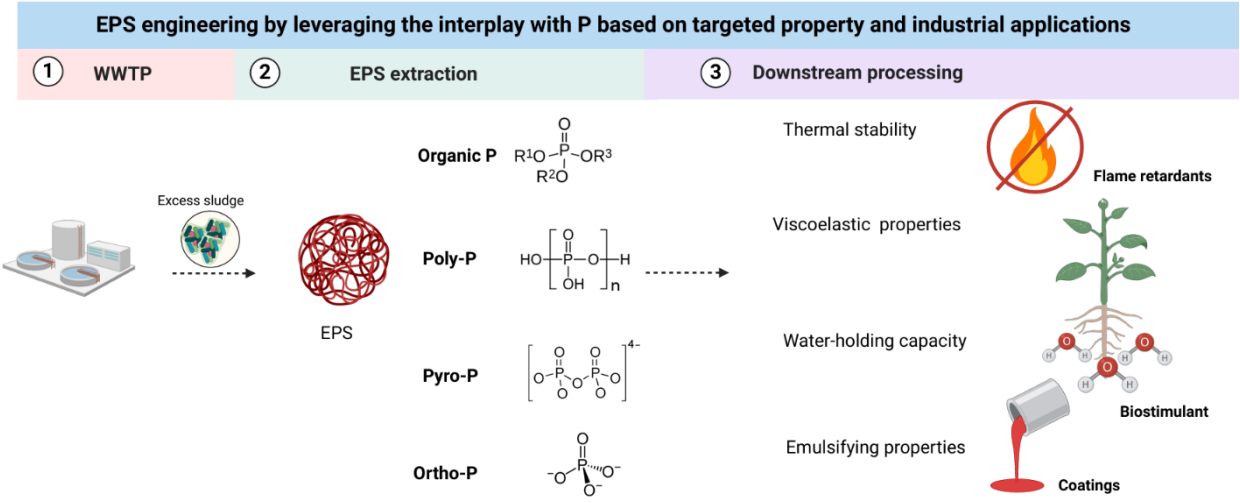

This chapter has been submitted to Water Research Journal and is under revision

This chapter was patented as:

METHOD FOR EXTRACELLULAR POLYMERIC SUBSTANCES EXTRACTION FROM AN AQUEOUS STREAM, PHOSPHORYLATED EXTRACELLULAR POLYMERIC SUBSTANCES, AND USE THEREOF.

Abstract

Extracellular Polymeric Substances (EPS) are ubiquitous in biological wastewater treatment (WWT) technologies like activated sludge systems, biofilm reactors, and granular sludge systems. EPS recovery from sludge potentially offers a high-value material for the industry. It can be utilized as a coating in slow-release fertilizers, as a bio-stimulant, as a binding agent in building materials, for the production of flame retarding materials, and more. P recovered within the extracted EPS is an intrinsic part of the recovered material that potentially influences its properties and industrial applications. P is present in EPS in different speciation (e.g., P esters, poly-P, ortho-P, etc.). Such P species are already intensively used in the chemical industry to enhance thermal stability, viscoelasticity, emulsification, water-holding capacity, and many other properties of some natural and petroleum-derived polymers. The translation of this knowledge to EPS is missing which prevents the full utilization of phosphorus in EPS. This knowledge could allow us to engineer EPS via phosphorus for specific target properties and applications. In this review, we discuss how P could affect EPS properties based on experiences from other industries and reflect on how these P species could be influenced during the EPS extraction process or in the WWTPs.

P salts Abbreviations

TSPP: Tetrasodium pyrophosphate

STPP: Sodium tripolyphosphate

STMP: Sodium trimetaphosphate

SPP: Tetrasodium pyrophosphate anhydrous

SAPP: Sodium acid pyrophosphate

TPP: Tetrapotassium pyrophosphate

SHMP: Sodium hexametaphosphate

5.1 Introduction

Extracellular polymeric substances (EPS) constitute an essential element within the matrix of microbial biofilms in diverse ecological contexts, particularly in wastewater treatment technologies, e.g., activated sludge systems, biofilm reactors, and granular sludge systems (L. Huang et al., 2022a). EPS has potential applications across industrial sectors such as agriculture, construction, textiles, paper industry, and flame retardants production (E. van der Knaap et al., 2019.; Henze et al., 2020; Feng et al., 2019; Kim et al., 2020; Lin et al., 2015). The Netherlands has established the world's first two demonstration facilities for EPS extraction from aerobic granular sludge systems (Bahgat et al., 2023; E. van der Knaap et al., 2019). These developments signify a pioneering advance in commercializing EPS recovered from wastewater sludge, emphasizing their potential significance in industrial contexts.

EPS extracted from waste sludge contains significant amounts of P (Zhang et al., 2013; Zeng et al., 2019). Bahgat et al., 2023 reported that 20% of the total P load to AGS WWTPs ultimately becomes incorporated into the EPS. P recovered within the extracted EPS is an intrinsic part of the recovered material that potentially influences its properties and industrial applications. P is already intensively used in various contexts to modify polymers to improve or endow many properties. For instance, chemical phosphorylation of polyesters and cotton in textiles and polyvinyl chloride in construction materials make these materials flame-resistant (Liang et al., 2013; Salmeia et al., 2016; ESPP webinar,

2020). Similarly, protein phosphorylation is applied in food industries to change the properties of substances such as egg white, potatoes, and rice to enhance wettability, dispersibility, and water absorption capacity (Y. Hu et al., 2023a; Z. Hu et al., 2019a; P. Li et al., 2020; Miedzianka & Pęksa, 2013a). So, phosphorus could be a way to engineer EPS by influencing its properties analogous to these polymers, thereby enhancing the significance of phosphorus within EPS.

Different P species would be expected to be found in EPS that are either microbially produced before extraction or chemically induced during EPS extraction processes. Expected species are organophosphorus groups in phosphorylated protein, sugars, and lipids and could also be polyphosphates, pyrophosphates, and orthophosphates (García Becerra et al., 2010; Huang et al., 2015; and Bahgat et al., 2023). All these possible P species are not only relevant for engineering EPS properties but could also be considered to be potential high-value phosphorus groups that could be extracted from WWTPs. These phosphorus compounds could replace some of the elemental phosphorus, P_4, derivatives that are necessary to make flame retardants, lubricants, detergents, and others in the industrial sector, representing 2% of the P rock demand (Blank, 2023; ESPP webinar, 2020; Jupp et al., 2021). So, utilizing these P groups incorporated in recovered EPS to engineer and design its properties would create an industrial niche for recovered P and EPS from WWTPs.

While there is little literature addressing the influence of P on EPS properties and possible industrial applications, the influence of P has been

extensively reported in other contexts. In this review, first, we focus on identifying P groups realistic to be present in EPS from WWTPs, collecting knowledge from various disciplines to review how P can influence polymer properties and giving indications on how this is important for EPS developments. Finally, we give ideas on how to manipulate P chemistry to engineer EPS and give a critical outlook on what research gaps we suggest to be addressed.

5.2 P species in EPS

Phosphorus, a Group 15 element, has five electrons in its outermost electron shell. It can form up to five covalent bonds by donating these electrons, such as when it combines with four oxygen atoms to create orthophosphate. Orthophosphate exhibits chemical versatility, forming various esters (P-O-C) with alkyl and aryl hydroxyl groups, as well as acid anhydrides (P-O-P). The ability of phosphate to form esters (nucleic acids in RNA, DNA, and phosphoproteins) and anhydrides (ATP, polyphosphate) which are stable at ambient temperatures in water, makes it ideal for the synthesis of biological molecules that predominate in living organisms (Hunter, 2012). It was reported by Stephanopoulos et al., 1998 that the dry biomass of E. coli consists of about 55% protein (with P as a minor modification), 20% RNA (about 3.5% (w/w) P), 9% lipids mainly phospholipids (about 2% P), 6% cell wall constituents (very minor P), 4% free metabolites (as pH buffer, as pyrophosphate, or as activation group (e.g., glucose-6-P)), 3% DNA (about 3.5% (w/w) P), and 3% storage polymer (no P). However, the phosphorus composition of bacteria differs mainly when large amounts of energy-

rich phosphate bonds are used for energy storage like in polyphosphate (Blank, 2012). **Figure 5-1** shows the possible P species to be found in EPS either microbially made or chemically induced during EPS extraction.

5.2.1 Organic P

5.2.1..1 RNA, DNA, Phospholipids

Organic P-ester groups found in DNA, RNA, and phospholipids could end up in EPS. Phosphodiester bonds make up the backbones of DNA and RNA, genetic information carriers, as the phosphate is attached to the 5' carbon of one nucleoside and the 3' carbon of the adjacent nucleoside. RNA is not stable so it will possibly hydrolyze and form monoribonucleotides during the alkaline extraction of EPS as done in Epe and Zutphen installations in the Netherlands (Lemire et al., 2016). Phospholipids are also diester compounds that have both a hydrophobic and a hydrophilic component and contribute to the structure and function of cell membranes. Phospholipids from cell membranes could end up in extracted EPS or could split to free fatty acids and glycerophosphoric acid under alkaline conditions (Hartman et al., 1980), saponification reaction, during the alkaline extraction of EPS (Bahgat et al., 2023).

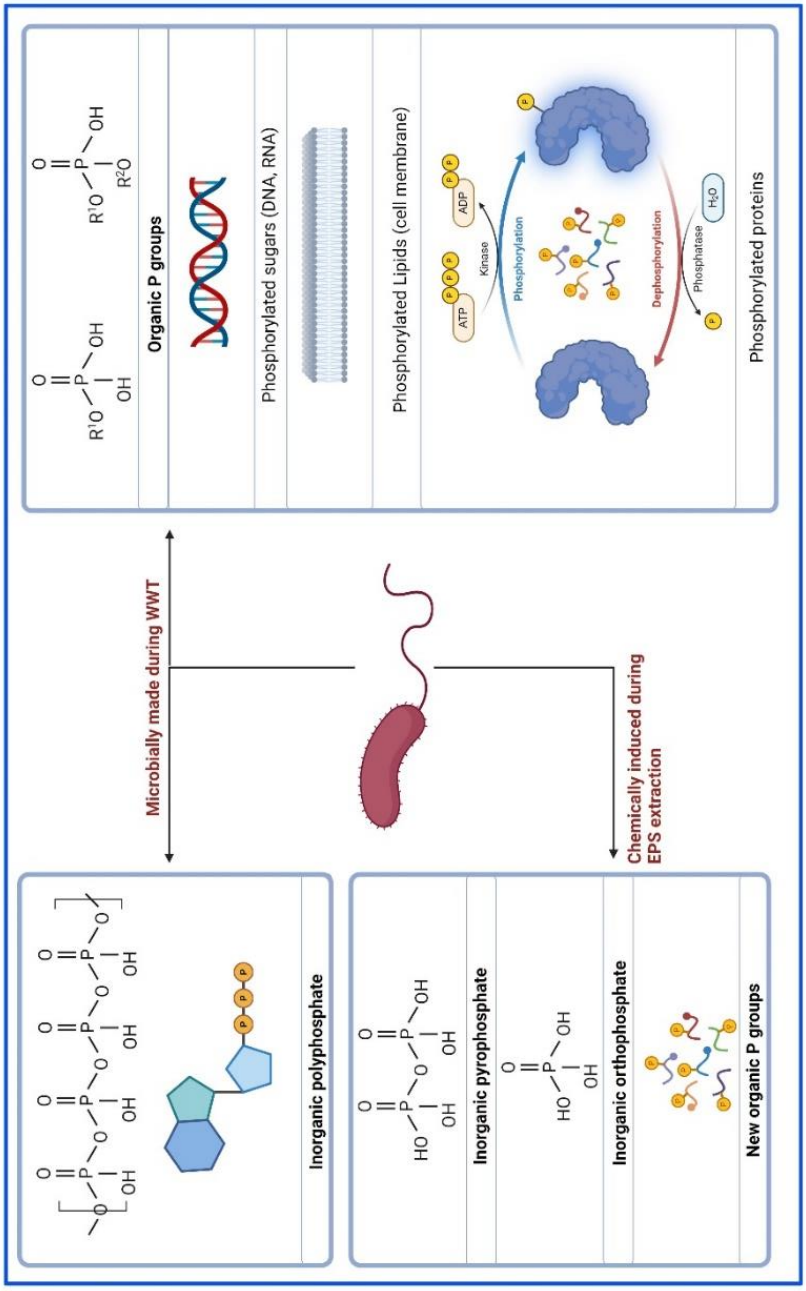

Figure 5-1: Expected P species in EPS either microbially produced or chemically induced during the EPS extraction

5.2.1..2 Phosphorylation

Phosphorylated proteins and sugars are essential components of microbial cells, involved in energy metabolism, signal transduction, enzymatic regulation, cellular structure, and stress adaptation, among other functions (Ardito et al., 2017). The only amino acids with a negative charge are Asp and Glu. Their carboxyl side chains carry a single negative charge and have a small hydrated shell. The phosphate group, characterized by a negative charge greater than 1 and a larger hydrated shell causes amino acids in phosphoproteins to function as novel chemical entities. This modification results in properties that differ from any natural amino acid and offers a way to diversify the chemical characteristics of protein surfaces (Hunter, 2012). Phosphorylated proteins and/or sugars inside cells could also end up in EPS but might also be induced chemically along the extraction process as discussed in section 5.4.2. Understanding biochemical phosphorylation in cells and pure chemical phosphorylation of polymers can help us evaluate the possible presence of phosphorylation and organic P species in EPS. Phosphorylation concept is discussed in the following two sections.

a. Biochemical Phosphorylation

Enzymatic phosphorylation in biochemistry is a highly endothermic reaction that uses a phosphate donor and an energy carrier and it occurs at a physiological pH of 7.4. ATP is a famous energy carrier in biochemistry, containing a phosphate anhydride bond (P-O-P), and it is often referred to as high-energy phosphate because it produces high free energy upon hydrolysis. That high free energy is needed so that the

overall reaction of phosphorylation proceeds with a negative ΔG^o for example glucose phosphorylation shown in equations (1), (2), and (3). **Figure 5-2** illustrates the free energies of hydrolysis (kJ/mol) for various phosphorylated compounds in cellular biology (Jakubowski et al., 2022; Smith, 2016). Thermodynamically favored reactions are determined by the energy levels, such as the utilization of ATP (higher energy compound) to produce Glucose 6-Pi and 3-phosphoserine (lower energy compounds). To maintain the energy source in the cells, ADP (lower energy compound) is phosphorylated to make ATP (higher energy compound) again using a proton gradient that provides the mechanical energy needed for phosphorylation. This reaction proceeds by the isolation of the ADP in close proximity to the phosphate, which results in a localized environment with very high phosphate/ADP activity coupled with low water activity, which is important to drive phosphorylation according to Le Chatelier's Principle (Pasek, 2020).

$$Glucose + P_i \rightarrow Glucose\ 6-P_i \qquad \Delta G_0 = 13.8\ kJ/mol \quad [1]$$

$$ATP + H_2O \rightarrow ADP + P_i \qquad \Delta G_0 = -31.4\ kJ/mol \quad (2)$$

$$Glucose + ATP \rightarrow Glucose\ 6-P_i \qquad \Delta G_0 = -17.6\ kcal/mol \quad (3)$$

b. Chemical Phosphorylation

Chemical phosphorylation is widely used in various industries for both natural and synthetic polymers to modify their properties, and it is primarily non-enzymatic (J. Chen et al., 2020; Y. Hu et al., 2022). The thermodynamics of chemical phosphorylation are driven by two main factors: 1) the abundance of the leaving group, and 2) the efficiency of the leaving group in providing the energy needed for phosphorylation

(Pasek, 2020). For example, phosphorylation by H_3PO_4 is a condensation reaction with H_2O as a leaving group. To push this reaction forward, the environment must have a high activity of the two reactants (phosphate and organic substrate) and an extremely low water activity. Therefore, this reaction requires dry conditions (Damer & Deamer, 2015) or the application of condensing agents that react with water to form new compounds, achieving the low water activity needed for phosphorylation to take place (Hulshof & Ponnamperuma, 1976). Additionally, phosphate (P_i) is also very low in energy, as shown in **Figure 5-2**, so extremely high temperatures are needed as a source of energy to induce phosphorylation (Gajewski et al., 1986). In contrast, salts containing high-energy phosphate anhydride bonds (P-O-P) are prevalent in the chemical industry. This route requires much lower activity of the P reagent and lower temperatures, and it occurs in aqueous environments because: 1) these salts have a high net energy, 2) these salts have leaving groups that withdraw electrons from the electrophilic P center, making it even more electron-poor and reactive (Klein, 2012a; Pasek, 2020), and 3) the leaving group is rarer than water, making phosphorylation more favorable. During phosphorylation, phosphate groups graft onto the structure by reacting with the side chain groups of the polymer, such as the hydroxyl groups of serine, threonine, and tyrosine, the amino groups of lysine, the 1 and 3 nitrogen atoms of the histidine ring, and the nitrogen atom of the arginine guanidine group in proteins. This forms different organic-P bonds, such as esters (P-O-C) and amidates (P-N-C) (Hadidi et al., 2021; Illy et al., 2015a; S. Liang et al., 2013; Schwenke et al., 2000). The extraction conditions of EPS, compared to

the phosphorylation conditions reported in the literature, could induce phosphorylation chemically as discussed in detail in section 5.4.2.

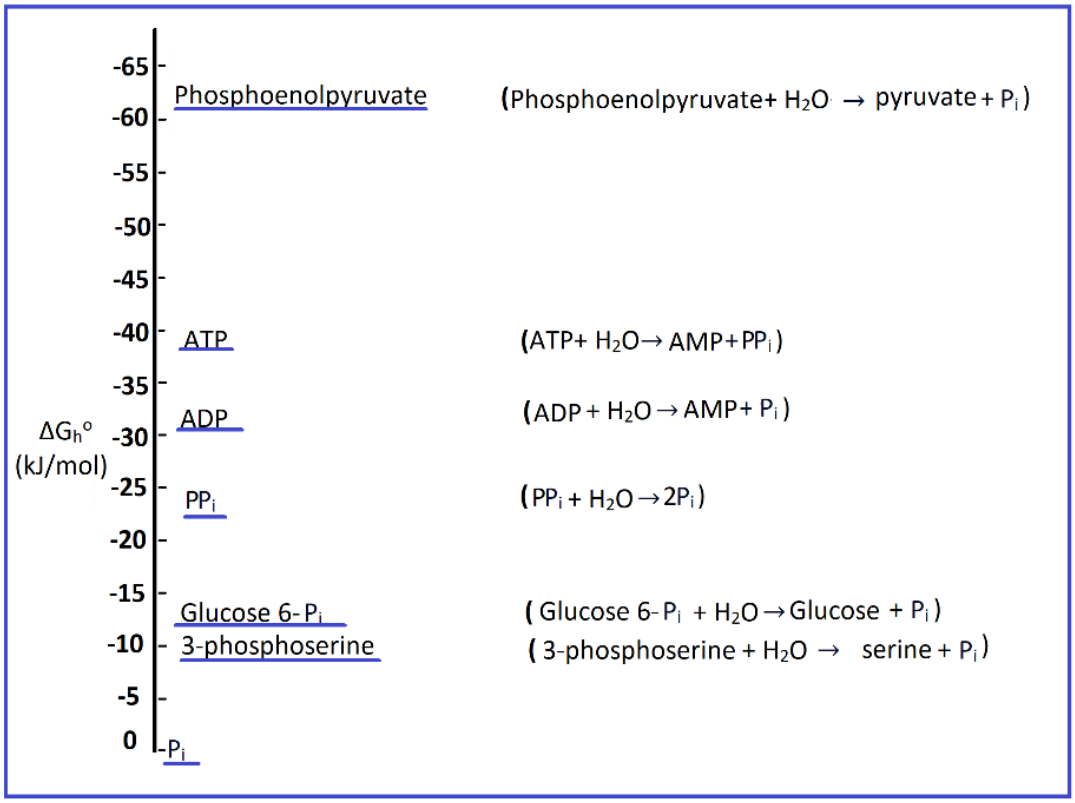

Figure 5-2: Gibbs free energy of hydrolysis (kJ/mol) of some high and low-energy phosphorus compounds compared to their cleavage products (adapted from Jakubowski et al., 2022; Smith, 2016)

5.2.2 Polyphosphates, pyrophosphates and orthophosphates

Polyphosphate is a linear polymer of a few to many hundreds of phosphates linked by a high-energy phosphate anhydride (P-O-P) bond (Akbari et al., 2021). Polyphosphate is used by many organisms instead of, or complementary to polysaccharides or lipids for energy storage, and the amount of polyphosphate can be as high as 30% of total cell mass (Blank, 2012). The phenomenon of intracellular Poly-P storage in phosphorus-accumulating microorganisms (PAOs) via luxury P uptake occurs in enhanced biological phosphorus removal (EBPR) system in WWTPs. The excess sludge produced contains around 90% of the total P load of the WWTP (Bahgat et al., 2023), mainly as polyphosphates. Polyphosphates can be hydrolyzed into pyrophosphate and subsequently pyrophosphate to orthophosphates along the EPS extraction process over time or under changing pH or temperature conditions (CHANG & RACZ, 1977; Hirota et al., 2010; Kuroda et al., 2002; McBeath et al., 2007). Pyrophosphate (PP_i) is the simplest form of polyphosphate that contains two phosphates. Orthophosphate (P_i) is the simplest and most stable form of phosphorus as it has higher resonance stabilization and greater delocalization of electrons.

Orthophosphate minerals such as struvite ($MgNH_4PO_4 \cdot 6H_2O$), calcium phosphate, and vivianite ($Fe_3(PO_4)_2 \bullet 8H_2O$) have been identified in WWTPs and sludge (Angela et al., 2011; Doyle & Parsons, 2002; Wilfert et al., 2018). These minerals may also end up in the EPS matrix based on the pH of the extraction process and the solubility of these minerals at that pH. Additionally, throughout the EPS extraction

process, phosphate minerals could form due to orthophosphate and other cations released from sludge into solution thus inducing supersaturation of these minerals, thus accumulating within the EPS.

5.3 P and functional properties

EPS showed significant potential as a flame retardant, agricultural bio-stimulant, and coating material (E. van der Knaap et al., 2019; L. M. Chen et al., 2024; N. K. Kim et al., 2022). EPS can benefit significantly from the incorporation of phosphorus groups into its structure to enhance its properties for these applications. EPS viscoelastic and water-holding properties are pivotal to further develop EPS as a bio-stimulant in agriculture to enhance soil quality. EPS versatility extends to coatings for seeds, slow-release fertilizers, and papers, as well as adhesive applications, with viscoelastic and emulsifying properties crucial for coating efficacy and durability. In the following sections, we look into how important the phosphorus groups described in section 5.2 could be for EPS properties to maximize its potential usage in those applications by gathering insights from different fields.

5.3.1 Thermal properties

Thermal stability is important to develop flame retardants (FRs) out of EPS. To understand how P could influence the thermal stability of EPS, first, the general mechanisms of P-containing FR will be discussed focusing on the P chemical groups expected to be found in EPS discussed earlier in the section 5.2. Then we look closer into biobased FRs (e.g., DNA, casein, phytic acid) as they are closely related to EPS in nature.

Finally, we focus on EPS to reflect what the existing knowledge means for EPS and its industrial application as a flame retardant.

5.3.1..1 Mechanisms of P-based flame retardants

P-based FRs are widely used due to their nontoxic degradation during the burning process, unlike halogenated FRs which are now considered global contaminants (Markwart et al., 2019). P-based FRs can be organic (e.g., phosphoesters, phosphonates, phosphinates) or inorganic (e.g., polyphosphates, phosphate minerals) (Aaronson, 1992; Naiker et al., 2023; Z. Liang et al., 2022). Flame retardants (FRs) act primarly in the condensed phase (forming a protective layer or char) but also in the gas phase (releasing flame-inhibiting gases) (Gaan et al., 2009; Naiker et al., 2023a; Salmeia, Jovic, et al., 2016). P-based FRs act in the condensed phase by enhancing the formation and stabilization of carbonaceous char on the material which isolates and protects the polymer from the flames. The char-forming products by the end of the burning process are difficult to generalize for all P-based FRs as it depends on multiple parameters, e.g., chemical structure, chemical bonds, intermolecular forces, rigidity, the oxidation state of P, combustion temperature, etc (Hu & Wang, 2019; Naiker et al., 2023; Schmitt, 2007; Cho et al., 2011; Schartel et al., 2016). P-based FRs can also act in the gas phase by forming P radicals such as PO•, PO2• and HPO2• upon heating (Scharte, 2010). These radicals trap the highly reactive radicals H• and OH•, the principal flame-propagating radicals, to terminate the exothermic reactions of the combustion cycle (Salmeia et al., 2015) , as shown in **Figure 5-3**(C). A chain reaction creates water molecules and other non-

flammable compounds dilute the gas phase which reduces the oxygen concentration (Levchik & Weil, 2005; Naiker et al., 2023; Shen et al., 2021). All these reactions together in the gas and the condensed phases cool down the system.

c. Organic P

Organophosphorus FRs are associated with the production of phosphoric acid when the system is heated and its role as a catalyst in the dehydration process of hydroxyl groups (Shen et al., 2022). Markwart et al., 2019 described that upon heating, P-ester bonds in organic P-based FRs are quickly decomposed to phosphoric acid via *cis*-elimination (main reaction) or hydrolyzation (minority reaction), as shown in **Figure 5-3**(A). During the burning process, enough energy is released to attack a non-bonding electron of the oxygen from the phosphoryl group (P=O) on the hydrogen of the second carbon from the alkoxy group. This reaction gives an alkene and a phosphorus compound with a hydroxy group. This reaction can be repeated as many times as there are alkoxy group bonds to the phosphorus. Then, the reaction of phosphoric acid in char formation depends on the polymer and its structure. For example, in the epoxy resin, as shown in **Figure 5-3**(A), the hydroxy group (P-OH) of the phosphoric acid is esterified with the hydroxy group of the undecomposed resin (HO-R) or with the aromatic alcohol (HO-Ar) which is the resin decomposition product, or polymerization takes place forming a polyphosphoric acid (inorganic glass). All these dehydration reactions create char precursors (Markwart et al., 2019; Naiker et al., 2023a; Weil & et Sergei V. Levchik, 2017).

Structural arrangements might also take place to facilitate the P-esters formation and consequently the char formation. Levchik & Weil, 2005 and Velencoso et al., 2018 reported that aromatic phosphate flame retardants, such as Resorcinol bis (diphenyl phosphate), first catalyze the Fries rearrangement during the burning process in polycarbonate/acrylonitrile butadiene styrene (PC/ABS) polymer to convert phenolic esters into hydroxy aryl ketones so phosphoric acid can react with the polymer by transesterification, forming P-ester groups.

d. Polyphosphates and pyrophosphates

Polyphosphates and pyrophosphates- based flame retardants were reported to behave similarly as the organic P-based flame retardants. Upon heating, phosphoric acid is also produced and acts as an acid catalyst in the dehydration process to form char as in ammonium polyphosphates (APP), and pyrophosphate piperazine (PAPP) flame retardants. Maqsood & Seide, 2019 investigated APP combined with cornstarch and reported APP decomposition to phosphoric acid, and ammonia. Phosphoric acid catalyzed the dehydration process of hydroxyl groups present in the starch, forming P-esters on that can later decompose, releasing carbon dioxide and water due to dehydration of the starch as described in **Figure 5-3**(B). Sun et al., 2023 also reported a similar mechanism for pyrophosphate piperazine (PAPP) that forms polyphosphoric acid substances upon heating when tested on Ethylene Vinyl Acetate polymer.

e. Orthophosphate minerals

Orthophosphate minerals such as $NH_4H_2PO_4$, $MgNH_4PO_4 \cdot 6H_2O$ (struvite), and hydroxyapatite were also reported in the firefighting industry (Z. Liang et al., 2022; Guo et al., 2018; A. H. Kim et al., 2021). Z. Liang et al., 2022 reported struvite efficiency as a fire extinguisher on burning oil samples as it acts both in the condensed phase by forming $Mg_2P_2O_7$, pyrophosphate, also called heat-resistant ceramic as a final pyrolysis product, and in the gas phase by releasing water, ammonia, and phosphorus oxygen which can absorb OH· and H· radicals in the flame. This mechanism contrasts with A. H. Kim et al., 2021's proposal, wherein struvite suspended with cellulose carriers was tested on wood. Struvite was proposed to act similarly to ammonium polyphosphate (APP), generating phosphoric acid under burning conditions, dehydrating alcohols, and forming unstable esters that decompose into char, as also reported by H. Guo et al., 2020 in their study on the flame retardancy mechanism of struvite mineralization treatment. Guo et al., 2018 also prepared cellulose nanofiber (CNF)- calcium phosphate hydroxyapatite (HAP) composite foams that showed excellent flame retardancy as HAP was thermally stable.

f. Additives that show synergy effects with P-FR

Some additives show synergy effects with P-FRs further enhancing the thermal stability of these flame retardants e.g., P-metal-based FR in the presence of multivalent cations or P-N-based FR in the presence of nitrogen-containing compounds. For example, Laoutid et al., 2021 reported that calcium-based minerals such as calcium hydroxides

combined with APP in ethylene vinyl acetate (EVA) polymers form a thicker homogenous char and significantly reduce the peak of heat release rate (PHRR) compared to when APP has been used separately thanks to the interactions with additives during combustion process. The presence of calcium hydroxide assisted in forming cohesive residues by deposition of calcium carbonate during the combustion induced by the chemical reaction between calcium hydroxide and the polymer (Laoutid et al., 2013; Rothon, 1999). It is also reported that when nitrogen is combined with phosphorus, it increases considerably the flame retardancy effect through the formation of more char (Vothi et al., 2019) as the result of intermolecular coupling via a transesterification reaction which continues until it removes all the hydrocarbons and forms a phosphorus-nitrogen compound-rich char which is thermally stable (Nguyen & Kim, 2008). Also, nitrogen-containing compounds release incombustible gases, such as nitrogen oxides (NOx), during combustion, which dilute the concentration of flammable gases, reduce the availability of oxygen, and suppress the spread of fire as for ammonium polyphosphates or melamine polyphosphate flame retardants (G. Wang & Bai, 2017).

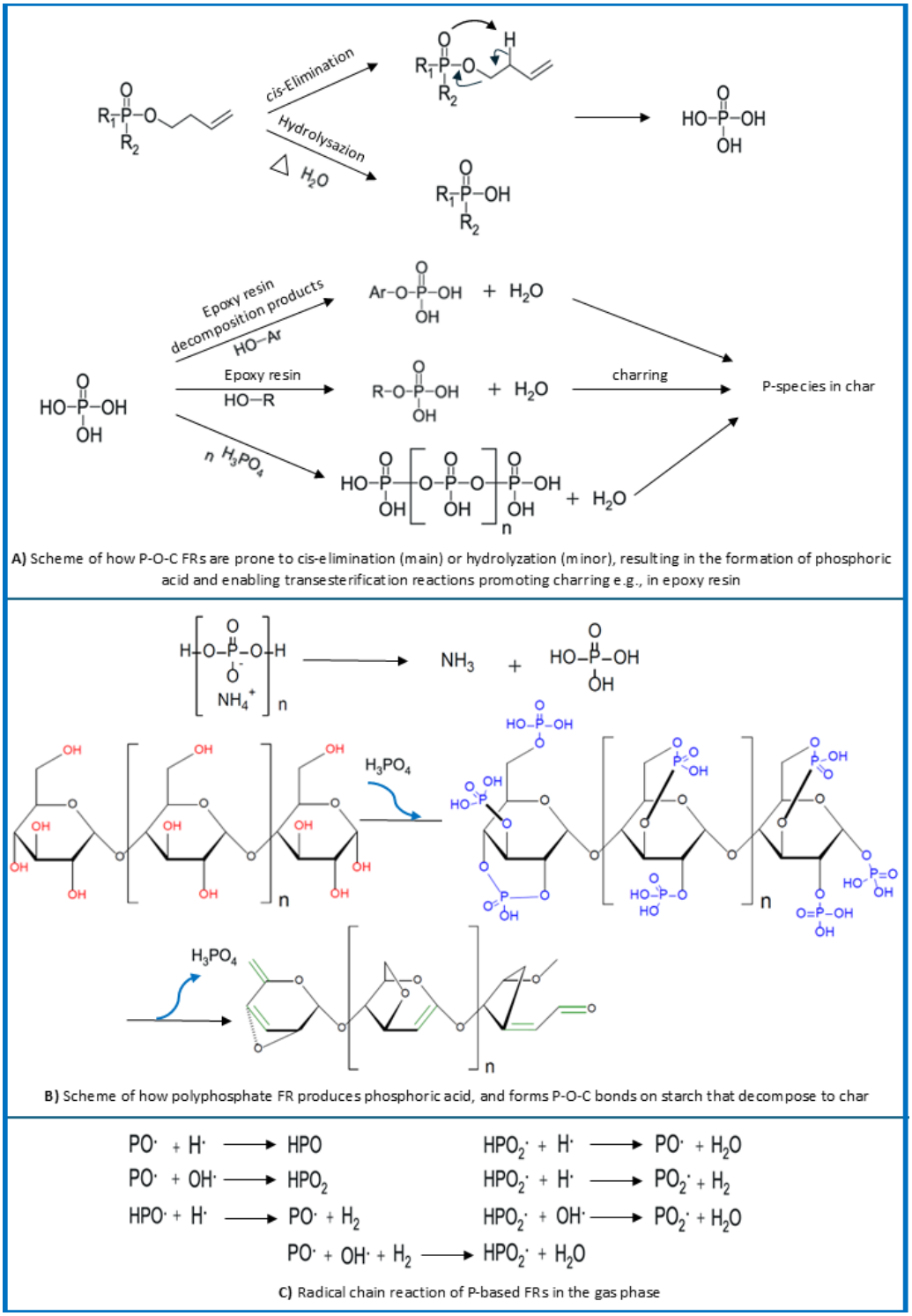

A) Scheme of how P-O-C FRs are prone to cis-elimination (main) or hydrolyzation (minor), resulting in the formation of phosphoric acid and enabling transesterification reactions promoting charring e.g., in epoxy resin

B) Scheme of how polyphosphate FR produces phosphoric acid, and forms P-O-C bonds on starch that decompose to char

$PO^{\cdot} + H^{\cdot} \longrightarrow HPO$
$PO^{\cdot} + OH^{\cdot} \longrightarrow HPO_2$
$HPO^{\cdot} + H^{\cdot} \longrightarrow PO^{\cdot} + H_2$
$PO^{\cdot} + OH^{\cdot} + H_2 \longrightarrow HPO_2^{\cdot} + H_2O$
$HPO_2^{\cdot} + H^{\cdot} \longrightarrow PO^{\cdot} + H_2O$
$HPO_2^{\cdot} + H^{\cdot} \longrightarrow PO_2^{\cdot} + H_2$
$HPO_2^{\cdot} + OH^{\cdot} \longrightarrow PO_2^{\cdot} + H_2O$

C) Radical chain reaction of P-based FRs in the gas phase

Figure 5-3: Examples from the literature of organophosphorus and poly-P FRs work in the condensed and gas phases **A)** (Markwart et al., 2019), **B)** (Maqsood & Seide, 2019), **C)** (Scharte, 2010)

5.3.1..2 Phosphorylated polymers

P-based FRs can be used as an additive (coating the material with a flame retardant as in section 5.3.1..1) or can be obtained by inducing phosphorylation of the material (performing chemical phosphorylation described in section (b)) to make the material inherently flame-retardant (Velencoso et al., 2018). Some naturally phosphorylated polymers, due to their inherent flame-retardant properties, have gained significant interest for flame retardancy applications because they are naturally phosphorylated, and elemental P_4 is not needed for their production as it is done for commercial P-based FRs. This section explores examples of naturally phosphorylated biopolymers e.g., DNA, casein, and phytic acid, as they are analogous to the EPS nature.

g. DNA

Deoxyribonucleic acid (DNA) has been reported as a flame retardant for different polymeric matrices as ethylene-vinyl-acetate (EVA), polypropylene (PP), and polyamide 6 (PA6) and 10 wt.% DNA showed good performances and a reduction in the PHRR of more than 50% in all polymeric matrices (Alongi et al., 2016). DNA is an effective flame retardant because its chemical structure contains P-esters as a phosphoric acid source, charring deoxyribose carbohydrates, and nitrogen-heterocyclic building blocks as blowing components forming ammonia and nitrogen inert gases during combustion (Alongi et al., 2013, 2015, 2016; Koedel et al., 2021). ATR-FTIR and TGA analysis showed the separation of sugar (phosphorus part) and nucleobase (nitrogen part) via scission. Phosphodiester sugars underwent dehydration,

polymerization, and reorganization through pyrolysis to form char as described earlier. Nucleobases reacted with each other, leading to dehydration and polymerization, also forming char. This suggests that there is a synergy effect between phosphorus and proteins contributing to the flame retardancy of DNA. DNA as a flame retardant for cellulose acetate (CA) polymer was also investigated by Koedel et al., 2021, and it was reported that flame-retarding effects of DNA on CA are concentration-dependent. The 10 wt.% DNA mixture exhibited the strongest PHRR reduction by 25.5%, twice as high as the PHRR reduction of 5 wt.% DNA mixture.

h. Casein

Casein has also been proposed as a bio-based flame retardant. Phosphorus is present inside micellar casein (0.7–0.9 wt.%); its structure is unclear, but it has a high P content in the form of colloidal CaP and P-ester bonds (phosphor-serine) (Uddin et al., 2020; Hindmarsh & Watkinson, 2017; Léonil et al., 2013). In earlier studies, casein exerted flame-retardant effects on cotton fabric (Carosio et al., 2014; Malucelli et al., 2014; Xu et al., 2019). Xu et al., 2019 have modified casein by introducing more P atoms to reach 7.2 wt.% to expand its application as a flame retardant in textiles. The P atoms were first introduced into casein by chemical phosphorylation to synthesize the casein-based FR, which was then grafted onto cotton fabrics by covalent bonds. During the burning process, the casein-based flame retardant changed the conventional pyrolysis route of cellulose as phosphoric acid was released and dehydration reactions occurred to form a strong char layer. This

study did not report specifically if colloidal CaP contributed to the flame retardancy effect or not; however, we propose that calcium would contribute to the flame retardancy of casein. Calcium phosphate could have formed hydroxyapatite while burning forming a thermal stable layer as mentioned earlier in section (e). Similarly, Uddin et al. 2020 reported that magnesium produced a thermally stable insulating magnesium oxide layer in casein-magnesium composites.

i. Phytic acid

Phytic acid (PA), or inositol hexaphosphate acid, is another phosphorus-rich natural substance explored as an eco-friendly FR. With a phosphorus content of 28 wt.%, PA serves as the primary phosphorus source in plant tissues, mainly in seeds, roots, and stems. Cheng et al., 2016 used PA to make poly (lactic acid) (PLA) fabric less flammable and reported that higher concentrations of PA led to a greater reduction in PHRR of the treated fabric. Liu et al., 2023 reported that an effective approach to maximize the flame retardancy of PA involves blending PA with other elements to create a compound or mixture, establishing a synergistic flame-retardant system such as a phytate metal system. Since PA has 6 negatively charged phosphate groups in its structure, it has a strong affinity for metals. It can form complexes with metal ions (magnesium, sodium, potassium), further enhancing the char layer formation.

5.3.1..3 Insights into Flame Retardancy in EPS

EPS, extracted from excess sludge, can replace traditional flame retardants in the chemicals industries. EPS is a gel-forming polymer that

consists of a mixture of proteins, free amino acids, sugars, and glycoconjugates (including glycoproteins and glycolipids) and other inorganic metals such as iron, calcium, phosphorus, etc (Bahgat et al., 2023; L. M. Chen et al., 2024; Komazin et al., 2019).

EPS extracted from AGS was reported to have 2-2.5% dry weight of phosphorus, with 25-30% of total P as free orthophosphates in the liquid fraction and 75%-70% is bound P (possibly organic, polyphosphates, pyrophosphate, mineral precipitates or others) (Bahgat et al., 2023). Kim et al., 2022 reported EPS as a possible bio-based flame retardant since polyvinyl alcohol (PVA) composites fully decomposed at 800°C, whereas approximately 31.7% residue remained in the EPS/PVA composite, and the EPS/PVA composite exhibited a 36.4% reduction in PHRR compared to PVA alone. Kim et al., 2020 also reported that EPS-AGS had better results than EPS-flocs. They contributed the difference to the phosphorus in the EPS because carbonated hydroxyapatite was a dominant composite in the remaining residue of EPS-AGS coated flax fabric after burning, unlike the residue of EPS-flocs coated flax fabric in which only amorphous phosphate was detected, suggesting that different P groups would contribute differently to the thermal stability. Carbonated hydroxyapatite is a thermally stable barrier contributing to the flame retardancy effect as explained in sections e) and f), and its formation could be explained that calcium phosphates, either present initially in EPS or formed during heating react with CO_2 produced while burning. Another possible mechanism is that organic P or poly-P in EPS releases H_3PO_4 upon heating and acts as a catalyzer forming the char layer as explained in sections c) and d). Also, EPS contains other

components that could contribute to flame retardancy such as nitrogen-containing compounds (similarly to P-N-based flame retardants and reports on DNA), charring sugars (similarly to reports on DNA), metals such as calcium, magnesium, iron (similarly to reports on phytic acid). All these components besides phosphorus could be a synergistic effect contributing to the flame retardancy of EPS. Therefore, although there is evidence that phosphorus components play a role, the exact mechanism of flame retardancy is still unknown and needs further investigation.

5.3.2 Physiochemical properties

The intercellular structures formed by EPS possess the inherent capability to retain moisture through two binding mechanisms: electrostatic interactions and hydrogen bonds (Neyens et al., 2004). EPS also carries a negative charge and selectively binds to divalent cations forming a stable gel that prevents water seepage from flocs pores which makes it a choice as a biostimulant in agriculture, horticulture, and forestry (Mangrum & Jenkins, 2020). Viscoelastic properties and water-holding capacity properties are important to develop EPS as a bio-stimulant. EPS can also be applied as a coating material for seeds, paper, slow-release fertilizers, and also as an adhesive material. Emulsifying properties are important for coatings applications to improve the performance and extend the shelf life of the coating, and viscoelastic properties are important to ensure the ability of making thin coatings and films out of EPS. For any industrial applications where an EPS system is used as a gel it would be important to know and even be able to influence the

viscoelastic properties. P could contribute to these properties and could be a way to tune the properties. So, in this section, we explore the mechanisms by which P influences these properties in different matrices as in food industries, such as in walnuts, egg whites, ovalbumin, potatoes, and rice proteins to understand how this knowledge translates to EPS (Y. Hu et al., 2023; Cen et al., 2022; Y. R. Wang et al., 2019; Anjaneyulu et al., 1989; Hsu & Chung, 2001).

5.3.2..1 Influencing the intermolecular forces of polymers via P salt addition

The combination of intermolecular forces of polymers leads to a well-developed structure causing specific polymer properties. For example, the three-dimensional protein structures are maintained by intermolecular forces such as covalent bonds (e.g. disulfide bonds), noncovalent bonds (e.g. hydrogen bonds), hydrophobic interactions, and electrostatic interactions (Castellanos et al., 2014; Hong et al., 2017). The properties of proteins can be modified by influencing these intermolecular forces via polyphosphates and pyrophosphates salts addition and introducing organic P groups (chemical phosphorylation, described in section b)) that increase the polymers electronegativity or influence the physiochemical environment (changes in pH and ionic strength).

j. Organic P

The properties of polymers can be modified by influencing intermolecular forces by introducing phosphate groups on the side chains of the polymers by phosphorylation. These new organic-P bonds increase the electronegativity of the polymer which enhance the ionic interaction

between phosphate groups and -NH_3^+ of amino acids (Criado-Gonzalez et al., 2020; T. Huang et al., 2019; Kaewruang et al., 2014b) and can form salt bridges in the presence of metal ions bridging between negatively charged P groups on the polymer molecules (Bryant & McClements, 2000; Lv et al., 2022;Arfat & Benjakul, 2013). Arfat & Benjakul, 2013 reported the enhancement in the gelation of phosphorylated protein isolate of yellow stripe trevally by the addition of zinc sulfate as zinc served as a cross-linker via a salt bridge between the negatively charged phosphate groups introduced by phosphorylation.

k. pH and ionic strength

P salt addition can also influence the intermolecular forces and polymer properties via physicochemical changes, pH, and ionic strength. When the pH of the polymer environment is close to the isoelectric point (pI) (pH point where a particular molecule carries no net electrical charge, equally positive and negative charges), the static repulsion between polymer molecules decreases, and it aggregates. However, at pH > pI, the polymer will have a higher negative charge; at pH < pI, the polymer will have a higher positive charge. That creates electrostatic repulsion forces and exposes the hydrophobic groups inside the polymer, influencing the intermolecular forces causing the swelling of the polymer chains (Duan et al., 2013; Lv et al., 2022). Ionic strength also influences intermolecular forces such as pH. Salt addition increases the negative charge of the polymer due to anion preferential binding, increases the electrostatic repulsion forces, and the exposure of the hydrophobic groups. Cations from the salt addition also form an ion cloud around the

polymer, resulting in local concentration difference and increased osmotic pressure, causing further swelling of the proteins filaments (Offer et al., 1989a; Puolanne et al., 2001). However, excessive salt can cause the ionic and hydrogen bonds between protein molecules to break and cause the system to collapse (Sow & Yang, 2015); hence, controlled pH and ionic strength are necessary to have the optimum effect on polymer properties upon salt addition. P salts are also commonly used in the meat industry because P has multiple negative charge which induces higher electronegativity and physiochemical changes with little salt addition. Also, it forms a sticky gel layer upon heating that greatly reduces water losses after cooking compared to other salts (Cao et al., 2020; Feiner, 2006; Offer & Trinick, 1983; SIEGEL & SCHMIDT, 1979; S. Q. Xu et al., 2009).

5.3.2..2 Viscoelastic properties

EPS exhibits both viscous and elastic characteristics when deformed under stress. As discussed in the earlier section, phosphorus influences the intermolecular forces of polymers and consequently their viscoelastic properties. Cen et al., 2022 phosphorylated fish gelatin (FG) using TSPP (50 Celsius, 30 mins, pH 7), and Kaewruang et al., 2014a did the same using STPP (65 Celsius, 1-3 hours, pH 5-11) and reported enhanced gelation and better gel strength of gelatine. The samples were dialyzed in both studies to confirm that the better gelation effect was due to bound phosphorus to the FG. Both studies showed that excessive phosphorylation (organic bound) or addition of orthophosphates (free) weakened the gel strength due to electrostatic repulsions between

protein molecules. Similarly Yu et al., 2024 reported that phosphorylated ovalbumin (OVA) addition to pork myofibrillar protein (MP) increased the gel hardness by 2.67-fold higher compared to the control; however, excess addition of phosphorylated OVA decreased the gel hardness which was attributed to the fact that excessive amounts of P-OVA weakened the interaction between MP and P-OVA and resulted in depolymerization (Walayat et al., 2021). Hence, the degree of phosphorylation is a crucial parameter to optimize, and residual free phosphate concentrations might have to be prevented or eliminated to prevent negative influences on gelation. Xiong & Ma, 2017 reported stronger intermolecular cross-linking, improved rheological properties, and increased rigidity of phosphorylated ovalbumin (OVA) using STPP within pH 5-9 and at 45 °C for 12 hours. MALDI-TOF/MS confirmed that phosphate groups were successfully grafted onto the OVA backbone through covalent interactions and C-O-P bond formation, and the number of phosphorylated peptides was similar over the pH range. Kaewruang et al., 2014a also reported that gelatin phosphorylation occurred over pH 5-11 but the alkaline pH range had the highest gel strength, which was interpreted due to a higher phosphorylation degree at alkaline pH. Miedzianka & Pęksa, 2013 also reported a higher phosphorylation effect at alkaline pH compared to lower pH while phosphorylating potato protein isolates at a pH range of 5.2-10.5 at room temperature for 30 mins. Phosphorylation at alkaline pH was also reported by SUNG et al., 1983 for phosphorylation of soybean protein (pH 10.5–12.5, 25–45 °C, for 3 h). Also, Woo et al., 1982 obtained stable phosphorylated bovine protein at pH 8.5, and the ^{31}P NMR spectral

data suggested that protein lysine and histidine residues have been phosphorylated. Hence, pH also plays a role in optimizing phosphorylation, and alkaline conditions seem to induce higher phosphorylation degree than acidic conditions. To understand the influence of pH on phosphorylation, it is important to think about the activity of the nucleophilic organic groups and the stability of the P salt leaving groups (Klein, 2012). Ideally, the pH should be such that the nucleophile is in its deprotonated, more active form, while the leaving group remains protonated enough to leave easily. OH^- is only active in alkaline conditions, where it is in its deprotonated form (Illy et al., 2015b; Li et al., 1997; Petreuş et al., 2003b). The unprotonated form of NH_2 groups is a good nucleophile as it has a pair of lone electrons on the nitrogen whereas acidic conditions will make it less active due to NH_3^+ formation, although it can still participate in nucleophilic attacks (Miedzianka & Pęksa, 2013; SUNG et al., 1983). Therefore, slightly alkaline conditions more optimal for higher phosphorylation than acidic conditions.

5.3.2..3 Water-holding capacity

Water holding capacity (WHC) is the ability of the polymer to hold water during the application of force, pressure, centrifugation, or heating (Ikeuchi, 2011; Zayas, 1997) Viscoelastic properties and WHC are related concepts as intermolecular forces influence both properties (Albarracín et al., 2011; Poornima & Dean, 1995) and the development of a three-dimensional network structure, capable of capturing water molecules and trapping them, leading to better WHC (Hughes et al., 2014;

X. Wang et al., 2017). Miedzianka & Pęksa, 2013 reported improved WHC in phosphorylated potato protein isolate after STMP treatment and dialysis to confirm that improved WHC was due to new bound phosphorus. Increased water holding capacity of phosphorylated soy protein isolate using STMP was also observed by SUNG et al., 1983 who confirmed phosphoesterification of serine residues and the phosphoramidation of lysine residues in soy protein and shift of pI (isoelectric point) of the protein approximately 0.8 pH unit because of the introduced negative phosphate groups. Yu et al. 2024 also reported that phosphorylated ovalbumin (OVA) addition to pork myofibrillar protein improved the WHC up to 76% due to the construction of more compact network structures, which facilitated the capture of water molecules and increased the WHC of the MP gel.

The combined effect of P salts via phosphorylation and physiochemical properties on WHC could also be concluded from the meat industry literature and knowledge on actomyosin ATPase cycle in nature. Anjaneyulu et al., 1989 studied the effect of SPP, SAPP STPP, and SHMP on the physicochemical properties of raw and cooked buffalo meat and patties. They reported a WHC increase of 3-4-fold depending on the type of phosphate and its concentration. Pyrophosphate was found to be significantly superior in increasing WHC and moisture retention % in raw and cooked buffalo patties than other polyphosphates due to its greater contribution in raising the pH of meat compared to polyphosphate salts (Kondaiah et al., 1985; Molins, 2018; Zayas, 1997). Gadekar et al., 2014 also reported a similar trend of enhanced WHC, moisture retention %, and decreased cooked losses in raw and cooked patties

using TPP and TSPP in goat meat. The increase of WHC in raw patties is associated with physiochemical changes, as discussed in section (k), but also due to phosphorylation as discussed in section (j). Although phosphorylation was not verified directly in those studies, based on the methodology used (heat treatment during cooking, high pH, P-O-P salts addition), this should have induced phosphorylation, which makes P-O-P salts superior in meat applications compared to other salts (e.g., NaCl). This can be confirmed by Trout & Schmidt, 1986 who reported that the improvement in protein functionality in meat products by *P-O-P* salts could not be explained only by pH or ionic strength changes as it also forms a sticky gel on the top of the cooked meat, binding meat pieces together (Offer et al., 1989; Offer & Trinick, 1983). P-O-P salts act to dissociate actomyosin via myosin phosphorylation, which frees myosin (increases its solubility) to participate in a greater number of molecular interactions (Jolley & Offer, 1984; SIEGEL & SCHMIDT, 1979b). Myosin was reported to be the main responsible protein for the binding together of meat pieces as it forms a sticky exudate on the surface of meat products. This effect is similar to the role of ATP in the actomyosin ATPase cycle, a fundamental process in muscle contraction, when it binds to myosin head and detaches it from the actin (L. Cao et al., 2020; Kodera & Ando, 2014; Cecchini et al., 2008). So, P-O-P salts added to meat products not only influence pH and ionic strength but also bind to myosin (phosphorylation concept kicks in), causing actin-myosin dissociation which enhances the gelling, texture, tenderness, and WHC of the meat. Since EPS could contain different P species as discussed in section 5.2, organic P species could influence

the intermolecular interactions between EPS proteins, or in general different P species could influence pH and ionic strength and consequently influence EPS viscoelastic and WHC properties.

5.3.2..4 Emulsifying properties

Phosphate esters are anionic emulsifiers that have many industrial applications (e.g., detergents, cleaners) because of their excellent surface properties, chemical stability, and biocompatibility (Zhao et al., 2020). These esters have a negative charge on the phosphate group acting as the hydrophilic part and the hydrocarbon chain is the hydrophobic part (Cooper, 1963). Enhancing the emulsifying properties of proteins through phosphorylation is also reported in food literature to enhance their stability against environmental stress (Chen et al., 2019; (Y. Hu et al., 2023). For example, Ovalbumin, the most abundant protein in egg white, treated with STPP with dry heating exhibited higher stability against flocculation, coalescence and phase separation compared to the native Ovalbumin due to the formation of phosphopeptide monoesters revealed by FTIR, XPS and ^{31}P NMR (Xiong et al., 2016). Z. Hu et al., 2019 also reported better stability and storage for phosphorylated rice bran protein under wide range of environmental conditions, phosphate esters and changes in the secondary and tertiary structure of the protein was observed upon the phosphorylation with STMP. Miedzianka & Pęksa, 2013 also reported better emulsifying activity for phosphorylated potato protein isolates over pH range of 5.2 to 10.5 and higher emulsifying activity at the alkaline range. As mentioned in section 5.2.1..1, phospholipids (P-diesters) are part of the cell membranes that

might end up in the EPS. Phospholipids were also reported to reduce the surface tension to levels ranging from 25 mN/m to 45 mN/m (Veldhuizen et al., 1998). García Becerra et al., 2010 reported that the surface tension of alkaline extracts of sludge decreased from 70 mN to around 35 mN/m increasing the pH from 7 to 13 due to the release of lipids, mainly phospholipids as detected by ^{31}P NMR. So, organic P might also be one of the factors contributing to EPS emulsifying activity and stability over time which boosts its possible applications as a coating material.

5.4 Outlook: EPS engineering via P

5.4.1 Translating Literature Knowledge to EPS

The previous sections show that different P species that are expected to be present in EPS after extraction are likely to influence properties such as flame retardancy, viscoelasticity, water holding capacity, emulsifying properties etc. The main influences of P groups in EPS that we anticipate are the following:

- For thermal stability: organic P, polyphosphates, and pyrophosphates in EPS could contribute significantly to its flame retardancy by forming phosphoric acid upon heating and its role as a catalyzer for the dehydration reactions forming the char layer. Orthophosphate minerals, if initially present in EPS or formed during burning, could also contribute to flame retardancy by forming a thermal stable layer e.g., hydroxyapatite. Or if all these P species were present in EPS, a synergic P and

multivalent cation flame retardant could be anticipated. The presence of glycoproteins and amino acids in EPS could also contribute to flame retardancy along P species creating a synergic P-N based flame retardant.

- For viscoelastic properties, water-holding capacity, and emulsifying properties: Organic P in EPS could contribute significantly to these properties, as it changes the surface chemistry by increasing its electronegativity and influencing the intermolecular forces. Polyphosphates, pyrophosphate salts or any other salts that could influence the pH or the ionic strength of the polymer would also influence the intermolecular forces and consequently the polymer properties. Around 15-20% TS of EPS extracted from AGS is salt (primary from the chemical additions in the extraction process, ends up as ash), as estimated by Bahgat et al., 2023. Such a high salt content could contribute significantly to these properties, so, washing experiments are recommended for the EPS to evaluate the influence of these salt on viscoelastic and water-holding capacity properties and if it is recommended to wash it or not for industrial applications. These washing experiments could also be designed to differentiate the influence of anions and cations to EPS. Since EPS is reported to be mostly negatively charged (L. Huang et al., 2022b; Sudmalis et al., 2020), it is expected that cations could also have a significant influence.

5.4.2 Engineering P species in EPS

Understanding and influencing the role of P species in EPS will open a new direction towards how to potentially maximize the effect of P on EPS by engineering certain P species in EPS, for instance, by inducing phosphorylation. Based on the phosphorylation conditions reported in sections b) and 5.3.2, EPS extraction conditions reported by Bahgat et al., 2023 (mainly the alkaline solubilization step) are very promising to induce purely chemical phosphorylation: 1) the sludge treated at this stage already contains significant amounts of polyphosphates (high energy P-O-P salt if not stored anaerobically in the buffer tank to provide the energy needed for phosphorylation), 2) the temperature is 80 Celsius (high temperatures promote the endothermic phosphorylation reaction), 3) the pH is alkaline ≈9 (potentially promoting higher phosphorylation degree compared to acidic conditions because slightly alkaline conditions deprotonate the nucleophilic hydroxyl and amino groups), and 4) the incubation time is 2 hours (in the same order of magnitude of phosphorylation incubation time in literature). The consequences of phosphorylation may vary depending on the polyphosphate concentrations in the sludge, EPS molecular conformation, the available phosphorylation sites, the extent of phosphorylation, operating pH, temperature, incubation time, and others. Future research should investigate all these different factors to assess the optimal conditions to promote better phosphorylation and better influence of EPS properties. The addition of external polyphosphates or pyrophosphate salts into the alkaline EPS extraction step could also be a way to engineer EPS properties if a higher P salt concentration is needed to promote

phosphorylation. Other ways to engineer or select different P species in EPS could be adding Ca^{2+}, $Fe^{2+,3+,}$ or Mg^{2+} in the WWTP or during the EPS extraction process to have higher multivalent cation content, reach supersaturation levels and obtain higher content of precipitated P minerals in EPS at optimal pH since metal content showed to enhance some properties as thermal stability (Bahgat et al., 2024). Future research on how to tweak the EPS extraction process and how it could change P speciation is necessary to assess if P is indeed influencing EPS properties. A further interesting approach could be to research how EPS P content and its properties could be influenced due to chemical differences in the influent stream, or operating conditions in WWTPs (upstream processing). Creating this knowledge could help to facilitate EPS engineering by leveraging the interplay with P based on the targeted property in relation to relevant industrial applications.

5.5 Conclusions

EPS contains different P species e.g., polyphosphates, pyrophosphates, organic-P, orthophosphates minerals, etc. either formed microbially or induced chemically during the WWT or EPS extraction process. Phosphorus and EPS interplay has the potential to enhance EPS utilization in the industry and elevate the value and quality of EPS and phosphorus recovery from WWTPs. This interplay can potentially promote EPS utilization as a flame retardant, slow-release fertilizer, bio-stimulant, coating material, or others by enhancing its thermal, viscoelastic, emulsifying properties, water-holding capacity, or others. Consequently, this advancement could facilitate the substitution of fossil-based polymers, and P_4 derivatives, and make the recovery process from WWTPs more economically viable. This review represents a critical step toward realizing a WWTP model that acts as a production facility that produces high-value products that fit into industrial niches. We recommend doing more P speciation research over-extraction and seeing how P speciation modifications are changing the properties.

References

Aaronson, A. M. (1992). Phosphorus Flame Retardants for a Changing World. https://doi.org/10.1021/bk-1992-0486.ch017

A.F. van Nieuwenhuijzen, E. Koornneef, P.J. Roeleveld, A. Visser, D. Berkhout, F. van den Berg van Saparoea, V. Miska, E. van Voorthuizen, & C. van Erp Taalman Kip. (2011). STOWA 2011-16. https://www.stowa.nl/publicaties/handboek-slibgisting

Akbari, A., Wang, Z. J., He, P., Wang, D., Lee, J., Han, I. L., Li, G., & Gu, A. Z. (2021). Unrevealed roles of polyphosphate-accumulating microorganisms. In Microbial Biotechnology (Vol. 14, Issue 1). https://doi.org/10.1111/1751-7915.13730

Albarracín, W., Sánchez, I. C., Grau, R., & Barat, J. M. (2011). Salt in food processing; usage and reduction: A review. In International Journal of Food Science and Technology (Vol. 46, Issue 7). https://doi.org/10.1111/j.1365-2621.2010.02492.x

Alongi, J., Carletto, R. A., Di Blasio, A., Carosio, F., Bosco, F., & Malucelli, G. (2013). DNA: A novel, green, natural flame retardant and suppressant for cotton. Journal of Materials Chemistry A, 1(15). https://doi.org/10.1039/c3ta00107e

Alongi, J., Cuttica, F., & Carosio, F. (2016). DNA Coatings from Byproducts: A Panacea for the Flame Retardancy of EVA, PP, ABS, PET, and PA6? ACS Sustainable Chemistry and Engineering, 4(6). https://doi.org/10.1021/acssuschemeng.6b00625

Alongi, J., Di Blasio, A., Milnes, J., Malucelli, G., Bourbigot, S., Kandola, B., & Camino, G. (2015). Thermal degradation of DNA, an all-in-one natural intumescent flame retardant. Polymer Degradation and Stability, 113. https://doi.org/10.1016/j.polymdegradstab.2014.11.001

Anjaneyulu, A. S. R., Sharma, N., & Kondaiah, N. (1989). Evaluation of salt, polyphosphates and their blends at different levels on physicochemical properties of buffalo meat and patties. Meat Science, 25(4). https://doi.org/10.1016/0309-1740(89)90047-8

Ardito, F., Giuliani, M., Perrone, D., Troiano, G., & Muzio, L. Lo. (2017). The crucial role of protein phosphorylation in cell signalingand its use as targeted therapy (Review). In International Journal of Molecular Medicine (Vol. 40, Issue 2). https://doi.org/10.3892/ijmm.2017.3036

Arfat, Y. A., & Benjakul, S. (2013). Effect of zinc sulphate on gelling properties of phosphorylated protein isolate from yellow stripe trevally. Food Chemistry, 141(3). https://doi.org/10.1016/j.foodchem.2013.05.112

Bahgat, N. T., Siddiqui, A., Wilfert, P., Korving, L., & van Loosdrecht, M. C. M. (2024). FePO4.2H2O recovery from acidic phosphate-rich waste streams. Water Research, 121905. https://doi.org/10.1016/j.watres.2024.121905

Bahgat, N. T., Wilfert, P., Korving, L., & van Loosdrecht, M. (2023). Integrated resource recovery from aerobic granular sludge plants. Water Research, 234. https://doi.org/10.1016/j.watres.2023.119819

Blank, L. M. (2012). The cell and P: From cellular function to biotechnological application. In Current Opinion in Biotechnology (Vol. 23, Issue 6). https://doi.org/10.1016/j.copbio.2012.08.002

Bryant, C. M., & McClements, D. J. (2000). Influence of NaCl and CaCl2 on cold-set gelation of heat-denatured whey protein. Journal of Food Science, 65(5). https://doi.org/10.1111/j.1365-2621.2000.tb13590.x

Cao, L., Hou, C., Hussain, Z., Zhang, D., & Wang, Z. (2020). Quantitative phosphoproteomics analysis of actomyosin dissociation affected by specific site phosphorylation of myofibrillar protein. LWT, 126. https://doi.org/10.1016/j.lwt.2020.109269

Cao, Y., Ma, W., Huang, J., & Xiong, Y. L. (2020). Effects of sodium pyrophosphate coupled with catechin on the oxidative stability and gelling properties of myofibrillar protein. Food Hydrocolloids, 104. https://doi.org/10.1016/j.foodhyd.2020.105722

Carosio, F., Di Blasio, A., Cuttica, F., Alongi, J., & Malucelli, G. (2014). Flame retardancy of polyester and polyester-cotton blends treated with caseins. Industrial and Engineering Chemistry Research, 53(10). https://doi.org/10.1021/ie404089t

Castellanos, M. M., Pathak, J. A., & Colby, R. H. (2014). Both protein adsorption and aggregation contribute to shear yielding and viscosity increase in protein solutions. Soft Matter, 10(1). https://doi.org/10.1039/c3sm51994e

Cecchini, M., Houdusse, A., & Karplus, M. (2008). Allosteric communication in myosin V: From small conformational changes to large directed movements. PLoS Computational Biology, 4(8). https://doi.org/10.1371/journal.pcbi.1000129

Cen, S., Zhang, L., Liu, L., Lou, Q., Wang, C., & Huang, T. (2022). Phosphorylation modification on functional and structural properties of fish

gelatin: The effects of phosphate contents. Food Chemistry, 380. https://doi.org/10.1016/j.foodchem.2022.132209

CHANG, C., & RACZ, G. J. (1977). EFFECTS OF TEMPERATURE AND PHOSPHATE CONCENTRATION ON RATE OF SODIUM PYROPHOSPHATE AND SODIUM TRIPOLYPHOSPHATE HYDROLYSIS IN SOIL. Canadian Journal of Soil Science, 57(3). https://doi.org/10.4141/cjss77-033

Chen, J., Ren, Y., Zhang, K., Qu, J., Hu, F., & Yan, Y. (2019). Phosphorylation modification of myofibrillar proteins by sodium pyrophosphate affects emulsion gel formation and oxidative stability under different pH conditions. Food and Function, 10(10). https://doi.org/10.1039/c9fo01397k

Chen, J., Ren, Y., Zhang, K., Xiong, Y. L., Wang, Q., Shang, K., & Zhang, D. (2020). Site-specific incorporation of sodium tripolyphosphate into myofibrillar protein from mantis shrimp (Oratosquilla oratoria) promotes protein cross-linking and gel network formation. Food Chemistry, 312. https://doi.org/10.1016/j.foodchem.2019.126113

Chen, L. M., Erol, Ö., Choi, Y. H., Pronk, M., van Loosdrecht, M., & Lin, Y. (2024). The water-soluble fraction of extracellular polymeric substances from a resource recovery demonstration plant: characterization and potential application as an adhesive. Frontiers in Microbiology, 15. https://doi.org/10.3389/fmicb.2024.1331120

Cheng, X. W., Guan, J. P., Tang, R. C., & Liu, K. Q. (2016). Phytic acid as a bio-based phosphorus flame retardant for poly(lactic acid) nonwoven fabric. Journal of Cleaner Production, 124. https://doi.org/10.1016/j.jclepro.2016.02.113

Cho, Y. H., Kim, K., Ahn, S., & Liu, H. K. (2011). Allyl-substituted triazines as additives for enhancing the thermal stability of Li-ion batteries. Journal of Power Sources, 196(3). https://doi.org/10.1016/j.jpowsour.2010.08.085

Cooper, R. S. (1963). Anionic phosphate surfactants. Journal of the American Oil Chemists Society, 40(11). https://doi.org/10.1007/BF02633868

Criado-Gonzalez, M., Wagner, D., Rodon Fores, J., Blanck, C., Schmutz, M., Chaumont, A., Rabineau, M., Schlenoff, J. B., Fleith, G., Combet, J., Schaaf, P., Jierry, L., & Boulmedais, F. (2020). Supramolecular Hydrogel Induced by Electrostatic Interactions between Polycation and Phosphorylated-Fmoc-Tripeptide. Chemistry of Materials, 32(5). https://doi.org/10.1021/acs.chemmater.9b04823

Damer, B., & Deamer, D. (2015). Coupled phases and combinatorial selection in fluctuating hydrothermal pools: A scenario to guide experimental

approaches to the origin of cellular life. Life, 5(1). https://doi.org/10.3390/life5010872

Duan, X., Li, M., Wu, F., Yang, N., Nikoo, M., Jin, Z., & Xu, X. (2013). Postfertilization changes in nutritional composition and protein conformation of hen egg. Journal of Agricultural and Food Chemistry, 61(49). https://doi.org/10.1021/jf403099q

E. van der Knaap, E. Koornneef, K. L., M. Oosterhuis, P. Roeleveld, & M. Schaafsma. (2019). Kaumera Nereda gum: samenvatting NAOP onderzoeken 2013-2018,2019. Retrieved February 18, 2020, from http://edepot.wur.nl/501893

ESPP webinar. (2020). Summary of joint European Commission-ESPP webinar on P4 (phosphorus) Critical Raw Material. www.phosphorusplatform.eu

Feiner, G. (2006). Meat Products Handbook: Practical Science and Technology. In Meat Products Handbook: Practical Science and Technology.

Gaan, S., Rupper, P., Salimova, V., Heuberger, M., Rabe, S., & Vogel, F. (2009). Thermal decomposition and burning behavior of cellulose treated with ethyl ester phosphoramidates: Effect of alkyl substituent on nitrogen atom. Polymer Degradation and Stability, 94(7). https://doi.org/10.1016/j.polymdegradstab.2009.03.017

Gadekar, Y. P., Sharma, B. D., Shinde, A. K., & Mendiratta, S. K. (2014). Effect of Different Phosphates on Quality of Goat Meat and Restructured Goat Meat Product. Agricultural Research, 3(4), 370–376. https://doi.org/10.1007/s40003-014-0129-3

Gajewski, E., Steckler, D. K., & Goldberg, R. N. (1986). Thermodynamics of the hydrolysis of adenosine 5'-triphosphate to adenosine 5'-diphosphate. Journal of Biological Chemistry, 261(27). https://doi.org/10.1016/s0021-9258(18)67153-4

García Becerra, F. Y., Acosta, E. J., & Grant Allen, D. (2010). Alkaline extraction of wastewater activated sludge biosolids. Bioresource Technology, 101(18). https://doi.org/10.1016/j.biortech.2010.04.021

Guo, H., Zparpucu, O., Windeisen-Holzhauser, E., Schlepütz, C. M., Quadranti, E., Gaan, S., Dreimol, C., & Burgert, I. (2020). Struvite Mineralized Wood as Sustainable Building Material: Mechanical and Combustion Behavior. ACS Sustainable Chemistry and Engineering, 8(28). https://doi.org/10.1021/acssuschemeng.0c01769

Guo, W., Wang, X., Zhang, P., Liu, J., Song, L., & Hu, Y. (2018). Nanofibrillated cellulose-hydroxyapatite based composite foams with excellent fire

resistance. Carbohydrate Polymers, 195. https://doi.org/10.1016/j.carbpol.2018.04.063

Hadidi, M., Jafarzadeh, S., & Ibarz, A. (2021). Modified mung bean protein: Optimization of microwave-assisted phosphorylation and its functional and structural characterizations. LWT, 151. https://doi.org/10.1016/j.lwt.2021.112119

Hartman, L., Cardoso Elias, M., & Esteves, W. (1980). Method for the determination of phosphorus in lipids and lipid-containing materials. The Analyst, 105(1247). https://doi.org/10.1039/AN9800500173

Hindmarsh, J. P., & Watkinson, P. (2017). Experimental evidence for previously unclassified calcium phosphate structures in the casein micelle. Journal of Dairy Science, 100(9). https://doi.org/10.3168/jds.2017-12623

Hirota, R., Kuroda, A., Kato, J., & Ohtake, H. (2010). Bacterial phosphate metabolism and its application to phosphorus recovery and industrial bioprocesses. In Journal of Bioscience and Bioengineering (Vol. 109, Issue 5). https://doi.org/10.1016/j.jbiosc.2009.10.018

Hong, T., Iwashita, K., & Shiraki, K. (2017). Viscosity Control of Protein Solution by Small Solutes: A Review. Current Protein & Peptide Science, 19(8). https://doi.org/10.2174/1389203719666171213114919

Hu, Y., Du, L., Sun, Y., Zhou, C., & Pan, D. (2023). Recent developments in phosphorylation modification on food proteins: Structure characterization, site identification and function. In Food Hydrocolloids (Vol. 137). https://doi.org/10.1016/j.foodhyd.2022.108390

Hu, Y., & Wang, X. (2019). Flame retardant polymeric materials: A handbook. In Flame Retardant Polymeric Materials: A Handbook. https://doi.org/10.1201/b22345

Hu, Y., Wu, Z., Sun, Y., Cao, J., He, J., Dang, Y., Pan, D., & Zhou, C. (2022). Insight into ultrasound-assisted phosphorylation on the structural and emulsifying properties of goose liver protein. Food Chemistry, 373. https://doi.org/10.1016/j.foodchem.2021.131598

Hu, Z., Qiu, L., Sun, Y., Xiong, H., & Ogra, Y. (2019). Improvement of the solubility and emulsifying properties of rice bran protein by phosphorylation with sodium trimetaphosphate. Food Hydrocolloids, 96. https://doi.org/10.1016/j.foodhyd.2019.05.037

Huang, L., Jin, Y., Zhou, D., Liu, L., Huang, S., Zhao, Y., & Chen, Y. (2022). A Review of the Role of Extracellular Polymeric Substances (EPS) in Wastewater Treatment Systems. In International Journal of Environmental

Research and Public Health (Vol. 19, Issue 19). https://doi.org/10.3390/ijerph191912191

Huang, T., Tu, Z. cai, Shangguan, X., Sha, X., Wang, H., Zhang, L., & Bansal, N. (2019). Fish gelatin modifications: A comprehensive review. In Trends in Food Science and Technology (Vol. 86). https://doi.org/10.1016/j.tifs.2019.02.048

Huang, W., Huang, W., Li, H., Lei, Z., Zhang, Z., Tay, J. H., & Lee, D. J. (2015). Species and distribution of inorganic and organic phosphorus in enhanced phosphorus removal aerobic granular sludge. Bioresource Technology, 193. https://doi.org/10.1016/j.biortech.2015.06.120

Hughes, J. M., Oiseth, S. K., Purslow, P. P., & Warner, R. D. (2014). A structural approach to understanding the interactions between colour, water-holding capacity and tenderness. Meat Science, 98(3). https://doi.org/10.1016/j.meatsci.2014.05.022

Hulshof, J., & Ponnamperuma, C. (1976). Prebiotic condensation reactions in an aqueous medium: A review of condensing agents. Origins of Life, 7(3). https://doi.org/10.1007/BF00926938

Hunter, T. (2012). Why nature chose phosphate to modify proteins. In Philosophical Transactions of the Royal Society B: Biological Sciences (Vol. 367, Issue 1602). https://doi.org/10.1098/rstb.2012.0013

Ikeuchi, Y. (2011). Recent advances in the application of high pressure technology to processed meat products. In Processed Meats: Improving Safety, Nutrition and Quality. https://doi.org/10.1533/9780857092946.3.590

Illy, N., Fache, M., Ménard, R., Negrell, C., Caillol, S., & David, G. (2015a). Phosphorylation of bio-based compounds: The state of the art. In Polymer Chemistry (Vol. 6, Issue 35). https://doi.org/10.1039/c5py00812c

Jakubowski, H., Flatt, P., Agnew, H., & Larsen, D. (2022). Fundamentals of Biochemistry, a free and new LibreText book for Undergraduate Courses. The FASEB Journal, 36(S1). https://doi.org/10.1096/fasebj.2022.36.s1.r4590

Jolley, P. D., & Offer, G. W. (1984). The Effect of Salt and Pyrophosphate on the Structure of Meat. Journal of Food Structure, 3(2).

Jupp, A. R., Beijer, S., Narain, G. C., Schipper, W., & Slootweg, J. C. (2021). Phosphorus recovery and recycling-closing the loop. In Chemical Society Reviews (Vol. 50, Issue 1). https://doi.org/10.1039/d0cs01150a

Kaewruang, P., Benjakul, S., & Prodpran, T. (2014). Characteristics and gelling property of phosphorylated gelatin from the skin of unicorn leatherjacket. Food Chemistry, 146. https://doi.org/10.1016/j.foodchem.2013.09.111

Kim, A. H., Yu, A. C., El Abbadi, S. H., Lu, K., Chan, D., Appel, E. A., & Criddle, C. S. (2021). More than a fertilizer: Wastewater-derived struvite as a high value, sustainable fire retardant. Green Chemistry, 23(12). https://doi.org/10.1039/d1gc00826a

Kim, N. K., Lin, R., Bhattacharyya, D., van Loosdrecht, M. C. M., & Lin, Y. (2022). Insight on how biopolymers recovered from aerobic granular wastewater sludge can reduce the flammability of synthetic polymers. Science of the Total Environment, 805. https://doi.org/10.1016/j.scitotenv.2021.150434

Kim, N. K., Mao, N., Lin, R., Bhattacharyya, D., van Loosdrecht, M. C. M., & Lin, Y. (2020). Flame retardant property of flax fabrics coated by extracellular polymeric substances recovered from both activated sludge and aerobic granular sludge. Water Research, 170. https://doi.org/10.1016/j.watres.2019.115344

Klein, D. (2012). Organic Chemistry with a Biological Emphasis, Volume 1. John Hopkins University, 1(January).

Kodera, N., & Ando, T. (2014). The path to visualization of walking myosin V by high-speed atomic force microscopy. In Biophysical Reviews (Vol. 6, Issues 3–4). https://doi.org/10.1007/s12551-014-0141-7

Koedel, J., Seibt, S., Callsen, C., Puchtler, F., Weise, M., Weidinger, A., Altstaedt, V., Ruckdäschel, H., Schobert, R., & Biersack, B. (2021). DNA as a Natural Flame Retardant for Cellulose Acetate Polymer Mixtures. ChemistrySelect, 6(15). https://doi.org/10.1002/slct.202004493

Komazin, G., Maybin, M., Woodard, R. W., Scior, T., Schwudke, D., Schombel, U., Gisch, N., Mamat, U., & Meredith, T. C. (2019). Substrate structure-activity relationship reveals a limited lipopolysaccharide chemotype range for intestinal alkaline phosphatase. Journal of Biological Chemistry, 294(50). https://doi.org/10.1074/jbc.RA119.010836

Kondaiah, N., Anjaneyulu, A. S. R., Rao, V. K., Sharma, N., & Joshi, H. B. (1985). Effect of salt and phosphate on the quality of Buffalo and Goat meats. Meat Science, 15(3). https://doi.org/10.1016/0309-1740(85)90036-1

Kuroda, A., Takiguchi, N., Gotanda, T., Nomura, K., Kato, J., Ikeda, T., & Ohtake, H. (2002). A simple method to release polyphosphate from activated sludgefor phosphorus reuse and recycling. Biotechnology and Bioengineering, 78(3). https://doi.org/10.1002/bit.10205

Laoutid, F., Lorgouilloux, M., Lesueur, D., Bonnaud, L., & Dubois, P. (2013). Calcium-based hydrated minerals: Promising halogen-free flame retardant and fire resistant additives for polyethylene and ethylene vinyl acetate

copolymers. Polymer Degradation and Stability, 98(9). https://doi.org/10.1016/j.polymdegradstab.2013.06.020

Laoutid, F., Vahabi, H., Movahedifar, E., Laheurte, P., Vagner, C., Cochez, M., Brison, L., & Saeb, M. R. (2021). Calcium carbonate and ammonium polyphosphate flame retardant additives formulated to protect ethylene vinyl acetate copolymer against fire: Hydrated or carbonated calcium? Journal of Vinyl and Additive Technology, 27(2). https://doi.org/10.1002/vnl.21800

Lemire, K. A., Rodriguez, Y. Y., & McIntosh, M. T. (2016). Alkaline hydrolysis to remove potentially infectious viral RNA contaminants from DNA. Virology Journal, 13(1). https://doi.org/10.1186/s12985-016-0552-0

Léonil, J., Michalski, M. C., & Martin, P. (2013). Les structures supramoléculaires du lait : Structure et impact nutritionnel de la micelle de caséine et du globule gras. Productions Animales, 26(2). https://doi.org/10.20870/productions-animales.2013.26.2.3142

Levchik, S. V., & Weil, E. D. (2005). Overview of recent developments in the flame retardancy of polycarbonates. In Polymer International (Vol. 54, Issue 7). https://doi.org/10.1002/pi.1806

Li, P., Jin, Y., & Sheng, L. (2020). Impact of microwave assisted phosphorylation on the physicochemistry and rehydration behaviour of egg white powder. Food Hydrocolloids, 100. https://doi.org/10.1016/j.foodhyd.2019.105380

Li, S., Liu, Q., De Wijn, J., Wolke, J., Zhou, B., & De Groot, K. (1997). In-vitro apatite formation on phosphorylated bamboo. Journal of Materials Science: Materials in Medicine, 8(9). https://doi.org/10.1023/A:1018546730925

Liang, S., Neisius, N. M., & Gaan, S. (2013). Recent developments in flame retardant polymeric coatings. In Progress in Organic Coatings (Vol. 76, Issue 11). https://doi.org/10.1016/j.porgcoat.2013.07.014

Liang, Z., Zhou, Z., Sun, Y., Huang, Y., Guo, X., Cai, G., Wang, M., & Zhang, H. (2022). Fire Extinguishing Performance of Chemically Bonded Struvite Ceramic Powder with High Heat-Absorbing and Flame Retardant Properties. Materials, 15(22). https://doi.org/10.3390/ma15228021

Liu, Y., Zhang, A., Cheng, Y., Li, M., Cui, Y., & Li, Z. (2023). Recent advances in biomass phytic acid flame retardants. Polymer Testing, 124. https://doi.org/10.1016/j.polymertesting.2023.108100

Lv, X., Huang, X., Ma, B., Chen, Y., Batool, Z., Fu, X., & Jin, Y. (2022). Modification methods and applications of egg protein gel properties: A review. Comprehensive Reviews in Food Science and Food Safety, 21(3). https://doi.org/10.1111/1541-4337.12907

Malucelli, G., Bosco, F., Alongi, J., Carosio, F., Di Blasio, A., Mollea, C., Cuttica, F., & Casale, A. (2014). Biomacromolecules as novel green flame retardant systems for textiles: An overview. In RSC Advances (Vol. 4, Issue 86). https://doi.org/10.1039/c4ra06771a

Mangrum, C. R. L., & Jenkins, D. (2020). The effect of divalent cation complexation on anaerobically digested enhanced biological phosphorus removal sludge dewatering performance. Water Environment Research, 92(5). https://doi.org/10.1002/wer.1259

Maqsood, M., & Seide, G. (2019). Investigation of the flammability and thermal stability of halogen-free intumescent system in biopolymer composites containing biobased carbonization agent and mechanism of their char formation. Polymers, 11(1). https://doi.org/10.3390/polym11010048

Markwart, J. C., Battig, A., Zimmermann, L., Wagner, M., Fischer, J., Schartel, B., & Wurm, F. R. (2019). Systematically Controlled Decomposition Mechanism in Phosphorus Flame Retardants by Precise Molecular Architecture: P-O vs P-N. ACS Applied Polymer Materials, 1(5). https://doi.org/10.1021/acsapm.9b00129

McBeath, T. M., Lombi, E., McLaughlin, M. J., & Bünemann, E. K. (2007). Polyphosphate-fertilizer solution stability with time, temperature, and pH. Journal of Plant Nutrition and Soil Science, 170(3). https://doi.org/10.1002/jpln.200625166

Miedzianka, J., & Pęksa, A. (2013). Effect of pH on phosphorylation of potato protein isolate. Food Chemistry, 138(4). https://doi.org/10.1016/j.foodchem.2012.12.028

Naiker, V. E., Mestry, S., Nirgude, T., Gadgeel, A., & Mhaske, S. T. (2023a). Recent developments in phosphorous-containing bio-based flame-retardant (FR) materials for coatings: an attentive review. In Journal of Coatings Technology and Research (Vol. 20, Issue 1). https://doi.org/10.1007/s11998-022-00685-z

Neyens, E., Baeyens, J., Dewil, R., & De Heyder, B. (2004). Advanced sludge treatment affects extracellular polymeric substances to improve activated sludge dewatering. Journal of Hazardous Materials, 106(2–3). https://doi.org/10.1016/j.jhazmat.2003.11.014

Nguyen, C., & Kim, J. (2008). Thermal stabilities and flame retardancies of nitrogen-phosphorus flame retardants based on bisphosphoramidates. Polymer Degradation and Stability, 93(6). https://doi.org/10.1016/j.polymdegradstab.2008.03.024

Offer, G., Knight, P., Jeacocke, R., Almond, R., Cousins, T., Elsey, J., Parsons, N., Sharp, A., Starr, R., & Purslow, P. (1989). The structural basis of the water-holding, appearance and toughness of meat and meat products. Food Microstructure, 8,(1).

Offer, G., & Trinick, J. (1983). On the mechanism of water holding in meat: The swelling and shrinking of myofibrils. Meat Science, 8(4). https://doi.org/10.1016/0309-1740(83)90013-X

Pasek, M. A. (2020). Thermodynamics of Prebiotic Phosphorylation. In Chemical Reviews (Vol. 120, Issue 11). https://doi.org/10.1021/acs.chemrev.9b00492

Petreuş, O., Bubulac, T., Petreuş, I., & Cazacu, G. (2003). Reactions of some phosphorus compounds with cellulose dissolved in aqueous alkaline solution. Journal of Applied Polymer Science, 90(2). https://doi.org/10.1002/app.12532

Poornima, C. S., & Dean, P. M. (1995). Hydration in drug design. 1. Multiple hydrogen-bonding features of water molecules in mediating protein-ligand interactions. Journal of Computer-Aided Molecular Design, 9(6). https://doi.org/10.1007/BF00124321

Pronk, M., van Dijk, E. J. H., & van Loosdrecht, M. C. M. (2020). Aerobic granular sludge. In Biological Wastewater Treatment: Principles, Modeling and Design (2nd ed.). https://doi.org/10.2166/9781789060362

Puolanne, E. J., Ruusunen, M. H., & Vainionpää, J. I. (2001). Combined effects of NaCl and raw meat pH on water-holding in cooked sausage with and without added phosphate. Meat Science, 58(1). https://doi.org/10.1016/S0309-1740(00)00123-6

Rothon, R. N. (1999). Mineral fillers in thermoplastics: Filler manufacture and characterisation. Advances in Polymer Science, 139. https://doi.org/10.1007/3-540-69220-7_2

Salmeia, K. A., Fage, J., Liang, S., & Gaan, S. (2015). An overview of mode of action and analytical methods for evaluation of gas phase activities of flame retardants. Polymers, 7(3). https://doi.org/10.3390/polym7030504

Salmeia, K. A., Gaan, S., & Malucelli, G. (2016). Recent advances for flame retardancy of textiles based on phosphorus chemistry. Polymers, 8(9). https://doi.org/10.3390/polym8090319

Salmeia, K. A., Jovic, M., Ragaisiene, A., Rukuiziene, Z., Milasius, R., Mikuioniene, D., & Gaan, S. (2016). Flammability of cellulose-based fibers and the

effect of structure of phosphorus compounds on their flame retardancy. Polymers, 8(8). https://doi.org/10.3390/polym8080293

Scharte, B. (2010). Phosphorus-based flame retardancy mechanisms-old hat or a starting point for future development? Materials, 3(10). https://doi.org/10.3390/ma3104710

Schartel, B., Perret, B., Dittrich, B., Ciesielski, M., Krämer, J., Müller, P., Altstädt, V., Zang, L., & Döring, M. (2016). Flame Retardancy of Polymers: The Role of Specific Reactions in the Condensed Phase. Macromolecular Materials and Engineering, 301(1). https://doi.org/10.1002/mame.201500250

Schmitt, E. (2007). Phosphorus-based flame retardants for thermoplastics. Plastics, Additives and Compounding, 9(3). https://doi.org/10.1016/S1464-391X(07)70067-3

Schwenke, K. D., Mothes, R., Dudek, S., & Görnitz, E. (2000). Phosphorylation of the 12S globulin from rapeseed (Brassica napus L.) by phosphorous oxychloride: Chemical and conformational aspects. Journal of Agricultural and Food Chemistry, 48(3). https://doi.org/10.1021/jf9907900

Shen, J., Liang, J., Lin, X., Lin, H., Yu, J., & Wang, S. (2022). The flame-retardant mechanisms and preparation of polymer composites and their potential application in construction engineering. In Polymers (Vol. 14, Issue 1). https://doi.org/10.3390/polym14010082

SHULTS, G. W., RUSSELL, D. R., & WIERBICKI, E. (1972). EFFECT OF CONDENSED PHOSPHATES ON pH, SWELLING AND WATER-HOLDING CAPACITY OF BEEF. Journal of Food Science, 37(6). https://doi.org/10.1111/j.1365-2621.1972.tb03688.x

SIEGEL, D. G., & SCHMIDT, G. R. (1979). IONIC, pH, AND TEMPERATURE EFFECTS ON THE BINDING ABILITY OF MYOSIN. Journal of Food Science, 44(6). https://doi.org/10.1111/j.1365-2621.1979.tb09116.x

Smith, S. K. S. (2016). Milo, Ron: Cell biology by the numbers. CHOICE: Current Reviews for Academic Libraries VO - 53, 10.

Stephanopoulos, G. N., Aristidou, A. a, & Nielsen, J. (1998). Metabolic Engineering: Principles and Methodologies. In Metabolic Engineering (Vol. 54).

Sudmalis, D., Mubita, T. M., Gagliano, M. C., Dinis, E., Zeeman, G., Rijnaarts, H. H. M., & Temmink, H. (2020). Cation exchange membrane behaviour of extracellular polymeric substances (EPS) in salt adapted granular sludge. Water Research, 178. https://doi.org/10.1016/j.watres.2020.115855

Sun, H., Chen, K., Liu, Y., & Wang, Q. (2023). Improving flame retardant and smoke suppression function of ethylene vinyl acetate by combining the

piperazine pyrophosphate, expandable graphite and melamine phosphate. European Polymer Journal, 194. https://doi.org/10.1016/j.eurpolymj.2023.112148

SUNG, H. -Y, CHEN, H. -J, LIU, T. -Y, & SU, J. -C. (1983). Improvement of the Functionalities of Soy Protein Isolate through Chemical Phosphorylation. Journal of Food Science, 48(3). https://doi.org/10.1111/j.1365-2621.1983.tb14882.x

Trout, G. R., & Schmidt, G. R. (1986). Effect of Chain Length and Concentration on the Degree of Dissociation of Phosphates Used in Food Products. Journal of Agricultural and Food Chemistry, 34(1). https://doi.org/10.1021/jf00067a011

Uddin, M., Kiviranta, K., Suvanto, S., Alvila, L., Leskinen, J., Lappalainen, R., & Haapala, A. (2020). Casein-magnesium composite as an intumescent fire retardant coating for wood. Fire Safety Journal, 112. https://doi.org/10.1016/j.firesaf.2019.102943

Veldhuizen, R., Nag, K., Orgeig, S., & Possmayer, F. (1998). The role of lipids in pulmonary surfactant. In Biochimica et Biophysica Acta - Molecular Basis of Disease (Vol. 1408, Issues 2–3). https://doi.org/10.1016/S0925-4439(98)00061-1

Velencoso, M. M., Battig, A., Markwart, J. C., Schartel, B., & Wurm, F. R. (2018). Molecular Firefighting—How Modern Phosphorus Chemistry Can Help Solve the Challenge of Flame Retardancy. In Angewandte Chemie - International Edition (Vol. 57, Issue 33). https://doi.org/10.1002/anie.201711735

Vothi, H., Nguyen, C., Pham, L. H., Hoang, D., & Kim, J. (2019). Novel Nitrogen-Phosphorus Flame Retardant Based on Phosphonamidate: Thermal Stability and Flame Retardancy. ACS Omega, 4(18). https://doi.org/10.1021/acsomega.9b02371

Walayat, N., Xiong, Z., Xiong, H., Moreno, H. M., Nawaz, A., Niaz, N., Hu, C., Taj, M. I., Mushtaq, B. S., & Khalifa, I. (2021). The effect of egg white protein and β-cyclodextrin mixture on structural and functional properties of silver carp myofibrillar proteins during frozen storage. LWT, 135. https://doi.org/10.1016/j.lwt.2020.109975

Wang, G., & Bai, S. (2017). Synergistic effect of expandable graphite and melamine phosphate on flame-retardant polystyrene. Journal of Applied Polymer Science, 134(47). https://doi.org/10.1002/app.45474

Wang, X., Xiong, Y. L., & Sato, H. (2017). Rheological Enhancement of Pork Myofibrillar Protein-Lipid Emulsion Composite Gels via Glucose Oxidase

Oxidation/Transglutaminase Cross-Linking Pathway. Journal of Agricultural and Food Chemistry, 65(38). https://doi.org/10.1021/acs.jafc.7b03007

Weil, E. D., & et Sergei V. Levchik. (2017). FLAME RETARDANTS, PHOSPHORUS. In In Kirk-Othmer Encyclopedia of Chemical Technology, édité par John Wiley & Sons Inc, 1 34. Hoboken, NJ, USA: John Wiley & Sons, Inc. .

Woo, S. L., Creamer, L. K., & Richardson, T. (1982). Chemical Phosphorylation of Bovine β-Lactoglobulin. Journal of Agricultural and Food Chemistry, 30(1). https://doi.org/10.1021/jf00109a013

Xiong, Z., & Ma, M. (2017). Enhanced ovalbumin stability at oil-water interface by phosphorylation and identification of phosphorylation site using MALDI-TOF mass spectrometry. Colloids and Surfaces B: Biointerfaces, 153. https://doi.org/10.1016/j.colsurfb.2017.02.027

Xiong, Z., Zhang, M., & Ma, M. (2016). Emulsifying properties of ovalbumin: Improvement and mechanism by phosphorylation in the presence of sodium tripolyphosphate. Food Hydrocolloids, 60, 29–37. https://doi.org/10.1016/j.foodhyd.2016.03.007

Xu, F., Zhong, L., Zhang, C., Wang, P., Zhang, F., & Zhang, G. (2019). Novel High-Efficiency Casein-Based P-N-Containing Flame Retardants with Multiple Reactive Groups for Cotton Fabrics. ACS Sustainable Chemistry and Engineering, 7(16). https://doi.org/10.1021/acssuschemeng.9b02474

Xu, S. Q., Zhou, G. H., Peng, Z. Q., Zhao, L. Y., & Yao, R. (2009). The influence of polyphosphate marination on simmental beef shear value and ultrastructure. Journal of Muscle Foods, 20(1). https://doi.org/10.1111/j.1745-4573.2008.00136.x

Yu, Z., Gao, Y., Wu, M., Zhao, C., Liu, X., Zhang, X., Zhang, L., & Chen, Y. (2024). Effects of phosphorylated ovalbumin on the quality of pork myofibrillar protein gel: an insight into gelling and physicochemical properties. Journal of Future Foods, 4(2). https://doi.org/10.1016/j.jfutfo.2023.06.006

Zayas, J. F. (1997). Functionality of Proteins in Food. In Functionality of Proteins in Food. https://doi.org/10.1007/978-3-642-59116-7

Zhang, H. L., Fang, W., Wang, Y. P., Sheng, G. P., Zeng, R. J., Li, W. W., & Yu, H. Q. (2013). Phosphorus removal in an enhanced biological phosphorus removal process: Roles of extracellular polymeric substances. Environmental Science and Technology, 47(20). https://doi.org/10.1021/es403227p

Zhao, T., Feng, N., Zhao, Y., & Zhang, G. (2020). Adsorption behavior and application performance of branched aliphatic alcohol polyoxyethylene ether

phosphate. Colloids and Surfaces A: Physicochemical and Engineering Aspects, 606. https://doi.org/10.1016/j.colsurfa.2020.125482

Chapter 6

General Discussion
Outlook

6.1 Integrated P and EPS Recovery Route from Aerobic Granular Sludge – Critical View of This Thesis

The integrated resource recovery approach offers significant economic advantages by combining the recovery of multiple elements within a single process, thereby reducing chemical costs, and waste production compared to standalone recovery methods. Additionally, these integrated solutions can produce unique, high-value products that are in high demand for niche industrial applications and are more environmentally friendly than commercial alternatives. However, some knowledge gaps and critical points require further attention:

1. The phosphorus present in sludge is distributed over multiple streams in the EPS extraction process (it was determined that approximately 60% of total phosphorus in sludge could be recovered: approximately 20% as an integral part of EPS, 30% from the acidic by-product stream as free orthophosphates, and approximately 10% from the liquid digestate released during anaerobic digestion of the alkaline pellet, also as free orthophosphate). So, recovering phosphorus from a single stream is insufficient given the increasing legal requirements for phosphorus recovery. Countries like Germany, Austria, and Switzerland have implemented regulations mandating that by 2033, all sewage works with a design capacity of ≥20,000 p.e. must recover 60% of the

inflow of phosphorus (ESPP, 2024). Therefore, achieving integrated phosphorus and EPS recovery necessitates phosphorus recovery from various streams to meet the 60% recovery target. While it might be argued that this requires more process equipment and that recovery efforts on a single phosphorus-rich stream, such as ash, would be preferable, the potential added value and market niche of phosphorus recovered within the EPS fraction justifies this integrated approach.

2. Recovering higher-value organic phosphorus compounds from WWTPs could potentially replace some organophosphorus compounds that currently rely on PCl_3, a precursor derived from the chlorination of P_4. These microbial-produced organic phosphorus compounds offer a sustainable and environmentally friendly alternative to PCl_3 derivatives, which present significant sustainability and safety challenges due to their corrosive nature, and high toxicity. PCl_3 is also listed as a precursor on Schedule 3 of the Chemical Weapons Convention (Jupp et al., 2021). While it is not possible to replace all P_4 derivatives with microbial-produced phosphorus compounds, reducing its consumption by utilizing organic P esters and polyphosphates produced by microorganisms in WWTPs, or by optimizing WWTPs operations to increase the content of these compounds, could significantly contribute to more sustainable P rock consumption and boost P recovery market from wastewater.

3. Recovering organic phosphorus products from WWTPs could be economically competitive, driving the phosphorus recovery market forward due to the higher value of these species compared to orthophosphate mineral precipitates. Recovering phosphorus as mineral precipitates, typically used as fertilizers like struvite and calcium phosphates, is not economically attractive since traditional commercial fertilizers cost about €1.6/kg P (Witek-Krowiak et al., 2022; Xu et al., 2023), while the recovery costs of phosphorus from wastewater are estimated at €2/kg P and can reach up to €8/kg P under certain conditions (Egle et al., 2015). Horstink et al. (2021) estimated the price of P_4 to be approximately €2.9/kg P, and the cost of P_4-derived chemicals is higher due to the additional processing required from P_4 or PCl_3. Therefore, recovering organic phosphorus products, which can function as P_4 derivatives, potentially offers a more economically competitive alternative to fertilizers. This highlights the need for the scientific community to re-evaluate phosphorus recovery from wastewater, focusing on higher-value products. However, even with the higher value of these recovered products, the costs might be not fully covered, emphasizing the necessity to target higher-value outputs while also working to reduce recovery costs.
4. The relevance of phosphorus chemistry in EPS to influence properties such as viscoelasticity, water-holding capacity, emulsifying properties, and thermal stability could

significantly enhance EPS's potential industrial applications as a flame retardant, biocomposite material, coating, or biostimulant. Integrating phosphorus chemistry innovatively with EPS would contribute to replacing some fossil-based polymers. However, there is a knowledge gap regarding the extent to which phosphorus influences these properties compared to other functional groups in EPS, such as carboxyl, amine, and sulfhydryl groups. It remains to be determined if phosphorus influence is indeed as significant as proposed in this thesis or if other groups have a more dominant influence. Further research is needed to understand how phosphorus content and speciation affect these properties. This can be achieved by selectively altering phosphorus content and determining the influence on its properties. For instance, increasing the organic phosphorus content through chemical phosphorylation, decreasing it using phosphatase enzymes, removing free orthophosphates from the EPS matrix using adsorbents, or addition of polyphosphates and pyrophosphates.

5. Building on the earlier discussion about high-value phosphorus recovery and its potential to advance the phosphorus recovery market, the valorization of strengite must also be evaluated for high-value applications such as electrode material manufacturing, catalysts, $LiFePO_4$ precursors, or flame retardants. Further research is needed to determine if strengite can effectively push the phosphorus recovery

market forward by providing such high-value applications or if it will be in the category of potential fertilizers facing similar obstacles as the current phosphorus recovery products. A promising aspect of strengite is its insolubility under acidic conditions, while heavy metals remain soluble, potentially resulting in a purer product compared to conventional phosphorus mineral products precipitated at higher pH levels. This purity could make strengite suitable for high-purity applications, warranting additional investigation. Recovering strengite could also be a way to advance vivianite purification and purity, and the concept needs to be evaluated in future research. As shown in **Figure 6-1**, by dissolving vivianite in HCl, then oxidizing Fe (II) to Fe (III) using H_2O_2 using the methodology established in chapter (3), precipitating strengite. As a result, we could get pure strengite (high solubility of heavy metals at low pH conditions) and recover 33% of the Fe as $FeCl_3$ solution (that could be recycled and reused in the WWTP).

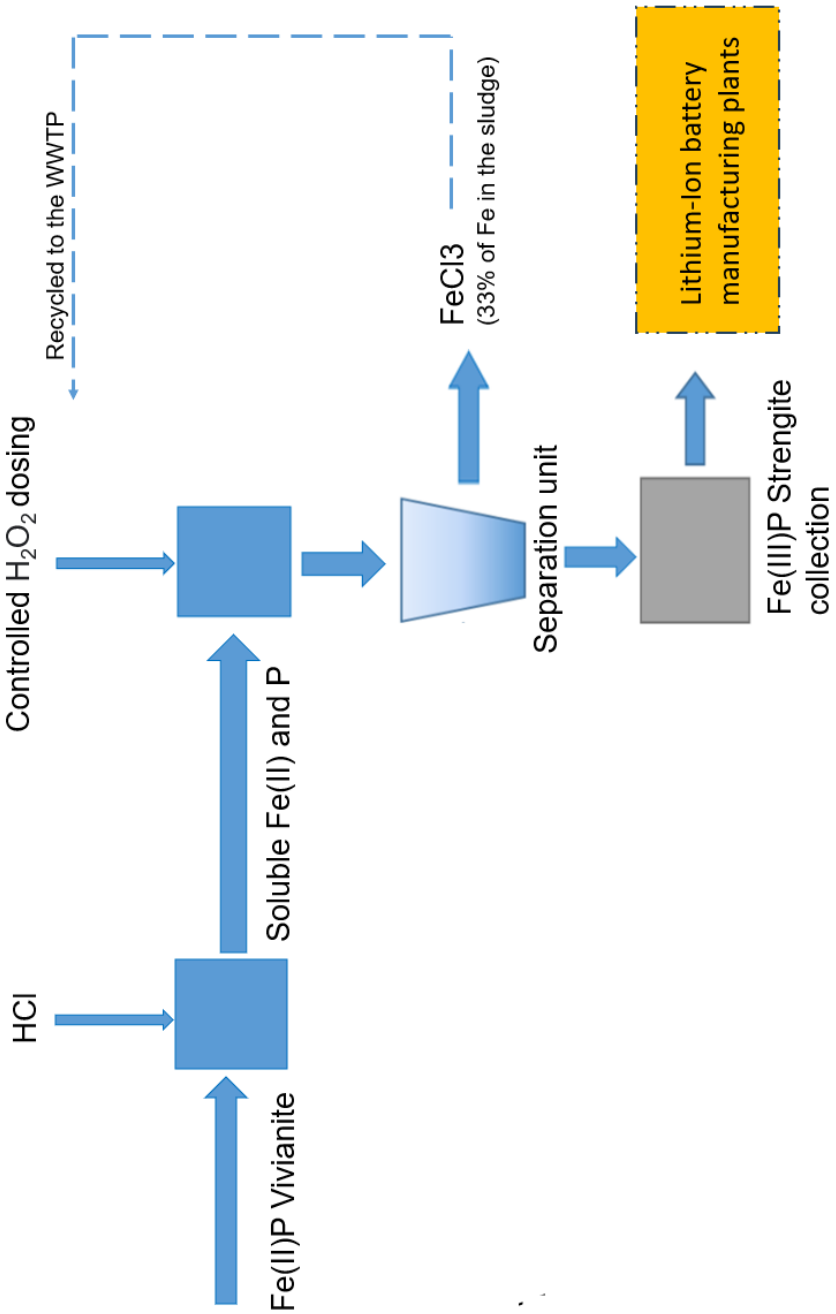

Figure 6-1: Using developed methodology in Chapter (3) to recover strengite-type compounds to purify vivianite (proposal for future applications)

6.2 Non-Integrated P Recovery Routes from Aerobic Granular Sludge – Alternatives to this Thesis

There are different approaches for recovering phosphorus from aerobic granular sludge. This thesis primarily examines an integrated approach that simultaneously recovers phosphorus and EPS; however, two possible non-integrated approaches for phosphorus recovery from AGS warrant further investigation. Subsequently, we discuss why the integrated approach tackled in this thesis is considered superior for maximizing the value of phosphorus removed from wastewater.

6.2.1 From the surplus AGS before EPS extraction

The excess sludge removed from AGS reactors is rich in phosphorus, predominantly in polyphosphates, and as apatite and non-apatite orthophosphate precipitates. The polyphosphates and orthophosphate precipitates within the sludge can be recovered by placing the sludge in a controlled reactor under anaerobic and acidic pH conditions as illustrated in **Figure 6-2**B) (Campo et al., 2023; Feng et al., 2020). Under these conditions, polyphosphates are released from the biomass into the liquid fraction, and the acidic environment increases the solubility of apatite and most of the non-apatite inorganic phosphorus fractions. The orthophosphate released into the phosphorus-rich liquid stream is then recovered through chemical precipitation.

Campo et al. (2023) reported that a maximum phosphorus recovery of 92.6% of total phosphorus was achieved after 12 days at pH 4 in laboratory batch experiments. Although this recovery percentage is higher

than the recovery obtained through our integrated phosphorus and EPS recovery approach, it has some drawbacks that make it less attractive in our opinion. First, it requires a significantly long time to achieve high phosphorus recovery. Second, all the phosphorus recovered is in a mineral form after precipitation. Third, the acid addition to mobilize the phosphorus from the sludge is chemically and economically intensive. In contrast, our approach offers some advantages. First, phosphorus mobilization/ recovery occurs within the time frame of the EPS extraction process, which takes only two hours. Second, part of the phosphorus is recovered as organic phosphorus, which has a higher value compared to mineral phosphorus. Third, the integration of EPS and phosphorus (and potentially methane) recovery makes it more economical and efficient in terms of chemical use in the process; and fourth, the unique integration of phosphorus chemistry and EPS in the final product broadens industrial applications for EPS as an alternative to fossil-based polymers and recovered P to P4 derivatives.

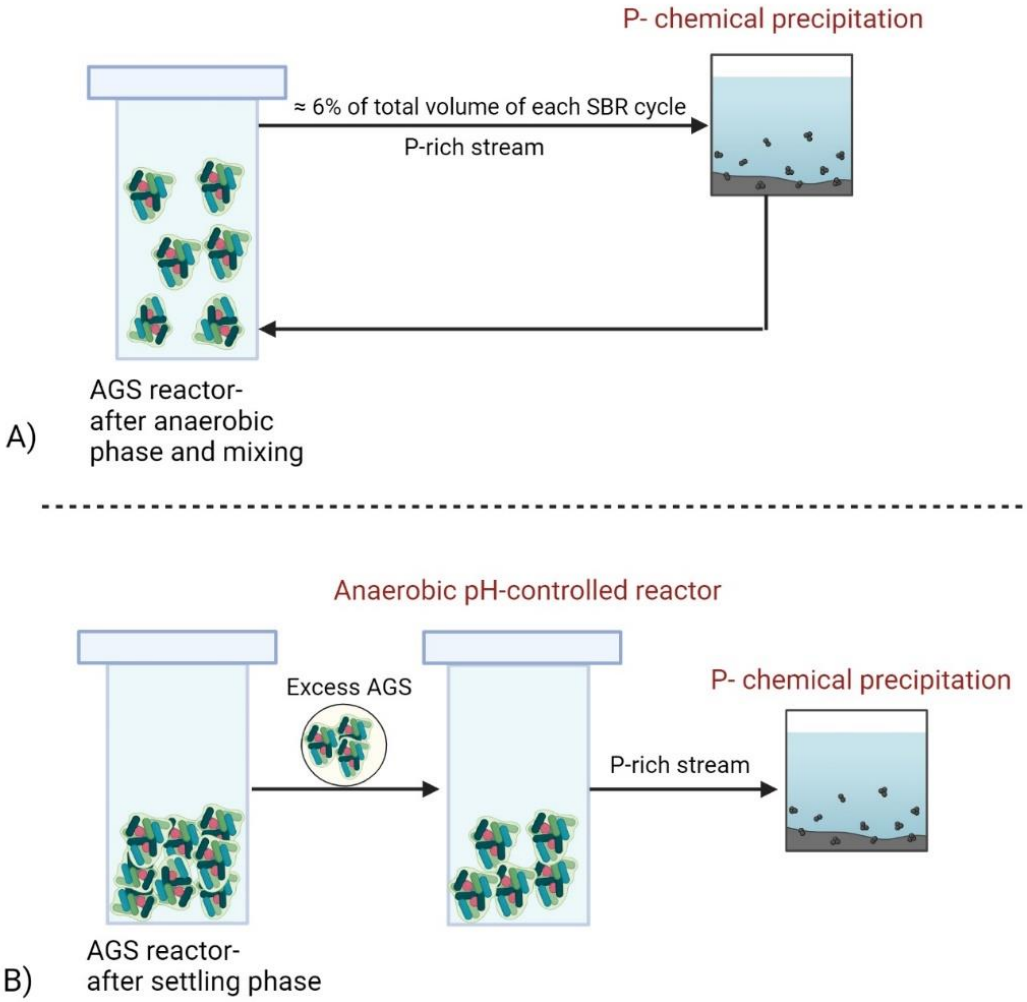

Figure 6-2:Other possible alternative routes for P recovery from AGS (not tackled in the thesis): A) at the end of the anaerobic phase, B) from excess sludge after anaerobic digestion

6.2.2 At the end of the anaerobic phase of the SBR cycle

Under anaerobic conditions, along with a carbon source in AGS reactors, the PAOs take up VFAs forming PHA while hydrolyzing polyphosphate to orthophosphates for energy production. This leads to phosphate being released into the bulk liquid and its concentration increases as monitored by the online sensors. This gives a chance to

recover phosphorus at this stage by, e.g., pumping the wastewater out to a separate reactor, adding metal ions, and precipitating the phosphorus, similar to the Phostrip process (Jeyanayagam et al., 2014; Salehi et al., 2018), then returning the wastewater to the AGS reactor to continue with the aeration phase as shown in **Figure 6-2**A). To elaborate more about the potential of the route, P mass balances with some assumptions could be helpful, taking Epe WWTP as an example. Based on the data collected in Chapter (2), Epe WWTP has a total P load of ≈ 45 kg P/day (the maximum P could be recovered daily), with two 4500 m^3 reactors working simultaneously. From the long-term graphs, the maximum P concentration after the anaerobic period is determined as ≈ 10 mg PO_4-P/L, as shown in **Figure 6-3**. This means that 45 kg P (the maximum P recovery per day) could be recovered from one cycle in one reactor assuming that the sludge bed at the bottom is negligible (in reality it will be < 45 kgP as it is impossible to empty the whole reactor because of the sludge bed). With two reactors and four cycles/day/reactor, 360 kg P/day could be recovered, which shows that potentially, in 1 day, the P load of 8 days could be recovered. This means that we only need to recover around 12% of the volume of each cycle to recover the total P load to the plant per day. However, we cannot recover 100% of the total daily P load to the WWTP as roughly 20-30% will be fixed in the sludge growth, and PAOs will need roughly another 20-30% to work properly. So, at maximum, 50% of the total P daily load could be recovered from the cycles. So, if Epe has 45 kg P/day, around 20 kg/day could be recovered from the cycles by treating around 6% of the total volume of each cycle.

Although the possible phosphorus recovery percentage from this approach is similar to or lower than that achieved through our integrated phosphorus and EPS recovery approach, it has several drawbacks that make it less attractive. First, the phosphorus concentration to be precipitated (approximately 10 mg $P\text{-}PO_4/L$) is relatively low for typical precipitation technologies like struvite, which has implications on the recovery feasibility. Second, all the recovered phosphorus is in a mineral form. Third, the effect of this approach on the activity of PAOs and the stable operation of AGS reactors is unknown, posing a risk. In contrast, our approach offers some advantages. First, the phosphorus concentration in the acidic by-product stream is very high (600 mg $P\text{-}PO_4/L$), making it highly feasible for precipitation. Second, part of the phosphorus is recovered as organic phosphorus, which is of higher value than mineral phosphorus. Third, as mentioned earlier, the unique integration of phosphorus chemistry and EPS in the final product expands industrial applications for recovery products. Finally, our recovery process occurs downstream of the wastewater treatment process, posing no risks to the performance of the treatment plant.

6.3 Outlook

6.3.1 Expanding the Scope of Phosphorus Recovery Beyond Mineral Precipitation

Microorganisms can produce well-defined products, such as polyphosphates or organic phosphorus esters, from complex matrices like wastewater. Implementing advanced phosphate biotechnology holds significant potential for contributing to the circular economy by closing the phosphate cycle.

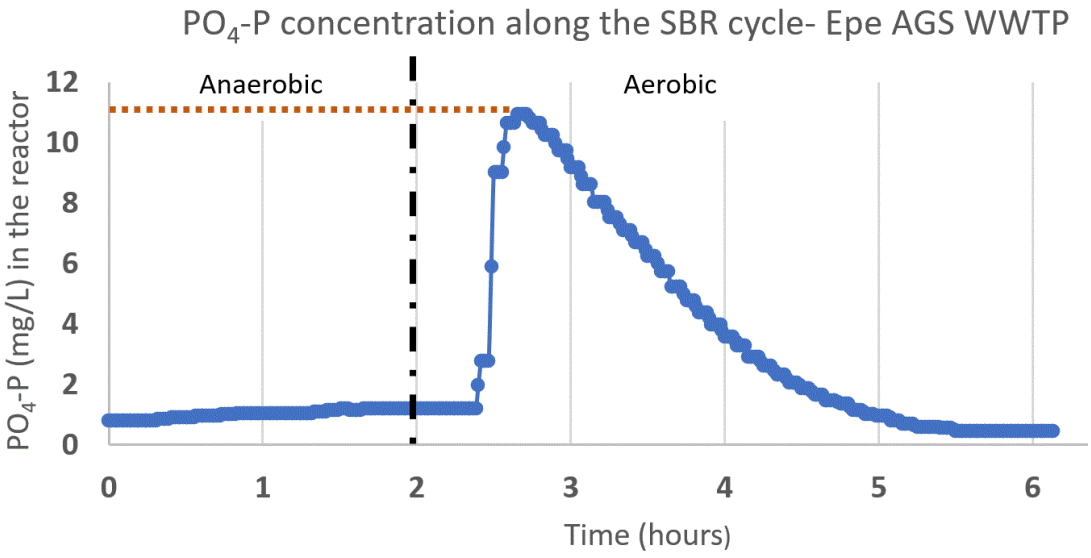

Figure 6-3: Online measurement data of PO_4-P concentration in an AGS reactor in Epe WWTP from the sampling campaign work performed in Chapter (2)

As explained in the introductory Chapter, these compounds are typically manufactured through cost- and energy-intensive thermal processing of phosphate rock due to their high industrial demand. Therefore, utilizing these phosphorus compounds naturally produced by microorganisms could promote more circular and economical phosphorus usage in high-value industrial applications, reduce reliance on mined phosphate, and mitigate its environmental impact. This introduces an intriguing perspective to the research track, from phosphorus in biotechnology to engineering applications. For example, recovering organic phosphorus, as demonstrated in this thesis, or extracting polyphosphate from sludge, as done in the Heatphos process, would enable using these microbial produced phosphorus molecules in industry. In

the Heatphos process, polyphosphates are released from sludge by heating it to 70°C for about one hour and then recovered by adding $CaCl_2$ (Takiguchi et al., 2003). Blank, 2012, 2023 described using microbial phosphorus in engineering applications as promising and referred to microorganisms as "designer bugs." However, there are knowledge limitations to achieving this goal. For instance, there is a lack of understanding of the interactions within microbial communities and the specific roles of different microbial species involved in enhanced biological phosphorus removal systems. Operators usually have limited options for troubleshooting during process upsets, highlighting the need for a deeper understanding of the underlying microbiological processes (Gebremariam et al., 2011).

6.3.2 Expanding the Scope of the Innovative Integration of Phosphorus and EPS to Engineer EPS

In **Chapter (5)**, we demonstrated that phosphorus chemistry can significantly influence the properties of EPS, including thermal stability, viscoelasticity, water-holding capacity, and emulsifying properties. In **Chapter (4)**, we identified various organic and inorganic phosphorus species in EPS, influenced by current practices in AGS WWTPs and the EPS extraction process. However, further research is needed to explore how to manipulate phosphorus chemistry in EPS. Phosphorus chemistry can be influenced both in WWTPs and during the EPS extraction process, offering opportunities to control and engineer phosphorus speciation in EPS and, consequently, tailor EPS its properties for specific applications. For instance, EPS has shown promising

potential as a flame retardant (Kim et al., 2020, 2022), likely due to its organic phosphorus content. Increasing the organic phosphorus species could potentially create a highly effective flame retardant from EPS. This enhancement could be chemically induced, analogous to the chemical phosphorylation of polymers. In **Chapter (5)**, we provided strong evidence that the current EPS extraction process is conducive to promoting phosphorylation. Phosphorylation may already be occurring, as suggested by our ^{31}P NMR results in **Chapter (4)**, which indicated an increase in organic phosphorus content during the alkaline extraction step compared to the initial sludge. Therefore, future experiments should aim to evaluate EPS phosphorylation to confirm whether the organic phosphorus ester content can be increased. These experiments should consider various factors, including pH, temperature, the concentration of P-O-P present in the initial sludge, the available functional groups in EPS that could undergo phosphorylation, and incubation time. All these factors would affect the phosphorylation outcomes. Advanced analytical techniques, such as mass spectrometry-based proteomics, should be used alongside ^{31}P NMR to achieve comprehensive results allowing for accurate identification of phosphorylation sites on EPS and providing a comprehensive overview of all phosphorylated and unphosphorylated proteins. This phosphorylation work is not only relevant to the EPS extracted from AGS but also many other materials could also profit from this work, e.g., EPS extracted from flocculant sludge (Dueholm et al., 2023), and lignocellulose extracted from plant biomass.

6.3.3 Towards the Future Vision of Aerobic Granular Sludge water-resource Facilities and Circularity

From the findings of this thesis, the future scheme of water resource recovery facilities of aerobic granular sludge WWTPs could be visioned, as shown in **Figure 6-4**. Since EPS recovery is likely the main driver for a recovery facility, we propose where to fit other recovery technologies within the extraction installation accordingly. Running this type of system differs significantly from managing a conventional WWTP. Utilities must consider strategies for implementing resource recovery, which might include either upgrading current WWTPs or partially delegating resource recovery activities. Another option could be to build centralized resource recovery facilities that receive and process aerobic granular sludge from multiple WWTPs. To achieve successful resource recovery, a holistic approach is needed with key points to be taken into consideration e.g., assessing the cost of recovery technologies, assessing the value and market potential of the recovered products, involving the stakeholders, promoting social acceptance, and building a value chain, thereby enabling the development of innovative processes that effectively recover marketable resource.

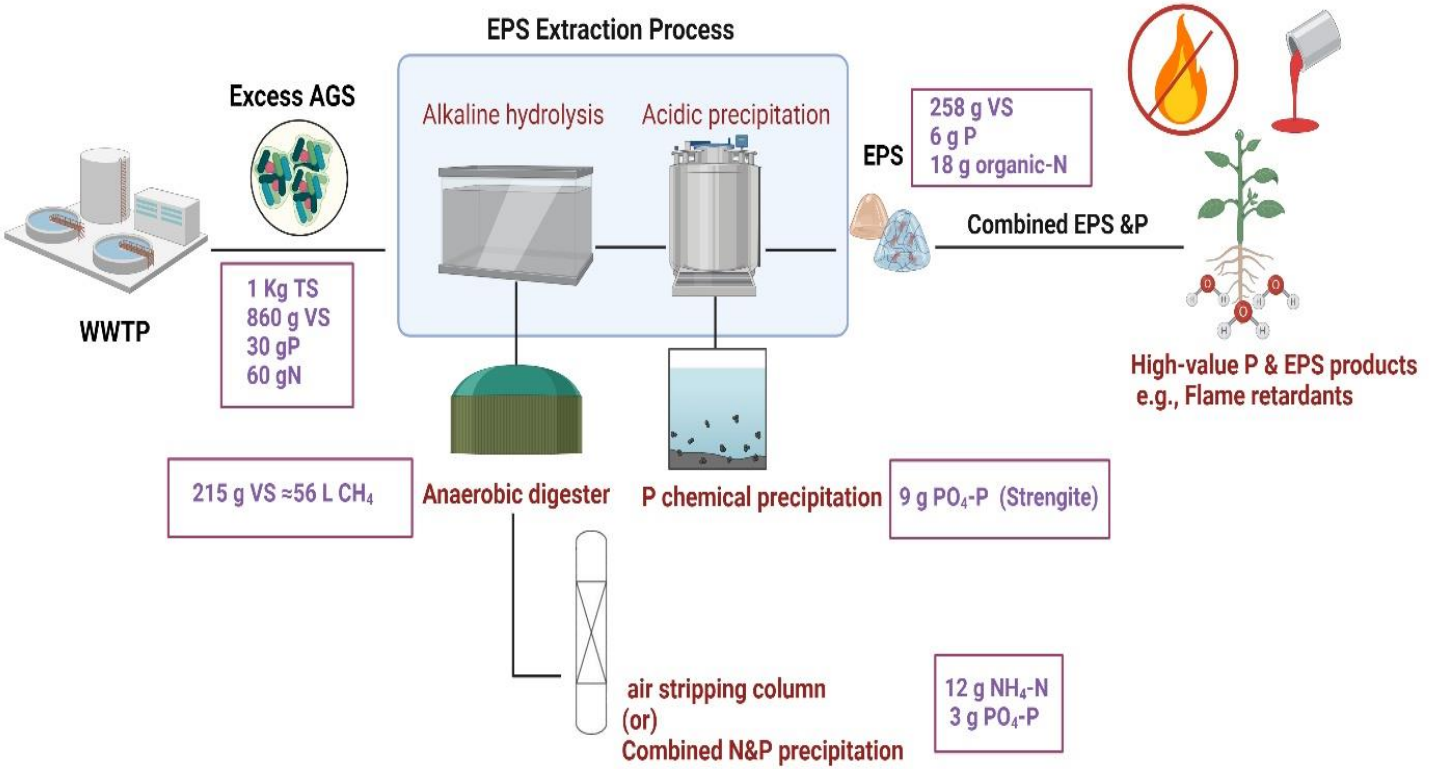

Figure 6-4: Proposed future scheme of integrated resource recovery from Aerobic Granular Sludge WWTPs to recover COD, phosphorus and ammonium

References

Blank, L. M. (2012). The cell and P: From cellular function to biotechnological application. In Current Opinion in Biotechnology (Vol. 23, Issue 6). https://doi.org/10.1016/j.copbio.2012.08.002

Blank, L. M. (2023). (Poly)phosphate biotechnology: Envisaged contributions to a sustainable P future. In Microbial Biotechnology (Vol. 16, Issue 8). https://doi.org/10.1111/1751-7915.14250

Campo, R., Czellnik, J. P., Lubello, C., & Lotti, T. (n.d.). Phosphorous recovery from waste aerobic granular sludge-ECOSTP2023 CONFERENCE PROCEEDINGS.

Dueholm, M. K. D., Besteman, M., Zeuner, E. J., Riisgaard-Jensen, M., Nielsen, M. E., Vestergaard, S. Z., Heidelbach, S., Bekker, N. S., & Nielsen, P. H. (2023). Genetic potential for exopolysaccharide synthesis in activated sludge bacteria uncovered by genome-resolved metagenomics. Water Research, 229. https://doi.org/10.1016/j.watres.2022.119485

ESPP. (2024, July). ESPP eNews no. 88 . https://www.phosphorusplatform.eu/scope-in-print/news

Feng, C., Welles, L., Zhang, X., Pronk, M., de Graaff, D., & van Loosdrecht, M. (2020). Stress-induced assays for polyphosphate quantification by uncoupling acetic acid uptake and anaerobic phosphorus release. Water Research, 169. https://doi.org/10.1016/j.watres.2019.115228

Gebremariam, S. Y., Beutel, M. W., Christian, D., & Hess, T. F. (2011). Research Advances and Challenges in the Microbiology of Enhanced Biological Phosphorus Removal—A Critical Review. Water Environment Research, 83(3). https://doi.org/10.2175/106143010x12780288628534

Jeyanayagam, S., Hahn, T., Fergen, R., & Boltz, J. (2014). Nutrient Recovery, an Emerging Component of a Sustainable Biosolids Management Program. Proceedings of the Water Environment Federation, 2012(2). https://doi.org/10.2175/193864712811693830

Kim, N. K., Lin, R., Bhattacharyya, D., van Loosdrecht, M. C. M., & Lin, Y. (2022). Insight on how biopolymers recovered from aerobic granular wastewater sludge can reduce the flammability of synthetic polymers. Science of the Total Environment, 805. https://doi.org/10.1016/j.scitotenv.2021.150434

Kim, N. K., Mao, N., Lin, R., Bhattacharyya, D., van Loosdrecht, M. C. M., & Lin, Y. (2020). Flame retardant property of flax fabrics coated by extracellular polymeric substances recovered from both activated sludge and aerobic granular sludge. Water Research, 170. https://doi.org/10.1016/j.watres.2019.115344

Salehi, S., Cheng, K. Y., Heitz, A., & Ginige, M. P. (2018). Re-visiting the Phostrip process to recover phosphorus from municipal wastewater. Chemical Engineering Journal, 343. https://doi.org/10.1016/j.cej.2018.02.074

Takiguchi, N., Kuroda, A., Kato, J., Nukanobu, K., & Ohtake, H. (2003). Pilot plant tests on the novel process for phosphorus recovery from municipal wastewater. Journal of Chemical Engineering of Japan, 36(10). https://doi.org/10.1252/jcej.36.1143

About the Author

Nouran Bahgat was born on September 16, 1995, in Cairo, Egypt. In 2013, she was among the top 150 students admitted to Zewail City of Science and Technology, founded by the Nobel Laureate Ahmed Zewail. There, she pursued a bachelor's degree in environmental engineering, studying various domains of chemistry, water resources engineering, wastewater treatment, and solid waste management. During her sophomore year, she began her first research project with her colleagues on developing polymeric networks for heavy metal contamination, supervised by Prof. Ibrahim M. El-Sherbiny. Nouran's growing interest in water led her to complete her bachelor's thesis on the feasibility of decentralized wastewater treatment systems and greywater reuse in urban areas in Egypt.

In 2018, Nouran received a Fellowship from Wageningen University and Research, allowing her to pursue a master's degree in water technology in the Netherlands, powered by Wetsus. For her MSc thesis, she worked within the biopolymer recovery research theme in Wetsus with Dr. Ruizhe Pei and Prof Alan Werker, investigating the stability of poly(3-hydroxybutyrate) in freshly produced PHB-rich biomass after mixed culture accumulation processes, addressing a crucial knowledge gap for industrial-scale production. In 2020, Nouran began her Ph.D. project on integrated phosphorus and extracellular polymeric substances recovery from aerobic granular sludge, initiated by TU Delft and the phosphate recovery research theme in Wetsus supervised by Prof. Mark van Loosdrecht, Dr. Philipp Wilfert, and Ir. Leon Korving. The outcomes of this four-year project, detailed in this thesis, led to four publications in Q1 journals and the granting of two patents. In recognition of her exceptional performance, she was honored with the prestigious Marcel Mulder Prize in 2024, awarded for outstanding contributions in the field of Water Technology.

List of Publications/Patents

*__Nouran T. Bahgat__, Philipp Wilfert, Stephen J. Eustace, Leon Korving, Mark C.M. van Loosdrecht, Phosphorous speciation in EPS extracted from Aerobic Granular Sludge, Water 2024. https://doi.org/10.1016/j.watres.2024.122077

*__Nouran T. Bahgat__, Aamash Sidiqqui, Philipp Wilfert, Leon Korving, Mark van Loosdrecht, FePO4.2H2O recovery from acidic phosphate-rich waste streams. WaterResearch, 2024 10.1016/j.watres.2024.121905

*__Nouran T. Bahgat__, Philipp Wilfert, Leon Korving, Mark van Loosdrecht, Integrated resource recovery from aerobic granular sludge plants, Water Research,2023.10.1016/j.watres.2023.119819

*R. Pei, __Nouran T. Bahgat__, M.C.M. Van Loosdrecht, R. Kleerebezem, A.G. Werker, Influence of environmental conditions on accumulated polyhydroxybutyrate in municipal activated sludge, Water Research,2023. 10.1016/j.watres.2023.119653

*Eslam G. Al-Sakkari, Omar M. Abdeldayem, Eslam E. Genina, Lobna Amin, __Nouran T. Bahgat__, Eldon R. Rene, Ibrahim M. El-Sherbiny, New alginate-based interpenetrating polymer networks for water treatment: A response surface methodology-based optimization study, International Journal of Biological Macromolecules, 2020. 10.1016/j.ijbiomac.2020.03.220

***MANUSCRIPTS UNDER REVISION**: **Nouran T. Bahgat et al** " Impact of Phosphorus on the Functional Properties of Extracellular Polymeric Substances Recovered from Sludge"- submitted to Water Research.

***Patent:** METHOD FOR EXTRACELLULAR POLYMERIC SUBSTANCES EXTRACTION FROM AN AQUEOUS STREAM, PHOSPHORYLATED EXTRACELLULAR POLYMERIC SUBSTANCES, AND USE THEREOF.

***Patent:** METHOD FOR PHOSPHATE AND/OR ARSENATE RECOVERY FROM AN ACIDIC STREAM, SYSTEM THEREFORE, AND USE OF A PRECIPITATE OBTAINABLE BY SAID METHOD.

Acknowledgments

Pursuing a PhD was a journey of self-discovery. It was a long and transformative experience, filled with new challenges, opportunities for growth, and the chance to meet diverse individuals from both academia and industry. Being abroad and engaging with talented, passionate colleagues from diverse cultures and academic backgrounds was an incredibly enriching experience. This journey would not have been the same without the people that made it possible. Even if I don't mention everyone by name, please know that your support is unforgettable to me, and I am truly grateful.

I would like to start with my supervisory team. **Philipp Wilfert, Leon Korving, and Mark van Loosdrecht**: Thank you for empowering me as the owner of my project, giving me the freedom to pursue my interests, providing constant support, and setting high standards for a stress-free academic environment. Working with you was a privilege, and you were the most significant factor in making my journey enjoyable. **Philipp**, I have always admired your fundamental and critical attitude throughout the project. Thank you for consistently providing honest, clear, and constructive not sugar-coated feedback. Also, I appreciate your patience—I can't count how many times I said, "I don't quite understand; could you explain that one more time?". **Leon**, thanks for always challenging me. You pushed me to engage with the industry on the practical applications of my research, participate in panel discussions, and present myself as a young water professional. Your encouragement to make my own decisions and stick to my time schedule was incredibly valuable. I will never forget your feedback on my presentation layouts. Your efforts have made the phosphate recovery team at Wetsus one of the strongest and most connected groups, creating a supportive environment where we always have each other's backs. **Mark**, thank you for sharing your wealth of knowledge with me and for all the engaging discussions and brainstorming sessions. I do admire your ability to identify what's interesting, and worth exploring, making significant impacts in our field. You're also a great teacher, and I've learned so much from you. I always felt like a priority, despite being distant from Delft campus and amidst your many other students.

Being part of the **WaterMining EU project** was an incredible experience, collaborating with numerous partners across Europe. Attending the annual consortium meetings was a true blessing, allowing us to connect in person in beautiful cities beyond Teams online meetings. I would like to extend a special thank you to **work package 4 partners**: Royal HaskoningDHV in the Netherlands, ACCIONA in Spain, and Aguas do Algarve in Portugal. **Mathijs**

Oosterhuis and **Eline van der Knaap**, I deeply appreciate your onsite support during the sampling campaign at Epe WWTP and the EPS extraction pilot, as well as your assistance in discussing the results. **Véronique Renard**, **Mar Micó Rec**, and **António Martins**, thank you for your invaluable feedback, and suggestions during our progress meetings. I also want to express my gratitude to **Alexander Groen** and **Frank van de Grootevheen** from Waterschap Vallei en Veluwe, and **Mark Smit** from Waterschap Rijn en Ijssel, for their unwavering support in sampling from the pilot plants at Epe and Zutphen WWTPs. Your openness and willingness to assist made everything so much easier. Thank you!

My journey at Wetsus began in 2018 when I started my master's degree in the Water Technology program. Over the past six years, I've received incredible support from technicians, the analytical team, administration, management, and all my fellow MSc, PhDs, and Postdocs. I want to give a special shout-out to the **1.18E office**—being part of two generations of this office allowed me to meet so many wonderful and kind people. Another special shout-out goes to **Ruizhe Pei** and **Alan Werker** from the bio-polymers recovery research theme. They introduced me to my first real research project during my MSc thesis and sparked my enthusiasm for research, which led me to pursue a PhD. Being part of the phosphate recovery team in my PhD was such a blessing. **Leon**, you did an awesome job picking this amazing group of people. **Thomas Prot**, I've lost count of how many times I said, "Just one quick question," and it turned into an hour-long chat! Thank you for always jumping in to help ASAP when I couldn't wait for an online meeting with Leon or Philipp. **Carlo Belloni**, you were my Wetsus PhD buddy and the first person I met on the phosphate team. Starting during the tough COVID times wasn't easy, but you really helped me settle in and get to know people. Thank you for always being so inclusive, welcoming, and kind. **Ha Nguyen**, I can still picture you in your big brown puffy jacket, walking through the atrium because you're always cold. Keep up the great work—you're next in line! **Sophie Banke**, Thanks for keeping tabs on me during the writing process and for all the hugs—couldn't have survived without them! Your efforts to mix and mingle at the Girona conference were truly top-notch! **Jessica Papera**, I know tackling a project like yours at Wetsus can be tough, but I'm confident you have got this! **Yuwei Huang,** you're the latest amazing addition to the team. Your artistic sense is exceptional, thank you for making my thesis cover look incredible! **Wokke Wijdeveld**, I was glad that you were part of the WaterMining project too. Sharing its activities with you made the whole experience even more enjoyable. **Simona Pruiti,** I bet you are going to miss having me next to you in the office, shouting out "OMG" every five minutes.

Your spirit and the toys on your desk made my writing phase so much more cheerful.

I would like to express my heartfelt gratitude to the TU Delft team. A special thanks to **Yuemei Lin**, **Stephen Picken**, and **Stephen Eustace** for their invaluable support throughout this journey, particularly in our discussions and assistance with measurements. **Ali Elahinik** and **Rodoula Ktori**, our time together during the WaterMinning activities was truly a blessing—I enjoyed every moment! **Anand Raja**, I greatly appreciate our collaboration in the last phosphorylation experiments and the lovely conversations we shared. You are one of the best personalities I encountered during my PhD.

The achievements of this thesis would not have been possible without the contributions of the students I had the pleasure of working with. It was a privilege to collaborate with such passionate and exceptional students. My heartfelt thanks go to **Aamash Siddiqui**, **Leo Sorin**, **Ana Catarina Lopez**, and **Basem Amireh**. I thoroughly enjoyed our time together, brainstorming as a mini phosphorus & EPS team at Wetsus and meticulously piecing together our findings. I trust you all will have a bright future and hopefully, our paths will cross again.

I also would like to thank **Berke Kisaoglan, Mirvahid Chehrghani, Elorm Obotey, Lourens van Langeveld, Yizhou Xing, Liang-Shin Wang, Widya Iswarani, Kecen Li, Jolanda Theeuwen**, **Lisette Cuperus**, **Irina Pozhidaeva, Ahmed Mahmoud** for all the nice conversations, coffee breaks, dinners, gatherings we had. It was a pleasure to get to know you all. **Yicheng Wang,** it has been reassuring knowing you were always there if I needed you. Now, it's time for me to leave you alone in the office—but I know you'll keep things awesome! **Yujia Luo,** you taught me that meaningful conversations aren't about how often you see someone, but about the depth and connection you share when you do. Thank you, **Olga Sojka**, for always reminding me that I'm doing great—it was the perfect pick-me-up during my down moments. **Angel Alonso**, you were like my office guardian, always offering incredible guidance when I needed it most, even after you flew the Wetsus nest! **Edward Kimani** and **Sebastian Castano,** we started our journey together in the Netherlands at the same time, from our Master's program to our PhDs. We witnessed each other growth. It's wonderful to have such confidants along the way. **Pamela Moussa,** Girl, I'm so glad you made it to Wetsus—I honestly can't imagine it without you. Thanks for always being there when I needed to vent out, suggesting those amazing restaurants, the fun sushi nights, Budapest, and Belgium trips with you and Talie. **Ruben Halfwerk,** you have been a great friend to me over the last few years. I will always cherish this amazing friendship. I know I've probably driven you crazy with endless questions about

illustrations, figures, layout design, microscopic pictures of crystals, and a million other things.

Last but not least, **Sarah Pinela**, You've always been there for me, both as a strong support and a cherished friend. Thank you for all the movie nights, Eurovision cheering nights, lazy lemon and Stek brunches, cooking traditional Portuguese dinners, those delicious Pastéis de Nata, and the thoughtful souvenirs from all your travels. **Talie Zarei**, I'll never forget our morning daily walks to Wetsus, coffee breaks and your endless supply of digestive biscuits. There are no "Toti, tomorrow 8?" messages anymore… Girls, it is hard to mention all the things we did together since we have seen each other almost every day since 2020. Inviting this new PhD to Proefverlof for the first time was an amazing idea from you both.

I want to extend my gratitude to my Egyptian friends—**Dalia Fleifel, Safwa Abu El Azaym, Randa Negm, Asmaa Samy, Gehad Nagy, Sarah Hazem, and Kareem Sherif**— For everything we've shared over the years and all the moments I will cherish forever, both online and offline, thank you. I'm grateful for the energy I gained from meeting you every vacation. **Hadeel, Alaa**, **Omar Magdi, Karim Elkholy, Mostafa Ahmed**, **Alaaeldin Elozeiri**, seeing you every now and then in the Netherlands was truly energizing for me, Thank you!

I am forever grateful to **Dr. Ahmed Zewail**, the Egyptian Nobel laureate, for establishing a modern educational institute that adopts a research-based education for undergraduate students in Egypt. My colleagues and I were lucky to study at **Zewail City** and receive full scholarships back in 2013. His meetings with us were always motivating, inspiring, and heart-warming. May he rest in peace :)

لماما وبابا، أغلى الناس على قلبي، شكراً على كل حاجة عملتوها ليا من وأنا صغيرة لغاية دلوقتي. أتمنى أكون دايمًا مصدر فخر ليكم. كله بفضل الله ثم بفضل مجهودكم. إخواتي **أحمد ونانسي،** شكراً لأنكم كنتوا دايمًا قدوة للنجاح في دراستي. **نانسي،** قدمتي لي دعم معنوي كبير، وخلّيتي دايمًا متصلة بمصر. مكالماتك انتي **وإسلام وجميلة** الجميلة كانت بتخلي ايامي أحلي.

وشكر خاص لعيلتي الكبيرة الرائعة اللي كانت معايا من وقت طفولتي وذكر خاص **لجدي علي، طنط سعاد، عمو هشام، خالو عبد الحميد، خالو محمد، رانيا، تامر، محمود، سارة، محمد، شيماء، علي، إبراهيم، ناجي، مصطفى، نجلاء، شادي، فادى، هادي، ليليا، ليديا.**

أحمد، كانت المرحلة الأخيرة صعبة، لكن تجاوزتها بكل ثبات بفضل وجودك فيها. شكراً على كل الثقة والدعم وعلى وجودك.